Hochschule für Angewandte Wissenschaften Hamburg
Hamburg University of Applied Sciences

Diplomarbeit

Studiendepartment Fahrzeugtechnik und Flugzeugbau

Identifying CO_2 Reducing Aircraft Technologies and Estimating their Impact on Global Emissions

Arno Apffelstaedt

08. Juli 2009

Hochschule für Angewandte Wissenschaften Hamburg
Fakultät Technik und Informatik
Department Fahrzeugtechnik + Flugzeugbau
Berliner Tor 9
20099 Hamburg

in Zusammenarbeit mit:

Deutsches Zentrum für Luft- und Raumfahrt e.V. (DLR)
Institut für Lufttransportkonzepte & Technologiebewertung
Blohmstraße 18
21079 Hamburg

Verfasser: Arno Apffelstaedt
Abgabedatum: 08.07.2009

1. Prüfer: Prof. Dr. Dieter Scholz, MSME
2. Prüfer: Dr.-Ing. Eike Stumpf

Industrielle Betreuung: Dr.-Ing. Eike Stumpf

Abstract

The strong growth in worldwide air traffic has raised concern on aviation's impact on climate change. According to latest scientific estimates, carbon dioxide is one of the main contributors of aviation to global warming, accounting for up to the half of its entire positive radiative forcing. As a reaction to these findings, there is an increased interest among the industry, scientific community and governments in possible approaches to mitigating the carbon footprint of aviation. Aircraft CO_2 emission is set by six technological key parameters, which define the range, the engine's efficiency, the aircraft's efficiency in terms of aerodynamics and weight, and the fuel efficiency in terms of heat content and fuel-specific CO_2 emission. A parametric study on the single influence of the parameters is conducted, which gives engine efficiency, fuel heat content and the zero-lift drag coefficient as the most powerful technological levers. Future aircraft technologies are identified through a literature study. Some of the most promising concepts for a medium-term application are found to be laminar flow technologies, geared and open rotor engine architectures, new materials for primary structures and bio-fuels. A method is developed and applied to assess the future fleet built-up through 2036. New aircraft programs as well as phase-out of in-service aircraft are considered. Individual aircraft's projected fuel efficiency and operational characteristics are introduced to assess the overall fleet's CO_2 emission development over the considered time frame. Three scenarios are established to simulate different future rates of technology progress and thus the possible implementation of identified technologies on future aircraft. Besides the individual aircraft's technological advances, further measures to reduce CO_2 emissions on a fleet level are analyzed: Bio fuels, shorter aircraft program cycles and shorter aircraft life. It is shown that the sole aircraft-related technology improvements will not be sufficient to reach such goals as 'carbon neutral growth' due to a constantly high traffic growth rate. Bio fuels seem to be the only solution for this problem, however, this technology is still immature and thus subject of high uncertainty in terms of economic viability as well as net-carbon footprint.

Hochschule für Angewandte Wissenschaften Hamburg
Hamburg University of Applied Sciences

DEPARTMENT FAHRZEUGTECHNIK UND FLUGZEUBAU

Identifying CO_2 Reducing Aircraft Technologies and Estimating their Impact on Global Emissions

Aufgabenstellung zur *Diplomarbeit* gemäß Prüfungsordnung

Background

European aeronautic research is driven by the ambitious goals of the Advisory Council for Aeronautics Research in Europe (ACARE) and its Vision 2020: A 50% reduction in aeronautic-related CO_2 emission in Europe is envisaged for 2020. The International Air Transport Association (IATA) has expanded this goal into a long-term global request for carbon-neutral air traffic by 2050. As a first step a technology roadmap is set up by international experts from industry and academia in a project organized by IATA. Generally speaking there exists a broad range of "technologies" that can be applied to reduce CO_2 emissions. On the one hand CO_2 emissions are influenced by the aircraft configuration and detailed design considerations. On the other hand it is of importance how aircraft are operated in the aviation system.

Task

A comprehensive listing of potential technologies for CO_2 reduction has to be set up and the global impact of the identified new technologies needs to be estimated. This review can be based on literature, the internet, and interviews with experts in the field. These inputs are then taken to estimate the global CO_2 reduction potential of the technologies based on aviation data bases, handbook methods and simple own models.

1. Parametric Assessment:
- Definition of the influencing physical variables which set the fuel consumption and CO_2 production of an aircraft.
- Formulation of an evaluation function suitable to measure the influence of these variables on fuel and CO_2 efficiency.
- Parametric application of the defined target function to assess the impact of each variable with regard to its physical constraints.

2. Technology Survey:
- Identification of current developments and possible future technologies with potential to reduce CO_2 emissions.
- Literature research on the technologies' potential to reduce CO_2 emissions and the timeline to be available for commercial aviation.

3. Fleet Forecast:

- Identification of the current world fleet composition, fuel consumption and CO_2 emissions.
- Estimation of the fuel consumption and CO_2 production of future aircraft equipped with new technology from the technology survey.
- Estimation of the future world fleet composition using generally acknowledged assumptions concerning growth rates, production rates and aircraft utilization cycles.
- Estimation of the future world fleet fuel consumption and CO_2 emissions.

The report has to be written in English based on German or international standards on report writing.

The thesis is supervised at the Deutsches Zentrum für Luft- und Raumfahrt e.V. (DLR) in Hamburg. Support is given by Dr.-Ing. Eike Stumpf.

Statutory Declaration

"I declare in lieu of an oath that I have written this diploma thesis myself and that I have not used any sources or resources other than stated for its preparation. I further declare that I have clearly indicated all direct and indirect quotations. This diploma thesis has not been submitted elsewhere for examination purposes."

July, 8th 2009 Arno Apffelstaedt

Content

List of Figures

List of Tables

Nomenclature

Symbols

a	speed of sound
AR	aspect Ratio
ASK	available seat kilometres
b	wingspan
BF	block fuel consumption
c_1	factor accounting for component weights driven by the maximum take-off weight
c_2	factor accounting for component weights driven by the payload
C_D	drag coefficient
C_{D0}	zero-lift drag coefficient
C_f	frictional coefficient
C_L	lift coefficient
D	drag
e	Oswald factor
f_L	seat load factor
g	gravitational constant
h	height, altitude
H	fuel heat content
k_R	cruise control factor
L/D	lift-to-drag ratio
LF	lost fuel fraction
m	mass
M	Mach-number
M_c	critical mach number
M_{dd}	drag-divergence Mach number
R	range
RPK	revenue passenger kilometres
S	wing area
SCE	fuel-specific CO2 emission
SFB	seat fuel burn
SR	specific range
T	thrust
$TSFC$	thrust specific fuel consumption
U	utilization
v	speed
W	weight
y	ratio of initial cruise lift coefficient to minimum lift coefficient

Greek Letters

η	engine efficiency
ρ	density

Subscripts

$( )_{AC}$	aircraft
$( )_{b}$	block
$( )_{Climb}$	climb
$( )_{CO2}$	CO_2
$( )_{Cr}$	cruise
$( )_{d}$	(per) day
$( )_{Div}$	diversion flight
$( )_{E}$	operational empty (weight)
$( )_{f}$	final
$( )_{F}$	fuel
$( )_{Hold}$	holding flight
$( )_{i}$	initial
$( )_{m}$	mission
$( )_{max}$	maximum
$( )_{md}$	minimum drag
$( )_{MTO}$	maximum take-off (weight)
$( )_{new}$	new aircraft
$( )_{P}$	payload
$( )_{prop}$	propulsive
$( )_{ref}$	reference aircraft
$( )_{Reserves}$	reserve (fuel)
$( )_{S}$	seats
$( )_{th}$	thermal
$( )_{TO}$	take-off
$( )_{Total}$	total (fuel)

Abbreviations

ACARE	Advisory Council for Aeronautics Research in Europe
ACC	active clearance control
ADS-B	Automatic Dependent Surveillance-Broadcast
APU	auxiliary power unit
ASC	active surge control
ATAG	Air Transport Action Group
ATC	air traffic control
ATM	air traffic management
BPR	(engine) by-pass ratio
BTL	biomass-to-liquid
BWB	blended wing body
CAEP	Committee on Aviation Environmental Protection
CANSO	Civil Air Navigation Services Organisation
CCD	continuous climb departure
CDA	continuous descend approach
CG	centre of gravity
CMC	ceramic matrix composites
CRTF	counter-rotating turbofan
CTL	coal-to-liquid
DOC	direct operating cost
EIS	entry into service
ETOPS	Extended Range Twin Engine Operations
ETS	Emission Trading Scheme
FAA	Federal Aviation Administration
FAME	Fatty Acid Methyl Ester
FESG	Forecasting and Economic Support Group (ICAO)
FPR	fan pressure ratio
GAO	Governmental Accountability Office
GDP	gross domestic product
GE	General Electric
GNSS	Global Navigation Satellite System
GTF	Geared Turbofan
GTL	gas-to-liquid
HLFC	hybrid laminar flow control
HP	high-pressure system
IATA	International Air Transport Association
ICAO	International Civil Aviation Organization
ICCAIA	International Coordinating Council of Aerospace Industries
IEA	International Energy Agency

IPCC	International Panel on Climate Control
LP	low-pressure system
MEA	more electric aircraft
MMC	Metal-Matrix-Composite
MRO	maintenance-repair-overhaul
NLFC	natural laminar flow control
OAG	Official Airline Guide
OPR	over-all pressure ratio
P&W	Pratt and Whitney
PMC	Polymer-Matrix-Composites
RAT	Ram Air Turbine
RQL	Rich Quench Clean
RR	Rolls Royce
SBAC	Society of British Aerospace Companies
SRA	Strategic Research Agenda
TAPS	Twin Annular Premixing Swirler
TBC	Thermal Barrier Coating
TBW	Truss-Braced Wing
TET	turbine entry temperature
UDF	un-ducted fan

"The most important and urgent problems of the technology of today are no longer the satisfactions of the primary needs or of archetypal wishes, but the reparation of the evils and damages by the technology of yesterday."

Dennis Gabor: *Innovations: Scientific, Technological and Social*, 1970

1 Introduction

1.1 Background and Motivation

Global air traffic has shown a strong and continuous growth since the beginning of the commercial jet age. Between 1960 and 2000, air travel has grown at an average rate of 9 % per year (data of FAA and IPCC in **Babikian 2006**) and at approximately 5.4 % between 1991 and 2007 (**Airline Monitor 2008b**). Barring any serious economic downturn or significant policy changes, air traffic is expected to experience similar growth rates in the future. For the years 2006 to 2036, a recent forecast of the International Civil Aviation Organization (ICAO) assumes an average annual growth of 5 % (**FESG 2008**). Even though the current financial crisis may constrain growth somewhat in the next few years, air traffic is expected to have recovered from this effect around the year 2012 (**Airline Monitor 2008b**, **OAG 2008**).

Historically, air travel has strongly contributed to the worldwide economic output. For 2007, the International Air Transport Association[1] (IATA) estimated aviation industry's share in worldwide gross domestic product (GDP) to be 7.5 % (**GAO 2009**). While a strong growth in traffic is likely to hold or increase that share, it also implies the risk of increasing the influence of aviation activities on the environment. Aircraft fuel burn per seat-km has been reduced by nearly 70 % since 1960 (**Greener By Design 2005**). Nevertheless, energy efficiency improvements were not able to keep pace with industry growth. As a result, global aviation's fuel use and emissions have continually been rising (**Babikian 2006**). Aviation's impact on the environment has become ever more important since the extent to which global warming can negatively influence living conditions on Earth is known. Aircraft engines emit several products that contribute to climate change, e.g. carbon dioxide (CO_2), nitrogen oxides (NO_x) and water vapour (H_2O). The International Panel on Climate Change (IPCC) estimates air traffic to account today for around 3 % of total human-generated positive radiative forcing[2] (**GAO 2009**). As air travel shows the fastest growth among all modes of transport and emissions at high altitude are affecting the climate potentially twice as severe as ground level emissions, its relative impact is expected to increase in the future (**Babikian 2006**, **IPCC 1999**, **Lee 1998**). Carbon dioxide emitted from aircraft engines plays a major role in the global warming potential of worldwide air travel: according to the latest IPCC estimate, about the half of global aviation's radiative forcing is attributed to the emission of CO_2 (**GAO 2009**). Thus, research into, and the identification of, CO_2 reducing aircraft technology is of high importance.

---

[1] IATA represents some 230 airlines comprising 93% of scheduled international air traffic (**IATA 2009b**).

[2] Radiative forcing expresses the change to the energy balance of the earth-atmosphere system in watts per square meter ($W \cdot m^{-2}$). A positive forcing implies a net warming of the earth and a negative value implies cooling (**Babikian 2006**).

Unfortunately, history shows that keeping up to usual rates of fuel-efficiency improvement may not be enough to fully offset the expected future increase in air traffic. As conventional technology is further assumed to approach its limit in efficiency (**Greener By Design 2005**), it is also questionable if aviation can even hold up to historical improvement rates without changing to radically different technologies and operations.

In response to this, several initiatives have been taken by governments and aviation stakeholders to foster research into new technologies and to provide incentives for implementing low-emission technologies on aircraft. They complement the United Nation's Kyoto Protocol of 1997, which sets binding, industry-unspecific targets for the reduction of greenhouse gases (**GAO 2009**). Three important initiatives should be named. First, to cap aircraft CO_2 emissions, the European Union (EU) plans to implement an emission trading program from 2012. The so-called European emission trading scheme (ETS) will include all flights to and from European airports. Airlines exceeding their individual emissions levels will need to purchase extra allowances (**GAO 2009**). Low-emission technology will then not only benefit the environment but also lower airline operating cost. Second, there is the goal of the Advisory Council of Aeronautical Research in Europe (ACARE), which aims at achieving a 50 % reduction in CO_2 emissions per seat-km for new aircraft entering service in 2020 (**SBAC 2008b**).[1] On the base of achieving the ACARE goals, already 200 research projects into emission and noise reduction had been funded by the EU in January 2009 (**Coppinger 2009**). Third, IATA just recently rescheduled its goal of 'carbon neutral growth' from 2050 to 2020 – that is, while the aviation industry keeps growing, global CO_2 emissions from aviation are not exceeding their 2020 level (**IATA 2009b**). IATA has set up a 'Technology Roadmap Project' to identify relevant technologies for achieving this goal.

Despite the various research activities, the question remains if implementing new technologies on planned future aircraft is enough to achieve these ambitious environmental targets. In general, it will take many years for new aircraft to work their way substantially into airline service (**Greener By Design 2005**). The impact of new technologies on world fleet CO_2 efficiency will then depend on multiple factors, such as year of introduction, market share and the retirement of old (i.e. considerably less efficient) aircraft. In this regard, insights into the benefit of new technologies require understanding of the make-up and fuel consumption of the future global aircraft fleet. If the beneficial impact of new aircraft alone should be too small for accomplishing environmental goals, technologies and operational instruments might become essential that are capable of providing benefits not only for new aircraft, but across the whole world fleet. There is a need to identify those in a relatively early stadium, as implementing them could allow air traffic to grow sustainably.

[1] Relative to a year 2000 reference aircraft.

1.2 Goals and Objectives

The primary objective of the thesis is to assess the capability of technological and operational measures to reduce individual aircraft and global aviation CO_2 emission. To achieve this primary goal, the following sub-ordinate, consecutive objectives can be set:

1. Identify technological key variables that set CO_2 emission of the individual aircraft and qualitatively understand their possible influence,
2. Identify general approaches and future technologies to reduce aircraft CO_2 emission,
3. Project the future development of global aviation CO_2 emission using different assumptions on the implementation of identified, CO_2 relevant technologies and operational instruments.

1.3 Methodology

The analysis consists of four phases of different nature. In the first phase, the influence of aerodynamic, engine, structural and fuel specific key variables on aircraft CO_2 emission is analyzed through a parametric study. A form of the Breguet range equation is derived that allows the calculation of block fuel weight from the predefined variables. It includes allowances for the fuel burned during taxiing, acceleration to cruise speed, climb to cruise altitude and en-route manoeuvring. These allowances are calculated from semi-empirical formulas to account for changes in aircraft efficiency. The block fuel weights and technological key variables of two actually existing passenger aircraft are chosen as reference for the parametric variations. One is representative of a modern short-haul narrow-body aircraft, the other of a modern long-haul wide-body aircraft. The technological variables are modified each in turn to estimate their influence on block fuel weight and thus CO_2 emission. Snowball effects on aircraft weight and drag polar are simulated using a simplified iterative approach.

In the second phase, a literature study is conducted to identify potential technologies for CO_2 reduction.

In the third phase, a forecast of the world fleet size and make-up up through the year 2036 is established, which allows the analysis of the impact of new technologies on global CO_2 emission. First, the make-up of the current world fleet of turbofan-powered passenger aircraft is determined. Using annual growth rates given by a recent ICAO forecast, the size of the future world fleet is projected. The ICAO forecast is used in its original form for the years 2017 through 2036, while, with respect to the current global economic downturn, the forecast is slightly adjusted down for the years 2009 through 2016. So-called *aircraft survival curves*

are then employed for computing future aircraft retirements. Based on literature research, especially on existing major studies on future aircraft deliveries, assumptions for consequent replacements, the emergence of new aircraft, the phase-out of current models and future market shares are made.

In the fourth phase, the future development of global aviation's CO_2 emission is projected. This is done using a bottom-up approach – that is, global fuel consumption and CO_2 emission are computed from the number and typical fuel consumption of individual aircraft flown in the world fleet. Fuel consumption and CO_2 emission of today's aircraft are found from the historical average of the recent years. Future aircraft that are equipped with promising new technology are assumed to consume less fuel and thus to be more CO_2 efficient. However, short- to medium-term and long-term aircraft projects are treated differently. The general design and technology of short- to medium-term aircraft projects is frozen and assumptions about fuel consumption are found from a literature study. The technological improvements found on long-term aircraft projects are less fixed. Thus, three different scenarios concerning the technological development and individual CO_2 emission are set up: a pessimistic, an optimistic and a 'most-likely' scenario. On the base of these scenarios, future global CO_2 emission is forecasted assuming new technologies find application only on new aircraft projects. Thereafter, different approaches to mitigating CO_2 emission further by using technological and operational measures that are capable of providing benefits to the whole world fleet are briefly analyzed.

1.4 Organization of the Thesis

The thesis examines aviation CO_2 emission first on the local level, i.e. aircraft level, and thereafter on the global level, i.e. world fleet level. The content of the single chapters is briefly summarized below. Chapter summaries at the end of chapters 2 to 6 shortly recapitulate the individual content and help guiding the reader through the thesis.

Chapter 2 provides an introduction into the understanding of the origin and consequences of aviation carbon dioxide and the influencing parameters of aircraft operation and design.

Chapter 3 investigates the possible impact of technological key design variables on aircraft fuel consumption and CO_2 emission.

Chapter 4 presents potential future technologies for CO_2 reduction.

Chapter 5 presents the approach and the results to forecasting the size and make-up of the future world fleet.

Chapter 6 presents the approach to determining individual aircraft CO_2 emission and transport performance and projects the development of future global CO_2 emission using different assumptions concerning the implementation of technologies and operational instruments.

Appendix A gives detailed information on the approach to calculating parametric variations in chapter 3.

Appendix B provides summarized information on CO_2 reducing technologies that were introduced in chapter 4 in tabulated form. In addition to the information given in chapter 4, the tables give information about major limitations, trade-offs and challenges associated with the technologies, the expected timeframe they could become available for commercial series production and their potential of reducing CO_2 emissions.

Appendix C provides data that is used to establish the fleet forecast in chapter 5 and the CO_2 forecasts in chapter 6.

Appendix D is a Compact Disc, which includes important, yet unreleased literature, detailed results of the parametric study and detailed results of the fleet and CO_2 forecasts.

2 Theory: Understanding Aircraft CO_2 Emission

This chapter provides an introduction into the understanding of the origin of aviation carbon dioxide. It is meant to emphasize the importance of limiting CO_2 emission and to set the scene for further discussion of possible approaches – i.e. technologies – to reducing CO_2. This is done in two separate parts. First, today's aviation emissions and their consequences for the environment and the airlines are briefly discussed. Second, influencing parameters of aircraft operation and technology are identified and examined concisely.

For a better understanding of the following sub-chapters, it is of help to recall the status quo of aircraft design. An example of today's dominant aircraft configuration is shown in Fig. 2.1: a classic swept-winged turbofan powered aircraft. Functions of providing volume for passengers, lift, stability and propulsion are separated. An optimized swept wing offers efficient high subsonic cruise flight. The aircraft is designed to use kerosene as fuel. Public, airlines, airports and manufacturers have adjusted the environment and their mindset to the configuration, which has now been dominant for half a century (**Greener By Design 2005**).

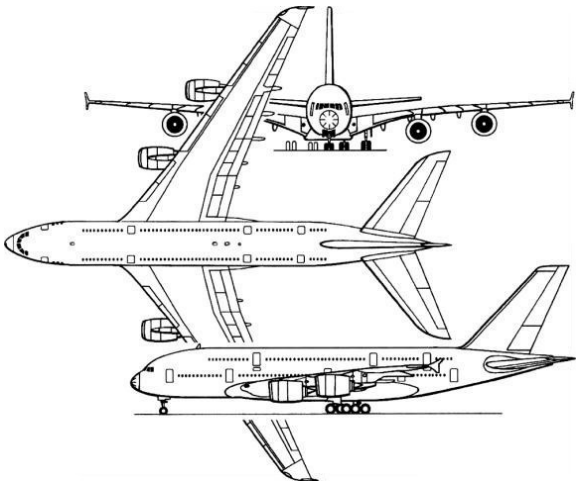

Fig. 2.1 Airbus A380-800 Schematic (**Jane's 2009**)

2.1 Sources and Consequences of Aviation Emissions

Fig. 2.2 shows the combustion process in a typical aircraft turbofan engine. In combustion engines, the ratio of fuel-to-air is called *stoichiometric*, when the mixture is chemically balanced and all fuel is combined with all free oxygen. The ideal or stoichiometric combustion of fossil fuels (i.e. hydrocarbons C_xH_y) forms carbon dioxide (CO_2) and water (H_2O) as combustion products. As ideal combustion does not exist, several other 'undesirable' by-products are emitted. In large part, these are nitrogen oxides (NO_x), carbon monoxide

(CO), unburned hydrocarbons (UHC) and soot particles. The emission of sulphur dioxides (SO_2) by airplanes is very low and can be neglected, as kerosene contains almost no sulphur (**Ruijgrok 2005**).

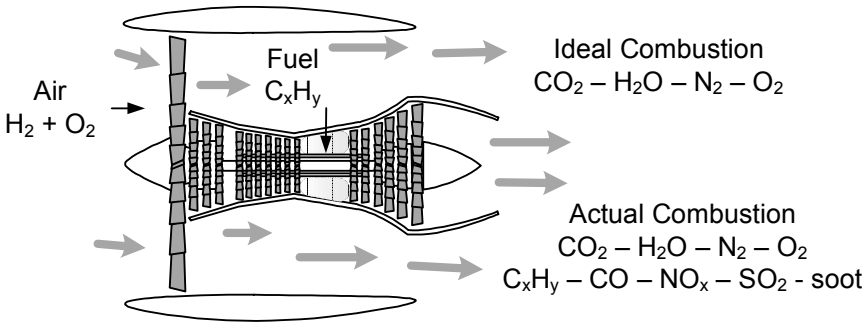

Fig. 2.2 The Combustion Process in a Turbofan Engine (reproduced from **Ruijgrok 2005**)

The amount of carbon dioxide (CO_2) and water (H_2O) emitted is directly proportional to the amount of fuel burned. Contrary, the formation of the undesirable products NO_x, CO, UHC and smoke is dependent on several factors of the combustion process:

- The amount of NO_x is related to the temperature of the burning gas and therefore increases with engine pressure ratio and thrust.
- Unburned hydrocarbons and carbon monoxide are the result of an incomplete combustion. They are strongly emitted when the fuel-to-air ratio is small and the oxidation process cannot be completed successfully. This is true for small mass flow rates at low thrust settings.
- Smoke or soot production occurs when too large fuel droplets and low oxygen come together, so that the fuel is not burned entirely. This may happen at high fuel-air ratios or if the fuel injected is not well atomized.

Table 2.1 summarizes above said and shows typical masses of emissions produced per unit mass of kerosene.

Table 2.1 Typical kerosene emission levels (reproduced from **Ruijgrok 2005**)

Substance	**Combustion product per kg fuel [kg]**	**Emission depends on**	**Impact on**
CO_2	3.15	Fuel consumption	Global atmosphere
H_2O	1.25		
CO	0.0004 - 0.065	Thrust setting:	Local air quality
UHC	0.0002 - 0.012	Max production at idle	
NO_x	0.004 - 0.030	Thrust setting:	Local air quality,
SO_x	0.00002 - 0.006	Max. production at full thrust,	global atmosphere
Soot	± 0.000015	i.e. take-off	

2.1.1 Air Pollution and Climate Change

Aviation emissions contribute to air pollution. According to **Ruijgrok 2005,** p. 1, the air is considered to be polluted, when the natural composition of the atmosphere is changed. In general, pollution can be of natural or anthropogenic source. Natural sources of pollution are for example volcanic eruptions or organic by-products of animals and plants such as pollen and methane. Today, emissions from power and heat generation through the burning of fossil fuels form the bulk of man-made pollutants. The different products emitted from aircraft engines have impacts on the local air quality and the global atmosphere, see Table 2.1. In more detail, burning kerosene or other hydrocarbons (C_xH_y) has the following harmful effects (**Ruijgrok 2005**):

- ***Global Warming*** or ***Enhanced Greenhouse Effect***: several combustion products settle in the atmosphere and cause the Earth's mean temperature to increase.
- **Acidification**: water vapour in the atmosphere combines with combustion products (nitrogen oxides NO_x and sulphur dioxides SO_2) and forms acid precipitation.
- **Ozone layer breakdown**: emitted nitrogen oxides participate in the destruction of the ozone layer and increase the risk of harmful ultraviolet radiation.
- **Photochemical air pollution**: nitrogen oxides may photo-react with oxygen and form ozone. Ozone is highly oxidative and poisonous. In the troposphere, it contributes to the global warming, near the ground it causes faster aging of plants and irritates eyes and mucous membranes.
- **Local air pollution**: the relatively motionless atmosphere near the ground does not foster the dispersion of the pollutants. A high concentration may lead to severe diseases and damage vegetation and buildings.

High air pollution from burning fossil fuels is thus a serious threat for both environment and living beings. It is therefore important to limit worldwide consumption. With growing world population and global living standard, especially in newly industrialising countries such as India and China, the number of consumers of fossil fuels is however rather increasing than decreasing. Low-emission technologies that allow for increased living standard while lowering air pollution are thus desirable.

While improving local air quality at airports has been of interest since the beginning of the jet age, the impact of man-made emissions on global warming has attracted wide public attention only recently. This is reflected by the fact that in the past, attention has been given mainly to the reduction of CO and UHC, which dominate at low thrust settings (**Ruijgrok 2005**). Further, international emission standards concerning CO, UHC and NO_x have first been set for the take-off and landing cycle by the International Civil Aviation Organization (ICAO) already in 1986 (**Greener By Design 2005**). The *Enhanced Greenhouse Effect* from emitting pollutants to the atmosphere that leads to global warming is however considered today the "most important issue in the long term" (**Greener By Design 2005,** p. 3), as climate change is

assumed to have long-lasting negative effects on the Earth's living conditions, such as rising sea levels and coastal flooding worldwide.

The most recent estimate of the International Panel on Climate Change (IPCC) concerning the impact of particular aviation emissions on global warming is shown in Fig. 2.3. Accordingly, CO_2 emissions account for about the half of the positive radiative forcing (warming effect) of aviation. Its impact might only be outclassed by the warming effect of so-called cirrus clouds. However, cirrus clouds are not considered in the calculations of the IPCC, as exact quantifications are not yet possible due to missing scientific understanding. A possible impact between 40 and 300 % of the influence of CO_2 has been reported (**GAO 2009**). There are also uncertainties concerning the radiative forcing of other non-carbon dioxide emissions, however, these are considerably lower.

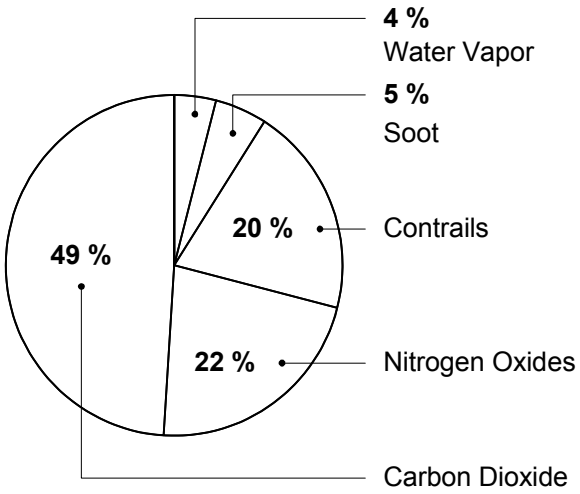

Fig. 2.3 Estimated Relative Contribution of Aviation Emissions to Positive Radiative Forcing (reproduced from **GAO 2009**, based on data from **IPCC 2007**) – **Note:** The relative contributions of emissions in this chart are an approximation because of the uncertainty surrounding the non-carbon dioxide forcing estimates, especially the contribution of cirrus clouds (**GAO 2009**).

Carbon dioxide (CO_2) emissions from aviation have the same radiative forcing as those from other industry sectors, as aviation CO_2 remains long enough in the atmosphere to be well mixed with the ground-emitted one (**GAO 2009**).[1] It is estimated that aviation accounts for about 13 % of all carbon dioxide emitted from transportation and for about 2 % of global CO_2 emissions, see Fig. 2.4. Of this 2 % estimate, 80 % account for civil commercial aviation including cargo (**GAO 2009**).

[1] This is different for other aircraft emissions, as for example nitrogen oxides. NO_x emissions have a higher warming effect at cruising altitudes because of the formation of ozone (**GAO 2009**, **Ruijgrok 2005**)).

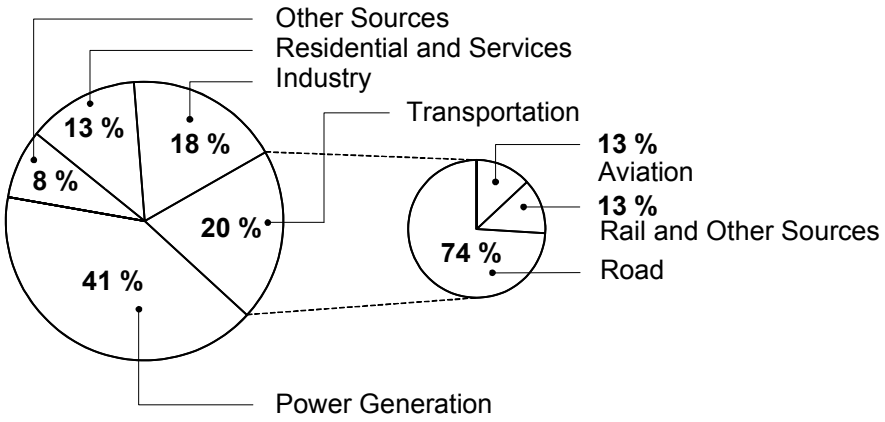

Fig. 2.4 Global Transportation and Global Aviation's Contribution to Carbon Dioxide Emissions 2004 (reproduced from **GAO 2009**, based on International Energy Agency and IPCC data)

Due to the warming effect of nitrogen oxides, contrails and cirrus clouds, global aviation's contribution to climate change is assumed higher than its 2 % share in global CO_2 emissions. According to **GAO 2009**, the IPCC estimated aviation emissions to contribute to about 3 % of the human-generated greenhouse effect in 2007. Due to uncertainties in calculating the impact of non-carbon dioxide factors, especially cirrus clouds, the relative share could however also be as low as 2 % or as high as 8 % (**GAO 2009**). Nevertheless, it is seen that success in limiting aviation's impact on global warming is strongly dependent on finding technologies that reduce carbon dioxide emission.

2.1.2 Cost of Emitting CO_2

Besides the environmental necessity, minimizing carbon dioxide emission can help reducing aircraft direct operating cost (DOC). This is primarily due to CO_2 emission being directly proportional to fuel consumption. As will be seen in the following chapters, reducing CO_2 is thus often realized by the means of reducing aircraft fuel burn. Fuel costs currently make up around 30 % of a large aircraft's DOC (**Babikian 2006**, **GAO 2009**, **Scholz 1999**). This share is likely to increase without new technology if crude oil prices should continue to rise. **GAO 2009** thus sees future fuel prices as a major factor in influencing the development of low-emission technologies for aviation. Most likely, fuel cost will however only provide an incentive for reducing CO2 emissions if fuel savings are greater than the improvement's additional life-cycle cost.

Another cost factor of emitting CO_2 for airlines might evolve from the implementation of emission taxes or emission trading programs (cap-and-trade programs). These governmental policy options would put a price on the emission of CO_2 and lead to higher direct operating costs if airlines do not invest in low-emission technologies (**GAO 2009**).

2.2 The Influence of Aircraft Operation and Technology on CO_2 Emissions

The mass of carbon dioxide emitted per kg of fuel burned can be assumed as a pure fuel-specific parameter. For example, kerosene emits 3.15 kg CO_2 per kg of burned fuel (**Ruijgrok 2005**). For a specific fuel, the total mass of CO_2 produced from engine start to shut-down is then a simple function of the block fuel mass. Therefore, before considering particular technologies to reduce CO_2 emission, it is worth thinking about the key variables which set fuel consumption and hence carbon dioxide emission of aircraft. In general, fuel consumption depends first, on the fuel efficiency of the aircraft – i.e. its technical ability – and second, on how it is operated – i.e. if it can fully exploit its technical ability. Typical commercial aircraft operation is now shortly described. The sub-chapter thereafter briefly discusses technological key variables that define aircraft fuel efficiency.

2.2.1 Aircraft Operation

Fig. 2.5 shows an ideal flight mission for an international flight. The numbered segments are: engine start and warm-up (1), pre-flight taxi (2), accelerate and take-off (3), climb to cruise altitude (4), cruise (5), descent (6) and landing taxi (7). From engine start to shut-down, aircraft weight is continuously decreasing as fuel is burned. For each segment, the difference of initial and final aircraft weight ($W_i - W_f$) then denotes the amount of fuel consumed. Fuel burned from the start of the engines to shut down is called block fuel $W_{F,b}$. Fuel consumed from take-off to touch-down is called mission fuel $W_{F,m}$. In addition to mission fuel, block fuel includes fuel burned during engine start and warm-up, pre-flight taxi and landing taxi.

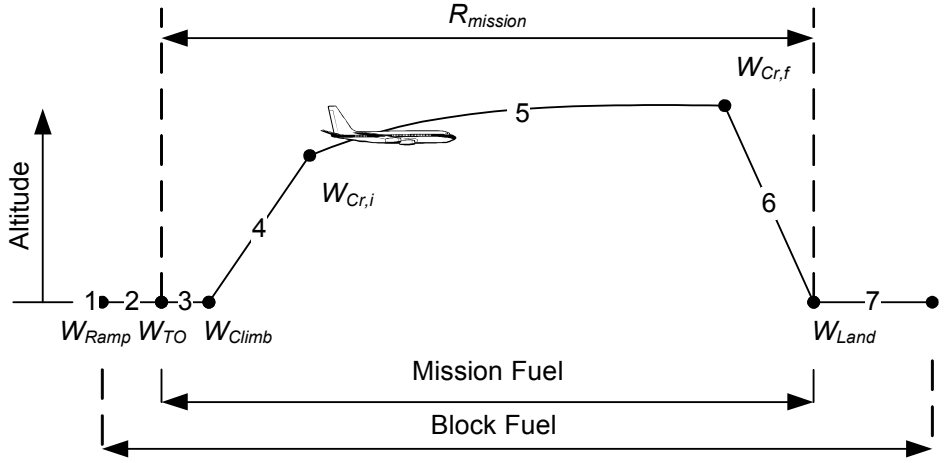

Fig. 2.5 Ideal Mission Profile for a Commercial Transport Aircraft (reproduced from **Roskam 1997**)

Best possible aircraft efficiency implies short as possible taxiways, continuous climb departures (CCD), most direct cruise flights that allow continuous altitude changes, continuous descent approaches (CDA) and no holding patterns. If the aircraft is allowed to fly a mission that is tailored to its particular needs, the flight profile shown in Fig. 2.5 is reasonably efficient. Unfortunately, airspace is not free and the aircraft is constrained to fly according to the rules of air traffic control (ATC). Efficiency is then lost due to (**Greener By Design 2002**):

- Extra ground time spent queuing and taxiing,
- Climb broken into segments including inefficient level flights,
- Cruise/En-route flight constrained to one particular altitude or few particular altitudes (if step-wise climbs are allowed),
- Non-direct flight paths due to different national/military/civil airspace areas with their own controls and restrictions,
- Non-direct flight paths due to outmoded ATC systems (i.e. waypoint beacons),
- Extra flight time spent in holding patterns, and
- Descent broken into segments including inefficient level flights.

Hence, an optimized air traffic environment, more advanced air traffic management (ATM) technology and improved operations could noticeably reduce fuel burn and CO_2 emissions. ATM stakeholders are currently working on establishing a so-called 4D traffic environment that would allow aircraft to operate more freely and closer to their optimum performance. The concept is briefly discussed in chapter 4.5.

2.2.2 Technological Key Variables

Consider a steady, level, powered flight: the aircraft is in cruise. The job of the aircraft engines is to overcome the airplane drag, i.e. to produce thrust as a counterforce. As in horizontal flight, lift is equal to aircraft weight W, the thrust T required can be defined by the lift-to-drag ratio L/D as shown below.

$$T = D = \frac{W}{L/D} \tag{2.1}$$

Theoretically, the aircraft can stay in this mode of flight as long as the engines produce enough thrust. This is dependent on the thrust specific fuel consumption of the engines, i.e.

$$TSFC = \frac{\text{fuel consumption in kg} \cdot \text{s}^{-1}}{\text{thrust output in N}} = \frac{\dot{m}_f}{T} = \frac{\dot{m}_f \, L/D}{W} \quad , \tag{2.2}$$

and the amount of fuel available. Hence, the instantaneous value of distance covered per unit quantity of fuel consumed, the so-called specific range

$$SR = \frac{\Delta R}{\Delta W_F} \quad , \tag{2.3}$$

is an expression of the momentarily aircraft performance. For a given cruise speed V, specific range can be written

$$SR = \frac{1}{TSFC \cdot g} \cdot v \cdot L/D \cdot \frac{1}{W} \quad . \tag{2.4}$$

Accordingly, performance is driven by the thrust specific fuel consumption, the lift-to-drag ratio, the (design) cruise speed and the aircraft weight (see e.g. **Gmelin 2008**). As proposed in **Torenbeek 1997**, for a more independent analysis of the variables, the overall engine efficiency is then introduced as

$$\eta \overset{def}{=} \frac{\text{Net Propulsive Power}}{\text{Heat Content of Fuel Flow}} = \frac{T \cdot v}{\dot{m}_f H} = \frac{\not{T} \cdot v}{TSFC \cdot \not{T} \cdot H} \quad , \tag{2.5}$$

where H is the calorific value of the fuel. Eq.(2.4) can be rewritten to give

$$SR = L/D \cdot \eta \cdot \frac{H}{g} \cdot \frac{1}{W} \quad . \tag{2.6}$$

Thus, specific range is an expression for the combined efficiencies of the airframe, the engines and the fuel.

Due to fuel burn, aircraft weight decreases during flight. The ratio of final to initial aircraft weight W_f/W_i indicates the amount of fuel burned for a certain range. Cruise range can be obtained from integration of the specific range (**Torenbeek 1997**), i.e.

$$R = \int_{W_f}^{W_i} \left(L/D\,\eta \cdot \frac{H}{g} \cdot \frac{1}{W} \right) \mathrm{d}W \quad . \tag{2.7}$$

Giving that the aircraft is allowed to maintain a constant lift coefficient and Mach number (i.e. assuming constant ($L/D \cdot \eta$)) through a constant climb during cruise (*cruise*/*climb*), Eq.(2.7) can be transformed to give fuel weight as

$$W_F = W_i \left[1 - \exp\left(- \frac{R}{L/D \cdot \eta \, H/g} \right) \right] \quad . \tag{2.8}$$

A more detailed analysis is possible if we write aircraft all-up weight as

$$W_i = W_E + W_P + W_F \quad , \tag{2.9}$$

where W_E is the aircraft empty weight and W_P is the payload. Rewriting Eq.(1.8) and inserting the above expression gives fuel consumption in kg per kg payload, i.e.

$$\frac{W_F}{W_P} = \left(1 + \frac{W_E}{W_P} \right) \left[\exp\left(\frac{R}{L/D \cdot \eta \, H/g} \right) - 1 \right] \quad . \tag{2.10}$$

Introducing the specific carbon dioxide emission *SCE* – i.e. the weight of carbon dioxide emitted per kg fuel burned – into above expression gives CO_2 production per kg payload as

$$\frac{W_{CO_2}}{W_P} = SCE \cdot \left(1 + \frac{W_E}{W_P} \right) \left[\exp\left(\frac{R}{L/D \cdot \eta \, H/g} \right) - 1 \right] \quad . \tag{2.11}$$

It is shown that fuel consumption – and hence CO_2 emission – for a given payload is set by six relatively independent variables, which are

- Aerodynamic efficiency *L/D*,
- Engine efficiency η,
- The ratio of empty weight to payload W_E/W_P,
- Energy content of the fuel per unit weight *H*,
- Specific carbon dioxide emission *SCE*, and
- Range *R*.

These parameters are now briefly analyzed.

Aerodynamic Efficiency *L/D*

An object moving through the air will experience a resultant force that is classically divided into two components, a component in the direction of the flow, the drag, and another component normal to the direction of flow, the lift. The ratio of these two, the lift-to-drag ratio of the aircraft *L/D*, is an important performance parameter, sometimes referred to as the aerodynamic fineness ratio or aerodynamic efficiency.

As the fuel consumption of the engines is generally thrust specific, the fuel flow rate is inversely proportional to the lift-to-drag rate. Hence, for reduced fuel consumption and less CO_2 emissions the ratio needs to be increased. For a given aircraft weight and lift, this is done by the means of reducing drag.

Fig. 2.6 shows a causal drag breakdown for a large modern swept-winged aircraft. It is seen that skin friction and lift-induced drag are the two main components. Skin friction drag is drag caused by the friction of the fluid particles on the aircraft surface. Lift-induced drag is mainly caused by trailing edge vortices at the wingtips. Form or pressure drag (afterbody/pressure drag in Fig. 2.6) is caused by the form of the object. It is high for bluff bodies, but plays only a minor role in the drag build-up of streamlined objects like aircraft. Interference drag – extra drag caused by bodies placed close to each other in an airstream – comes mainly from the interaction of the fuselage and engines with the wing. Wave drag results from local supersonic flows and shock waves over the wing and fuselage. For civil jet transports, the relative influence of wave drag on total drag is limited to relatively low values by the definition of the drag divergence Mach number ($\Delta C_D = 0.002$, Boeing definition). The expression parasite (or parasitic) drag generally terms the sum of the skin friction, pressure and interference drag of major aircraft components. In Fig. 2.6, the term 'Parasitics' stands for additional parasite drag that is due to things as control surface gaps, antennas and other extraneous items. Modern medium- and long-range aircraft feature cruise L/Ds between 16 and 19 (**Greener By Design 2003**, **Eurocontrol 2004a**).

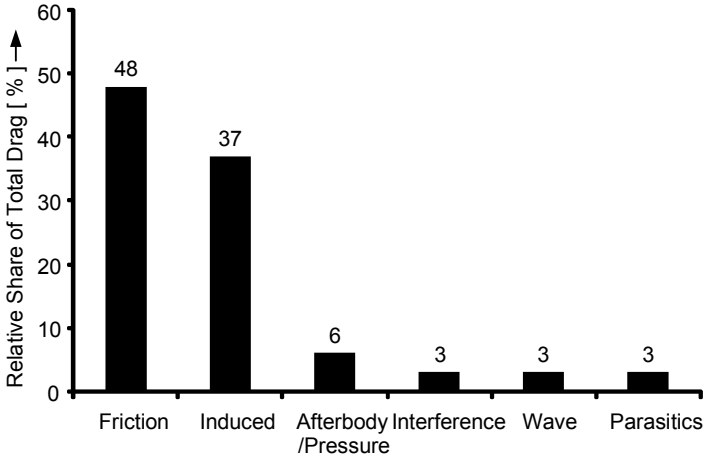

Fig. 2.6 Causal Drag Breakdown of a large modern swept-winged Aircraft (reproduced from **Greener By Design 2005**)

If we express the lift-to-drag ratio by the ratio of their coefficients C_L/C_D and we assume a parabolic drag polar, the expression to minimize is

$$C_D = C_{D0} + \frac{S}{\pi e b^2} \cdot C_L^2 \quad , \tag{2.12}$$

where C_{D0} is the zero-lift or parasite drag, which is the sum of the skin friction and form drag coefficients.[1] The second summand is called the lift induced drag, with S being the wing area, b the wing span and e the Oswald factor. For zero lift, the second term falls to zero and the total drag coefficient becomes C_{D0}. For jet transport, C_{D0} is dominant in cruise, whereas lift induced drag is dominant at take off (**Roskam 1997**). At high subsonic speeds, where wave drag occurs, the total drag coefficient leaves the parabolic function. However, as wave drag is low for subsonic civil aircraft, the parabolic drag polar has been found to yield adequate results up to their regular cruise Mach number (**Roskam 1997**).

As friction, induced and form drag together account for around 90 % of the aircraft drag in cruise (see Fig. 2.6), for simplification, the parametric study in chapter 3 is based on the parabolic drag polar and the variation of the coefficients C_{D0}, e and b. A closer look at all forms of drag – i.e. their origin and possible ways of reduction – is provided in chapter 4.1.

Engine Efficiency η

The majority of today's civil transport aircraft are flying with (high by-pass) turbofan engines, because of their high efficiencies, especially near transonic flight speeds. Smaller regional jets frequently use turboprop engines, being highly efficient at lower flight speeds.

Fig. 2.2 shows the schematic of a simple two-shaft turbofan. Thrust is provided by two airstreams, the primary airstream of the engine core and the secondary airstream of the fan. The ratio of the two mass flows, the by-pass ratio (BPR), is around 8 to 9 for large civil turbofan engines currently in production (**Gmelin 2008**). The engine is shrouded by the nacelle and mounted to the aircraft wings or fuselage using pylons.

The influence of the aircraft engines on fuel consumption can be divided into three parameters of different nature:

- Engine drag (including nacelle and pylon drag),
- Engine weight (including nacelle and pylon weight) and
- Thrust Specific Fuel Consumption.

Engine, nacelle and pylon drags are mainly driven by the size of the intake/fan, the wetted area of the nacelle, the interaction between nacelle and pylon and the interaction of the pylon

[1] The parabolic drag polar assumes that skin friction and form drags are not dependent on the production of lift. "In reality it has been found that such a simple split is difficult to achieve. The main reason is that in many airplanes parts of the parasite drag can become dependent on lift" (**Roskam 1997,** p. 146)

with the wing (**Gmelin 2008**). While interference drags from the interaction of the pylon, engine and wing are regarded as parts of the over-all aircraft drag, internal drags from the inlet and nacelle are most often accounted for as a reduction in installed thrust (**Roskam 1997,** p. 146). Thus, they can be seen as an increase in thrust specific fuel consumption.

Engine, nacelle and pylon weights are regarded as component weights of the aircraft empty weight. However, reducing the component weights plays an important role in realizing higher engine efficiencies, for example when increasing the fan diameter. Over-all engine weight is driven by the size of the engine, the number of engine parts, the materials used and the manufacturing and construction methods (**Gmelin 2008**).

Thrust specific fuel consumption, as defined in Eq.(2.5), is a function of the flight speed V, the calorific value of the fuel H and the over-all engine efficiency η.
Engine efficiency η can be expressed as the product of the thermal efficiency of the gas turbine η_{th} and the propulsive efficiency of the jet η_{prop}. With $TSFC$ and η being inversely proportional, we can write

$$TSFC \propto \frac{1}{\eta} = \frac{1}{\eta_{th}} \cdot \frac{1}{\eta_{prop}} \quad . \tag{2.13}$$

For a given fuel, the calorific value H in Eq.(2.5) is constant. Providing a constant flight speed, thrust specific fuel consumption can then be reduced by increasing thermal and propulsive efficiencies.

Today's state-of-the-art turbofans feature thermal efficiencies in the order of 50 % and propulsive efficiencies of 70 to 80 % (**Gmelin 2008**). This results in over-all efficiencies around 35 to 40 %. The theory of thermal and propulsive efficiencies and means to reduce thrust specific fuel consumption are more closely looked at in chapter 4.2.

The Ratio of Empty Weight to Payload W_E/W_P

Aircraft weight W can be split into payload W_P, fuel weight W_F and operating empty weight W_E. Payload is the carrying capacity of an aircraft, i.e. the sum of the weight of the passengers and cargo to be transported. The output of a vehicle is to transport payload from A to B, reducing payload will result in lower efficiencies and is thus not useful. Consequently, reducing aircraft weight efficiently means reducing fuel and empty weight for a given payload.

Operating empty weight is the sum of the aircraft structural weight, the engines' weight, the landing gear weight, the weight of the fixed equipment – i.e. galleys, seats, furnishing, etc. –,

the weight of the trapped fuel and the weight of the crew. Weight saved on any particular component will decrease empty weight. Component weights are set by the specific strength of the material used, the construction methods, additional load factors (reserve and gust load factors) and the design range. Further, aircraft empty weight increases during the aircraft's life. This is due to repairs, dirt, trapped fuel and moisture retaining insulations.

For example, the specific empty weights per kg design payload of the reference aircraft in chapter 4 are 2.74 kg for the medium-range narrow-body and 4.69 kg for the long-range wide-body aircraft (**Eurocontrol 2004a**). A closer look at the influencing factors and resulting possible methods and technologies to reduce empty weight are provided in chapter 4.3.

Fuel-specific Energy Content *H* and Carbon Dioxide Emission *SCE*

H is the energy produced per kg fuel burned. Today's commercial aircraft are generally powered with Jet A-1, a kerosene jet fuel with a calorific value *H* around 43 $MJ \cdot kg^{-1}$ (**Exxon 2008**). The carbon dioxide emission per kg of burned kerosene Jet A-1 is around 3.15 kg (**Ruijgrok 2005**). Both weight specific heat content *H* and *SCE* are fuel-specific. Improving the values is thus possible by using an alternative fuel. Alternative fuels and their potential for lowering CO_2 emission are briefly discussed in chapter 4.4.

Range

Per definition of Eq. (2.10) and (2.11), fuel consumption and CO_2 emissions per unit payload increase with increasing range. Traditionally, range has not been seen as a variable to be optimized, but as an (unchangeable) input to design, as the transport performance of any vehicle is generally transporting a given payload over a given distance.

It is the case for aircraft however, that fuel weight and range are not linearly dependent (see Eq.(2.8)). Increasing range ultimately increases (initial) aircraft weight. On long ranges, "... a substantial fraction of the fuel used for the first third of its [the aircraft, author's note] journey is two carry the fuel for the last thirds of the journey ..." (**Greener By Design 2003,** p. 30). Carrying extra weight decreases the aircraft's fuel efficiency: a long-range aircraft burns more fuel per passenger and km than a medium-range aircraft (with an identical payload and similar aerodynamic and engine efficiencies). This effect is amplified by snowballs (see description below) on aircraft empty weight, as wings, undercarriage etc. need to carry the extra fuel load.

When considering the cruising flight only, fuel efficiency increases continuously with shorter design ranges. However, this is untrue for the realistic case where the aircraft burns additional

fuel for climbing to cruise altitude and accelerating to cruise speed. This 'lost fuel', see chapter 3.1.2, offsets the benefit for very short design ranges. The optimum range yielding lowest fuel burn per seat and km is thus a medium one. As design range is a parameter that mainly affects aircraft structural weight, approaches to reducing CO_2 emissions by changing design range are included in chapter 4.3, *Aircraft Empty Weight*.

Snowballs on the Variables

The term "snowball effect" describes the phenomenon of local small changes growing to large global ones due to general interdependencies of parts in the overall system. As aircraft all-up weight, empty weight and fuel weight are interrelated, changes of even small significance to one of the influencing variables (L/D, η, W_E, W_P, H and R) will have a significantly larger impact on fuel consumption than indicated by the initial change.

Simply put, all aircraft components can be assigned to one of two categories: those which characteristics – i.e. size and weight – are driven by the payload and those which characteristics are driven by the maximum take-off weight. For example, consider the schematic of the classic cantilever configuration in Fig. 2.1. Geometry and accordingly weight of the mid-fuselage is mainly determined by the payload. The number of passengers and their designated comfort also drives the number and weight of the seats, the galleys, etc. Contrary, the characteristics of the wings, the empennage, the engines and the undercarriage are mainly functions of the maximum take-off weight. This can be mathematically expressed by the following equation (found in **Küchemann 1993** and adopted by **Greener By Design 2003**, **Greener By Design 2005**, **Green 2006** and **Nangia 2006**).

$$W_E = c_1 W_{MTO} + (c_2 - 1) W_P \quad , \tag{2.14}$$

where W_{MTO} is the maximum take-off weight, c_1 is a factor accounting for weights driven by W_{MTO} and (c_2-1) is a factor accounting for weights driven by the payload.

As Eqs. (2.14) and (2.9) show, take-off weight and empty weight are interdependent. Consequently, there is a snowball effect. Weight saved on any particular component will also decrease wing, empennage, engine and undercarriage weight, i.e. the variable c_1. As W_{MTO} is further a function of fuel weight, all methods that reduce fuel burn will also decrease c_1. The changes in maximum take-off weight allow wings, the empennage and engines to be resized. Wetted area and associated drag decreases, which again reduces fuel burn etc. However, the changes will get infinitesimally small at one point and the process comes to end. Payload-driven weights, represented by the variable c_2, can be assumed to be not affected (**Greener By Design 2005**, **Green 2006**).

2.3 Chapter Summary

In this chapter, the consequences of aviation carbon dioxide emission have been qualitatively assessed. It has been shown that limiting CO_2 emission is not only important to mitigate air traffic's impact on climate change, but also to keep airline direct operating cost low. It has further been found that the mass of CO_2 emitted from aircraft engines depends on the fuel used and the mass of fuel burned. As a consequence, technological key variables have been identified that set fuel consumption and thus CO_2 emission of aircraft. For a given payload and range, these variables define the aircraft's CO_2 efficiency in terms of aerodynamic efficiency, engine efficiency, empty weight and fuel used. The variables thereby further define major research disciplines (i.e. fields of interest) into CO_2 reducing aircraft technologies. In the following chapter, the possible impact of the variables on aircraft fuel burn and CO_2 emission is quantified through a parametric study.

3 Parametric Study

This chapter analyses the general impact of the previously introduced variables on aircraft fuel consumption and CO_2 emission. First, a method is set up that allows to estimate block fuel burn and hence CO_2 production on basis of the aforementioned variables. Second, two reference aircraft from the *Eurocontrol Base of Aircraft Data* (BADA) aircraft performance database are chosen. One is representative of a modern short-haul narrow-body aircraft, the other of a modern long-haul wide-body aircraft. Third, based on performance data given in BADA, variables and block fuel burn for the reference aircraft is determined. Fourth, fuel burn of improved/worsen aircraft is estimated by modifying each parameter in turn. Snowball effects are simulated using a simplified iterative approach.

3.1 Estimating Fuel Burn and CO_2 Emissions

As **Torenbeek 1997** depicts, "accurate calculations of the fuel load required for various flight segments can only be done when sufficiently detailed data are available in the form of drag polars, engine thrust and fuel flow diagrams, design weights, etc". Unfortunately, when estimating fuel consumption of future aircraft, such detailed information is not available. A simplified approach to estimate the fuel efficiency quite accurately is needed. This problem is quite similar to the difficulties encountered when predicting fuel loads in preliminary aircraft design. The calculations presented in the following sub-subchapters are hence primarily used in this field of knowledge. The following approach to estimating fuel consumption is mainly based on the assumptions and methods found in **Torenbeek 1997**, **Roskam 2002**, **Greener By Design 2003** and **Greener By Design 2005**.

According to Fig. 2.5, mission fuel is the fuel burned in the segments (3) to (6), i.e. when the aircraft is in the air. Fig. 3.1 shows recordings of altitude (red), Mach number (blue) and fuel flow (magenta) over distance for a long-range mission. It is seen that fuel flow is highest at take-off (3) with the engines running at full thrust. The aircraft is then in the climb segment (4) for approximately 300 km. With increasing altitude and lower engine throttle, fuel flow reduces. The bulk of fuel is clearly burned in segment (5), which is the cruise flight. One can clearly observe that the ever-decreasing aircraft weight continuously reduces required thrust and thereby fuel flow in cruise. Thrust requirements for descent (6) are low and hence the engines consume only small amounts of fuel. Finally, a short rise in fuel flow occurs as thrust is increased for landing.

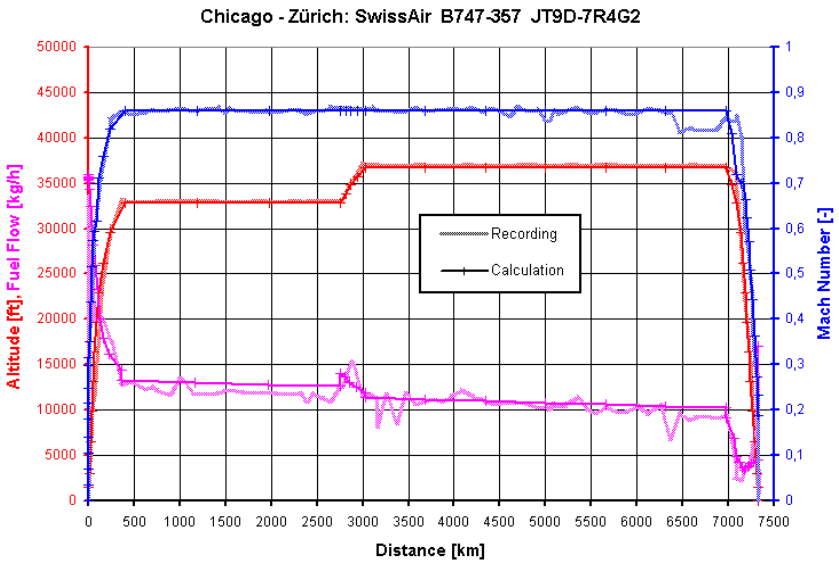

Fig. 3.1 Comparison of Calculated and Recorded Fuel Flow on a Long-Range Mission (**Plohr 2009**)

As observable from Fig. 3.1, a long-range flight mission can be split into one fuel intensive phase, the cruise, and several fuel un-intensive phases, e.g. climb and descent. If detailed data are not available, it is therefore acceptable for medium and long-range flights to estimate the mission fuel weight on the basis of primarily the cruise fuel requirements. Hence, the amount of fuel required for a 'hypothetical cruising flight' **Torenbeek 1997** over the complete mission range is calculated first. Further allowances for the fuel un-intensive flight segments are then added afterwards.

3.1.1 Estimation of Cruise Fuel

For a given aircraft and fuel, the ratio of empty weight to payload and the calorific value of the fuel is fixed. Cruise fuel consumption, according to Eq.(2.10), is then minimized by maximising the parameter $\eta \cdot L/D$. As both parameters are functions of the flight speed V, the expression will become maximal for one certain flight speed V and a certain corresponding L/D.[1] For maximum range – i.e. minimum fuel consumption – this speed and lift-to-drag ratio is to be maintained for the entire cruise flight. Maintaining the L/D is possible if the aircraft is allowed to climb continuously during cruise. To determine cruise fuel load for this special case, Eq.(2.10) is applicable.

[1] Maximum L/D is reached for the lift coefficient that results in the minimum drag, i.e. $C_{L,md}$. For a given aircraft weight, maximum L/D implies a certain cruising speed, which is generally called V_{md}, minimum drag speed. However, as for jet aircraft, the over-all engine efficiency η is a function of the flight speed as well (reconsider Eq.(2.5)), the expression $\eta \cdot L/D$ becomes maximal for a $V \neq V_{md}$ and an $L/D \neq (L/D)_{max}$ (**Scholz 1999**).

For the most cases, operational and safety issues make it impossible to control the flight so that both, *L/D* and speed, are constant. If ATC regulations relegate the aircraft to a constant altitude, it is possible to maintain either the flight speed or the lift-to-drag ratio. For the latter option, flight speed needs to be reduced during cruise. This cruise technique yields a good range and fuel consumption, but increases the total flight time (**Torenbeek 1997**). As long as airlines aim at minimizing flight times, it is therefore unlikely to be implemented. Contrary, the other option, a horizontal cruise with constant Mach number and variable *L/D* is a common cruise technique for civil aviation. For shorter ranges and the case that the initial cruise lift-to-drag ratio is near $(L/D)_{max}$, the fuel consumption is then only slightly higher than for the cruise/climb (**Torenbeek 1997**). However, the longer altitude and speed are maintained, the further cruise *L/D*s shift of this optimum. The latter is the reason why on long-range flights, pilots may get permission to change altitudes stepwise (as observable in Fig. 3.1) and thereby change to *L/D*s that are more favourable.

For the purpose of this paper, a refined version of the standard Breguet range equations, developed by **Torenbeek 1997**, will be used to estimate fuel burn in cruise. It features a 'cruise control factor k_R' that allows covering all practical cruise procedures. Cruise fuel load is then given as

$$W_{F,cr} = W_{Cr,i} \cdot \frac{R/(H/g)}{\eta_i \cdot (L/D)_i + 0.5 k_R \cdot R/(H/g)} \quad , \tag{3.1}$$

where the index *i* denotes for *initial cruise condition*. The cruise control factor for cruise/climb is typically

$$k_R = 1 + \frac{R/(H/g)}{6 \cdot \eta_i (L/D)_i} \quad . \tag{3.2}$$

For a horizontal cruise with constant Mach number, the fuel consumption is higher and k_R will be less than 1.0. If the ratio of initial lift coefficient to minimum drag lift coefficient $y = C_{L,i}/C_{L,md}$ is known, k_R can be determined from

$$k_R = \left(1 - \frac{R/(H/g)}{6 \cdot \eta_i (L/D)_i}\right) \frac{2y^2}{1+y^2} \quad . \tag{3.3}$$

For a step/climb procedure, k_R will be in between the value of the cruise/climb and the horizontal cruise flight, the value $k_R = 1$ "will usually be adequate" **Torenbeek 1997,** p. 316.

3.1.2 Estimation of 'Lost Fuel'

The over-all fuel consumption of a civil transport aircraft on a regular mission can be split into 'useful fuel' that actively transports the aircraft over the mission range and 'lost fuel' that is burned additionally. Following the approach of **Torenbeek 1997**, fuel burned for anything else than cruise is referred to as lost fuel. Fuel is then 'lost' for

- Pre-flight ground operations, i.e. engine start, warm-up and taxiing
- Accelerating the aircraft to cruise speed, i.e. take-off and acceleration during climb
- Lifting the aircraft to cruise altitude, i.e. climb
- En-route manoeuvring and
- Post-flight ground operations, i.e. landing taxi and shut-down

In preliminary aircraft design, the fuel fractions for these segments are often approximated from historical/statistical values. They are mostly given as mission weight/mass fractions W_f/W_i, where the index f denotes for final, the index i for initial aircraft weight (see e.g. **Roskam 2002** and **Raymer 1992**). Different assumptions found in literature concerning mission fuel fractions were assessed and the most realistic one for each mission phase was adopted. The process is documented in Appendix A.1. The methods/fractions finally used are given below. For the purpose of the parametric study at hand, semi-empirical methods rather than fixed mission weight fractions seem to be more suitable for the in-flight segments. These can be found in **Torenbeek 1997**. They take account of major changes in the mission profile and aircraft efficiency and therefore agree with the basic idea of a parametric study, where improved/worsen efficiencies need to be analyzed.

Engine Start and Warm-Up, Pre-Flight Taxiing

The weight fractions are calculated from information on typical taxi-fuel given in the ground handling manuals for the Airbus A320 (**Airbus 2007a**) and the Boeing 777 (**Boeing 2007b**). The typical mission weight fraction for the A320 (0.967) is considered as being representative for short-haul narrow-body aircraft, the typical mission weight fraction calculated for the B777 (0.98) is considered as being representative for long-haul wide-body aircraft.

Take-Off and Climb to Cruise Altitude

Fuel for take-off and climb to cruise altitude is calculated in two steps. First, a cruising flight over the climbing distance is assumed. Second, the additional fuel weight for accelerating the

aircraft to cruise speed and lifting it to cruise altitude is calculated from a semi-empirical formula that is found from an energy balance in **Torenbeek 1997** and an estimation of over-all engine efficiency during climb from **Greener By Design 2003**,

$$\Delta W_F = W_{TO} \frac{\left(h_{Cr} + \frac{v_{Cr}^2}{2g} \right)}{0.21\left(H/g \right)} \quad , \tag{3.4}$$

where ΔW_F is the fuel consumed, h_{Cr} the initial cruise altitude and v_{Cr} the initial cruise speed. For example, the lost fuel for accelerating and lifting a kerosene-powered (H = 43 MJ·kg^{-1}) turbofan to an initial cruise altitude of 35 000 ft (10 668 m) and accelerating it to 0.84 Ma would then calculate to 1.5 % of take-off weight.

En-Route Manoeuvring

To account for the additional fuel burn from en-route manoeuvring, a semi-empirical formula from **Torenbeek 1997** is adopted:

$$\Delta W_F = W_{TO} \frac{0.0025}{\eta_{Cr}} \quad , \tag{3.5}$$

where η_{Cr} is the over-all engine efficiency for cruise. For modern turbofans with cruise efficiencies around 35 to 40 %, the additional fuel for manoeuvring is then around 0.71 to 0.63 % W_{TO}.

Descent

A cruising flight over the descent distance (as proposed by **Torenbeek 1997**) seems tolerable for current aircraft and ATC regulations and is assumed for the following parametric calculations.

Post-Flight Ground Operations

In agreement with the considerations for pre-take-off fuel weight further above, a fuel weight of 0.33 % W_{TO} for narrow-bodies and of 0.2 % W_{TO} for wide-bodies will be applied for

landing-taxi. This is admissible as taxi fuel flow (idle) for a given engine is independent of aircraft weight according to **ICAO 2009a**. Hence, assuming a similar taxiing time, landing-taxi fuel and pre-flight-taxi fuel will be nearly identical. It should be noted that fuel for landing-taxi is typically taken from the reserves and will not be separately added to the calculations of the take-off fuel weight fraction.

3.1.3 Estimation of Mission and Block Fuel

Mission fuel is the fuel burned from take-off to touch-down. Combining the findings from the sections further above, mission fuel can be calculated from

$$W_{F,m} = W_{F,Lift\&Accelerate} + W_{F,Manoeuvre} + W_{F,Cr} \quad \text{, i.e.} \tag{3.6}$$

$$W_{F,m} = W_{TO}\left[\frac{\left(h_{Cr} + \frac{v_{Cr}^2}{2g}\right)}{\eta_{Climb}\left(H/g\right)} + \frac{0.0025}{\eta_{Cr}} + \frac{R/\left(H/g\right)}{\eta_i\left(L/D\right)_i + 0.5k_R \cdot R/\left(H/g\right)}\right] \quad . \tag{3.7}$$

For a given aircraft, fuel, cruise altitude and cruise speed, the first and second term – accounting for the *lost fuel* – are constant. If we write LF_m for the mission lost fuel fraction, Eq.(3.7) can be simplified to give

$$W_{F,m} = W_{TO} \cdot \left[LF_m + \frac{R/\left(H/g\right)}{\eta_i\left(L/D\right)_i + 0.5k_R \cdot R/\left(H/g\right)}\right] \quad . \tag{3.8}$$

It becomes clear that for a fixed flight altitude, lost fuel is independent of range. In this case, its impact on over-all mission fuel is inversely proportional to mission range.

To assess the block fuel of an aircraft, aircraft movement on ground and engine warm-up need to be taken into account. As the distance covered is rather small, mission range is unaffected. With LF_G being the lost fuel fraction for ground movements, block fuel then calculates to

$$W_{F,b} = W_{F,Pre\text{-}flight} + W_{F,m} + W_{F,Post-Flight} \quad \text{, i.e.} \tag{3.9}$$

$$W_{F,b} = W_{TO} \cdot \left[LF_G + LF_m + \frac{R/\left(H/g\right)}{\eta_i \cdot \left(L/D\right)_i + 0.5 \cdot k_R \cdot R/\left(H/g\right)}\right] \quad , \tag{3.10}$$

where LF_G is 0.0066 for narrow-bodied and 0.004 for wide-bodied aircraft.

3.1.4 Estimation of Reserve Fuel

For safety reasons, the aircraft needs to carry extra fuel reserves to account for holding flights, flights to alternate airports etc. On an ideal mission as shown in Fig. 2.5, only fuel taken for landing taxi is taken from the reserves **Torenbeek 1997** and the bulk of reserve fuel remains unburned. In the real world however, a considerably larger part is consumed due to holding patterns being common especially at busy airports. Moreover, transporting fuel reserves increases aircraft take-off weight, and thereby required thrust and fuel consumption. Hence, for the estimation of block fuel burn and CO_2 emissions, reserve fuel loads should be considered at least when calculating aircraft all-up weight.

Required reserve fuel weights are imposed by regulation authorities. For the purpose of the parametric study, European rules to calculate reserve fuels are adopted.[1] These are defined by the Association of European Airlines (AEA) as: 5% of the mission fuel for contingency reserve; a diversion flight over 370 km for short- and medium-range aircraft, or a diversion flight over 463 km for long range aircraft; and after this, a 30 min holding flight at 1500 ft (457 m) altitude.

Diversion fuel can be calculated simply from a cruise flight over the diversion distance. For the rather short distance we can assume a constant cruise/climb, i.e.

$$W_{F,Div} = W_{Cr,f}\left[1-\exp\left(-\frac{R_{Div}}{\left(L/D\right)_{Div}\eta_{Div}\,H/g}\right)\right] \quad , \tag{3.11}$$

where the index *div* denotes for diversion flight. It is important to notice that for the most cases, *L/D* and η for diversion will be less than for a regular cruise flight. This is due to diversion flights mostly being operated at considerably lower altitudes (and hence at lower speeds). An altitude of 10 000 ft (3048 m) will be implemented for our study. The speed for determining η_{div} will be taken as 250 knots (128.6 m·s^{-1}), which is the maximum allowable speed at that altitude.

---

[1] For US Airlines, the reserve fuel is set in the Federal Aviation Regulations (FAR) Part 121. The exact definitions differ for domestic and international flights (including ETOPS). For domestic flights, typical reserves are 130 nm (241 km) diversion and 30 min holding at 1 500 ft (457 m) (**Torenbeek 1997**). International flights require extra reserve fuel for an extension of the cruise flight that lasts for 10 % of the total time required for the regular mission. Further, the diversion flight is longer. The aircraft needs to be able "to fly to the most distant airport specified in the flight release". If no alternate airport is specified, the cruise flight is to be extended by two hours (**FAA 2009**).

Fuel for the holding flight is calculated using a formula for maximum endurance taken from **Gollnick 2008**,

$$W_{F,Hold} = W_{Div,f}\left[1-\exp\left(-\frac{t_{Hold}v_{Hold}}{(L/D)_{\max}\,\eta_{Hold}\,H/g}\right)\right] \quad , \tag{3.12}$$

where t_{Hold} and v_{Hold} are the duration and speed of the holding flight. $(L/D)_{\max}$ is calculated from

$$(L/D)_{max} = \sqrt{\frac{\pi e b^2}{4C_{D0}S}} \quad , \tag{3.13}$$

where e is the Oswald factor, b is the wing span, C_{D0} is the drag at zero lift and S is the wing reference area. Finally, contingency reserves are simply taken as 5% of the mission fuel calculated from Eq. (3.7).

3.1.5 Estimation of CO_2 Emissions

The amount of CO_2 emitted from aircraft jet engines is a function of the specific CO_2 production of the fuel – i.e. the mass of CO_2 emitted per kg of fuel burned – and the total amount of fuel burned. Hence,

$$W_{CO_2} = SCE \cdot W_F \quad , \tag{3.14}$$

where *SCE* is the specific carbon dioxide emission of the fuel. Thus, reasonably accurate estimations of the CO_2 emitted in different flight segments are possible by simply multiplying mission segment fuel with the fuel's *SCE*. For example, for kerosene, *SCE* is 3.15 and block CO_2 emissions can be estimated using following expression.

$$W_{CO_2,b} = 3.15 \cdot W_{F,b} \tag{3.15}$$

3.2 Reference Aircraft

As shown above, aircraft fuel burn and CO_2 emission can be estimated on the basis of different variables that define the mission and the efficiency of the aircraft aerodynamics, engines, empty weight and fuel. The impact on fuel efficiency of variations in a single parameter is measureable only in the context of the airplane entity, i.e. if the remaining parameters are known. It is thus necessary to find an adequate set of parameters that serves as basis for variations. The combined set defines the reference fuel burn and thereby represents a specific aircraft, i.e. the reference aircraft. Concerning future improvements, it increases the informative value of the study if reference parameters are not chosen randomly, but correspond to the technological performance of today's state-of-the-art aircraft. Hence, for the parametric study at hand, performance data of real existing is used. Reference parameters are conducted from the *Eurocontrol Base of Aircraft Data* (BADA) aircraft performance database.

3.2.1 Selected Reference Aircraft

The impact of technologies on fuel and CO_2 efficiency is different for aircraft of different size, payload and design mission length. For the mission length, this is mainly due to W_F/W_{TO} being considerably larger for long-range aircraft. Thus, a similar percentage change in fuel weight on both aircraft generates a larger percentage change in maximum take-off weight on the long-range aircraft. Further, as many of the large aircraft components are functions of W_{MTO}, snowball effects from changes in fuel weight affect the empty weight of a long-range aircraft more significantly. It is thus assumed that the result is a higher benefit from technological improvements for long-range aircraft.

To verify above thesis, it was decided to perform parametric analyses on two real existing aircraft models that were designed for different stage lengths. The Airbus A320-212 (Option 2) aircraft is selected to represent medium-range narrow-body aircraft. The reference for long-range wide-body aircraft is the Boeing 777-200ER. "Option 2" and "ER" refer to extended range options. The design range for the A320 is 3045 nm (5640 km). For the B777-200ER, two further range-options are available. The one, which serves as reference in the study at hand, is the higher take-off weight option and features a design range of 7380 nm (13 668 km). Both aircraft are among the best sold and most flown in their corresponding seat and range category. On the 20th of November 2008, 1884 Airbus A320 and 401 B777-200ER were in service (**MRO Prospector 2008b**). A summary of basic information on both aircraft, reproduced from **Jenkinson 2005** and **Jane's 2009**, is given in Table 3.1. Fig. 3.2 shows computer renderings of the two aircraft.

Fig. 3.2 Renderings of the Reference Aircraft Airbus A320 (left) and Boeing 777 (right) (**Airbus 2009c**, **Boeing 2009b**)

Table 3.1 Basic Information on the Reference Aircraft (reproduced from **Jane's 2009** and **Jenkinson 2005**)

Aircraft	**A320-212 Option 2**	**B777-200ER**
Configuration	Classic Cantilever, Backward Swept Wing, Positive Dihedral, Circular Cross Section	Classic Cantilever, Backward Swept Wing, Positive Dihedral, Circular Cross Section
Classification	Short- to Medium-Range, Single-Aisle Narrow-Body	Long-Range, Twin-Aisle Wide-Body
Certification	November 8th 1988	January 17th 1997
Power Plant	2x CFM-56/5A3	2x P&W 4090, RR Trent 895, GE 90-94B
Engine Classification	Wing-Mounted, 6.0 BPR	Wing-Mounted, 5.7-6.4 BPR (P&W 4090, Trent 895), 9.0 BPR (GE 90)
Passenger Capacity (Typical)	150 (Two Class)	310 (Three Class)
Design Payload	14 250 kg	29 450 kg
Design Range	5640 km	13 668 km
Cruise Mach Number	0.78	0.84
Maximum Take-Off Weight	77 000 kg	287 000 kg

3.2.2 Reference Fuel Burn and Efficiency Parameters

For the calculation of fuel burn and CO_2 emission of the reference aircraft, required parameters of aerodynamic and engine efficiency are calculated from aircraft performance data files given in BADA (**Eurocontrol 2004a**). The build-up of the files, selected parameters and intermediate calculations are described in Appendix A.2.

It is assumed that the aircraft are flying a mission identical to their design specification, i.e. R = design range, W_P = design payload. Further, both aircraft start their cruising flight at an initial altitude of 35000 ft (10668 m). The "lost fuel" for lifting the aircraft to cruise altitude and accelerating the aircraft to cruise speed is then calculated from Eq.(3.4). The initial cruise weight (and subsequently initial L/D) can be determined by subtracting this fuel weight from the maximum take-off weight. Efficiency parameters of the reference aircraft at the beginning of the cruise flight are listed in Table 3.2.

Calculated fuel weights are shown in Table 3.3. Shown are results for three different calculations, i.e. cruise techniques: assuming first, a constant climb during cruise (cruise-climb), second, a cruise with several, but discrete altitude changes (step-climb) and third, a cruise at constant altitude and constant Mach number (decreasing L/D). These are computed using Eqs.(3.7) and (3.10) and different cruise control factors as proposed by **Torenbeek 1997**, see chapter 3.1.1.

Table 3.2 Efficiency Parameters of the Reference Aircraft on a Mission according to Design Specifications (Aircraft data from **Eurocontrol 2004a**, Fuel Data from **Ruijgrok 2005**)

Parameter		**A320-212 Option 2**	**B777-200ER**
W_{MTO}	[kg]	77 000	287 000
Initial Cruise Altitude	[m]	35 000	35 000
Cruise Mach	[-]	0.78	0.84
Design Payload	[kg]	14 250	29 450
Design Range	[km]	5640	13 668
Aerodynamics[1]			
Wing Area S	[m^2]	122.6	427.8
Wing Span b	[m]	34.1	60.9
C_{d0}	[-]	0.024	0.0185
k-Factor	[-]	0.0375	0.0425
Oswald Factor e	[-]	0.895	0.8639
L/D_{max}	[-]	16.667	17.832
$L/D_{initial}$	[-]	15.988	17.546
Engine			
$TSFC_{Cr}$	[kg·min^{-1}·kN^{-1}]	1.0009	0.8568
η_{Cr}	[-]	0.3223	0.4055
Fuel			
H	[MJ·kg^{-1}]	43.0	43.0
SCE	[-]	3.15	3.15

[1] Valid for a cruise (clean) wing configuration.

Table 3.3 Fuel Weights of the Reference Aircraft for different Cruise-Techniques (calculated)

Mission Section		A320-212 Option 2	B777-200ER
Lost Fuel			
Lift& Accelerate	[kg]	1117	4305
Manoeuvre	[kg]	600.6	1779
Ground	[kg]	513.0	1148
Cruise Fuel			
Cruise-Climb	[kg]	17 060	101 841
Step-Climb	[kg]	17 139	103 178
Horizontal, Const. Mach	[kg]	17 756	107 797
Mission Fuel			
Cruise-Climb	[kg]	18 778	107 925
Step-Climb	[kg]	18 857	109 259
Horizontal, Const. Mach	[kg]	19 474	113 878
Block Fuel			
Cruise/Climb	[kg]	19 291	109 069
Step/Climb	[kg]	19 370	110 407
Horizontal, Const. Mach	[kg]	19 987	115 026
Specific Seat Info			
Specific Seat Fuel	[l/100km]	≈ 2.94	≈ 3.36
Specific Seat CO_2	[kg/100km]	≈ 7.40	≈ 8.47

As observable from Table 3.3, fuel weights for the different flight techniques differ considerably only for long distances (777-200ER). Concerning the parametric calculations below, it is assumed that the aircraft is allowed to climb continuously during cruise, i.e. to perform a cruise-climb procedure. This allows keeping cruise Mach number, engine efficiency η_{Cr} and aerodynamic efficiency L/D constant during the entire cruise flight. It is believed that trends in efficiency improvements are similar for all cruise techniques.

3.2.3 Reference Empty Weight

Table 3.2 shows efficiency parameters of the reference aircraft. In the following subchapter 3.3, these parameters – namely the zero-lift drag coefficient, the wing span, the Oswald factor, the over-all propulsive efficiency, the heat content of the fuel and the specific CO_2 emission – are to be varied separately and the impact on fuel consumption and CO_2 emission to be measured. To calculate variations in the aircraft empty weight and to make calculations possible that take into account snowball effects, it is important to calculate some further reference values. These are the reserve fuel weight, the aircraft empty weight and the factors c_1 and c_2. The two latter ones will help to divide empty weight into two parts. First, a weight fraction that is influenced by the new total fuel weight, i.e. component weights that change with maximum take-off weight, and second, a weight fraction that is mainly dependent on the payload. In the following, components belonging to the first group – i.e. the wing, the

engines, the undercarriage etc. – will be referred to as c_1-components. Accordingly, components of the second group are named c_2-components.

Reserve fuel weight is calculated according to European (AEA) specifications, as defined in sub-subchapter 3.1.4. The range for the diversion flight is taken as 370 km for the A320 and related parametric variations, and as 463 km for the B777-200ER and related parametric variations. $(L/D)_{Div}$ and η_{Div} are calculated similar to the aerodynamic and engine efficiencies for the cruising flight (see Appendix A.2). However aircraft weight is calculated for the end of the cruise flight ($W_{TO} - W_{F,m}$), ρ_{Div} is the density at 10 000 ft (3048 m) and v_{Div} is 250 knots (128.6 m·s^{-1}). For the calculation of the holding flight, the cruise correction factor (for the computation of *TSFC*) is dropped and flight speed taken as 250 knots. Finally, we add 5% of $W_{F,m}$ as contingency reserve fuel. It is then possible to calculate expected empty weight from

$$W_E = W_{MTO} - W_P - W_{F,m} - W_{F,Reserves} \quad . \tag{3.16}$$

The empty weight fraction that is directly related to payload is expected to be a function of the design range. [1] **Green 2006** suggests the following relationship.

$$c_2 = 1 + \frac{2}{1 + \exp\left[-0.693\left(\frac{R}{3000} - 1\right)\right]} \quad , \tag{3.17}$$

which yields in a value of 2.3 for the design range of the A320 and 2.84 for the design range of the 777-200ER. c_2 is related to payload and empty weight as defined in chapter 2.2.2. Accordingly, if c_2 is known, c_1 can be calculated from

$$c_1 = 1 - \left(c_2 \cdot \frac{W_P}{W_{MTO}}\right) - \left(\frac{W_{F,Total}}{W_{MTO}}\right) \quad , \tag{3.18}$$

where $W_{F,Total}$ is the total transported fuel weight, i.e. $W_{F,m} + W_{F,Reserves}$. For a better understanding, the definitions of c_1 and c_2 are given below.

---

[1] Green 2003,2006 and **Nangia 2006** concentrated on finding a representative value for the factor c_2. A constant value of c_2 (as proposed by **Küchemann 1993**) does not seem to represent modern aircraft very well. Analyzing real aircraft data (**Nangia 2006**), c_2 seems to be rather a function of the aircraft's design range. The reason for c_2 to change with range is a difference in the ratio of design payload to maximum payload for short and long-range aircraft. According to real aircraft data given in **Nangia 2006**, this ratio is approximately 0.8 for design ranges around 3000 km and approximately 0.5 for design ranges around 9000 km. As c_2-component weights are driven by the maximum payload, but are defined by the design payload – i.e. Eq.(3.19) –, c_2 is ultimately larger for lower ratios (longer ranges).

$$c_2 \overset{def}{=} \frac{\left(W_P + \Delta W_{E,Payload-Driven}\right)}{W_P} \tag{3.19}$$

$$c_1 \overset{def}{=} \frac{\Delta W_{E,MTO-Driven}}{W_{MTO}} \tag{3.20}$$

It now becomes clear that for a constant design range and payload, both fractions remain constant. If the take-off weight changes, the weights of the c_1-components have to change concomitantly. Payload-driven c_2-component weights will only change if their specific weight changes and not due to snowballs.

Calculated reserve fuel, empty weight, c_1 and c_2 for the two reference aircraft for the assumption of a cruise-climb are presented in Table 3.4 below. For comparison and validity of the selected approach, the real aircraft empty weight and design fuel (total fuel) weight, reproduced from BADA (**Eurocontrol 2004a**) and **Jenkinson 2005** are also given. It is seen that calculated total fuel weight and empty weight are close to the values given in literature.

Table 3.4 Empty Weight, c_1 and c_2 of the Reference Aircraft (Calculated vs. Literature)

Parameter		**A320-212 Option 2**	**B777-200ER**
As calculated from Eqs. in Chapter 3.1 and Aircraft Efficiencies according to Eurocontrol 2004a			
Reserve Fuel Weight	[kg]	3597	12 529
Total Fuel Weight (Cruise-Climb)	[kg]	22 328	120 451
Empty Weight	[kg]	40 422	137 099
c_1	[-]	0.2851	0.2886
c_2	[-]	2.2958	2.8432
$\Delta W_{E,MTO-Driven}$	[kg]	21 957	82 828
$\Delta W_{E,Payload-Driven}$	[kg]	18 465	54 282
As calculated from Actual Total Fuel Weight and Actual Aircraft Fuel Weight			
Total Fuel Weight (**Jenkinson 2005**)	[kg]	23 750	119 327
Empty Weight (**Eurocontrol 2004a**)	[kg]	39 000	138 100
c_1	[-]	0.2667	0.2920
c_2	[-]	2.2958	2.8432
$\Delta W_{E,MTO-Driven}$	[kg]	20 535	83 818
$\Delta W_{E,Payload-Driven}$	[kg]	18 465	54 282

3.3 Methodology to Calculate Parametric Influence

In this subchapter, pre-calculated efficiency parameters of the reference aircraft are modified, each one in turn, to measure their possible theoretical influence on fuel burn and CO_2 emission. The aim is the production of results that show theoretical qualitative trends, which can be used to understand the general relations. This aim is reached by producing quantitative results for the fuel consumption, which are then compared to the reference aircraft. However, the quantitative results are not claimed to be more than reasonable trends. It is important to realize that the study at hand is based on a simple parametric variation of reference constants (the simplifications are listed in this chapter further below). In the real world however, the design of a new aircraft is a highly complex matter. To produce accurate quantitative estimations, much more detailed and time-intensive aircraft design tools are to be used. However, the results are then accurate for one design and aircraft only. The informative value for other aircraft, even if similar in range and payload, would still only be of qualitative nature: in the form of trends. The simple parametric variation is therefore regarded as being adequate for the purpose of this thesis.

For the following study, efficiencies of the two reference aircraft are varied and fuel consumption and CO_2 emission of the improved/worsen aircraft are determined. The design parameters range, payload, cruise speed and initial cruise altitude are held constant. For each variation, four different results are produced:

1. **No snowball effects:** The size, weight and drag of all components that are not directly affected remain constant. Hence, empty weight of the new aircraft is identical to the empty weight of the reference aircraft, and so is the drag polar. As the take-off weight reduces due to a reduced fuel consumption, C_L decreases. These results are not representative of a new aircraft design. However, they show the possible impact of technologies if implemented as a retrofitting. Further, the amplifying effect of snowballs is easier to observe.
2. **Snowball effects on c_1-components:** The weights of W_{MTO}-driven components change proportional to the take-off weight. It is assumed that the weight fraction c_1 remains constant. Thus, empty weight is reduced. However, even the weight of components change, their size and the drag polar are assumed to remain unaffected. Similar to case one, C_L decreases due to a reduced take-off weight and a constant initial cruise altitude.
3. **Snowball effects on c_1-components and the drag polar, constant aspect ratio:** The weights of c_1-components change proportional to the take-off weight, see case two. Further, wing area changes with take-off weight. For this calculation, wing loading and aspect ratio are held constant. Hence, the influence of C_L on aircraft drag (the k-factor, see Eq.(3.17)) is unaffected. However, as the wing area decreases, the ratio of wetted area to wing area is enlarged. This is due to the area of the fuselage being payload-driven and thus constant. According to Eq.(4.1), this will increase the zero-lift drag coefficient C_{D0}. To account for this snowball effect, an assumption of **Greener By**

Design 2003, p. 81 is adopted: C_{D0} of the reference aircraft is "... divided equally between the profile drags of the wing, fuselage and a group containing the empennage, nacelle and other components ...". The wetted areas of the c_1-components, i.e. the wing and the group containing the empennage, nacelle, etc., change with wing area and do not affect C_{D0}. The increase in the profile drag coefficient of the fuselage is inversely proportional to the change in wing area, i.e.

$$C_{D0} \sim \frac{1}{S} \sim \frac{1}{W_{MTO}} \quad . \tag{3.21}$$

For a constant wing loading, the new aircraft's C_{D0} becomes

$$C_{D0,new} = \frac{2}{3} C_{D0,ref} + \frac{1}{3} C_{D0,ref} \cdot \frac{1}{\left(\frac{W_{MTO,new}}{W_{MTO,ref}} \right)} \quad , \tag{3.22}$$

where the first summand accounts for the profile drags of the wing and the "group of other components" and the second summand accounts for the drag of the fuselage. The index *new* denotes for the new aircraft, the index *ref* for the reference aircraft.

4. **Snowball effects on c_1-components and the drag polar, constant wing span:** Most of the assumptions for these calculations are identical to the ones introduced for the third case. However, instead of assuming a constant aspect ratio wing, the wing span is held constant. Thus, the *k*-factor will change and influence the lift-dependent part of the drag polar.

The calculations for all cases follow the calculation scheme introduced in subchapter 3.2. For the first and second case calculations, wing area is constant and the lift coefficient for the initial cruise condition is determined from $W_{Cr,i}$, which in turn is a function of the new take-off weight. The new take-off weight is however an output-value of the calculations. *L*/*D*, fuel weight and take-off weight are therefore computed inside an iterative loop. This is also necessary for all calculations of the third and fourth case: C_{D0} and W_{MTO} are interrelated (see Eq.(3.22)). Wing loading for case three and four is held constant. It then results from Eq.(3.18) that $C_{L,i}$ is identical with the initial lift coefficient of the reference aircraft. For demonstration, Fig. 3.3 shows a schematic of how W_{MTO} for the different cases is estimated for a change in engine efficiency.

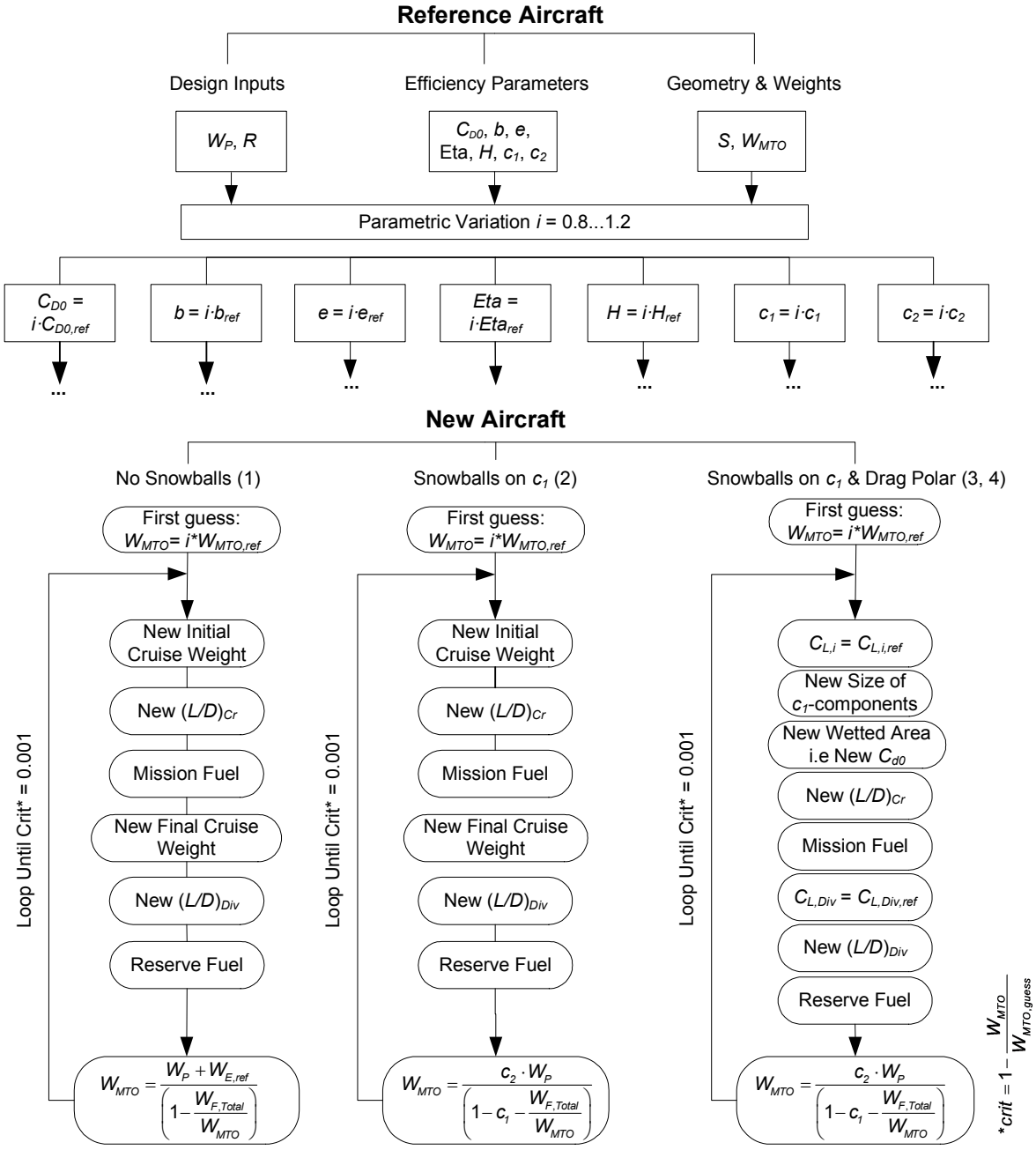

Fig. 3.3 Schematic for the Iterative Computation of New Maximum Take-Off Weight

3.3.1 Restrictions and Simplifications of the Model

It is necessary to always bear in mind that the calculations are based on simple variations of reference values. Thus, in general, it is possible to represent aircraft that are very "similar" to the reference. Fig. 3.4 shows a visualization of how a new aircraft would look like for the assumptions made. For the cases one (1) and two (2), take-off weight decreases without influencing the size of the components: the outer appearance of the aircraft is identical with

the reference. This is different for the third and fourth case calculations where c_1-components shrink with decreasing weight, while c_2-components (i.e. the fuselage) stay constant in size.

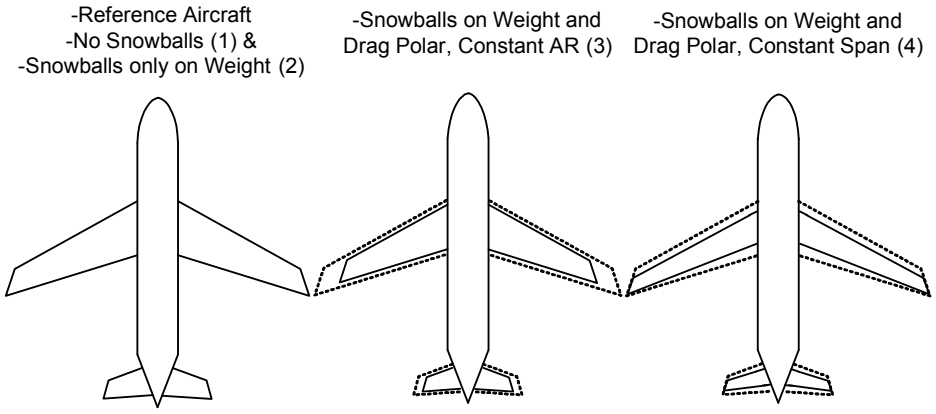

Fig. 3.4 Visualization of the Assumptions Concerning Wing and Fuselage Areas

From Fig. 3.4 it becomes evident what the restrictions and simplifications of the model are:

- The study represents only classic cantilever aircraft: Radical new aircraft configurations such as the Blended Wing Body (BWB) or the Truss-Braced Wing (TBW) aircraft cannot be simulated by a variation of the chosen parameters, as the lift distributions and drag polars are not similar to the classic cantilever aircraft.
- The model can represent the benefits of new technologies only as an improvement in one of the chosen parameters. If real existing technologies are to be connected with the variations shown, it is important to bear in mind that in the real world, many technologies entail changes in the over-all aircraft design. For example, the application of laminar flow technologies generally requires a reduction of the wing sweep or even forward-swept wings. However, a change in sweep angle is not considered for this study. Similarly, most experts believe the mounting of un-ducted or open rotor fans to the wings to be unrealizable. Most open rotor concepts therefore use tail-mounted engines. Further, the cruise Mach would have to be decreased for open-rotor application. Both aspects, a change to rear-mounted engines and a reduction of the cruise Mach number are not simulated. In summary, to accurately calculate pros and cons of a single new technology, a more detailed analysis/aircraft design study would be needed.
- The study presumes that the size and weight of all aircraft components can be assigned clearly to either a group being influenced by the payload or a group being driven by the maximum take-off weight. It is probable that for the case of a real aircraft such a simple split is not as easily achieved. Moreover, there is a multitude of additional variables influencing the size and weight of aircraft components.
- The parametric variation for the case of no snowball effects (case one) represents a rather conservative approach: With constant initial cruise altitude, the initial lift coefficient is decreasing with take-off weight. Theoretically, a higher C_{Li} could be

maintained if the initial cruise altitude would be increased with decreasing weight. For a constant lifting area, this would result in very high initial altitudes. This procedure needs to be scrutinized closely. With ever decreasing aircraft weight, altitudes could increase to ones where the aircraft systems or the engines are unable to operate. Moreover, due to ATC regulations, aircraft are not free in choosing their flight altitudes. Assuming $h_{Cr,i}$ to be constant seems a more realistic approach. However, this results in lift coefficients that are less favourable and thus, in more moderate fuel savings.

- For the case of a decreasing wing size and constant aspect ratio (case three), a larger part of the wing will be influenced by the airflow around the fuselage. This will affect the character of the lift distribution and lead to a different Oswald factor. This aspect is not covered in the model.
- For the case of a decreasing wing area and constant span (case four), the length of the wing chord is reduced. This will lead to a reduced moment of inertia. To compensate for the loss in stiffness, the specific strength or thickness of the material needs to be increased. For this study, it is assumed that new materials will be at hand that allow for the weight fraction of the wing being unaffected.
- **The informational value of the results for the increase in wingspan is rather low.** The degree of simplification for the study at hand is considerably larger for the calculations of the increase in wingspan than for variations in the rest of the other parameters. This is due to the wingspan affecting more than simply the *k*-factor. A change in wingspan would normally result in a completely different lift distribution. Especially for our case, where the wing area is constant (case one) or reduced (case three), the wing gets more slender with increasing span. The reduced wing chord would then also decrease the zero-lift drag coefficient. As all these changes can only be sufficiently accounted for in a more complex wing design study, the curves at hand should be interpreted with extra caution.

3.4 Results

Most realistic trends for the impact on fuel consumption and CO_2 production are produced from calculations of the cases one and three. Case one is considered as being representative of a retrofitted aircraft, as snowball effects are generally disregarded. The aircraft thus profits only from instantaneous improvements of the parameters and from a reduced fuel weight. Further, $C_{L,i}$ decreases due to a smaller initial cruise weight at an unchanged initial cruise altitude. Contrary, the results of case three take into account a re-sizing of the aircraft: c_1-components decrease in size and weight. The wing loading is identical with the reference aircraft and so is the initial cruise lift coefficient. As wing area is reduced, the aspect ratio is held constant and wing span reduces concomitantly. This is a more realistic and conservative belief than the assumption of a constant span (case four), as the stresses acting on the wing

box – which are functions of the lift, the wing area and the length of the wing chord $y(x)$ (**Seibel 2003**) – are then comparable to the reference aircraft. Hence, there is no need for extra allowances due to a required change in the specific strength or thickness of the wing box material. The following analysis of a variation in reference parameters will therefore be focusing on the results of the cases one and three. The assumptions and results of the cases two and four are less representative of reality and are thus regarded as being of only low value for the discussion below. Detailed results for all four cases are enclosed as *Microsoft Excel* spreadsheets on a compact disc in Appendix D.

The calculation of cruise and block fuel is based on the assumption of a constant cruise/climb, i.e. the cruise correction factor k_R is calculated from Eq.(3.2). It should be noted that for the retrofitted aircraft, $C_{L,i}$ shifts further off the minimum drag lift coefficient $C_{L,md}$ as take-off weight decreases. As the cruise correction factor for a horizontal flight (Eq.(3.3)) is a function of the ratio of initial to minimum drag lift coefficient, the difference between the cruise/climb block fuel and the horizontal cruise block fuel will be larger for the retrofitted than for the reference aircraft. The results are presented in graphical form in Fig. 3.5 through Fig. 3.8. The percent change in block fuel is plotted against the percent change in the reference parameter. Shown are only parametric changes that lead to a positive effect on block fuel consumption. To reduce fuel burn, the parameters C_{D0}, c_1, (c_2-1), W_E/W_{MTO} need to be minimized (Fig. 3.5 and Fig. 3.7), whereas the parameters e, b, H and η are to be maximised (Fig. 3.6 and Fig. 3.8).

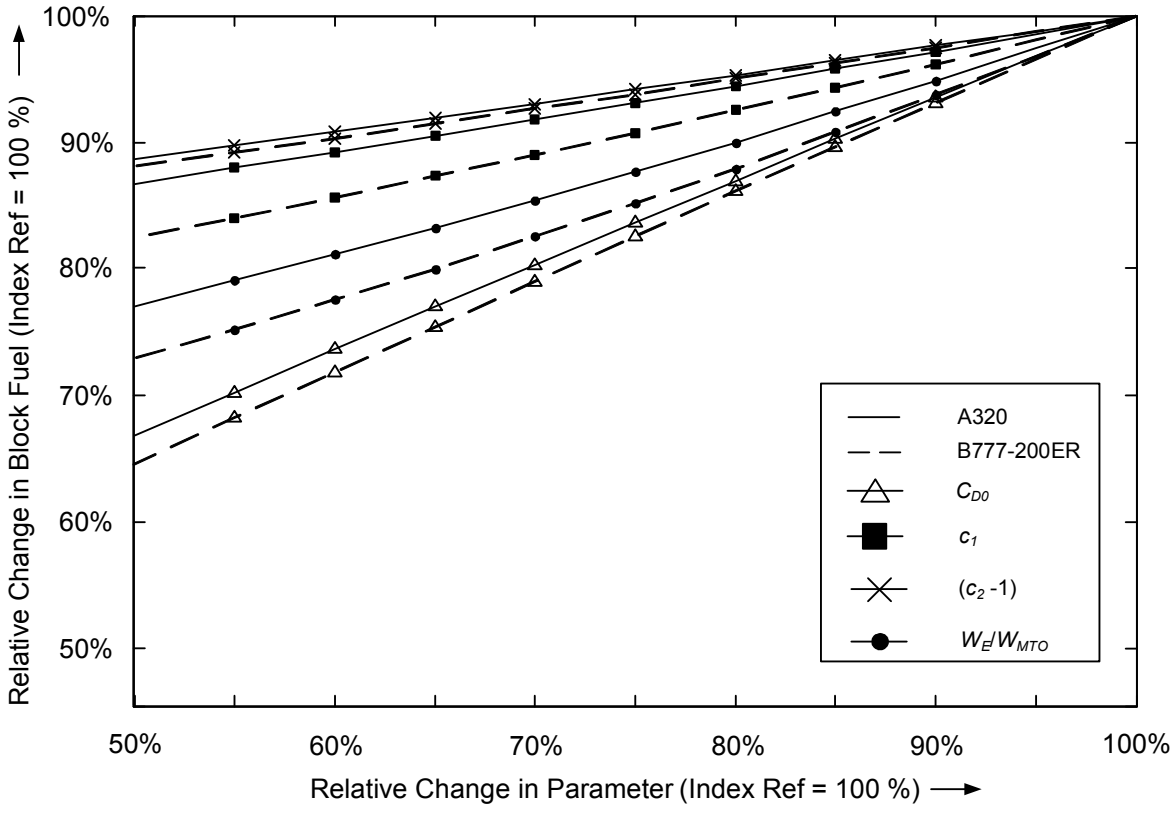

Fig. 3.5 Results of Parametric Variation Case (1) 'Retrofitted Aircraft' – C_{D0}, c_1, c_2, W_E/W_{MTO}

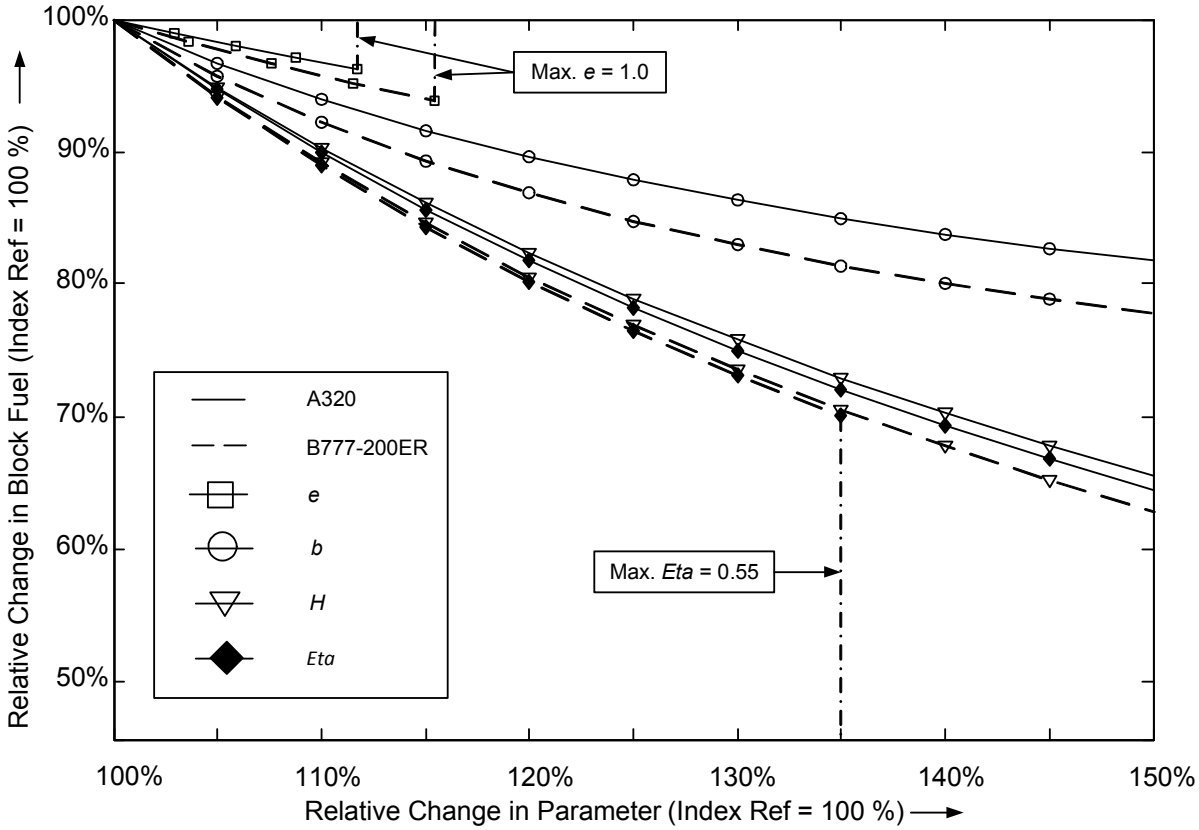

Fig. 3.6 Results of Parametric Variation Case (1) 'Retrofitted Aircraft' – *e, b, H, η*

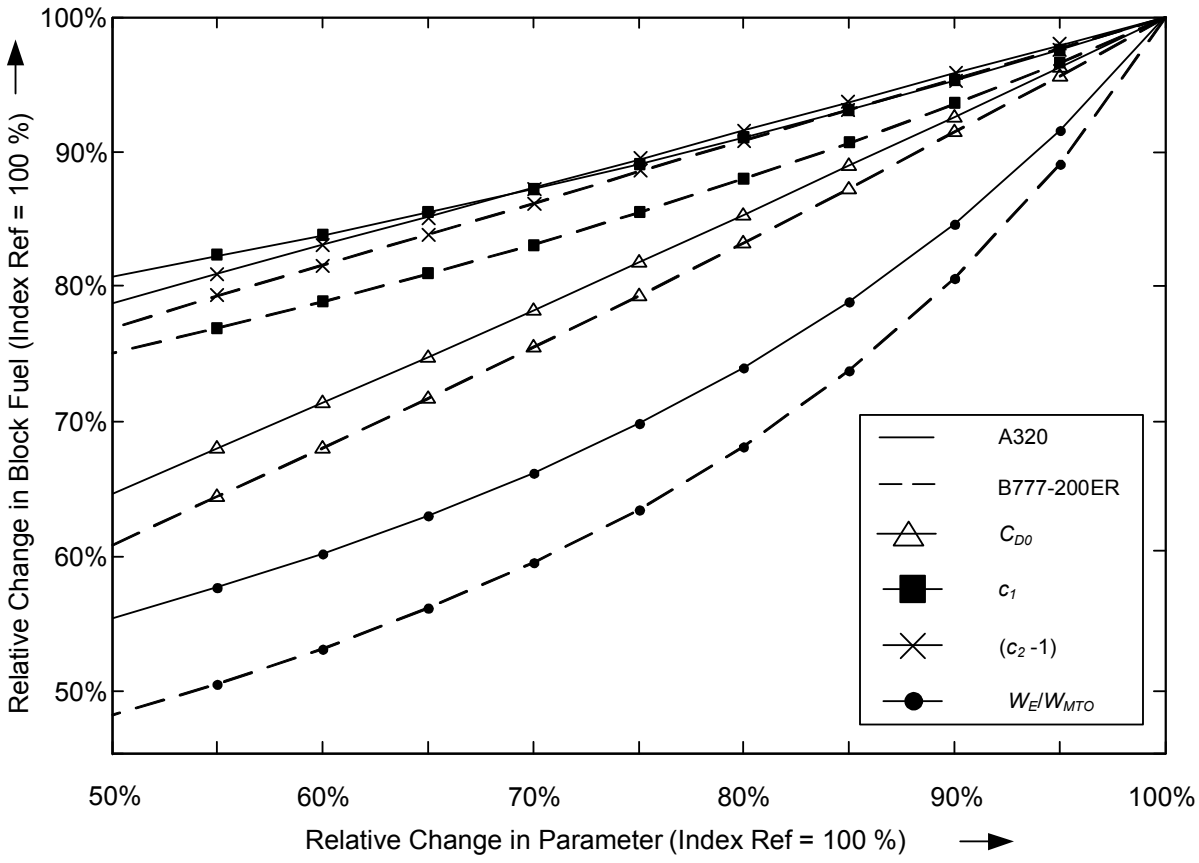

Fig. 3.7 Results of Parametric Variation Case (3) 'Re-Sized Aircraft' – C_{D0}, c_1, c_2, W_E/W_{MTO}

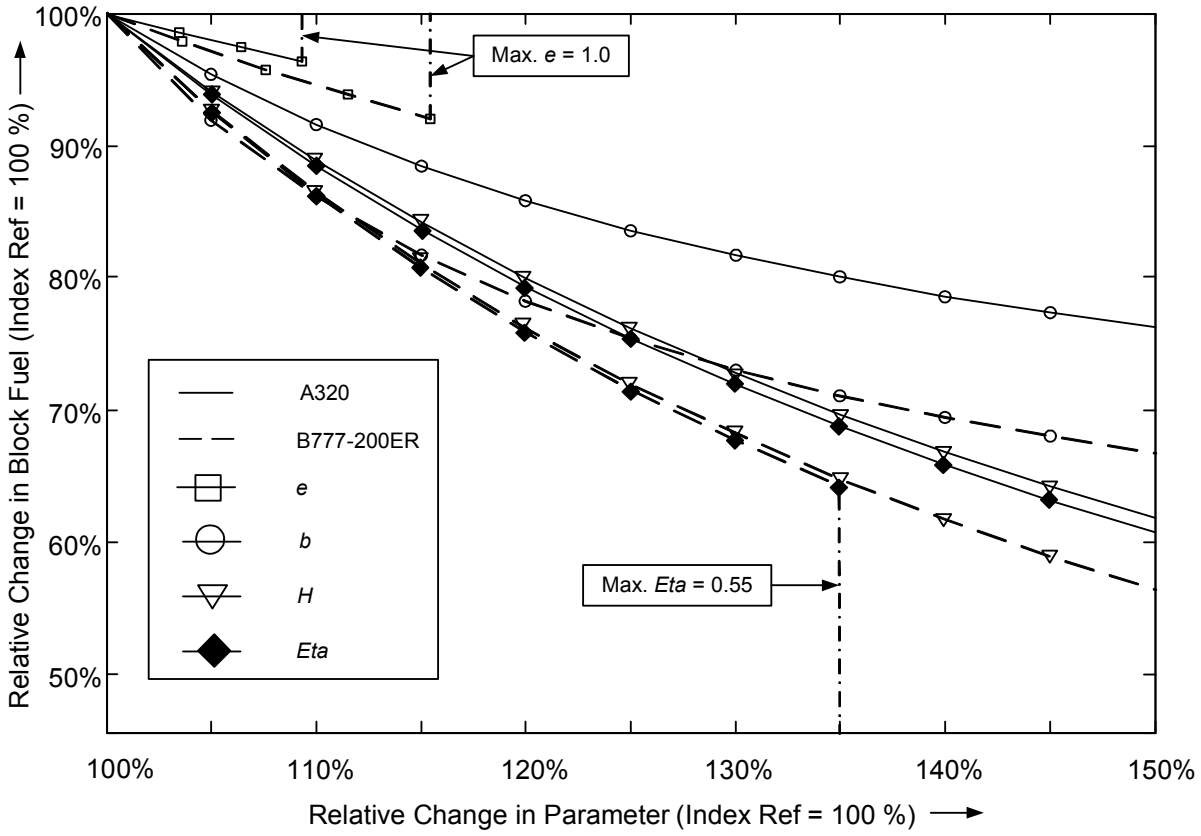

Fig. 3.8 Results of Parametric Variation Case (3) 'Re-Sized Aircraft' – *e, b, H, η*

3.5 Analysis and Interpretation of Results

It can easily be observed that for all parameters, the fuel saving potential is first, larger for the long-range aircraft and second, larger for the re-sized aircraft. Former is mainly due to the fuel weight of the long-range aircraft being larger than the fuel weight of the medium-range aircraft. An identical percentage change in fuel weight will have a larger effect on the take-off weight of the Boeing B777 than on the take-off weight of the A320. Latter is grounded on the benefit of a reduction in weight of c_1-components (snowballs on weight) and on the benefit of a lift coefficient that is not decreasing with take-off weight. It is further seen that the percentage change in fuel consumption is smaller than the percentage change in parameter for many curves.

For a more detailed analysis, it is helpful to recall the equation that is used to calculate mission fuel, i.e.

$$W_{F,m} = W_{TO} \cdot \left[\frac{\left(h_{Cr} + \frac{v_{Cr}^2}{2 \cdot g} \right)}{0.21 \cdot \eta_{Climb} \cdot (H/g)} + \frac{0.0025}{\eta_{Cr}} + \frac{R/(H/g)}{\eta_i \cdot (L/D)_i + 0.5 \cdot k_R \cdot R/(H/g)} \right] \tag{3.23}$$

where $(L/D)_i$ is calculated from

$$(L/D)_i = \frac{C_{L,i}}{C_{D0} + \frac{S}{\pi b^2 e} \cdot C_{L,i}^2} \tag{3.24}$$

and take-off weight is given by

$$W_{TO} = W_E + W_P + W_{F,Total} = \left[c_1 \cdot W_{MTO} + (c_2 - 1) \cdot W_P \right] + W_P + W_{F,Total} \tag{3.25}$$

3.5.1 Aerodynamic efficiency

The influence of changes in aerodynamic efficiency on block fuel consumption is represented by the curves for zero-lift drag C_{D0}, the wing span b and the Oswald factor e. Both, wing span and Oswald factor influence the k-factor, i.e. the lift-dependent part of the drag. C_{D0} is the dominant part in the over-all drag of both reference aircraft. It accounts for 64 % of the drag of the A320 and for 59 % of the drag of the B777-200ER. Accordingly, reducing C_{D0} seems to have a higher fuel saving potential than increasing the Oswald factor e or the wing span b for rather large parametric changes. Nevertheless, induced drag is inversely proportional to the square of the wing span. Hence, the curve of the wing span shows a steeper decline in fuel consumption than the curve of C_{D0} for small parametric changes. However, as already mentioned above, the curve for the increase in wing span needs to be considered with extra caution. Even if higher wing root bending moments are neglected, increasing the wing span has impacts on the lift distribution, the Oswald factor and the zero-lift drag coefficient that cannot be simulated in this parametric study.

The fuel saving potential from increasing the Oswald factor e is strictly limited to only a few percent. The maximum realizable e is 1.0. For a wing in isolation in inviscid flow, this would imply an elliptical loading. As **Greener By Design 2005** depicts, today, e does not only account for the departure from the elliptical lift distribution, but also for the lift-dependent part of the skin-friction and pressure drags. It can further be assumed that trim drag from the down-force on the horizontal stabilizer (which is also lift-dependent) is also considered in the deviation of e from unity. The reference aircraft feature Oswald factors of 0.895 (A320) and 0.864 (B777-200ER). In theory, e could be improved by +12 % on the A320 and by +16 % on

the B777. The maximum possible fuel savings would then be around 6 to 8 % (see Fig. 3.6 and Fig. 3.8). In practice, it is probable that new aircraft will feature Oswald factors that are closer to unity, but will not reach 1.0. First, the prospect to decrease the lift-dependent part of profile drag considerably is small. Second, the classical elliptical span loading is not always favourable, as much lift on the outer wings increases the wing root bending moment (**Greener By Design 2005**).

In summary, the reduction of the *k*-factor seems to be limited to very small changes, at least for the classic cantilever. From literature and the parametric study, we might reasonably assume that reducing C_{D0} seems to have the highest fuel saving potential from the aerodynamics' point of view. Interestingly, for both the retrofitted and re-sized aircraft, the relationship between a change in C_{D0} and the corresponding change in block fuel is nearly linear. Further, snowball effects increase the impact of a reduction in C_{D0} only very slightly. The reason for this is probably the decrease of the wing size and the corresponding increase in C_{D0}. As a result, the effective ('global') decrease in C_{D0} is less than indicated by the factor *i*. For example, decreasing the zero-lift drag coefficient of the Airbus A320 on all components by 30 % ($i = 0.7$) results in an effective 'global' decrease of only 28 %. With decreasing wing area, the fuselage, which accounts for around one-third of the zero-lift drag of today's aircraft (**Greener By Design 2003**), becomes the dominant factor in aircraft drag. The negative snowball on aircraft drag shows that new technologies could be implemented with a larger benefit if wing area and fuselage area would not be separated as they are today.

In the long term, the departure from the classical cantilever configuration could enhance chances for more radical drag reductions. The blended-wing-body (BWB) concept is promising in terms of merging the wing and fuselage and foster C_{D0} reduction, whereas truss-braced wing (TBW) and joined- or box-wing aircraft could considerably increase the effective wingspan and thereby decrease the induced drag.

3.5.2 Engine efficiency and fuel heat content

For the retrofitted aircraft, the parameter with the highest impact for both aircraft is the engine efficiency η. For parametric changes up to +20 % for the long-range and up to +10 % for the medium-range aircraft, the percentage change in block fuel is larger than the percentage change in parameter. Due to beneficial snowball effects, fuel savings that surpass the percentage change in parameter are possible for the re-sized aircraft even up to +20 % for the medium-range and up to +30 % for the long-range aircraft.

In general, *H* and η both influence the same superordinate parameter *TSFC*. For identical parametric changes, the resulting impact on block fuel should hence be the same. The reason for the small deviation of the *H*-curve from the η-curve is the definition of manoeuvre fuel in

Eq.(3.5): the only influencing parameter is the engine efficiency. Eq.(3.5) is a semi-empirical expression. From the physics' point of view, manoeuvre fuel is a function of *TSFC* and will thus be influenced by *H* as well. It is therefore expedient to consider the curve for engine efficiency to be representative of both, changes in η and changes in *H*.

History shows that reducing thrust specific fuel consumption (*TSFC*) by increasing the engine efficiency has also a realistic retrofitting potential (see e.g. several CFM-56 engine generations on the A320 and B737 aircraft). This is due to the engine being removable – i.e. also exchangeable if the specific weight and size remain constant – on many aircraft. As the engine is thus more independent from the over-all system, there is a chance to employ technological innovations more easily.

As shown on the η-curves of the long-range aircraft, an increase in engine efficiency is limited by physics. The Boeing B777-200ER is equipped with engines that already provide high cruise efficiencies of 40.55 %. According to Fig. 4.14 and **Gmelin 2008**, maximum obtainable efficiencies with conventional technology are 60 % for the thermal and 92.5 % for the propulsive efficiencies. This limits over-all engine efficiency in cruise to 55.5%. For the Boeing B777 aircraft this limit is reached for $i = 1.36$. The cruise efficiency of the CFM-56 engines is lower (32.23 %). A parametric multiplier of $i = 1.72$ is theoretically possible for the A320 before physical limits are touched. In practice, it is uncertain if the physical limits are reachable with conventional aero-engines. If low NO_x levels become obligatory, thermal efficiency could be limited to 55 % (**Gmelin 2008**). Further, according to today's knowledge, propulsive efficiencies as high as 92.5 % are feasible only by using open-rotor configurations. As economical cruise Mach numbers for un-ducted fans are however limited to around 0.78, they are unlikely to be put into service on long-range aircraft as the B777.

Lower *TSFCs* then become possible only by increasing the weight specific energy content of the fuel. Liquid Hydrogen (LH_2) features an of 119 $MJ \cdot kg^{-1}$: a multiplier of 2.76 in comparison to kerosene. Unfortunately, the use of liquid hydrogen as aviation fuel has multiple disadvantages (see chapter 4.4.2). For the near-term, increasing thermal and propulsive efficiency will thus be the more realistic way to reduce *TSFC*. In the long-term however, physical limits will necessitate a departure from conventional aviation engines and fuels.

3.5.3 The Ratio of Empty Weight to Payload and Take-Off Weight

Reductions in the specific weight of aircraft components are pictured by the curves of c_1, (c_2 - 1) and W_E/W_{MTO}. Reducing empty weight for a given take-off weight – i.e. the factor W_E/W_{MTO} – results in enormous fuel reductions, especially for the calculation including snowball effects. A reduction of 'only' 10 % reduces block fuel by 15 % on the medium-

range aircraft and by 20 % on the long-range aircraft. This is consistent with information given by **Gmelin 2008**, which says that weight reductions produce a percentage reduction in fuel burn 1.5 times the weight reduction on short- to medium-range flights and 2.0 times the weight reduction on long-range flights.

It is important to realize that even though a 10 % reduction in W_E/W_{MTO} sounds moderate, it can only be accomplished by more substantial reductions in component weights. The curve for W_E/W_{MTO} could mislead to the assumption that all component weights are functions of take-off weight. If this would be the case, a 10 % reduction in W_E/W_{MTO} calculated simply to a 10% reduction in component weight. Unfortunately, only c_1-components are dependent on take-off weight, whereas c_2-components are payload-driven. The design payload is held identical to the reference throughout the parametric study. With decreasing fuel weight, take-off weight reduces, and thus, the ratio of payload-driven empty weight to take-off weight does even increase. To achieve a concomitant 10 % reduction in the ratio of payload-driven weights to take-off weight – i.e. $(c_2\text{-}1)\cdot W_P/W_{MTO}$ – and in the ratio of take-off weight driven weights to take-off weight – i.e. c_1 – on the A320, all c_2-weights (fuselage, furnishings, etc.) need to be reduced by 27 %. As c_1-components are snowball affected, their specific weights need to be reduced by only 10 %. It is of course also possible to reduce W_E/W_{MTO} only by reducing either c_1 or (c_2-1). For the A320, the necessary component weight reduction would then calculate to 35% for all related components. Howsoever, the required component weight reduction is considerably higher than 10%. It is therefore advisable to base the analysis rather on the curves for c_1 and c_2, as the reduction in parameter is then similar to the necessary reduction in component weight.

Snowball effects are large for all reductions in empty weight. Thus, reducing component weights is a powerful means of saving fuel especially for re-sized aircraft. The benefit for a re-sized aircraft is approximately 1.5 to 2.0 times the benefit for a retrofit. As the substitution of structural components also involves high risk and costs, reductions in empty-weight as a means of increasing fuel efficiency of an existing aircraft will generally focus on reducing the weights of furnishing and fixed equipment, i.e. c_2-components. The benefit is depending on the fraction of c_2-components in empty weight. According to Eq. (3.17), c_2-components for our case account for around 46 % of empty weight on the A320. For example, a 10 % reduction in ($c_2 - 1$) then reduces fuel burn by 3.4 %.

3.5.4 Negative Trends

When assessing real aircraft technologies, it is important to bear in mind that they eventually change one parameter for the worse while improving another. For example, implementing a boundary layer suction system on the wings that decreases C_{D0} will increase the weight of the wings, i.e. the parameter c_1. The over-all benefit of the system will then be lower than

indicated by the C_{D0} curves in Fig. 3.5 and Fig. 3.7. This is true for many other 'technologies' as for example liquid hydrogen, which increases H but requires larger and heavier fuel tanks due to pressurization requirements.

3.5.5 The Influence of Design Range on Fuel Efficiency

Design range has not been included as a variable to the parametric study at hand. The reason for this is given below.

Recent studies (**Greener By Design 2003; Green 2006**) suggest the most fuel efficient design range to be around 4000 km. Assuming identical aerodynamic and engine efficiencies, the fuel burn per seat and km is noticeably increased for very long ranges. The absolute magnitude of the fuel penalty is however not clear. Calculations and data given by **Green 2006** and **Nangia 2006** for a design range of 15 000 km vary between 140 % and 210 % compared to the fuel burn of R = 4000 km. Similar to the parametric assessment at hand, Green uses Küchemann's weight model (the constants c_1 and c_2) to separate between payload-driven and W_{MTO}-driven weights. The large discrepancies come from different assumptions concerning the weight factor c_2. If c_2 is taken as a constant, fuel penalty results only from an increased fuel weight and increased weights of W_{MTO}-driven components. If Eq.(3.17) is used however, c_2 increases with range and there is an additional fuel penalty due to increased weights of W_P-driven components. Eq. (3.17) was derived by **Green 2006** using actual aircraft data. This suggests the large fuel penalty (210 %) to be the more realistic result. However, due to the large discrepancy in Green's results, it is decided to exclude the range as a variable from the parametric assessment for the study at hand. This is in accordance with the conclusions in **Green 2006,** p. 516:

> *The simple weight model proposed by Küchemann ... is probably adequate for making illustrative comparisons. ... To make a really credible assessment of the variation of PFE [Payload Fuel Efficiency, author's note] with design range, however, a model is needed which realistically incorporates the effects of all the practical design constraints.*

Green's results concerning shorter-than-optimum ranges are more consistent. The fuel penalty seems to be much less. The ratio of seat fuel burn for 2000 km and seat fuel burn for 4000 km for all assumptions concerning c_2 is only around 1.07 (**Green 2006**). A qualitative illustration of how fuel efficiency changes with design range when calculated according to **Green 2006** is given in Fig. 3.9.

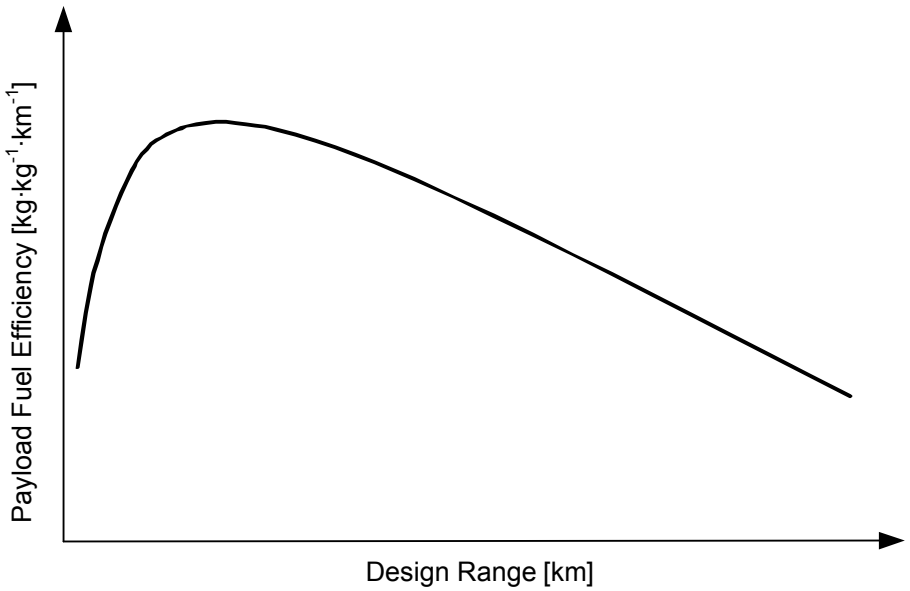

Fig. 3.9 Quantitative Illustration of the Influence of Design Range on Fuel Efficiency (reproduced from **Green 2006**)

The reason for the curve in Fig. 3.9 to drop sharply for very short design ranges is the influence of the lost fuel. For a given initial cruise altitude, additional fuel burned for ground operations, lifting the aircraft to cruise altitude and accelerating it to cruise speed is per definition (see sub-subchapter 3.1.2) independent of range. Thus, the impact on payload fuel efficiency PFE, which is the product of range and payload divided by the block fuel weight, is larger for short-range flights. According to **Torenbeek 1997**, fuel for lifting and accelerating the aircraft "... amounts to about 5 % of over-all fuel for very long-range flights (approximately 12 000 km), up to about 25 % ... for relatively short ranges, down to 1000 km".

The quintessence of the recent paragraphs is that while primarily being a design specification, design range is also a variable that strongly influences fuel and CO_2 efficiency. There seems to be an optimum design range that yields the lowest fuel consumption per passenger-km for a given L/D, η and H. For today's technology, this optimum is a medium design-range. The reasons for short and long design ranges to be less efficient are different in nature. High fuel weight and resulting high structural weights are the explanation for long-range aircraft to be less efficient in cruise. Contrary, the efficiency for short design ranges drops due to extra fuel burned for other-than-cruise segments.

3.6 Chapter Summary

In this chapter, the difference in influence of major aerodynamic, engine, structural and fuel efficiency handles on aircraft CO_2 emission has been examined. A form of the Breguet range equation has been employed to calculate the reduction in block fuel weight (i.e. block CO_2 emission) for gradual improvements in the single parameters. Calculations have been performed both regarding and not regarding snowball effects on the structural weight and drag polar. The CO_2 reduction potential due to technological improvements for retrofits and new aircraft has thus been exemplarily quantified.[1] It has been shown that there is a coupling between the reduction potential and the design range, as calculations have been performed on a short-haul and a long-haul aircraft. Where applicable, theoretical improvement limits have been highlighted. It is now easier to qualitatively rate technologies according to their CO_2 improvement potential given that they change one of the defined parameters. This allows for a qualitative verification of the assumptions concerning efficiency improvements due to new technologies implemented on future aircraft, see chapter 6.1.2 and Appendix C. These and other potential technologies for the reduction of aircraft CO_2 emission by improving the variables in question are included in the technology survey following this chapter.

[1] Note that the calculations are valid only for a qualitative understanding of the reduction potential as several simplifications were incorporated, see chapter 3.3.

4 Technology Survey

A brief overview of approaches and techniques to lower CO_2 is given below. The technologies are presented in the context of their super-ordinate research discipline or field of interest, e.g. *Engines & Power – Improving thermal efficiency*. Single sub-ordinate technologies to one approach, e.g. *Advanced Ni-based Superalloys*, will not be separately listed in the main body, or only if they can serve as example for the general idea. However, brief information on single technologies is given in Appendix B.

The technology survey at hand focuses on technologies that could be available in the near to medium future if the reduction of CO_2 emissions is the primary objective of research and development. It also gives an outlook on more radical and groundbreaking technologies that will only be realizable in the long term. However, this outlook is confined to the 2050 timeframe. Thus, technologies that have an even more distant time horizon – e.g. terrestrial lasers that power the aircraft's propulsion systems (**Curry 2008**) – are disregarded.

4.1 Aerodynamics

For a given lift requirement, maximum aerodynamic efficiency L/D is achieved by minimizing aircraft drag. In chapter 2.2, five different forms of aircraft drag are identified, which are skin friction, form, induced, wave and interference drag. Approaches to drag reduction for all forms are presented in turn below.

4.1.1 Reducing Friction Drag

Friction drag results from shear stresses due to friction of the viscous fluid against the surface of the aircraft. For a given flight speed and altitude, skin friction drag is mainly defined by the frictional coefficient C_f and the size of the wetted surface area. The frictional coefficient is dependent on the character of the boundary layer, which tends to be thin and laminar at the front of the object, e.g. the wing, but becomes turbulent and thicker towards the rear (**Schlichting 2001**).

In a turbulent boundary layer, wall shear stresses and therefore friction coefficients are higher, because there is a lot of vertical (up and down) movement of air particles. The difference in frictional coefficients is seen in Fig. 4.1. It is also observable that skin friction rises sharply at the transition from laminar to turbulent boundary layer. The transition is affected by multiple

factors such as Reynolds number, pressure gradient, surface curvature, free stream turbulence and surface roughness (**Roskam 1997**).

In laminar boundary layers, surface roughness contributes to friction drag only if the so-called *critical roughness height* is exceeded. This is the height where roughness leads to an early transition to turbulent flow (**Schlichting 2001**). Today's transport aircraft are flying with virtually all turbulent boundary layers (**Greener By Design 2003**). In turbulent boundary layers, the *allowable roughness height* is of particular importance as it indicates the minimum quality of the skins to ensure that there is no friction drag rise due to roughness (**Schlichting 2001**). It is also important to remind that friction drag is driven by the wetted area. As for example, the non-lifting fuselage of a typical swept wing aircraft causes a large wetted area and therefore an immense friction drag rise.

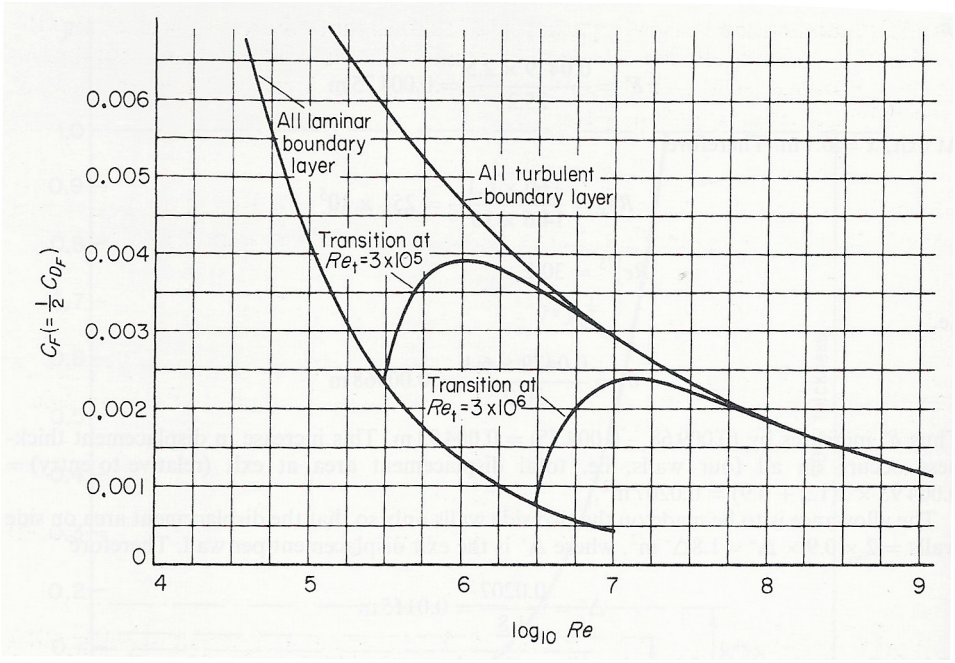

Fig. 4.1 Two-dimensional Surface Friction Drag Coefficients for a Flat Plate. Here *Re* = Plate Reynolds number, Re_t = Transition Reynolds number, C_F = Skin Friction Force per Surface (unit width) (**Houghton 2003**)

Reducing Friction Drag of Fully Turbulent Boundary Layers

According to today's knowledge, methods of reducing the frictional coefficient of already turbulent boundary layers are quite limited. Classically, the surface roughness can be minimized to give lower friction coefficients. There has been a lot of research in the field of paints and coatings (drag-reduction coatings) through the last decades and modern manufacturing and painting processes guarantee very **smooth aircraft outer surfaces**. There might be potential for further drag reduction by even smoother paints and coatings. However,

regarding modern manufacturing and painting processes, the increase in efficiency is regarded as being rather small. Contrary, there could still be a large potential for lower skin friction by reducing the risk of early laminar-turbulent flow transition initiated by small aircraft components. New rivet-free manufacturing methods and materials could enhance smoother aircraft skins. For the fuselage, drag reductions could be achieved if the influence of windshield wipers, doors, windows and pitot probes could be lessened.

It should also be noted, that friction drag increases with a poor airframe condition. Dirt, the absence of seals and chipped paint can seriously affect the smoothness of the outer surfaces. One square meter of rough surfaces leads to additional fuel burn up to 105 kg on a typical Airbus A330/340 flight (**Airbus 2004**). Newest polymer coatings are said to fill in the "naturally occurring peaks and valleys of the paint surface" (**Esler 2008**) and making the aircraft less susceptible to dirt. The potential drag saving is however assumed as low.

Another way of influencing the frictional coefficient is by **disrupting span-wise cyclic flows** that are a major characteristic of turbulent flows. These streaks of low- and high-speed flows create wave-like disturbances that generate additional wall friction and drag (**Lockerby 2008**). Both passive (e.g. *riblets*, *dimples*, Helmholtz resonators) and active (travelling surface waves using active skins) are known. Traditionally, a drag reduction potential in the order of 5 to 10 % is presumed (**Houghton 2003**). Most recent research activities using Helmholtz resonators indicate very high drag savings (up to 40 %) (**Lockerby 2008**). However, these are only first calculations that still need to be validated by tests of a larger scale.

Reducing Friction Drag by Maintaining Laminar Flow

As was exemplarily shown for a flat plate in Fig. 4.1 above, attaining laminar flow over a surface results in frictional coefficients clearly below the frictional coefficients of turbulent flows. Laminar flow technologies delay the transition from laminar flow to turbulent flow and thereby reduce skin friction drag. A postponed transition to turbulent flow also decreases the pressure drag (form drag) from boundary layer growth. Laminar flow control is regarded as being one of the few aerodynamic technologies to enable substantial improvement in fuel efficiency up to 30% (**Greener By Design 2005**, **Houghton 2003**). The technologies can be divided into natural laminar flow technologies, where laminar flow is achieved passively, and hybrid laminar flow technologies, where the boundary layer is kept laminar by actively influencing it.

Natural laminar flow control (NLFC) is generally limited to relatively short wing chords and low wing sweep. The technique is such likely to find application only on commercial aircraft up to the size of an Airbus A320 or Boeing 737. However, even for these aircraft, considerable changes from the current design (e.g. a lower wing sweep or forward swept

wings) are necessary. **Hybrid laminar flow control** (HLFC) allows laminar flow to be maintained over wings with a larger wing chord (Reynolds number) and leading edge sweep and is therefore applicable to a greater range of aircraft than natural laminar flow (**Greener By Design 2005**). It however requires a considerable power input and a smooth wing with seamless high-lift devices. Contamination of the suction surface is another challenge that needs to be addressed. Both techniques are not yet ready for commercial series production, but could be available in the 2025 timeframe (**IATA 2008a**).

Reducing Friction Drag by Reducing the relative wetted Area

Reducing the relative wetted area, which is the sum of all outer surface areas divided by the base area of the wing, is another powerful means of reducing friction drag. This is obvious from the following equation, which is taken from **Greener By Design 2003**.

$$C_{D0} = \frac{\sum C_{f,i} k_{p,i} S_i}{S} \quad , \tag{4.1}$$

where $C_{f,i}$ is the average skin friction coefficient on an individual component, $k_{p,i}$ is the ratio of form drag to skin friction drag at zero lift (the form factor) for an individual component, S_i is the surface area of the component and S is the wing area. The ratio of wetted area to lifting area S_{wet}/S_{lift}, or the relative wetted area, is an indicator of how much surface of the aircraft is actually lifting. The ideal ratio S_{wet}/S_{lift} would be 2.0, as this would mean only lifting parts. On a conventional airplane, the cylindrical fuselage is non-lifting. However, it strongly contributes to the wetted area and therefore to the friction drag of the airplane. Conventional aircraft hold ratios of about 5.0 (B707-320) to 6.5 (DC9-30) (**Roskam 1997**).

Reducing the wetted area of classic cantilever aircraft is rather difficult. The size and wetted area of the fuselage is mostly set by the design passenger load and the defined passenger comfort (**Roskam 1997**). The wetted area of the engine nacelles is driven by the diameter and length of the engine – i.e. the by-pass-ratio and size of the engine core – and is likely to rather increase than decrease in the near future. Aircraft components that offer potential are thus only the fin and horizontal tail. **Reducing the size and wetted area of the fin and horizontal tail** is generally possible by reducing the required trim load or by improving their aerodynamic performance, e.g. by achieving laminar flow on their surfaces (**Courty 2008**). Methods for reducing the required trim ability of the horizontal tail are mentioned in the context of reducing trim drag in sub-chapter 4.1.4. On many aircraft, the required trim load from the fin is defined by the case of flying with one engine out. The deflection of the vertical tail is then necessary to ensure zero yawing.

The departure from the classic cantilever aircraft promises more radical drag savings. Flying wing concepts achieve relative wetted areas closest to the optimum. They achieve this by having no separate body, only a single wing: see in Fig. 4.2, part 4. **The blended-wing-body** (BWB) or hybrid-wing-body (Fig. 4.2, part 2) falls in between the flying wing and a classic cantilever and is the most-likely concept to find application in civil aviation. The principle behind the blended wing-body is to merge the wings with the fuselage and thereby reducing non-lifting fuselage and tail surfaces. According to **Greener By Design 2003**, the reduction in relative wetted area leads to an increase in *L/D* of 15%. **IATA 2008a** indicates a reduction of 25% in per-seat fuel burn. It is likely that BWB configurations will find their first large-scale application in a military freighter or tanker aircraft, as serious problems concerning passenger transports (e.g. a pressurized cabin, emergency evacuation, etc.) still need to be resolved (**Greener By Design 2005**).

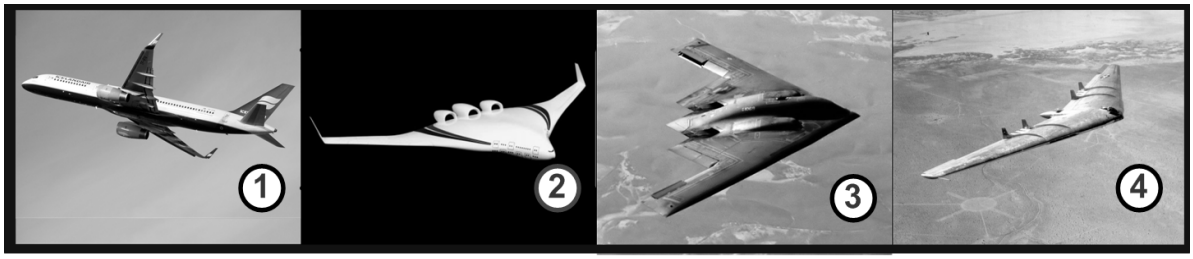

Fig. 4.2 Progression of aircraft design from conventional cantilever (1) to flying wing (4) (**Herbert 2007**)

4.1.2 Reducing Form Drag

Form drag is caused by the separation of flow from the object moving through the air. The less streamlined an object, the more difficult it will be to keep the flow attached to the surface. "Form drag is overwhelmingly the main contribution to the overall drag of bluff bodies like the cylinder, whereas in the case of streamlined bodies skin-fraction drag is predominant, form drag being less than ten percent of the overall drag" (**Heinze 2005,** p. 522).

Flow separation also occurs on streamlined objects, when the air particles in the boundary layer do not have sufficient energy to reach the trailing edge. This is especially true for the rear section of an airfoil (beyond the point of maximum thickness), where the boundary layer flow has to resist the increasing pressure while moving downwards. From the point of separation, the boundary layer thickens rapidly, causing a so-called wake and a large form drag. Generally, turbulent boundary layers are less susceptible to separation, as the fluid particles near the surface possess more energy (due to higher velocity) to resist the pressure increase (**Roskam 1997**, **Heinze 2005**). Thus, keeping form drag to a minimum is reached by postponing or avoiding flow separation.

Form drag of the fuselage is dependent on the ratio of fuselage diameter to fuselage length. Fuselages should not only be streamlined at the nose (see Fig.5.20, chapter 2), but also at the tail, to prevent drag rise due to so-called base areas (**Roskam 1997**). Staying with the conventional cantilever configuration, fuselage diameter and length is typically driven by the number of passengers to be transported and the designated passenger comfort, i.e. headroom, seats abreast etc. In long-term, the fuselage and wings should not be separated as they are today. BWB configurations allow for fuselages designs that are aerodynamically considerably improved and do not limit passenger comfort.

On modern transport aircraft, form drag accounts for less than ten percent of overall drag (**Houghton 2003**, **Greener By Design 2005**). As it cannot be terminated completely, the possible benefit of a further reduction in form drag seems small for the classic cantilever wing configuration. Large parts of form drag arises from flow separation at small aircraft components such as protuberances, antennas etc. By paying attention to detail design, form drag can already be considerably reduced (**Roskam 1997**, **Bouteiller 2008**).

Theoretically, form drag can further be reduced by some form of **active or passive separation control**. Unfortunately, both of them have serious drawbacks. Passive devices lead to increased drag at cruise when they are not required (**Houghton 2003**). Active systems increase aircraft weight, require system power and regular maintenance. With form drag being already low, "the potential returns are small on modern aircraft" (**Greener By Design 2005**, p. 21). Separation control becomes increasingly interesting for future aircraft such as the Blended Wing Body (BWB). The reason for this is that separation control can be used on a conventional configuration only on the wings, where the resulting drag reduction would be rather small. On a BWB, separation control could be used over large part of the fuselage, where it would have a much larger impact on the over-all drag.

4.1.3 Reducing Lift-induced Drag

Induced Drag is a drag form directly related to the production of lift. Simply put, trailing vortices at the wing tips produce a downwash velocity, which causes the flow over that section of the wing to deflect slightly from its original direction. Hence, the wing is effectively not attacking the airflow at the geometric angle of attack α, but at a reduced (effective) angle of attack ($\alpha - \varepsilon$). Similarly, the produced lift is inclined backwards, as shown in Fig. 4.3. The effective direction of lift can then be divided into a vertical component actively producing lift, and a horizontal component producing drag. This drag is known as the lift induced drag or vortex drag (**Houghton 2003**). By definition of the parabolic drag polar, see Eq.(2.12), vortex drag is inversely proportional to the Oswald factor e and to the square of the wing span b.

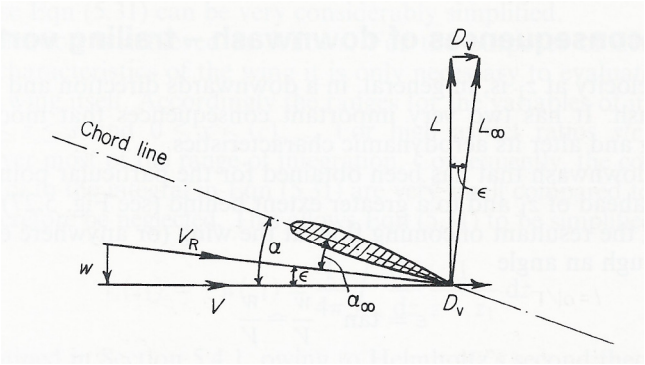

Fig. 4.3 The Inluence of Downwash on Wing Velocities and Forces: w = Downwash; V = Forward Speed of Wing; VR = resultant oncoming Flow at Wing; α = Incidence; ε = Downwash Angle, L∞ = two-dimensional Lift; L = Wing Lift; DV = Trailing Vortex Drag (**Houghton 2003**)

The traditional definition of the lift-induced drag accounts however only for the main wing. In reality, the departure of *e* from unity is not only accounting for the deviation from the elliptically shaped lift distribution, but also for other than vortex-dependent sources of lift induced drag. In general, these are the lift-dependent parts of the profile drag. These arise from a growth of the boundary layer and vary (same as the vortex drag) as the square of the lift **Greener By Design 2005**. For the purpose of this paper, it is assumed that trim drag, arising from a down-force on the horizontal stabilizer, is also accounted for in the Oswald factor.

Reducing Induced Drag by Increasing the Oswald Factor

For a given wing aspect ratio, i.e. $AR = b^2/S$, vortex drag is at its minimum for an Oswald factor $e = 1.0$. For a wing in isolation in inviscid flow this is true for an elliptic wing loading (Heinze 2005, Schlichting 2001).

The strength of trailing edge vortices, i.e. the classical induced drag, can be reduced by **the use of wingtip devices or non-planar wing extensions**. The device being the longest in service is the simple winglet shown in Fig. 4.4. It is in use for example on the Boeing B747-400 and Airbus A330/340 and reduces total drag by about 2.5% (**Houghton 2003**). Today, more advanced systems are in operation (wingtip fence, blended winglet, raked wingtip) that reduce drag by up to 5.0 % (**IATA 2008a**). Improved versions of these and more uncommon devices (spiroid wingtip, multiple (active) winglets) could find application on future aircraft. The different forms are listed in Appendix B.1. One should however bear in mind that the potential for fuel burn reductions by bringing *e* closer to unity is strictly limited (see results of the parametric study in chapter 3.3).

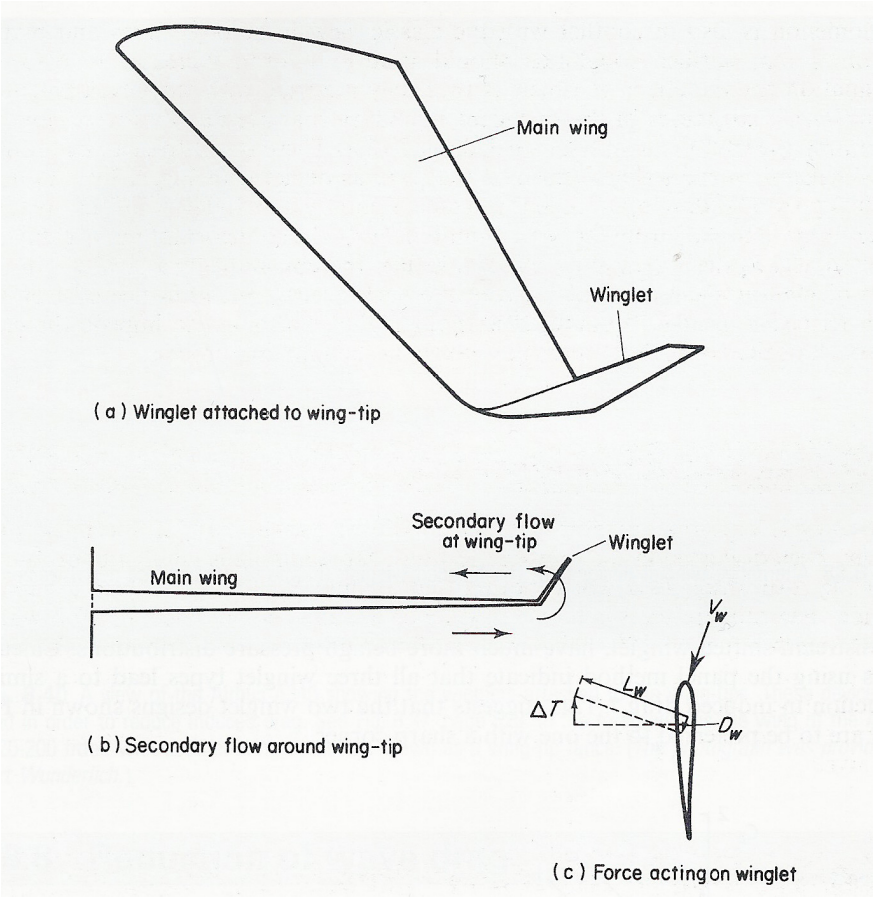

Fig. 4.4 Using Winglets to reduce induced Drag (**Houghton 2003**)

The control of wingtip vortices could possibly enable further benefits for the air traffic system. Large wingtip vortices cause turbulences to the air behind the aircraft. To avoid danger, following aircraft are required to fly at some distance from the first. The strength of the vortex and therefore the horizontal spacing is dependent on the aircraft weight (**Truman 2006**). Wingtip devices weaken the wingtip vortices and thereby lower the risk for following aircraft. If the majority of (large) aircraft would be equipped with well working devices, horizontal spacing could be reduced and thus terminal space capacities increased. This would lead to further fuel and CO_2 savings (**IATA 2008a**).

As **Roskam 1997** define it, trim drag caused by down- and up-forces on the horizontal tail is lift-dependent and thus part of the lift-induced drag. In general, the required trim force defines the size and angle of attack for the horizontal tail. This force is driven by the location of the centre of gravity (CG), the location of the thrust-line, i.e. the location of the engines, and the stability margin. Thus, **reducing trim load** is possible by a rearward centre of gravity, fuselage mounted engines and a reduced stability margin. Trim drag accounts for 0.5 to 5% of total airplane drag (**Roskam 1997**). This defines the maximum aerodynamic benefit of reducing this parameter. If the tailplane size would be reduced concomitantly, parasite drag and weight associated with it would be less. The resulting snowball effects will therefore decrease fuel consumption by a greater amount.

For a conventional aircraft in trimmed flight, the horizontal tail is producing a down-force. Thus, flying with an aft centre of gravity can help to minimize trim drag. This can be achieved for example by moving heavy equipment to the back of the aircraft, manage the passenger-seating configuration or by developing fuel burn sequences between fuel tanks (**Viscotchi 2006**). Controlling the position of CG in flight is possible by pumping fuel into special trim tanks in the aft of the aircraft. This is done for example on the Airbus A330 and A340 aircraft. This is called active stability. If the size of the horizontal plane is reduced concomitantly, **Greener By Design 2003** believes fuel reductions of 1 to 2% to be realistic for this technology.

Reducing Induced Drag by Increasing the Wing Span

A greater wingspan has two positive effects. First, the lifting area is increased. Second, the influence of trailing edge vortices on the inner wing is reduced, i.e. induced drag is lessened. Theoretically, wingspan has a strong decreasing effect on vortex drag and CO_2 emission, as it is seen from the results of the parametric study. Unfortunately, as **Greener By Design 2005** depicts, on current aircraft, "the balance between wing span and wing weight is close to optimum". With conventional technology, the benefit of a further increase in wingspan is nearly always offset by increased wing weight and fuel consumption. For the current design, a cylindrical fuselage with cantilever wings, **Greener By Design 2005** lists three possibilities to increase wingspan without weight penalties:

- The use of new high strength, lightweight materials,
- The use of turbulent boundary layer control to allow for thicker wing profiles and hence lower wing bending moments,
- The reduction of the cruise Mach number to reduce form and wave drag to allow for thicker wing profiles and/or lower wing sweep and thus lower wing bending moment.

For very large aircraft, as has been seen on the Airbus A380, the maximum wingspan is imposed not by weight but by airport regulations. The "80 m box" limits maximum wingspan on ground. To allow for a more optimum wing design, folding wing tips would be an option (**Greener By Design 2005**, **IATA 2008a**).

Dramatic changes in wingspan seem to be realizable only with alternative aircraft configurations. **Strut- or truss-braced wing (TBW) concepts** could considerably enhance aerodynamic efficiency of a conventional take-off and landing aircraft (**IATA 2008a**). The essential idea is to support the wing with a truss or a strut and thereby reducing the wing root bending moment.

A similar principle of weight reduction by partly unloading the main wing is found in the concept of **joined-wing and box-wing aircraft**. The joined-wing aircraft concept features tandem wings that join between 60 and 100% of the front wing. While the rearward wing is swept forward and attached to the tail, the front or main wing is swept backwards: the result is a diamond-shaped form from both the top view and the front view (**Mello 2006**, **Kroo 2006**). The concept of the box-wing aircraft is very similar. The most obvious difference is the connection of the front and rear wing: while the wings of the former join directly, the wings of the box-wing are connected by endplates. This reduces potential interference problems at the wingtips: flow fields of both wings are more isolated (**Sweetman 2000**).

4.1.4 Reducing Interference Drag

On component level, interference drag is extra drag caused by bodies placed close to each other in an airstream. The total drag of the bodies will nearly always be higher than the sum of the individual drags. This is especially important for the arrangement of wings, engines and fuselage, where the drag increment consists of parasitic drag caused by the interference with the boundary layer and induced drag due to a change in lift distribution.

Interference drag can be minimized by finding an appropriate geometric layout of all airplane components and by well-designed fairings and fillets (**Roskam 1997**). Today's aircraft feature very sophisticated designs to minimize interference drag. On a classic cantilever, the future drag reduction by a further refinement of engine/wing and fuselage/wing intersections is therefore small. A better integration of the fuselage with the wing will ultimately lead to the concept of a blended-wing-body aircraft. Since the De Havilland Comet in the 1950s, no aircraft buried the engines in the wing or the fuselage. With engine efficiency being one of the most powerful means to reduce fuel consumption (see the parametric study in subchapter 3.3) and η increasing with higher BPR, it is a reasonable belief that in the near future aircraft engines will be too large in diameter to be embedded in a classic cantilever configuration. Buried engines show further disadvantages in terms of maintainability, exchangeability and protection against engine burst (**Greener By Design 2005**). For BWB aircraft however, several buried concepts have been proposed that show benefits not only in terms of interference, but also reduce weight and eliminate aircraft control surfaces (**Greener By Design 2005**, **IATA 2008a**).

4.1.5 Reducing Wave Drag

Wave Drag is drag asscoiated with compressibility effects at high-speed flight. Flow over a curved surface (outside the boundary layer) shows local velocities significantly different to

the speed and Mach number of the free flow. Hence, local velocities exceeding the speed of sound (M > 1.0) may already occur at subsonic cruising speeds (**Roskam 1997**, **Heinze 2005**). For a given aircraft (or wing/profile) and angle of attack, the *critical Mach number* M_c of the free flow indicates the first emergence of such local sonic conditions. A further increase beyond M_c will result in local supersonic flows that terminate in shock waves proportional in size and strength to the flight Mach number.. The increase in aircraft drag is directly related to the strength of the shock waves. Wave drag will grow steadily until a strong enough shock wave separates the boundary layer (**Roskam 1997**). Similar to the effect of flow separation described above, the drag coefficient will increase abruptly. This effect is called drag divergence, the related flight Mach number *drag divergence Mach number* M_{dd}.

Theoretically, the emergence of wave drag could thus be avoided by flying at lower Mach numbers. However, for today's turbofan-powered aircraft, the most efficient cruise Mach number is "... part way up the drag rise ..." (**Greener By Design 2005**, p. 21), as propulsive efficiency increases with flight speed. To increase η_{prop}, aircraft flying at high subsonic speeds should have drag divergence Mach numbers as high as possible. To achieve high cruising speeds at relatively low wave drag, modern transport aircraft use so-called *supercritical airfoils*. These specially tailored airfoils allow supersonic flows and shock waves to develop, but keep them at minimum strength. Another very common technique is to sweepback the wing and thereby reducing the effective Mach number of the airflow advancing the wing.

There have been studies on more un-common techniques to reduce wave drag. Some of them use passive systems (e.g. bumps or porous regions) on the wing to **spread the shock into multiple shocks of lower strength**. Active systems are supposed to do the same by boundary layer blowing or suction. As with active systems for laminar control, this will probably increase wing weight and maintenance costs (**Greener By Design 2005**). Even not found in literature, it is however imaginable that in the long-term, a single system could fulfil the demands of both, laminar control and active wave drag reduction.

The contribution of wave drag to over-all airplane drag is small (< 5 %, **Greener By Design 2005**). Nevertheless, reducing wave drag can extensively contribute to fuel savings. This is less due to the simple reduction of drag, but to the regained possibility of reconsidering the wing design. Un-sweeping the wing would then not only allow for a lighter wing structure, but also for an increased wingspan and a wider application of laminar flow technologies.

4.1.6 Reducing Off-Design Flying Time

Conventional wings in cruise condition are generally designed to meet the requirements at a fixed design point. Flying at optimum L/D is then possible by keeping a constant angle of attack. If also the cruise Mach number should be kept constant, the aircraft needs to constantly

climb during cruise to compensate for the loss in fuel weight. The so-called cruise-climb procedure is however generally not possible as, for safety reasons, air traffic control relegates the aircraft to a constant altitude.

Using a mission-adaptive wing could help shifting average flight *L*/*D* closer to optimum. The general approach is allowing the wing to change its section airfoil shapes during flight and thus to be continuously tailored to each flight segment (**IATA 2008a**). In a discrete manner, this is already done on currently active aircraft. Trailing edge (flaps) and leading edge (slats) devices vary camber and shape of different wing sections for take-off, climb-out, cruise, approach and landing. From this, the progress to a truly mission-adaptive wing can be divided into multiple steps. The first one is to allow for a continuous variation of flaps and slats. The variation can then be automated for all flight segments to ensure that the devices are always in optimum position. A similar system is projected to be on-board the Airbus A350 (**Kingsley-Jones 2006**). More advanced mission-adaptive wings would then use so-called *active* or *smart* materials, e.g. piezoelectric devices and shape-memory alloys. This would allow for a fully morphing wing doing without additional leading and trailing edge devices as it is shown in Fig. 4.5 (**IATA 2008a**).

In the long-term, a mission-adaptive wing could not only benefit lift-to-drag ratios, but also allow for an increased buffet boundary (i.e. divergence drag Mach number), increased flight speed and reduced wing structural weight (**IATA 2008a**).

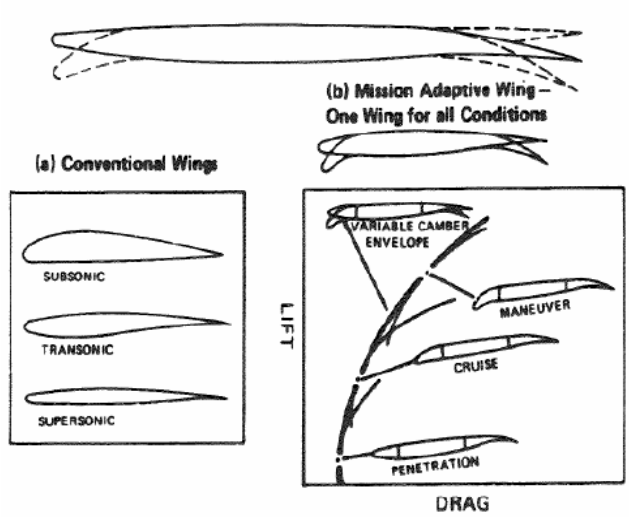

Fig. 4.5 Variable Camber Wing Concept (**IATA 2008a**)

4.2 Aircraft Engines and Secondary Power

Maximum engine efficiency is achieved by maximising thermal and propulsive efficiencies. As on today's aircraft, either the engines or a gas-turbine auxiliary power unit (APU) powers the aircraft systems, fuel consumption is further a function of the energy needed for secondary power. Means to lower the amount of CO_2 emitted by increasing engine efficiency or lowering fuel consumption of the aircraft systems are presented below.

4.2.1 Increasing Thermal Efficiency

Modern aero engines, i.e. turbofans, can easily be split into two components: The core engine with the primary flow, and the secondary flow provided by the fan. In this context, thermal efficiency can be seen as the efficiency of the core gas turbine as a heat engine. Thermal efficiency is then defined as

$$\eta_{th} \overset{def}{=} \frac{\text{Mechanical Work Output}}{\text{Heat Energy Input}} \quad . \tag{4.2}$$

Assuming fully efficient (100 %) core engine components, η_{th} is simply a function of the over-all pressure ratio (OPR) (**Kurzke 2009**). For real engine components with lower efficiencies, η_{th} is however also dependent on the temperature of the gas leaving the combustion chamber, i.e. entering the high-pressure turbine. This temperature is frequently called turbine-entry-temperature (TET) (**Gmelin 2008**) or burner exit temperature (**Kurzke 2009**). For temperatures up to 2 000 K, TET is a function of the injected fuel-air ratio only. Above 2 000 K, TET becomes dependent on the pressure as well.[1]

The influence of TET and OPR on thermal efficiency is shown in Fig. 4.6 where *T4/T2* denotes the ratio of turbine entry temperature to the temperature at the inlet. The dashed line at the top shows thermal efficiency for fully efficient engine components, i.e η_{th} being independent of TET. The uppermost solid line (*T4/T2* = 10.3) denotes the maximum efficiencies achievable with component efficiencies of 90 % at the maximum realizable turbine entry temperature. This implies a TET around 2 500 K[2], which is a maximum for burning kerosene (**Kurzke 2009**).

---

[1] It should be noted, that the relation of turbine inlet temperature to fuel-air ratio is not linear as indicated by engine theory. Hence, peaks in TET and fuel-air ratio are not identical, i.e. maximum TET does not occur at stoichiometric combustion (**Kurzke 2009**).

[2] The engine inlet temperature *T2* is 244 K for a flight at 11 km altitude, Mach 0.8 (**Kurzke 2009**).

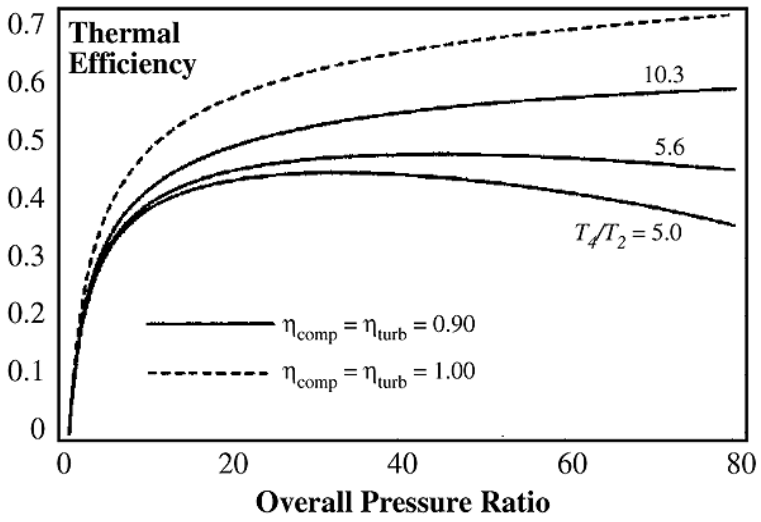

Fig. 4.6 Thermal Efficiency over OPR and TET (**IPCC 1999**)

Today's state-of-the-art turbofan engines hold pressure ratios in the region of 45 and TETs around 1 700 K. With component efficiencies of 90 %, this yields in thermal efficiencies in the order of 45 to 50 % (**Gmelin 2008**). According to Fig. 4.6, an further increase in thermal efficiency is achievable by increasing component efficiencies, by changing to higher burning temperatures (TET) or by higher over-all pressure ratios (OPR).

It is important to realize that all parameters mentioned above are strongly coupled. For example, an increase in component efficiencies with constant OPR shifts the optimal turbine entry temperature to lower values (**Kurzke 2009**). Similarly, as observable from Fig. 4.6, engines with lower TET have their maximum efficiency at lower over-all pressure ratios. Simply put, there is an optimum for every parametric combination.

Increasing thermal Efficiency by Increasing TET

The maximum turbine entry temperature is mainly set by the heat resistance of the turbine material. Technological enablers for higher TET are thus new, **highly heat-resisting materials**. It is anticipated (**Gmelin 2008**, **IATA 2008a**) that the next considerable step in temperature will be contributed to the use of ceramic materials for turbine components. So-called ceramic-matrix-composites (CMCs) combine both light weight and higher heat resistance. According to **Gmelin 2008**, the use of ceramic materials could increase maximum TET to 1944 K.

The natural thermal resistance of turbine materials can be increased by using so-called thermal barrier coatings (TBCs) and internal turbine cooling. Both technologies are already in use on current engines: "In fact, many of today's turbine engines operate at turbine inlet

temperatures which are above the melting point of the materials used" (**Roskam 1997**, p. 249). However, improvements are possible by new coating materials and by a more efficient cooling system. New coating materials include CMC and Niobium-Silicon (Nb-Si) (**IATA 2008a**). Moreover, according to **IATA 2008a**, current engines do not fully exploit the performance improvements of current TBCs. This is due to state-of-the-art TBC performance not being considered fully monitorable and reliable. Advances in TBC reliability could thus allow for a higher TET.

An advance in internal turbine cooling is imaginable by the concept of ***cooled cooling air***. Today, cooling air for the turbine blades is taken directly from the compressor. The idea is to lower the temperature of the cooling air by guiding it along the secondary (fan) flow. This could provide higher heat resistance of the turbine material and lower the pressure losses on the compressor (**Gmelin 2008**, **Bock 2007**).

Higher turbine inlet temperatures, i.e. higher combustion temperatures, lead to an increase in NO_x production. This has become increasingly important over the last few years due to growing environmental concerns. It is prospected that future aircraft regulations will not only limit the NO_x emission on ground, but also in cruise (**SBAC 2008b**). With current technology, the room for higher TET is therefore also limited by future emission regulations. There are however promising technological concepts that may allow for an increased TET while keeping constant or reducing NO_x emissions. **New low-NO_x combustor technology** entering service from the year 2010 on allows for a successive improvement of the fuel burning process. Low NO_x (lean-burn) combustors in development include the Twin Annular Premixing Swirler (TAPS), the TALON X and the Rich Quench Lean (RQL) combustors (**IATA 2008a**).

Increasing thermal Efficiency by Increasing OPR

Increasing OPR is realizable by a faster running engine core and more efficient compressor stages. To allow for an increased rotational rate of compressor parts and the associated temperature rise, **compressor materials with a higher heat resistance** are needed. Today, titanium is the state-of-the-art material for compressors (**IATA 2008a**). So-called titanium metal-matrix-composites (Ti-MMCs) are the most promising future choice. These consist of layers of monolithic titanium and composite material, which is made of metal and reinforced carbon. Ti-MMCs are said to increase both heat resistance and specific strength (**IATA 2008a**). Thus, also weight savings are possible.

Compressor efficiency is inversely proportional to the clearance between the compressor rotor blades and the casing. More efficient compressor stages could become possible by using **active clearance control** (ACC). Further, towards low mass flow rates, the stable operation

of compressors is limited by the surge line, which indicates the occurrence of serious flow instabilities (**Willems 1998**). Compressor efficiency at low mass flow rates could thus be increased by actively suppressing these instabilities: a technique called **active surge control** (ASC), which works by injecting air onto the rotor tips. Both ACC and ASC are investigated in the European *new engine core concepts* (NEWAC) project under the names *Active Core Engine* and *Flow Controlled Core Engine* (**NEWAC 2009**, **Bock 2007**).

Increasing thermal Efficiency by Minimizing Pressure Losses

Pressure losses are lower if bleed air taken from the engine core is reduced. For the compressor, this concerns cooling air taken for the turbine blades. For constant TET, the need for cooling air decreases with increasing heat resistance of the turbine material or the concept of cooled cooling air (see above). NEWAC's Active Core Engine project (**NEWAC 2009**) investigates the application of an active cooling system. While on current engines a fixed amount of the air delivered by the high-pressure compressor is used for cooling, the new system should control this amount actively and thereby reduce unnecessary pressure losses.

Further pressure losses occur from bleed air taken for the hydraulic and pneumatic aircraft systems. The bleed air is generally taken from the airflow behind the LP compressor. Thereby aircraft engines lose some of their efficiency to the systems, especially during descent when the engines are in idle. **A More Electric Airplane** (MEA) is often regarded as the next step to allow for a *no bleed* engine and higher engine efficiency. This implies the (wider) use of electricity instead of pneumatic and hydraulic energy as a power source for the aircraft systems (**Daggett 2003a**, **Gmelin 2008**), see chapter 4.2.3 below.

Increasing thermal Efficiency by Inter-cooling and Recuperation

A further efficiency increase can be obtained by a different over-all thermodynamic cycle, e.g. by using a recuperative system. In this case, the rise in turbine inlet temperature is partly achieved by recycling heat from the exhaust gases (**Boggia 2004**, **Gmelin 2008**). This reduces specific energy needed from the fuel and results in a lower amount of fuel being injected, thus lower fuel consumption. Engine efficiency can further be increased by inter-cooling the air exiting the LP compressor and entering the HP compressor. This is generally done using the colder air of the secondary (fan) flow. As the HP compressor needs less energy to compress the cooler air, the energy input (fuel amount) can be decreased (**Boggia 2004**, **Gmelin 2008**).

Both concepts are expected to show highest efficiencies if combined. This results in a thermodynamic cycle called ***Inter-cooled Recuperative Engine*** (IRA) Cycle. A possible

architecture is shown in Fig. 4.7. The inter-cooling makes the process of recuperation more effective, as the temperature difference between the exhaust gas stream and the compressor exit stream is higher (**Gmelin 2008**).

The IRA-cycle is most efficient at rather low over-all pressure ratios (OPR < 30), see Fig. 4.8. This helps reducing engine weight (lower stage count) and NO_x emission, which increase with OPR. The IRA cycle is also investigated in the NEWAC project. However, due to the high complexity of the system, inter-cooled recuperative systems are expected to enter series production not until 2020 (**Gmelin 2008**).

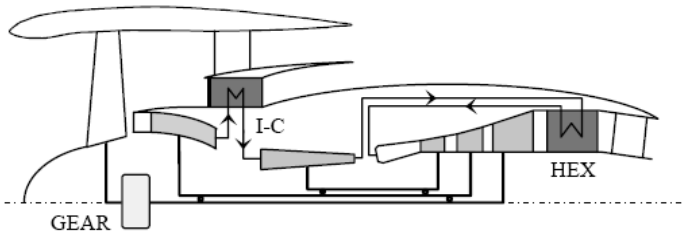

Fig. 4.7 Concept of a Three-Spool Geared Turbofan with Intercooler (I-C) and Recuperator (HEX) (**Boggia 2004**)

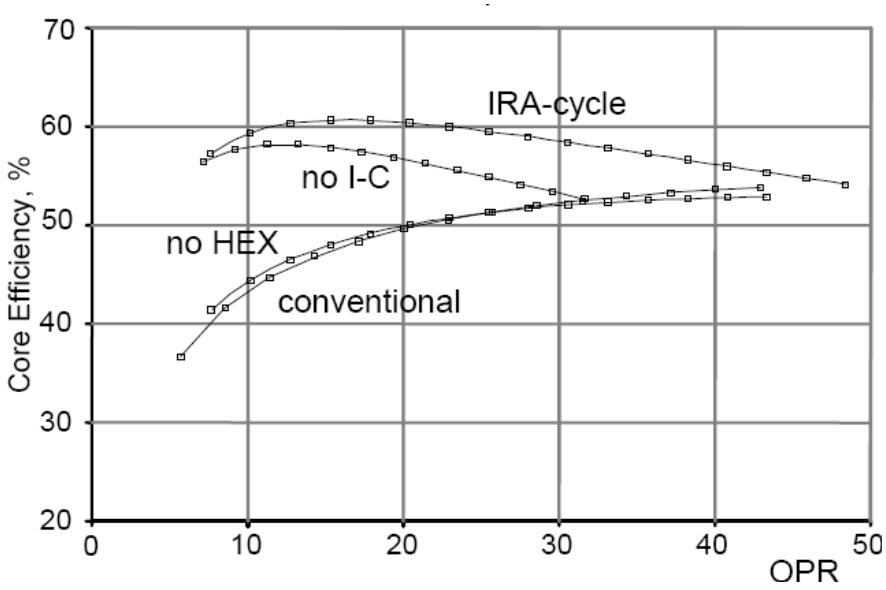

Fig. 4.8 Core Efficiency (η_{th}) vs. OPR – Conventional, Inter-cooled, Recuperative and IRA-Cycle (**Boggia 2004**)

4.2.2 Increasing Propulsive Efficiency

The over-all propulsive efficiency of a jet engine is the amount of mechanical energy output that is effectively used to propel the aircraft, i.e. the energy amount that actually produces thrust. Hence

$$\eta_{prop} \overset{def}{=} \frac{\text{Propulsive Output}}{\text{Mechanical Work Output}} \tag{4.3}$$

The over-all propulsive efficiency η_{prop} represents the propulsive efficiency of the fan, the component efficiencies of the low-pressure system driving it and the propulsive efficiency of the core stream. It further includes losses due to nacelle and engine drag, as internal engine drags are considered as an increase in specific thrust (**Gmelin 2008**).

Increasing propulsive Efficiency by Lowering Specific Thrust

η_{prop} is mainly influenced by the ratio of exhaust speed to flight speed. An ultimate propulsive efficiency would imply a ratio of 1.0, a value clearly not realizable, as the engine produces thrust by ejecting air at a higher velocity than that of the aircraft (**Greener By Design 2003**). To produce a given thrust with lower exhaust speeds, the mass flow through the engine needs to be increased by **higher by-pass ratios** (BPR), i.e. an increase in fan diameter for a given core size. For a conventional turbofan, an increase in fan diameter is unfortunately always accompanied by an increase in nacelle diameter and length. Nacelle drag increases roughly as the square of fan diameter (**Greener By Design 2003**). Moreover, weights of the fan and nacelle increase. Today's high-tech engines feature by-pass ratios in the order of 8 to 9. These ratios are the outcome of a carefully balanced approach, where the increase in fan diameter and the resulting increase in weight and drag are at an optimum for current technology. On current engines, the fan accounts for 20 to 30 % of over-all engine weight (**Mecham 2006**). New technologies will allow for a further reduction in specific thrust, i.e. for larger fan diameters.

According to (**Gmelin 2008**), new lightweight materials and construction methods for the fan blades and housing will shift the optimum to by-pass ratios around 10 to 12 in 2012. On today's civil aircraft, these components are mainly made of solid titanium-alloys. Promising future materials are carbon fibre reinforced polymers (polymer matrix composites, PMCs) for weight reduction. Nevertheless, titanium is still assumed being a future fan material. New manufacturing methods allow for constructing hollow titanium fan blades that achieve considerably lighter fan architectures than today's state-of-the-art designs and are still rugged enough to survive damages by foreign objects (**IATA 2008a**).

For simple two spool architectures, there is a trade-off between increasing the propulsive efficiency the large fan by reducing the rotational rate of the shaft and increasing the efficiency of the coupled internal turbine. Whilst the first is inversely proportional to the rotational rate, the latter increases with a faster running engine core. Clearly, more turbine stages are able to compensate for the loss in speed, but this increases engine size and accordingly weight and drag. For an optimal design of both components, fan and LP turbine need to be de-coupled. This is possible either by implementing a third spool (consisting of an additional compressor and an additional turbine) or by the concept of **a geared turbofan** (GTF). Former is already in use on modern turbofan engines, latter is said to enter the market in 2013 (**Gmelin 2008**, **IATA 2008a**). A schematic showing the concept of the GTF is given below (Fig. 4.9).

Decoupling through gearing is said to have advantages over the three-spool concept. Instead of adding further turbine and compressor stages, the existing number can be decreased as the faster running LP compressor and turbine are more efficient. This allows for a shorter and lighter core engine (**Gmelin 2008**, **IATA 2008a**). Due to the high turning speed, the LP system is able to operate with a shaft of a smaller diameter. This allows for an easier integration of the LP shaft and further weight reductions (**Gmelin 2008**). Moreover, the slow rotational speed of the fan enables a reduction of the number of fan blades to about the half of previous-generation turbofans and a reduction of blade-specific weight (**IATA 2008a**). Even though the gearing mechanism adds extra weight to the engine, the GTF is therefore still lighter than conventional turbofans. Geared turbofan concepts are expected to increase BPR up to 15.0 and reduce fuel consumption by 6 to 15 % compared to the CFM56 and V2500 (**Gmelin 2008**, **IATA 2008a**). The first GTF series model is assumed to enter service in 2013 on regional and small narrow-body aircraft. An application to larger aircraft is presumably not possible as quick. With increasing fan diameter, the gear requires additional cooling and probably large heat exchanging elements (**Gmelin 2008**).

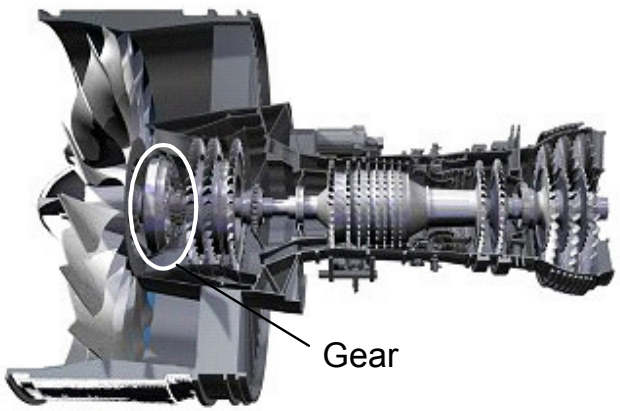

Fig. 4.9 Concept of the Geared Turbofan (**Volvo Aero 2007**)

Higher by-pass ratios hold improvements in efficiency and fuel burn only, when the fan pressure ratio (FPR)[1] is adjusted to the new design. More precisely, optimal fan pressure ratio decreases with higher BPR. This can be explained as follows. With increasing BPR and constant fan pressure ratio, the energy needed from the turbine to turn the larger fan increases, until at some point all energy is consumed by the fan and the velocity of the core exhaust stream ultimately falls to zero. To avoid this, the fan pressure ratio needs to be reduced. The optimal fan pressure ratio is generally found for $c_9 = c_{19}$, i.e. the exhaust speeds of the primary (core) stream and the secondary (fan) stream are identical. The optimal FPR for modern turbofans (BPR 8-9), flying at Ma 0.8, is around 1.7 to 1.8. An increase to by-pass ratios around 12 shifts the optima to 1.4 to 1.5 (**Bräunling 2004**, p. 393). It is important to note that the sensitivity for the optimum increases with by-pass ratio, i.e. it becomes more difficult putting optimal engine performance into practice. A variable fan exhaust nozzle, as used for flight-testing the geared turbofan of Pratt & Whitney, is able to vary fan pressure ratios during flight (**Norris 2008a**). A similar system could one day appear in a series production to ensure optimized flight performance (**Norris 2008a**, **Gmelin 2008**).

Very low fan pressure ratios are not realizable with conventional fan technology, as airflow through the multiple fan-blades is always forced to reduce its speed. Increasing flow speed further is only realizable by reducing the number of blades. However, a single fan will then not be capable of producing the required thrust. Theoretically, this could be compensated by a second fan stage that is rotating in the opposite direction, a concept known as the ***Counter Rotating Turbofan*** (CRTF), see Fig. 4.10. The CRTF could either be driven by two counter-rotating LP turbines or only one LP turbine with a gear on the second fan (**Gmelin 2008**). As **Gmelin 2008** reports, FPR lower than 1.3 will not result in further efficiency improvements for shrouded turbofans. This results in fan diameters 30 to 40 % larger than current ones and a propulsive efficiency around 87 %. However, open rotor concepts (see below) are not constrained to this limit and will eventually feature even lower fan pressure ratios. A tandem counter-rotating fan architecture further allows for removing fixed stator vanes that are currently found after the fan stage. This reduces internal engine drag and weight (**IATA 2008a**).

[1] The fan pressure ratio is the ratio of fan exhaust pressure to the fan inlet pressure.

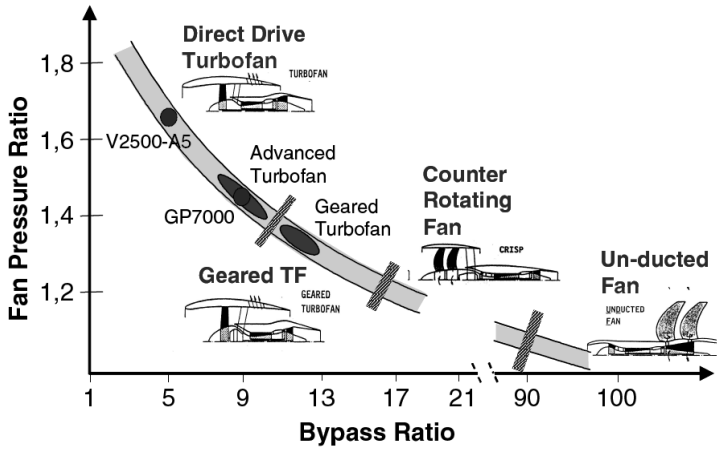

Fig. 4.10 Turbofan Engine Concepts with varying By-pass and Fan Pressure Ratio (**Riegler 2007**)

Reducing the nacelle drag is another possibility to increase propulsive efficiency. The application of natural laminar flow designs (Boeing 787 nacelle) or artificial laminar flow control by suction (hybrid laminar flow control, HLFC) has a large drag reduction potential. As **Greener By Design 2003**, p. 37 depicts, "Flow control by suction is probably more practicable on the nacelle than on any part of the aircraft because of the proximity of a source of power to drive the suction system". If achieved with small weight penalty, positive snowball effects (larger diameter fan etc.) could improve efficiency beyond the simple drag reduction. However, as laminar flow (either natural or hybrid) is still vulnerable to system failure (contamination of the surface, damage of the suction surface), first applications will not be able to take advantage of afore mentioned effects.

Open rotor, un-ducted fan (UDF) or open *Propfan* concepts (see Fig. 4.11) do completely without a nacelle. The resulting decrease in drag and weight allows for an immense increase fan diameters and BPR (>> 20), see Fig. 4.10. To allow for low enough FPRs, most open rotor concepts incorporate two counter-rotating fans. A *TSFC* reduction of 15 to 30 % is prospected (**Gmelin 2008**, **IATA 2008a**). However, there are still numerous challenges concerning the wide-range use propfans. Due to the large fan diameters and the resulting increase in tip speeds, open rotors are efficient only when flying at relatively low speeds (< 0.8 Ma): see Fig. 4.12. This restricts practical application to short- and medium-range flights (up to around 3700 km) (**Gmelin 2008**). Further, due to the missing nacelle, current open rotor demonstrators produce considerably more noise and vibration than their shrouded competitors do. The large diameter fans bring further challenges for the engine-airframe integration (**IATA 2008a**). As **Gmelin 2008** states, propfans are alternatives for short- to medium ranges and small to medium thrust classes only.

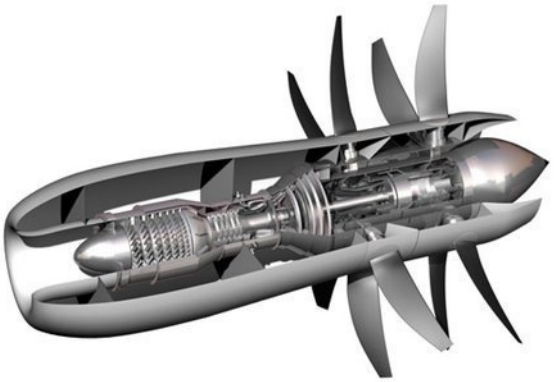

Fig. 4.11 Open Rotor (Propfan) Pusher Concept with Two-Stage Counter Rotating Fans (**Bateman 2009**)

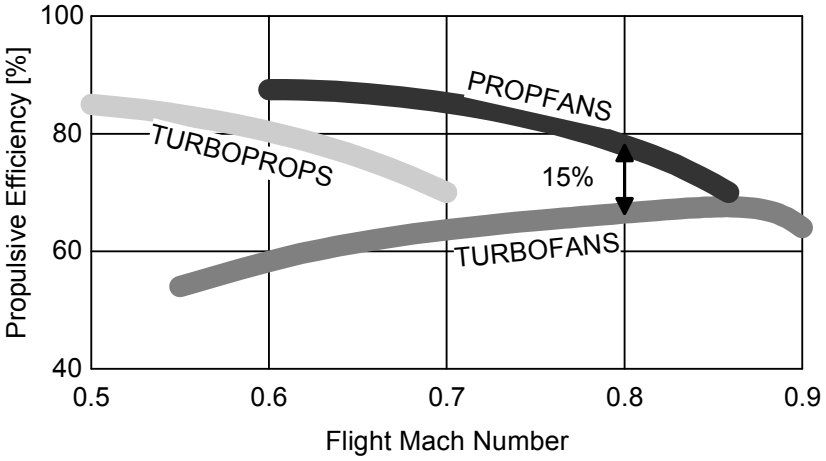

Fig. 4.12 Comparison of Propulsive Efficiencies of Turboprops, Turbofans and Propfans (reproduced from **Roskam 1997**)

4.2.3 Increasing Fuel Efficiency of Secondary Power

Today, about 5 % of aircraft block fuel consumption is due to production of on-board power (**Scholz 2009**). The power requirements can be divided into power consumed by equipment required to operate the aircraft safely (i.e. technical loads) and power consumed by equipment desired to increase passenger comfort and satisfaction (i.e. commercial loads). There are traditionally three different types of secondary power found on board, which are hydraulic, pneumatic and electrical power.

During flight and taxiing, energy for all of the three is normally provided by the aircraft engines. This is done either by taking power off the shaft (electric and hydraulic) or by taking bleed air off the engine core (pneumatic). Energy can also be provided by other power

sources, which are the auxiliary power unit (APU), batteries, a ram air turbine (RAT) or ground power (airport equipment). The APU is a small gas turbine device mostly located at the tail and is mainly used prior to flight to start the main engines and to allow the air condition system to work. However, it works also as a back-up system in flight to ensure working aircraft systems if one of the main engines or generators fails. This is especially important for aircraft flying Extended Range Twin Engine Operations (ETOPS), where the APU is declared as a safety critical device. If the aircraft is on-block, the systems are most of the time supplied by ground power. Batteries and RATs are power sources generally needed only for redundancy (**Scholz 2009**).

Staying with the current philosophy of power generation, over-all fuel efficiency of secondary power can be increased by increasing efficiency of the sub-parts. This implies better efficiency of the consumers and better efficiency in power generation. Some potential enablers are light-emitting diodes (LEDs) for cabin lighting (**IATA 2008b**), Fly-By-Light Control Systems (i.e. fibre-optic links between the flight computer and the flight controls) and a more efficient gas turbine APU (**IATA 2008a**). Another option is to smooth out the peaks in power demand, e.g. by deploying flaps sequentially rather than all at once (**EU 2004a**).

Changing to more electric systems is seen as another enabler of fuel-efficient secondary power generation. This is said to have several benefits. First, electric systems tend to be more energy efficient and reliable. Second, power supply can be configured to better match respective power demands.[1] Third, bleed air from the engines is no longer required. This reduces pressure losses and increases engine efficiency. However, if all-electric systems are the better choice is not indisputable. As traditionally pneumatic systems, e.g. wing anti-ice and air condition packs, need to be electrically powered, more power needs to be taken off the engine shaft. Further, current electric systems are said to be heavier than their pneumatic and hydraulic counterparts (**EU 2004a**). The first commercial application of a 'no-bleed' system is found on the Boeing 787 (assumed service entry in 2010). Despite the above-mentioned disadvantages, Boeing argues that over-all system power taken off the engines is thereby reduced by up to 35 % (**Sinnett 2007**).

Another possibility is to change the fundamental principle of secondary power production, that is, discontinue using the aircraft engines as the primary energy source. The simplest approach is using a more efficient gas-turbine engine throughout the entire flight. Replacing the APU by **a fuel cell or a gas turbine-fuel cell hybrid** could bring further benefits. This is especially interesting as fuel cells work with hydrogen and thus do not emit any CO_2 (**IATA 2008a**, **Scholz 2009**). However, it is assumed that it will take several decades until fuel cell technology has matured enough to be used for the over-all production of secondary power, see

[1] To function on command, today's hydraulic and pneumatic systems maintain constant pressure levels, i.e. require constant power. In comparison, electric power can be provided almost instantaneously and thus needs to be supplied only when needed (**EU 2004a**).

Fig. 4.13. Further, all-electric aircraft system architecture is generally seen as being essential for full applicability. A technology that is rather unlikely to improve to being useful for air transport, but produces fully regenerative energy and is theoretically imaginable as a secondary power source, is solar power (**IATA 2008a**).

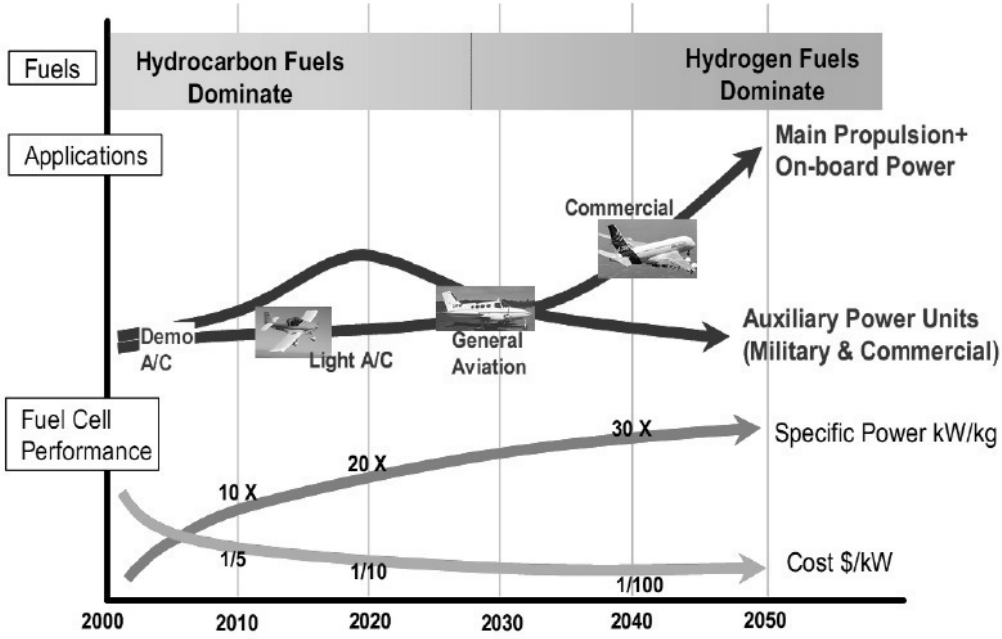

Fig. 4.13 Envisioned Application of Fuel Cell Technology in Aviation (**Maclin 2003**, found from **IATA 2008a**)

Not strictly increasing efficiency of secondary power production, but however decreasing fuel consumption by working on the systems, is the so-called landing gear drive. This is an electric motor or a series of electric motors added to the nose or main landing gear. It would allow shutting down the engines for landing taxi or when stuck in lengthy outbound taxiing queues. The electric motors would then be powered by the APU. Certification work for one such system has already started (**Forrester 2009**). As the system allows for autonomous pushback, CO_2 emitted from ground services (pushback tugs) can also be reduced. According to the developing company, about 65 % of total taxi fuel can thus be saved on a typical Boeing 737 flight. This calculates to an absolute fuel saving of around 200 kg fuel or 635 kg CO_2 per flight (**Forrester 2009**, **WheelTug 2009**).

4.2.4 Potential Future Improvements

Disregarding the potential of recuperative systems, a literature review suggests maximum achievable thermal efficiencies in the order of 58-62 %, with maximum TET of 2500 K, fully efficient components and pressure ratios above 80 (**Gmelin 2008**, **Greener By Design 2003**,

IPCC 1999, **Kurzke 2009**). Thus, compared to today's state-of-the-art engines (50-55 %), a potential improvement of 3 to 12 % seems reasonable.

Fig. 4.14 shows theoretical and practical limits for further over-all engine improvements. A future reduction in fuel consumption of 25 to 30 % is thus achievable. This indicates an over-all engine efficiency of 55 %, with η_{th} (60 %) and η_{prop} (92.5 %) at their theoretical limits. If environmental (NO_x) regulations limit turbine inlet temperatures to lower levels, the potential for further improvements is limited to values around 20 to 25 %. The theoretical limit for propulsive efficiency can be achieved most likely only with open rotor configurations (**Gmelin 2008**).

CO_2 production resulting from secondary power could theoretically be eliminated if all power was produced from a fuel cell or a bio-fuel powered gas turbine APU. This calculates to a reduction in over-all fuel consumption of around 5 % (**Scholz 2009**), presuming the new system architecture does not increase aircraft all-up weight and drag.

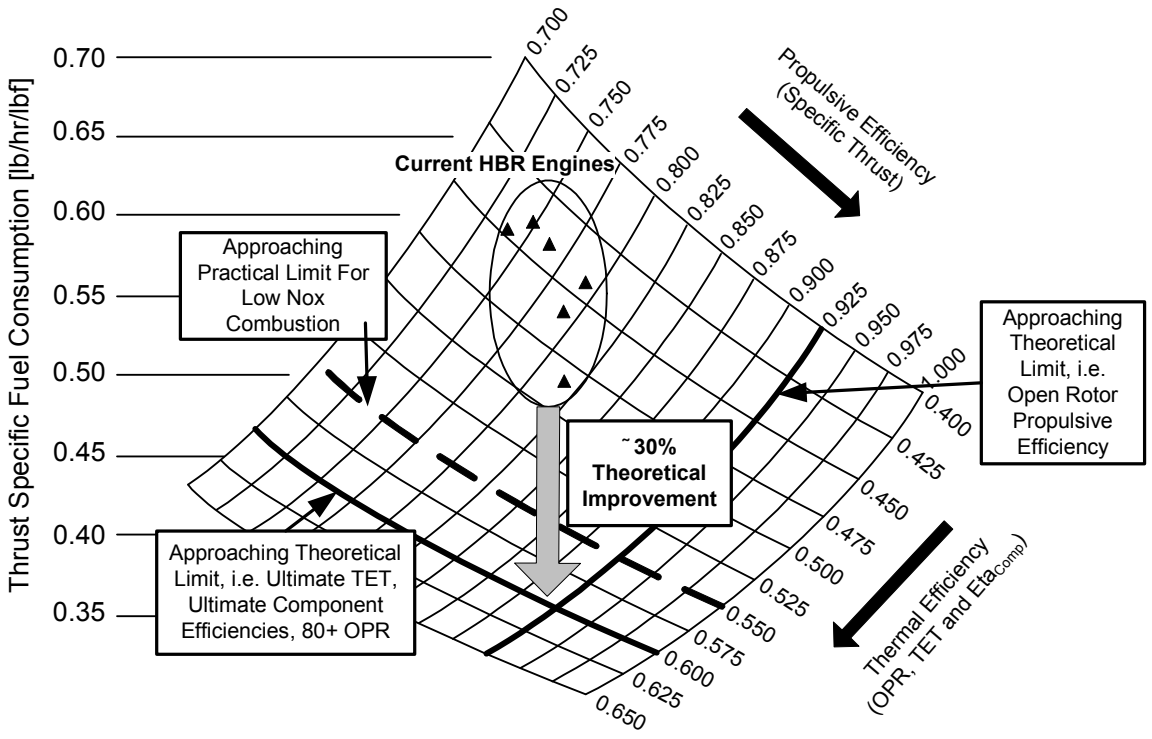

Fig. 4.14 Uninstalled SFC as a Function of Thermal and Propulsive Efficiency (Copyright Rolls Royce plc, reproduced from **Greener By Design 2005**)

4.3 Aircraft Empty Weight

As was shown by the parametric study in chapter 3, reducing empty weight strongly contributes to fuel savings. For the purpose of this section, aircraft empty weight is divided into two elements: structure weight and systems/fixed equipment weight (including the weight of the trapped fuel and the crew). Means for reducing empty weight by reducing weight of the two elements are regarded in turn below. It should be borne in mind that for re-sized aircraft, snowball effects amplify component weight reductions: the ultimate weight saving on the aircraft is larger than the initial weight saving on the component.

4.3.1 Reducing Structure Weight

For this analysis, the following parameters are assumed being set: design payload, design range, systems/fixed equipment weight, aerodynamic and engine efficiency. The weight of the airframe (i.e. fuselage, wings and empennage) is then mainly driven by the geometrical layout of the aircraft, the specific strength of the materials used and additional load multipliers, which are structural reserve factors and gust load factors.

Staying with the dominant configuration, a conventional cantilever aircraft with back-swept wings and wing-mounted engines, the most obvious means of reducing empty weight is by **using lighter and stronger materials.**

Following the trend of the last decades, the relative share of composite materials is likely to increase for both structural and interior components. About 15 % of empty weight is composite material in large aircraft currently under production. This value could increase up to 65 % for an aircraft produced in 2020, see Fig. 4.15. A resultant airframe weight reduction of 10 to 20 % is projected (**Greener By Design 2005**, **IATA 2008a**). Even though composites are often regarded as the more advanced material, also new light metal alloys such as aluminium-lithium (Al-Li), aluminium-magnesium-scandium (Al-Mg-Sc) and advanced titanium alloys offer significant weight and strength benefits. Hybrid alloys such as glass-fibre-reinforced metal alloys (GLARE, CentrAl) and aramid-fibre-reinforced metal alloys (ARALL) are said to combine the benefits of composites and metal and thereby lead to even higher weight savings. Finally, research at the basic level could bring out new *nanomaterials* and technologies that improve the performance of classic composites up to a possible 30 % weight reduction (**Greener By Design 2005**, **IATA 2008a**).

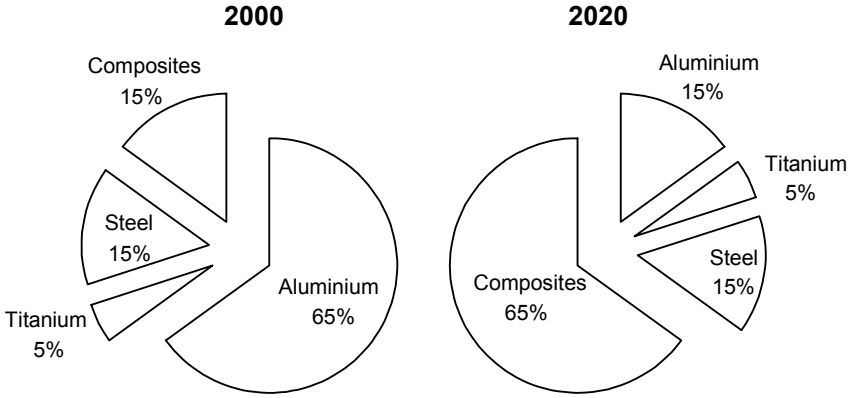

Fig. 4.15 Materials Weight Distribution – Typical for 2000, Conjectural for 2020 (reproduced from **Greener By Design 2005**)

Regarding metallic structures, today's aircraft structural design largely fulfils traditional lightweight construction philosophy. This is seen for example on the design of the wing, which fulfils multipurpose functions (e.g. integral wing-tanks), is unloaded by carrying fuel and engines and is built of mostly integral structures to reduce component material to a minimum (**Seibel 2003**). However, further improvement through new manufacturing technologies is imaginable. New joining methods such as friction stir welding and laser beam welding could offer reduced empty weight by lighter, rivet-free joining (**IATA 2008a**).

Today, fibre reinforced composite structures are designed as if they were built of metal ('black metal design'). This however does not fully exploit the potential of the new materials. The departure from traditional construction schemes for composite structures could thus offer considerable weight benefits. On the one hand, this requires more research into basic composite construction methods. On the other hand, manufacturers and regulation authorities need to transform design and certification principles to facilitate the implementation of the former.

There is a chance to decrease wing loads and thus weight by **active load alleviation** systems. These systems make use of the wing's control surfaces to reduce or distribute loads. Especially the influence of gust load factors and additional manoeuvre loads can thereby be minimized. Similar systems are already found on in-production aircraft such as the Airbus A340-500/600 and the Boeing 777 Freighter. More advanced systems are under development, which aim at combining the benefits of a mission-adaptive wing for both aerodynamic shaping (see sub-chapter 4.1.6) and load reduction (**IATA 2008a**). Wing loads in general may be decreased also by an active wing vibration damping using smart materials, for example so-called *Magnetic Shape Memory Materials* (**EU 2004b**).

In the long-term, rethinking the general layout of aircraft could help structural loads to be lessened. Especially **new airframe configurations** such as the hybrid- or blended-wing-body

(BWB), the truss-braced wing (TBW) and joined/box-wing concepts offer radical weight savings (**IATA 2008a**, **Mello 2006**, **Grasmeyer 1998**, **Scholz 1999**).

As shortly discussed in chapters 2.2.2 and 3.5.5, for today's aircraft, the optimum range is assumed a medium one (around 4000 km). Longer design ranges affect the fuel efficiency negatively, because of the increase in required fuel and structural weight. According to the case studies found in **Greener By Design 2003** and **Green 2006**, the approach of **multi-stage long distance travel** (also known as multi-sector journeys) can considerably reduce fuel consumption on ultra-long ranges. Thereby the aircraft is not designed to travel the entire distance in one flight, but to make refuelling stops at intermediate airports. It needs to be investigated if this procedure is of low customer acceptance as flight time is increased and if it increases direct operating costs due to a higher maintenance requirement (more cycles) and more landing fees. A similar approach is the idea of civil air-to-air refuelling (**Truman 2006**). However, as this requires large changes to the ATM system and on-board equipment and further has serious safety issues, this can be assumed realizable only in the very long-term.

There were also some more uncommon approaches to reducing aircraft weight identified. First, with today's and future aircraft being more reliable and equipped with structural and system health monitoring systems[1], certification authorities could allow for a design with reduced structural reserve factors and reduced fuel reserve requirements. Second, a design for **reduced aircraft life** could allow for lower fatigue requirements (thus reduce aircraft weight) and accelerated fleet turnover (**Greener By Design 2005**). These approaches however need further investigation. Reducing safety factors and fuel reserves comprises the risk of low passenger acceptance. An increased fleet turnover from a reduced aircraft life means higher production and retirement rates. Increased life-cycle CO_2 emissions from powering the production and recycling the aircraft need to be assessed, before a final statement about the ecological benefit can be drawn. A short case study delivering a first estimate to the impact of an accelerated fleet turnover is provided in chapter 6.3.2.

4.3.2 Reducing System and Fixed Equipment Weight

Aircraft systems (less the aircraft engines) and passenger support services account currently for around 13 % of total empty weight (**Greener By Design 2003**). At the flight system level, new technologies for flight control (Fly-By-Light, wireless flight control) offer large potential for component weight reduction. The weight of high-lift systems could be reduced using new variable camber and morphing wing concepts (**IATA 2008a**).

---

[1] Structural health monitoring is the process of identifying changes to the material and/or geometric properties of the structure to detect small damages before they can cause major problems (Farrar 2007).

Aircraft engines contribute approximately 10 % to total empty weight. Promising technologies for weight reduction include polymer matrix composites (PMC) for the fans, *Blisk*[1] and *Bling*[2] technology and metal matrix composites (MMC) for the compressors and ceramic matrix composites (CMC) for the turbines (**IATA 2008a**). Improved aerodynamic design of the turbomachinery can help to increase stage loadings and reduce the number of stages for a given over-all pressure ratio (OPR) (**Greener By Design 2003**). This would reduce the weight of the core engine. Further weight savings could be reached by no-bleed engine architecture (**Sinnett 2007**). However, the intention behind reducing component weights on aircraft engines is not always a reduction in over-all engine weight. In many cases, the weight benefit will be used to allow for greater by-pass ratios or higher OPR, see subchapter 4.2.

The landing gear accounts for about 7 to 10 % of over-all empty-weight (**Roskam 2002**). As for the other systems, weight reductions in the near future are expected from replacing the traditional hydraulic actuation with an electric one. In the field of new materials, recent developments include titanium and composite application for parts traditionally made of steel. In the medium term, titanium matrix composites promise further weight reductions as they show properties exceeding the ones of titanium and steel. The material and manufacturing costs are however too high for current application (**Messier-Dowty 2005**). It has been proposed that aircraft could generally do without a landing gear or only a lightweight emergency one if terrestrial (automated) take-off and landing system would become available at the airports (**Truman 2006**). This would not only reduce empty weight by up to ten percent, but also reduce drag and noise when approaching the airport, improve airframe design (landing gear integration) and increase the volume of the cargo compartment. The fuel savings were probably immense. However, because this implies a wide range intervention into the airport infrastructure and aircraft design, this is assumed being a far-future technology (> 2030).

Generally, research into lighter materials and reduced weight of single components will allow for weight savings in internal furnishings, passenger equipment and different systems. Some promising concept are so-called *High-Strength Glass Microspheres* to reduce weight of interior plastics, high power LEDs for cabin lighting and wireless optical connections for in-flight entertainment (**IATA 2008b**). Even though the benefit of the single technologies is rather small, the cumulative weight savings could help decreasing interior weights considerably. It should however be noted that component weight reductions on the system level are often offset by increased passenger demands concerning comfort and entertainment (**Greener By Design 2005**).

---

[1] A *Blisk* (Blade Integrated Disk) is a compressor component that combines both disk and compressor blades in one integrally manufactured part. It offers up to 50% component weight saving (**Greener By Design 2005**).

[2] A *Bling* (Integral Bladed Metal Matrix Ring) is an advanced Blisk that offers more significant weight reductions by increased inner diameters. It offers up to 70% component weight saving (**Greener By Design 2005**).

Finally, the system weight increase due to moisture in aircraft insulations can be actively minimized for example by using so-called *zonal dryers* or some sort of drain apparatus for the insulations (**Gupta 1985**, **enviro.aero 2008**).

4.4 Alternative Fuels

Beside its weight, the general impact of the fuel used on aircraft CO_2 emission is through the fuel heat content *H* and the specific carbon dioxide emission *SCE*. As both parameters are set from the fuel regarded, this chapter gives a brief overview over potential kerosene alternatives and their influence on the parameters.

H is a weight specific parameter. It defines the energy produced per kg fuel burned. This is an important factor, as the higher the heat content per unit weight, the lower the fuel weight for a given mission. However, aircraft fuels need not only to have a high energy content per unit weight, but also by unit volume. If the heat content per unit volume is low, the same amount of transported 'energy' needs larger tanks. For example, "The volumetric heat of combustion for LH_2 [liquid hydrogen, author's note] is so poor that it would force airplane design compromises" (**Daggett 2006**, p. 2).

Concerning the fuel's *SCE*, alternative fuels that are termed CO_2 neutral or 'climate friendly' must be separated into two categories. The first group consists of fuels with low or no carbon content, e.g. liquid hydrogen. Their ratio of CO_2 emitted to energy released during combustion is low on the local level, i.e. the aircraft is effectively producing less emissions. The second group of fuels consists of the so-called bio-fuels. Their 'local' *SCE* does not differ greatly from the one of kerosene. As biomass (woodchips, straw, switch grass, etc.) is the feedstock however, "the CO2 absorbed by the plant matter during its lifetime will offset the emissions produced when the fuel is burnt" (**SBAC 2008a**, p. 4). As a result, their 'global' *SCE* can be assumed lower. The ultimate benefit is then dependent on the savings in life-cycle CO_2 emission: see Fig. 4.16. Shown on the right hand side is the life cycle for an aviation bio-fuel, which transportation and production is powered by conventional fuel, e.g. gasoline, coal and natural gas. While all of these processes emit CO_2, only the emissions produced by the aircraft can be assumed as having been absorbed by the feedstock. To offer very high emission benefits, feedstock for the entire production and transportation cycle should thus be of a renewable source. Life-cycle carbon dioxide emissions must also be considered when comparing other, non-biological fuels to kerosene, as for example liquid hydrogen. If their production is powered by fossil fuels, there is a risk that their global *SCE* is considerably larger to that of kerosene.

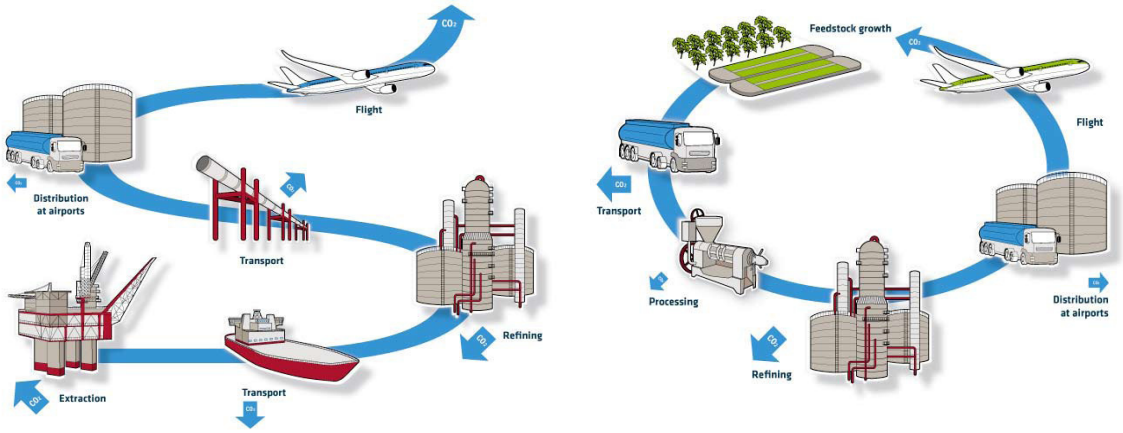

Fig. 4.16 Schematic of Life-Cycle CO_2 Emission of Kerosene (left) and Bio-fuel Produced Using Conventional Fuels (right) (**ATAG 2009**)

There are further requirements alternative aviation fuels need to satisfy. **SBAC 2008a** lists the following characteristics that the fuel needs to have to ensure safe and efficient operation:

- High energy content (per unit weight and volume) – to minimize fuel burn, operating costs and CO_2 emissions
- Low freeze point – to ensure that the fuel does not freeze at altitude
- Good flow properties (lubricity, low leakage, etc.) – to ensure that the fuel will flow as required through the aircraft fuel system
- Excellent thermal stability – to provide required heat sink capability
- Suitable flash point – to ensure that the fuel can ignite in air as required
- Good storage stability – to ensure that the quality of the fuel is maintained with time
- Compatibility with materials and components (e.g. pumps, seals, valves) in the fuel system

As **SBAC 2008a** further writes, fuel supply and storage systems and engine and aircraft systems of current aircraft have been specifically designed for optimal performance with kerosene. Using a fuel with very different properties would thus need high redesign effort and cost. For the near-term application, so-called ‘drop-in replacements’ (fuels that are compatible with existing systems) are therefore regarded the only wide-range alternative for kerosene. In the long-term however, aircraft may be specifically designed for a ‘non drop-in replacement’ such as liquid hydrogen. In addition to the possible benefits of higher fuel heat content and a lower *SCE*, alternative fuels are attractive if they reduce the dependency on crude oil.

4.4.1 Bio-Fuels

In this context, bio-fuels term fuel produced from biomass. Biomass feedstock for bio-fuels can be separated into oil/fat-based biomass and cellulose-based biomass. Depending on the nature of feedstock, different forms of fuels can be produced, see Fig. 4.17. For aviation, the most important bio-fuels are biomass-to-liquid (BTL) and hydrogenated oils.

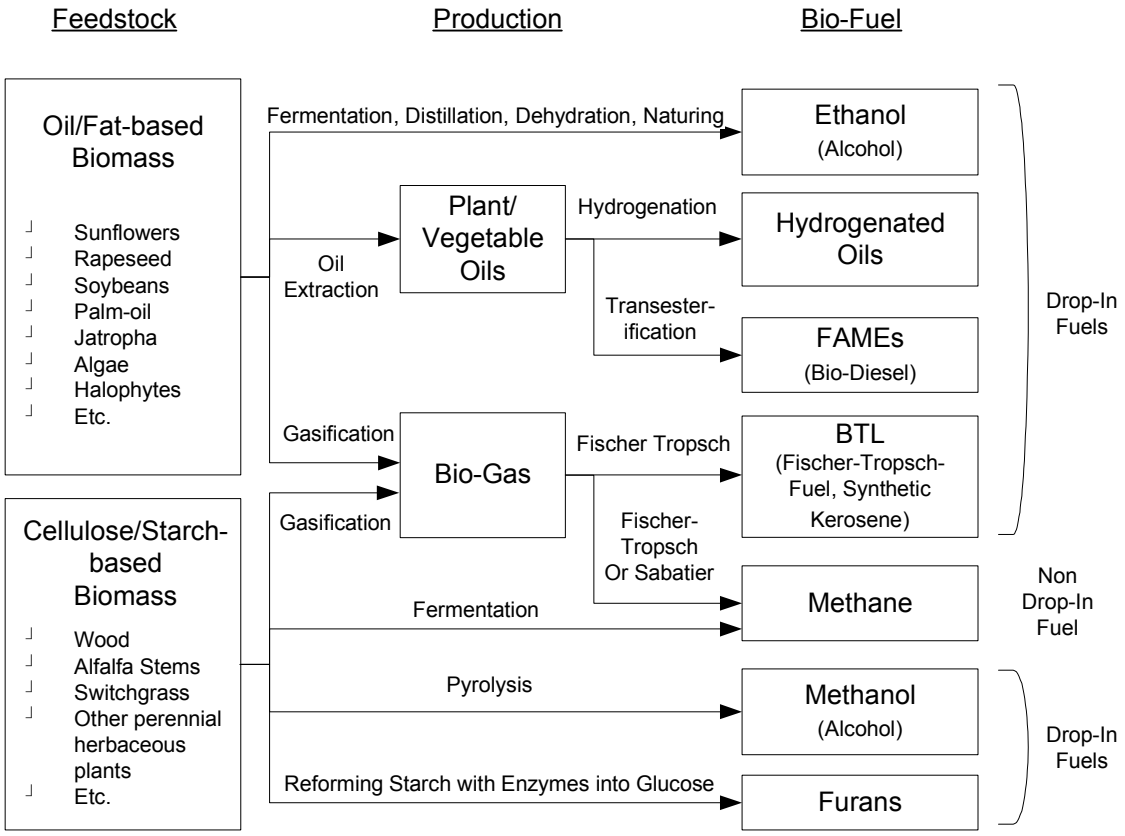

Fig. 4.17 Schematic of the Production Processes for Bio-Fuels (produced from information in **SBAC 2008a** and **IATA 2008a**)

BTL is a fuel based on the Fischer-Tropsch process. Similar fuels can also be produced from Coal (CTL) and natural gas (GTL), which are non-biological and not renewable (see sub-chapter 4.4.3). The generic name for Fischer-Tropsch fuels is XTL. XTL is also known as synthetic kerosene, as the properties are very similar. In these terms, the end product is thus a very good drop-in choice. If biomass is also used to power the production of BTL, life-cycle CO_2 emissions can be reduced down to 40-10 % of the ones of kerosene (**SBAC 2008a**, **IATA 2008b**). However, up to date, the production process using biomass is very inefficient and a massive amount of biomass is needed to produce a relatively small quantity of synthetic kerosene. Life-cycle CO_2 emissions from BTL that is produced using conventional (fossil) fuel can be even greater than the ones from GTL or kerosene (**SBAC 2008a**). A major disadvantage of BTL is its high production cost and the resultant high fuel cost (**SBAC 2008a**). Nevertheless, the first commercial BTL plant has already been built in Germany and

is said to start commissioning soon. The plant will produce BTL from forest residues and waste wood (**Shell 2008**).

Hydrogenated oils can be produced only from oil/fat-based plant matter. The development is in a rather early stage (**SBAC 2008a**). However, the hydrogenation process is well-known in oil refining to improve product quality (**IATA 2008a**). If the vegetable/plant oil has a similar structure to kerosene, the end product is believed to show similar properties. Gaining approval by regulatory bodies is thus expected to be unproblematic. Hydrogenated oils are also cheaper in production and resultant end price than BTL. The major challenge is however to find appropriate feedstock. Conventional land-grown crops such as soybeans and rapeseeds would take up an immense amount of cultivatable land that is currently used for human food production. Two promising concepts that could avoid this problem are currently under investigation. The first is using algae, which promises a high yield rate and can be cultivated in seawater. The second is growing so-called halophytes for oil production. These plants can be grown using salt water in deserts and on wasteland. However, both concepts are still very immature and need to show their feasibility (**SBAC 2008a**). If hydrogenated oils can reduce life cycle CO_2 emission in comparison to kerosene is still unclear, as the production process is not sufficiently developed. According to **SBAC 2008a**, the production process is likely to be less energy-intensive than BTL but more intensive than FAMEs (see below). In the end, similar as for BTL, the benefit is dependent on whether the production is powered by renewable or conventional fuel.

The energy density per weight (42 $MJ \cdot kg^{-1}$) of **2,5-Dimethylfuran** (Furans, Furanics, HMF fuel) and its specific weight (890 $kg \cdot m^{-3}$) is close to kerosene's. It is thus expected that these fuels have a high potential to be a good drop-in product (**IATA 2008a**). Further, the cost of production is expected to be similar to conventional fossil fuel (**Jong 2008**). Furanics are a next generation bio-fuel, which means that the product is still in development and is expected to be available not before 2010 (**IATA 2008b**). Further, the benefit regarding CO_2 emissions is still unclear. If, during the production, the amount of CO_2 emitted is less or equal to the emissions from producing kerosene, the life-cycle CO_2 emissions will be lower. Furanics can be produced from biomass that allows the production of glucose (**Jong 2008**).

The other bio-fuels producible show rather low near-term application potential for aviation. FAMEs (Fatty Acid Methyl Esters, Transesterification fuels) are produced, similar to hydrogenated oils, from vegetable or plant oil. The name 'bio-diesel' generally stands for FAMEs. FAMEs can be used for ground transportation without any significant technical issues, but their low heat content per unit weight, their high freeze point and low thermal stability make the application difficult in air transportation. Even if the problems of thermal stability and freeze point may be solved, they can be used only in rather small portions (20-30 %) in a FAME/kerosene blend. As the production of FAMEs is less energy intensive than the production of hydrogenated oils, the most effective use of oil/fat-based feedstock is in land-based transport. It has therefore been argued that dedicated available land should rather

be used for the production of FAMEs for ground transportation than for hydrogenated oils for aviation (**SBAC 2008a**).

The alcohols ethanol and methanol have very low energy densities (27.2 $MJ \cdot kg^{-1}$ and 19.9 $MJ \cdot kg^{-1}$) compared to kerosene (42.8 $MJ \cdot kg^{-1}$). They are therefore regarded as not being suitable for a commercial use in aviation (**SBAC 2008a**, **IATA 2008a**). (Liquid) Methane produced from biomass is a cryogen and is briefly discussed in the next sub-chapter.

In general, bio-fuels can be termed **first (1st), second (2nd) or third (3rd) generation bio-fuel**. This definition applies to the feedstock, not to the end-product. While 1st generation bio-fuels are ethically questionable as they are mainly produced from food crops such as sugarcane and soybeans, 2nd generation bio-fuels are generally produced from non-food feedstock such as jatropha palms and chamomile. 2nd generation bio-fuels are also said to yield higher energy efficiencies, lower life-cycle CO_2 emission and lower production costs and end prices (**Sims 2009**). However, 2nd generation bio-fuels are still produced from land-grown feedstock and thereby might compete with land for food production and forests. This is different for 3rd generation bio-fuels, which are produced for example from forest residues or oil-based algae.

4.4.2 Cryogenic Fuels: Liquid Hydrogen and Methane

Cryogens such as liquid hydrogen and liquid methane can be considered as the long-term solution for reducing CO_2 emissions. While the higher energy content and lower *SCE* compared to kerosene show a high potential for reducing both fuel consumption and CO_2, large changes to the aircraft design and infrastructure become necessary. Further, challenges in producing the fuel with low energy input exist and need to be solved before a large-scale application is imaginable.

Liquid hydrogen (LH_2) shows a high energy content per unit weight (119.7 $MJ \cdot kg^{-1}$) and its combustion emits no CO_2 (**IPCC 1999**). This is the reason why it is often seen as the most environmentally fuel available. However, it also has large drawbacks. First, LH_2 is not a source of energy in itself (**Daggett 2006**). An immense amount of energy is needed to produce LH_2 from a large source of clean water. This increases life cycle CO_2 emissions if the energy comes from burning fossil fuels. Second, large changes to the aircraft design become necessary. Even though LH_2 holds a high energy content per unit weight, the energy content per unit volume is very low (8.4 $MJ \cdot m^{-3}$) compared to kerosene (33.8 $MJ \cdot kg^{-1}$) (**IPCC 1999**). This requires larger on-board fuel tanks. Further, as the hydrogen needs to be transported in its liquid form, it needs to be constantly pressurized. The heavy cryogenic fuel tanks increase aircraft empty weight. Insulation and pressurization requirements do not allow the fuel to be stored in the wings as it is done with kerosene. Alternative fuel locations, for example in the fuselage, need to be found (**Daggett 2006**). However, as the fuel is still considerably lighter

than kerosene, it holds the potential for decreasing maximum take-off weight and accordingly engine thrust and weight. The outcome of a NASA study on how a hydrogen-powered conventional aircraft could be designed is seen in Fig. 4.18. According to **Daggett 2006**, the ultimate benefit in terms of energy consumption is depending on the mission length of the aircraft. Long-range aircraft have a greater benefit from the light fuel. The mission fuel weight is then less than for a kerosene-powered aircraft. The opposite is true for short ranges, where the heavy fuel tanks are the dominant factor. On the local level, CO_2 emissions will be zero for all cases. Life-cycle CO_2 emissions depend on the energy consumed and on the production of the fuel. If the production process is produced using renewable or nuclear energy, life-cycle CO_2 can be strongly reduced or even eliminated (**SBAC 2008a**).

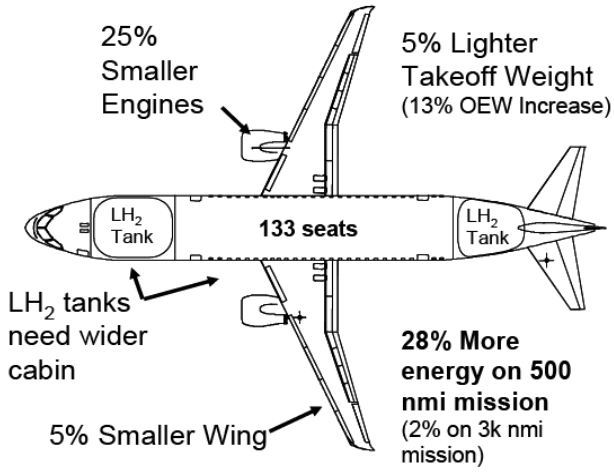

Fig. 4.18 Boeing 737-sized Aircraft designed to use Liquid Hydrogen (**Daggett 2006**)

Traditionally, **liquid methane** can either be obtained from the fermentation or gasification of biomass (see Fig. 4.17), or from geological deposits of methane or methane hydrates (in deep ocean floors/ under permafrost regions) (**SBAC 2008a**). Recent research activities indicate that methane could eventually also be produced from captured CO_2 using a photocatalyst nano-material and electricity (**Nanotechnology 2009**). According to **IPCC 1999**, tables 7-10 and 7-11, burning methane emits only 2.5 kg CO_2 per kg of fuel burned, which is about 20 % less than the *SCE* of kerosene. Liquid methane further holds a higher specific heat content *H* (50 $MJ \cdot kg^{-1}$). The combined benefit reduces energy specific CO_2 emission (in $kg \cdot MJ^{-1}$) by 25 % in comparison to kerosene (**IPCC 1999**). If produced from biomass or captured carbon dioxide, the benefit in terms of life-cycle CO_2 would be significantly greater. Similar to liquid hydrogen, the great drawback of liquid methane are the required changes to the aircraft and the airport infrastructure. Pressurized tanks for liquidation increase aircraft weight. However, as the fuel properties are closer to kerosene's than LH_2's, the increase in tanks size and reduction in take-off weight would not be as large as for liquid hydrogen (**SBAC 2008a**). As for LH_2 powered aircraft, there is an energy benefit for long ranges and a penalty for short ranges. If the penalty exceeds 25 %, the higher energy need offsets the lower *SCE* and there is no reduction in local CO_2 emissions compared to kerosene.

4.4.3 Other alternative Fuels

Synthetic kerosene (Fischer-Tropsch fuels, XTL) can also be produced **using natural gas** (GTL) or coal (CTL). The similarity to conventional kerosene is large. As no changes to the fuel system, aircraft or infrastructure are hence needed, GTL and CTL are ready drop-in fuels. A 100 % CTL aviation fuel received regulatory approval in April 2008. Regarding life-cycle CO_2 emissions, CTL is considerably worse than kerosene. Life cycle CO_2 emissions of GTL are generally nearly identical to those of kerosene. If the producing plant features a carbon capture and storage system (CCS), life cycle CO_2 will be slightly lower (**SBAC 2008a**, **Shell 2009**). One should however bear in mind that CTL and GTL fuels use non-renewable energy sources and should thus be treated only as an interim solution for the case of crude oil running short.

In the long-term, a large **electric-powered passenger aircraft** might become reality. Electricity could theoretically be carried in low-weight high-capacity batteries, produced on-board through wind-, solar-, or nuclear-powered generators or even be supplied in flight by a terrestrial laser (**Curry 2008**, **IATA 2008a**, **Truman 2006**). Today, the performance of electrical propulsion systems and sub-systems for storage and energy production is still far too low to enable commercial, electric-powered flight (**IATA 2008a**). There is however a trend to a more electric aircraft architecture (MEA) observable on the aircraft's system-level. The experience with electric aircraft systems and related technologies will most probably enable the development of more efficient electric sub-systems, which one day could make all-electric aircraft technologically feasible.

4.4.4 Assessment of alternative Fuels

Table 4.1 shows the results of an assessment conducted by **SBAC 2008a**. It evaluates the fuels with respect to their suitability for aviation (how close they are of being a drop-in replacement) and life-cycle CO_2 emissions.

From the assessment of **SBAC 2008a**, BTL seems to be the best choice for a near-term application (potentially available within the next five years). BTL can reduce life-cycle CO_2 emissions by up to 90 %, if the production runs with renewable energy (**SBAC 2008a**). This is in coherence with the findings of IATA's Technology Roadmap project in **IATA 2008b**, which identified BTL as the best alternative. A drawback of BTL is its high production and resultant fuel cost. The benefits of hydrogenated oils could exceed the ones of BTL in the medium-term, as the production costs are lower. However, first possible implementation of hydrogenated fuels is assumed five to ten years away (**SBAC 2008a**). The biggest challenge today concerns the finding and cultivating of appropriate oil-based feedstock. Fig. 4.19 shows

a diagram of land areas equivalent to produce enough fuel from oil-based matter to completely cover the current annual fuel consumption (250 billion litres) of the aviation industry. It is seen that algae holds the highest potential as the feedstock does not compete with land for food crop or forest and yields a high oil-output rate (**ATAG 2009**). In comparison, land-grown crops such as camelina and jatropha need farmlands that exceed the size of that of the world's annual corn crop production. However, the fuel production process from algae is still under development and today's forecasts concerning the maximum achievable quota of bio-fuels in aviation hold a high uncertainty (see also chapter 6.3.1).

Table 4.1 Evaluation of alternative Aviation Fuels (reproduced from **SBAC 2008a**)

Alternative Fuel	Suitability for Aviation	Life-Cycle CO2 Emissions
CTL	++	--
GTL	++	--
BTL	++	++[a]
FAMEs – conventional	00	00[b]
FAMEs – algae etc.	00	00[b]
Hydrogenated Oils – conventional	++	00[c]
Hydrogenated Oils – algae etc.	++	00[c]
Liquid Hydrogen	--	++[d]
Liquid Methane	--	00
Alcohols (Ethanol / Methanol)	--	00[e]
++	Drop-in Replacement	Much better than kerosene
00	Some Specification Challenges	Better than kerosene
--	Significant Specification Challenges	Comparable to/ worse than kerosene

[a] Will only be '++' if production powered by renewable energy. If powered by fossil fuels: '00'.
[b] 20-30 % kerosene blend, non-energy intensive farming methods.
[c] Due to the infancy of development, it is difficult to conclude about the environmental benefits.
[d] Will only be '++' if production powered by renewable energy. If powered by fossil fuels: '--'
[e] Will only be '00' if produced from biomass. If produced from petroleum or natural gas: '--'.

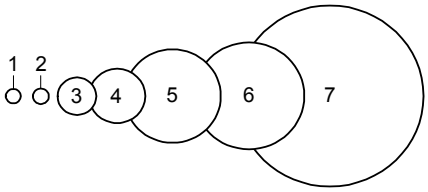

1. Algae:	68 000	km^2
2. Ireland:	70 000	km^2
3. Montana:	380 000	km^2
4. World Annual Corn Crop:	809 000	km^2
5. Camelina:	2 000 000	km^2
6. Jatropha:	2 700 000	km^2
7. Australia:	7 617 930	km^2

Fig. 4.19 Land Areas Equivalent to Produce Enough Fuel to Completely Supply the Aviation Industry (250 billion litres) (reproduced from **ATAG 2009**)

In the long-term, cryogenic fuels could find application in aviation, even though large changes to the transport system are required. Liquid hydrogen is attractive due to its zero life-cycle CO_2 if produced with renewable or nuclear energy. Liquid methane could eventually be produced from captured CO_2 with low energy (**Nanotechnology 2009**) and thus holds potential for large carbon dioxide benefits. A detailed assessment of potential alternatives to

kerosene as aviation fuel has been recently conducted by the IATA. For further information see **IATA 2008c**.

4.5 Air Traffic Management

Defining the most efficient air traffic environment[1] (and air traffic management) in terms of fuel and CO_2 savings is rather simple: each aircraft should be operating according to its individual best possible performance. For the aircraft in the air, this implies for example continuous climb departures (CCDs), most direct routes (while taking advantage of actual wind conditions), optimal flight altitudes for all phases of flight, take-off and landing paths that connect perfectly to the en-route structure (without loitering phases) and continuous descent approaches (CDAs). In ATM terms, this practice would be called performance-based or user-preferred trajectories. For the aircraft on ground, best possible fuel performance implies short as possible taxiing (landing to stand) and ground holding (stand to take-off) times.

4.5.1 Enabling user-preferred Trajectories

Today, trajectories are still far from being performance-based. Aircraft are bound to operate in a highly fixed route and terminal network. This involves for example ATC-assigned flight altitudes, approaches to mandatory holding fixes and flight paths along waypoint beacons. To say it in the words of the **ATA 2009**: "... aircraft don't fly in a straight line. Instead, they fly in the direction of one ground-based navigation aid and then another, literally connecting the dots as they methodically zigzag their way across the sky to their final destination."

This has security, navigation and traffic management reasons. In simple terms, today's air traffic technology, which is largely based on radar data (**Takemoto 2007**), is not yet able to allow for such unrestricted operation as user-preferred trajectories while keeping up to safety requirements. This applies to both air traffic control and aircraft. Further, especially in Europe, the air space is broken into multiple national military and civil areas with their own controls and restrictions. To enable truly performance-based trajectories in the long-term, two major goals can thus be specified:

[1] Neglecting far-future operations like formation flying and air-to-air refueling as proposed e.g. in **Truman 2006**.

- Technological evolution to a so-called *4D ATM Environment* (**Hering 2004**) and
- A global air space that is largely un-restricted,

where '4D environment' is a synonym for the ability of the air traffic system to continuously localize aircraft in four dimensions, i.e. latitude, longitude, altitude and time. In other words, each active participant to the system knows about the actual position of the others. This is seen as the key enabler for performance- and business-based trajectories (**Eurocontrol 2008**).

Major technologies for the establishment of a 4-dimensional localization and air traffic control are a Global Navigation Satellite System (GNSS, GPS, Galileo) and a technique called **Automatic Dependent Surveillance-Broadcast** or ADS-B. The former is necessary for the individual aircraft to determine its current position. The latter is used to sent this information together with further data from the aircraft's flight monitoring computer (type of aircraft, flight speed, flight number, whether the aircraft is turning, climbing or descending) to surrounding aircraft and ground stations (**Takemoto 2007**). It is then possible for both ATC and pilots to see the real-time display of air traffic.

The real fuel benefit is however expected to come from further consecutive tools and procedures to the ADS-B system. They will allow for example for a safe reduction in vertical and lateral separation and thus higher capacities, automated CCDs and CDAs, flight levels according to aircraft weight and most advantageous winds, more direct landing paths and fast re-routing of flights. When fully implemented, most of this is expected to be possible with only very few instructions from ground-based controllers as close-by aircraft 'communicate' directly through ADS-B (**Takemoto 2007**). A brief listing of some of the single tools and procedures is found in Appendix B.5.

The implementation of a fully efficient 4D management is however longsome. According to **Eurocontrol 2008**, a working 4D environment with business-preferred trajectories is only available past 2020. This is mainly due to the complexity of the system, as performance-based trajectories can only work safely from the moment all aircraft and airports are equipped with the necessary equipment. Until then, a successive improvement of the air traffic is envisaged. This implies the gradual replacement of conventional operations with new, more efficient ones. Systematically, regulation authorities will also make carrying of specific navigational equipment mandatory for all aircraft, as for example a GNSS system in the European airspace from the year 2015 on (**Eurocontrol 2008**). Detailed information on the planned steps to a full 4D environment and related technical enablers can be found for the European airspace at *The European Air Traffic Master Plan Portal* (**Eurocontrol 2009**) and for the US airspace at *Next Generation Air Transportation System – Joint Planning Environment* (**JPDO 2009**).

4.5.2 Possible Future Improvement

According to **Grimme 2008**, Eurocontrol estimates the influence of air traffic management on global aviation emissions to 7.0-11.0 %. The Civil Air Navigation Services Organisation (CANSO), which is a global association of ATM stakeholders, believes that the global ATM system is already between 92 and 94 % efficient, which is consistent with the assessment of ATM efficiency by the IPCC (**CANSO 2008**). This calculates to a theoretical potential for future improvement of around 6 to 8 %. However, according to **CANSO 2008,** p. 2, a 100 % efficient system is not achievable "... due to necessary operating constraints and interdependencies, such as Safety, Capacity, Weather, Noise and fragmentation of the airspace". On the base of this finding, CANSO has set up efficiency goals up to 2050, which are reproduced in Table 4.2.

Table 4.2 CANSO ATM Efficiency Aspirational Goals (**CANSO 2008**)

	Year	Global ATM Efficiency
Baseline	2005	Between 92 % and 94 %
Goal 1	2012	Between 92 % and 95 %
Goal 2	2020	Between 93 % and 95 %
Goal 3	2050	Between 95 % and 98 %

CANSO 2008 sees an achievable improvement in ATM efficiency of around 4 % for 2050. This sounds rather small. It must be noted however, that the ATM system has to similarly cope with immensely increased air traffic. If the air traffic system would be managed as hitherto, ATM efficiency would then significantly decay. A large part of future ATM improvement will thus not show in fuel efficiency, but in an increased airspace and airport capacity. Regarding this effect, the 'net' efficiency gains are larger than 4 %.

4.6 Chapter Summary

A survey of potential technologies for CO_2 reduction comprising improvements in aerodynamics, engine & power, empty weight, alternative fuels and air traffic management (ATM) has been carried out. After the possible CO_2 benefits for the single aircraft have been assessed, it is now possible to project the over-all benefit for the future global aviation system, once a forecast of the size and make-up of the future world fleet has been established in the next chapter.

5 Global Fleet Forecast

The following two chapters expand the scope of the analysis to a global level. Thereby it is tried to give answers to the question if technological innovations provide an opportunity not only to lower CO_2 emissions of a single aircraft, but also to diminish the over-all 'carbon footprint' of aviation. Fig. 5.1 shows a schematic illustrating the approach to estimating current and future global CO_2 emission.

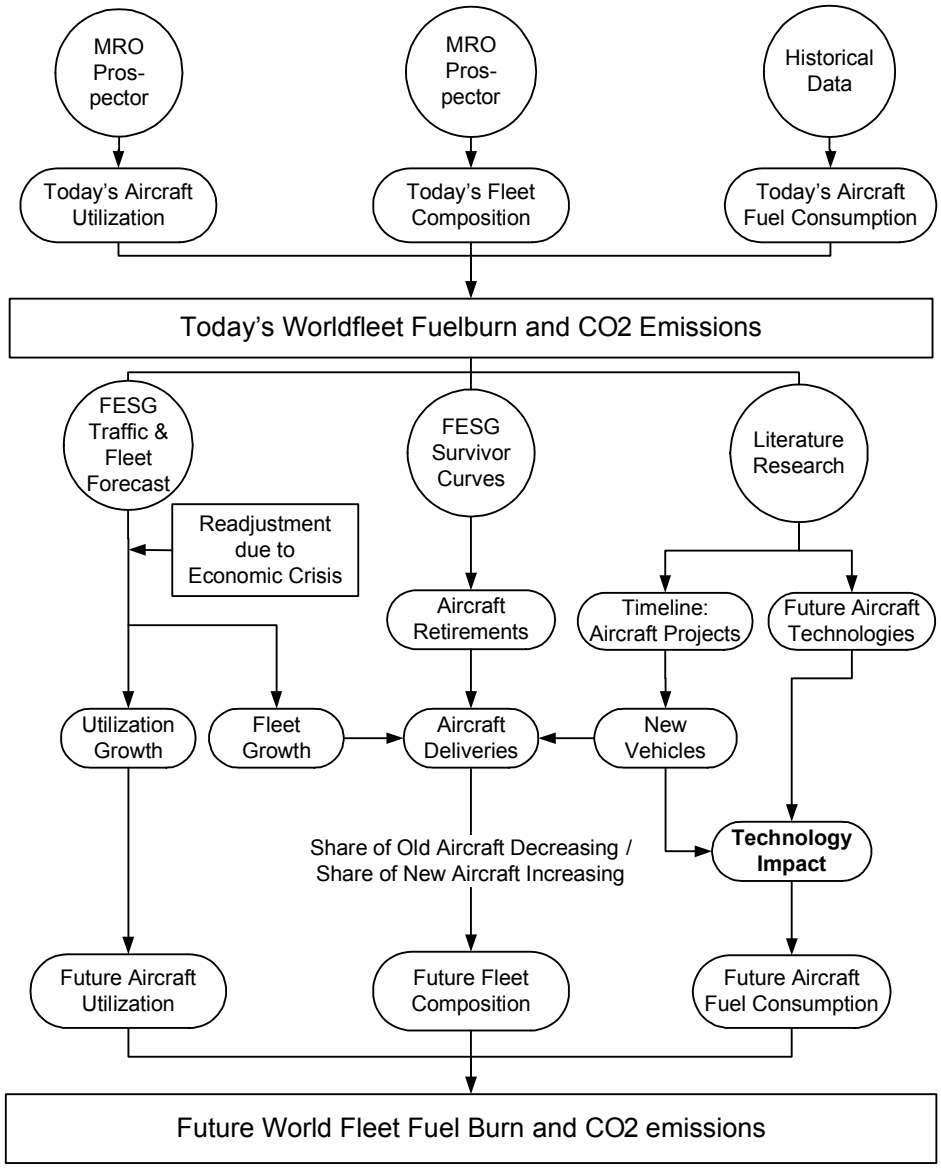

Fig. 5.1 Schematic of the Approach to Computing Future World Fleet CO_2 Emissions

First, the size of today's world aircraft fleet is determined. A simplified, but reasonably representative model of the latter is then established by focussing the study on commercial, turbofan-powered passenger aircraft. The make-up of this simplified 'world fleet' is determined from fleet data given in the online database *MRO Prospector* (**MRO Prospector**

2008b). Second, a fleet size forecast is established on the basis of a consensus-based ICAO forecast (*FESG* forecast). With respect to the current global economic downturn, the growth rates for the first decade are adjusted down. Third, based on an extensive literature research, assumptions for future retirements and consequent replacements, the emergence of new aircraft, the phase-out of current models and future market shares are made. This results in a forecast of the size and make-up of the passenger world fleet up to the year 2036: see Fig. 5.1 'Future Fleet Composition'.

In the chapter following this one, typical fuel consumption of active aircraft is determined from historical data. Further, fleet data of the MRO Prospector is used to compute average daily aircraft utilization and subsequently CO_2 emissions of the simplified world fleet in 2008. After that, assumptions concerning technological innovations on future aircraft are made. From this, improvements in fuel efficiency of future aircraft are estimated: see Fig. 5.1 'Future Aircraft Fuel Consumption'. Growth rates concerning general aircraft utilization are found from re-adjusting FESG assumptions with respect to the economic crisis: see Fig. 5.1 'Future Aircraft Utilization'. Finally, the CO_2 emission of the future world fleet is estimated on the base of three scenarios concerning the technological evolution in the next decades: a pessimistic, an optimistic and a trend scenario.

5.1 Aircraft in Scope

As of April 9th 2009, the world fleet of commercial aircraft consisted of 26 213 aircraft. Of these, 23 945 were in service and 2268 were stored (**MRO Prospector 2008b**). Hence, there were 23 945 aircraft regularly producing CO_2 emissions by burning fossil fuel. This number accounts for several dozen aircraft types and sub-types ranging from the Airbus A300-600 Freighter to the Yakolev Yak-40. It should however be possible to model the most important behaviour and characteristics of the entire world fleet with a considerably smaller group of aircraft. Having this in mind, it was decided to concentrate the study only on aircraft types

- ... that are used to transport passengers, i.e. passenger or 'combi'[1] aircraft,
- ... that are powered by turbofan engines,
- ... that feature a capacity of at least fifty passengers and
- ... of which at least ten aircraft are in service (excluding the Airbus A380).

It was further decided that **Russian-built aircraft would not be regarded** in the study as information on these type of aircraft was found to be very difficult to obtain.

---

[1] A combi aircraft is an aircraft that is used to transport both, cargo and passengers. For example, Boeing B747 combi aircraft "… feature a large side cargo door on the main deck for cargo loading in the aft section, and passenger accommodations in the forward two- thirds section of the airplane", **Boeing 1996**.

This search pattern eliminates a large number of aircraft types, but still results in an active fleet of 14 401 aircraft (as of November 20th 2008, **MRO Prospector 2008b**). Thus, in terms of aircraft in service, 60 % of the entire world fleet is still included. According to the *Airbus Global Market Forecast 2007-2026* (**Airbus 2007b**), the number of passenger aircraft in 2006 was 20 094, of which 5586 were aircraft with fifty seats or less. This calculates to 14 508 aircraft in 2006 that correspond to above defined pattern (including Russian aircraft). According to **Airbus 2007b**, this number is expected to grow up to 32 785 aircraft in 2026. Assuming an exponential growth, the annual growth rate for the years in between is 4.08 %. Hence, the fleet of November 2008 (after one year and ten month of growth) is expected to be 15 635 aircraft. Our reduced 'world fleet' accounts for 92 % of this number and is thus considered to be representative for the entire fleet of turbofan-powered passenger aircraft with more than 50 seats capacity. The aircraft models included in the forecast, together with their respective fleet size as of November 2008, are found in Table 5.1.

5.2 Traffic and Fleet Growth

In order to forecast the developments in global CO_2 emissions over the next decades, it is necessary to understand that the aircraft world fleet is not constant, but time-sensitive. The number of active aircraft in the world will change with the changing demand for air-traffic, usually with a short time-delay.

World air traffic can be described by the cumulative revenue passenger miles (RPM) or revenue passenger kilometres (RPK). For a single flight, RPKs are the distance flown multiplied with the passengers travelled. The distance flown can alternatively be expressed by the product of speed and time, which in aviation terms is block speed v_b times aircraft utilization U.[1] An indicator for the number of passengers is the so-called *load-factor*, which is the ratio of seats sold to seats available. It is then possible to write global air traffic per year as

$$\mathrm{RPK} = \sum_{j=1}^{n_{AC}} \left(f_L \cdot n_S \cdot U \cdot v_b \right)_j \quad , \tag{5.1}$$

where f_L is the average load-factor, n_S is the number of seats per aircraft, U is the average utilization in hours per year, v_b is the average block speed in km·h^{-1} and n_{AC} is the number of active aircraft in the world fleet. Generally, all of these factors are demand-sensitive. If we consider only near- and medium-term developments, n_S and v_b can be assumed as being

[1] Block speed is the average speed over a specific distance "block-to-block", i.e. gate-to-gate. Utilization is the number of hours an aircraft is actually on a mission, i.e. "off-block" or "off-gate". The term generally refers to a period of one day (daily utilization) or one year (yearly utilization).

constant. Load-factor, average aircraft utilization and number of aircraft react to changes in demand more sensitively. This is shown in Fig. 5.2, which shows historical annual growth rates for the three factors and air traffic. The most sensitive parameter is the load factor, which absorbs small fluctuations in demand 'automatically'. Small load factors are however not desirable, as they make a flight less profitable. If demand drops sharply, airlines will therefore react with reducing flights, i.e. the average daily utilization of the aircraft. The least sensitive one is the number of active aircraft. A reason for this is that airlines are planning purchases of new aircraft in the long term. A downturn in air traffic will thus not lead to an immediate cancellation of all aircraft orders and deliveries or to a sell-out of aircraft to reduce the active fleet.

All of these effects are clearly observable in Fig. 5.2. A good example is the drop of all curves for the year 2001 as a reaction to the terrorist attacks in September: Airlines were not able to react immediately; a decline in the load factor was unavoidable for 2001. In 2002, the airlines were able to recover the load factor completely by further decreasing aircraft utilization. The aircraft fleet reacts naturally slower and not as sensitive to external factors. While air traffic shows negative growth for the year 2001, the aircraft fleet still increased by more than 3 %. A similar phenomenon is observable for positive trends, as for example the sharp rise in air traffic in 2004. Nevertheless, a long-term economic crisis as actually predicted for the next years will certainly have an impact also on the growth rates of the world fleet and expected growth will be lower than for the last decade. This will be discussed later.

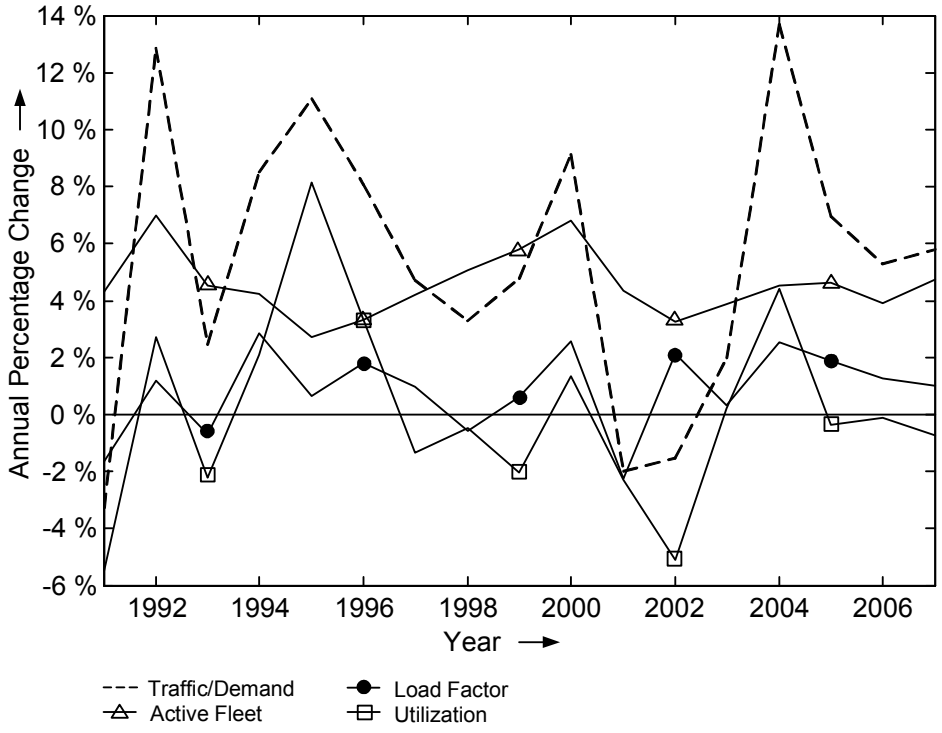

Fig. 5.2 Historical Annual Growth Rates of the Active Passenger World Fleet, Traffic, Load Factor and Utilization (reproduced from **Airline Monitor 2008b**)

5.2.1 Fleet Growth according to the FESG

To estimate the future growth of the chosen world fleet of passenger aircraft, a reasonably reliable air traffic forecast is needed. Both, Airbus and Boeing prepare yearly forecasts that cover the subsequent twenty years and are accessible to public, see for example **Airbus 2007b** and **Boeing 2009c**. However, single manufacturer forecasts have a high potential to be politically motivated. A more independent forecast is provided by the Committee on Aviation Environmental Protection (CAEP), which is a working group of the International Civil Aviation Organization (ICAO). The CAEP holds another sub-group, the Forecasting and Economic Support Group (FESG). This sub-group consists of members from manufacturers (aircraft and engines), airlines, airports and government officials. At regular intervals, the FESG, together with other sub-groups of the CAEP prepare a 'consensus-based' forecast for the next twenty to thirty years. In this case, *consensus-based* terms a forecast that is developed by combining already existing forecasts (provided by the ICAO and manufacturers) to an essential one.

For the study at hand, the most recent FESG forecast, presented on June 11th 2008, is used. The underlying forecasts are taken from Airbus, Boeing, General Electric, ICAO and Rolls Royce (**FESG 2008**). They all feature an identical time scope from 2006 to 2026. The FESG decided to extend this time scope by ten years (up to the year 2036).

The passenger aircraft forecast developed by the FESG features growth rates for nine generic seat categories: 20-50, 51-100, 101-150, 151-210, 211-300, 301-400, 401-500, 501-600 and 601-650 seats. The real aircraft – found from the search pattern defined in the section above – are assigned to these categories. As the final seating capacity of an aircraft varies with airline and route, it is then necessary to gather actual data on the capacity of active aircraft. This is done using 2008 OAG data (**OAG data 2007**). The OAG data software *MAX* is based on a large airline schedule database. Available seats per aircraft type for all included flights of the year 2008 are analyzed. By doing so, it is possible to answer the question on how many aircraft of each type are regularly flown in each seat category. Some aircraft can be assigned clearly to one category, for example the Boeing B757-300 aircraft with 100 % of its active fleet flown with 211 to 300 seats. The most aircraft however touch at least two categories, for example the Boeing B777-200ER with 53 % featuring a capacity below and 47 % featuring a capacity above 300.

Table 5.1 shows the resulting breakdown of the active passenger fleet 2008 into the respective seat categories. **OAG data 2007** does not include scheduled flights for the MD11 aircraft. As the average seat capacity is similar to the A330-300 aircraft (**Grimme 2008**), the fleet is split accordingly into 76 % flown in the 211-300 seat segment, and 24 % flown in the 301-400 seat segment. Further, as the MAX version used originates from December 2007, scheduled flights for the Airbus A380 are based on only two aircraft. Both of them (operated by Singapore Airlines) are equipped with only 471 seats. It is expected however, that a good part of the

aircraft yet to be produced will feature more than 500 seats. An equal split into 50 % operated with a seat number above and 50 % operated with a seat number below 500 is assumed. The fleet of passenger aircraft at hand does neither include aircraft that are flown in the category of 20 to 50 seats, nor in the one of 600 to 650 seats.

Table 5.1 Active Fleet of 2008 Assigned to Generic FESG Seat Categories (Derived from **OAG data 2007**)

Aircraft Name	**Active Fleet 2008**	**Relative Share of Active Fleet in Seat Category as of 2008**						
		51-100	**101-150**	**151-210**	**211-300**	**301-400**	**401-500**	**501-600**
	[-]	**[%]**	**[%]**	**[%]**	**[%]**	**[%]**	**[%]**	**[%]**
A300-Classic/600	14/117	-/-	-/-	-/12	100/88	-/-	-/-	-/-
A310	93	-	-	82	18	-	-	-
A318/A319	59/1061	22/-	88/95	-/5	-/-	-/-	-/-	-/-
A320/A321	1884/476	-	60/2	40/95	-/3	-/-	-/-	-/-
A330-200/300	313/249	-/-	-/-	-/-	94/76	6/25	-/-	-/-
A340-200/300	228	-	-	-	94	6	-	-
A340-500/600	25/80	-/-	-/-	20/-	68/11	12/89	-/-	-/-
A380-800	9	-	-	-	-	-	50	50
B717	133	20	80	-	-	-	-	-
B727	62	-	60	40	-	-	-	-
B737-200/300	268/847	15/-	85/100	-/-	-/-	-/-	-/-	-/-
B737-400/500	408/328	3/1	67/99	30/-	-/-	-/-	-/-	-/-
B737-600/700	65/923	-/-	100/100	-/-	-/-	-/-	-/-	-/-/
B737-800/900	141/83	-/-	20/-	80/71	-/29	-/-	-/-	-/-
B747-100/200	15/25	-/-	-/-	-/-	-/60	100/4	-/36	-/-
B747-300/400	42/436	-/-	-/-	-/-	24/15	26/64	48/20	-/-
B757-200/300	736/51	-/-	<1/-	66/-	34/100	-/-	-/-	-/-
B767-200/200ER	26/75	4/4	-/-	84/84	12/12	-/-	-/-	-/-
B767-300/300ER	97/482	-/-	-/1	9/58	91/41	-/-	-/-	-/-
B767-400ER	37	-	-	-	100	-	-	-
B777-200	85	-	-	-	53	47	-	-
B777-200ER/LR	401/22	-/-	-/-	-/-	53/14	47/86	-/-	-/-
B777-300/300ER	60/163	-/-	-/-	-/-	33/14	52/86	15/-	-/-
BAe146	220	95	5	-	-	-	-	-
CRJ-700/900	333/178	100/100	-/-	-/-	-/-	-/-	-/-	-/-
DC-9/10	163/20	14/-	86/-	-/-	-/100	-/-	-/-	-/-
E-170/175	144/104	100/100	-/-	-/-	-/-	-/-	-/-	-/-
E-190/195	184/23	100/52	-/48	-/-	-/-	-/-	-/-	-/-
Fokker 70/100	42/202	100/59	-/41	-/-	-/-	-/-	-/-	-/-
MD-11	22	-	-	-	76	23	-	-
MD-80/90	762/110	<1/-	92/78	8/22	-/-	-/-	-/-	-/-
Total	**14401**	**10**	**44**	**25**	**14**	**6**	**1**	**<1**

5.2.2 Effects of the Actual Economic Downturn

The FESG Forecast of summer 2008 expects global traffic to grow by 5.1 % p.a. in average for the years 2007 to 2016 **FESG 2008**. The most experts have assumed a growth rate in traffic around 5 % for 2008 until the first indications for a financial crisis showed. However, in July 2008, **Airline Monitor 2008b,** p. 7 writes

> *"A year ago, and even in the January update, we thought that world traffic in 2008 would be about 5.5 %, similar to the results for 2007. That is no longer the case – despite the fact that the first quarter was up about 4 %, we now expect the year to come in at less than 2 %. Moreover, we judge that the increase in 2009 may not be much better."*

About the same time, in August 2008, the Official Airline Guide (OAG) "... adjusts its fleet forecast for 2017 down by more than 3500 aircraft", **OAG 2008**. The expected growth in the number of active aircraft was adjusted down from 24 282 to 20 693 in 2017 (with a base of around 17 000 in 2007). The FESG forecast expects the active fleet of 2006 (18 773 aircraft) to grow up to 25 906 in 2016, which is nearly identical in terms of number of additional aircraft (ca. 7000) with the OAG forecast before readjustment. Since summer 2008, the economic crisis seems to have gotten even worse. According to **Flight Global 2009**, IATA believes air traffic to shrink by 5.7 % in 2009. This is considerably more than the experienced 2 % dip due to the tragic occurrences on September 11th 2001. Further, while latter is a shock reaction of passengers that vanished relatively fast, the crisis is able to cripple airline economics for a noticeably longer term. Already in July 2008, as the effects of the crisis were still hard to grasp, **Airline Monitor 2008b** expected growth rates not to fully regain until 2012. As fleet growth is a function of traffic, it is reasonable to say that it will drop at least as much as in 2001 and not post rise as quickly (**OAG 2008**). With respect to these recent developments, for the purpose of this paper, the FESG forecast for the years 2009-2016 is adjusted down. For orientation, the readjusted OAG forecast (**OAG 2008**) is used. It is shown in Fig. 5.3.

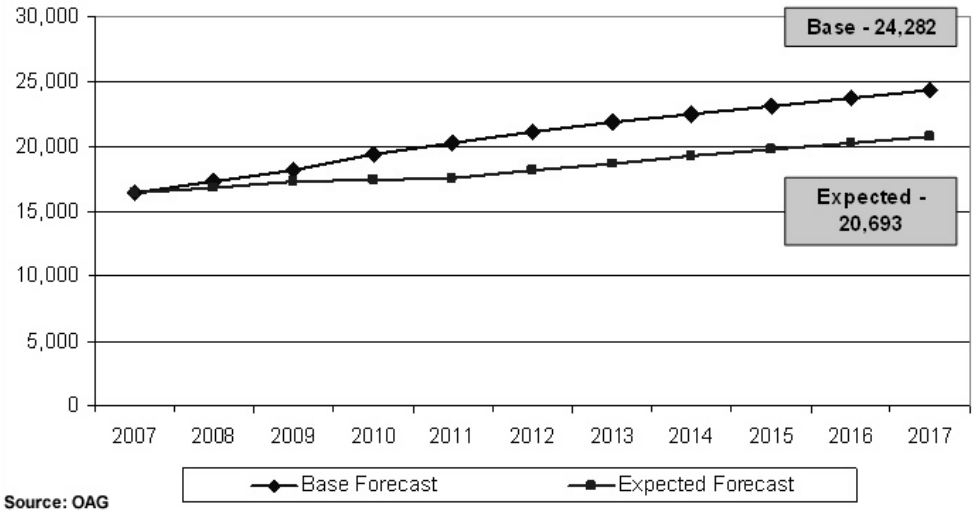

Fig. 5.3 Re-adjusted OAG Global Passenger Installed Fleet Forecast (**OAG 2008**)

According to the graph shown in Fig. 5.3, the annual growth rate for the years 2009 to 2011 is decoupled from the growth rate of the years 2012 to 2015. As suggested by **OAG 2008** and **Airline Monitor 2008b**, a very low growth of only 25 % of the original FESG growth rates will be applied until 2012. This correlates with a growth of the total fleet of 1.1 % p.a. From 2012 on, **OAG 2008** and **Airline Monitor 2008b** expect the economy to slowly regain historical rates. Thus, 75 % of the FESG forecast is expected (3.2 % growth p.a.). In 2016, air traffic is assumed to have fully recovered and the FESG forecast to be applicable in its original form.

5.2.3 Finally Applied Growth Rates

Table 5.2 gives the total number of active aircraft for each capacity class in 2008 and the expected annual growth for each decade. The original FESG growth p.a. was calculated from the absolute 'number of aircraft' given for 2006, 2016, 2026 and 2036 in **FESG 2008** assuming an exponential growth over ten years, i.e. from

$$n(t) = n_0 \exp(kt) \quad , \tag{5.2}$$

where n is the number of aircraft after the time t in years, n_0 the initial fleet size and k the annual growth rate. For the category of 501 to 600 seats, an exponential curve does not seem to be applicable due to the small initial fleet size of only five aircraft. A linear growth shows more realistic results and is thus applied. The conclusive growth of the pre-defined world fleet model up to the year 2036 is shown in Fig. 5.4.

Table 5.2 Annual Fleet Growth Rates as Applied to the Generic Seat Categories (Re-Adjusted FESG Forecast based on **FESG 2008** and **OAG 2008**)

Seat Category	**51-100**	**101-150**	**151-210**	**211-300**	**301-400**	**401-500**	**501-600**
Active Fleet of Base Year (2008)	1452	6318	3635	1961	899	132	5
% Fleet Growth p.a.							
2009-2011	2.48	0.62	1.17	1.07	1.20	2.45	1.98[1]
2012-2016	7.43	1.87	3.51	3.20	3.59	7.34	5.93[1]
2017-2026	4.04	2.13	3.16	3.88	4.54	8.92	18.7[1]
2027-2036	3.31	2.09	2.84	3.87	4.76	6.13	63.1[1]

[1] Linear Annual Gradients

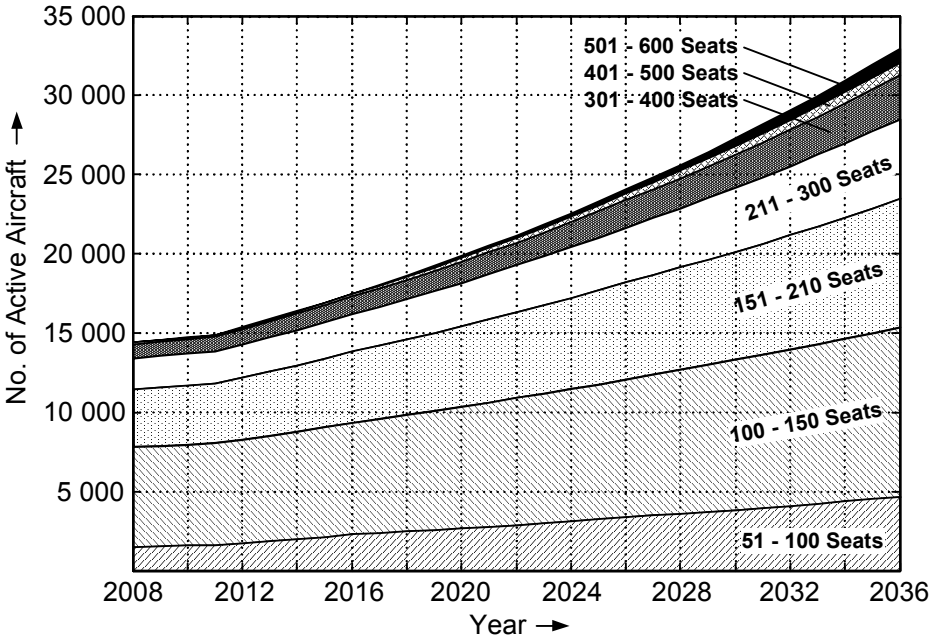

Fig. 5.4 Expected Growth of the Pre-Defined World Fleet of Passenger Aircraft

As shown in Fig. 5.2, airlines will react on the economic downturn as well by lowering the utilization of aircraft in service. This is also projected in a recent fleet and utilization forecast by **OAG 2009**: "We are projecting a worldwide drop of – 4 % in average aircraft utilization in 2009 compared to 2008, with only modest recovery in 2010. Normal levels of aircraft utilization growth are not expected to return until 2011." To factor this in the forecast at hand, utilization for all active aircraft is lowered by 4 % for 2009 and a zero growth is expected for the years 2010 and 2011. From 2012 on, normal utilization growth rates according to the FESG forecast (**FESG 2008** are adopted. For the purpose of this paper, assumptions on utilization are important for the calculation of global CO_2 emissions, see chapter 6.

5.3 Aircraft Retirements

New aircraft will not only enter the market to allow for traffic growth but also to replace old aircraft. Technically, aircraft life is given by the number of maximum allowed load cycles, i.e. by the number of flights. In reality however, the decision to retire an aircraft is mostly driven by economics: "Its owners decided they would be better off with the airplane out of service than they would be to keep it flying" (**Feir 2001,** p. 1). Reasons for the retirement might be a more efficient aircraft entering the market, stricter airworthiness requirements that lead to high maintenance costs, low passenger acceptance, a change in the route network of the airline, etc. An aircraft may further change the operator several times during its life. Small airlines, especially in developing regions, tend to buy aircraft that were already in use for

some years. More solvent airlines generally keep their aircraft fleet more modern and efficient, by buying aircraft directly from the manufacturer and selling them earlier.

Aircraft are sold best when they are relatively new on the market but already have proven their profitability. This may lead to a peak in sales for a couple of years and to an immense number of this type of aircraft entering the world fleet at a certain time. As all these aircraft have about the same life expectancy, they also tend to be retired around the same time. The great number of retirements results in an increase in demand for new aircraft. Peaks in new, more CO_2 efficient aircraft entering the world fleet may therefore be a result of high retirement rates rather than high traffic growth rates. For our study of passenger aircraft, it is important to expand the definition of retirement also on freighter conversions. It is however important to bear in mind that even if freighter conversions are subtracted from the passenger fleet and thereby reduce CO_2 emission, they continue being in service and emitting CO_2.

The typical useful life of an aircraft today is around 25 to 35 years. However, assuming a specific age, say 30 years, to forecast aircraft retirement would misrepresent reality. In the real world, some aircraft will leave the active fleet prior to the age of 25, whereas others of the same type will be operated for more than 35 years. A more accurate method to predict aircraft retirements is the use of so-called 'aircraft survival curves'. Survival curves plot the percent of still active aircraft (that originate from a specific year of delivery) over time, see Fig. 5.5. Historical retirement recordings show that real world survival rates are thereby represented reasonably accurate (**Feir 2001**). For the study at hand, aircraft survival curves defined by **Waitz 2006** and **FESG 2008** are used to forecast aircraft retirements. These curves were developed from year-end 2006 fleet data and historical retirements up through 2006 (**FESG 2007**). According to **FESG 2008**, fleets of the aircraft models shown in Table 5.1 can be assigned to four different survival curves, see Fig. 5.5. The survived percentage of aircraft for each group is calculated from

$$S = A + B \cdot t + C \cdot t^2 + D \cdot t^3 + E \cdot t^4 \quad , \tag{5.3}$$

where t is the time since the entry into service in years and A to E are coefficients given in Table 5.3. For each curve, Eq.(5.3) is valid only for a specific range of time (see Table 5.3). This is not a problem for the DC10, B727 and MD11 aircraft, as first, all aircraft fall into the specific age range and second, the validity ends with nearly all aircraft being retired ($S \rightarrow 0$). However, this is not true for the aircraft belonging to the first group. Using Eq.(5.3), the curve ends with still more than 20 % of the aircraft being in service. Assuming that survival falls to zero for the following year would lead to unrealistic peaks in the number of aircraft being retired. To allow for a realistic calculation of retirements beyond the age of 39, survival rates for the ages 40 to 50 are given in **FESG 2007**. They are reproduced in Table 5.4. Survival curves as defined by Eq.(5.3) are plotted in Fig. 5.5. The dashed line shows the just mentioned extension of curve 1 by the values given in Table 5.4.

Table 5.3 Coefficients for Calculating Aircraft Survival Rates (**FESG 2007**)

Aircraft	Coefficients					Valid for t
	A	B	C	D	E	[a]
Group 1	1.03366	-0.02355	$3.62 \cdot 10^{-3}$	$-1.807300 \cdot 10^{-4}$	$2.288650 \cdot 10^{-6}$	16 to 39
Group 2	1.00016467	-0.01361884	$4.37137 \cdot 10^{-3}$	$-3.2873 \cdot 10^{-4}$	$5.507300 \cdot 10^{-6}$	14 to 33
B707/727	1.85535	-0.07665	$7.8 \cdot 10^{-4}$	-	-	23 to 43
MD11	1.1135	-0.060022	-	-	-	5 to 18

Table 5.4 Survival Rates for Group 1 Aircraft Ages 40 to 50 (**FESG 2007**)

t	**[a]**	**40**	**41**	**42**	**43**	**44**	**45**	**46**	**47**	**48**	**49**	**50**
S	[-]	18.0%	15.8%	13.3%	11.2%	9.5%	7.5%	5.8%	4.5%	2.6%	1.3%	0.0%

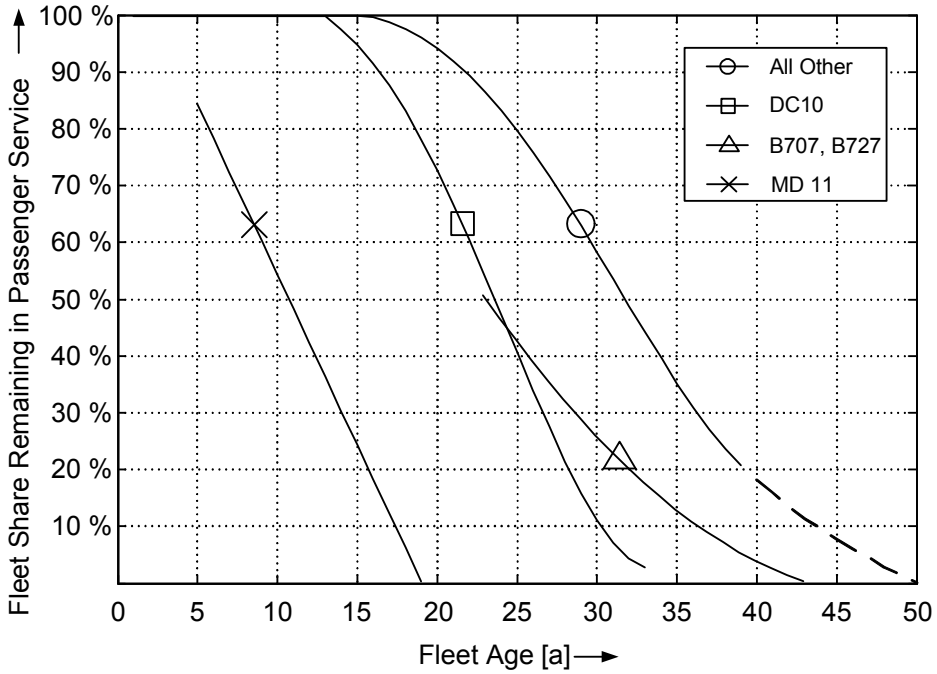

Fig. 5.5 Assumed Aircraft Fleet Survival Curves for the Calculation of Future Retirements (calculated from **FESG 2008**)

As observable from Fig. 5.5, there is no definite peak in retirement rates for a single aircraft family. There is rather a phase where the yearly retirement rate is at its maximum. For modern aircraft, this is the time span between 25 to 35 years, where each year around 4-5 % of the original fleet are retired. However, 20 % of the original fleet is retired prior to the age of 25 and 20 % past the age of 40. According to their curve, MD11 aircraft are 'retired' early and at a constant yearly retirement rate. It is important to bear in mind that for the purpose of a passenger aircraft forecast, the curve for the MD11 is not accounting for actual retirements, but mainly for freighter conversions.

As **Waitz 2006,** p. 28 explain, "Computing the retirement percentages for passenger aircraft using the FESG provided curves requires a multi-step process". First, aircraft entry-into-service dates are obtained from the Ascend Database in **MRO Prospector 2008b**. From these,

the average age of the active fleet is calculated. After that, the hypothetical fleet of the year zero, according to the retirement curve, is computed by projecting the actual number of aircraft back in time. The remaining number of aircraft for a year still to come is then computed by applying the retirement curve to this 'original' fleet. Finally, the difference between this value and the baseline fleet size – the number of aircraft retired – is calculated.

For the study at hand, it is assumed that airlines will replace a retired aircraft with an identical one if the model is still in production. Retirements of out-of-production models however increase the world-wide demand for new aircraft: all in-production models that belong to the same seat category are treated as potential replacements. The final decision for a certain model is thus depending only on the market shares. The number per year and seat category of these 'free market' retirements are shown in Fig. 5.6.[1]The sharp rise in annual retirements in the seat categories 101-150 and 151-200 is due to the end of production of the A320 and B737 in the late 2010s and early 2020s.

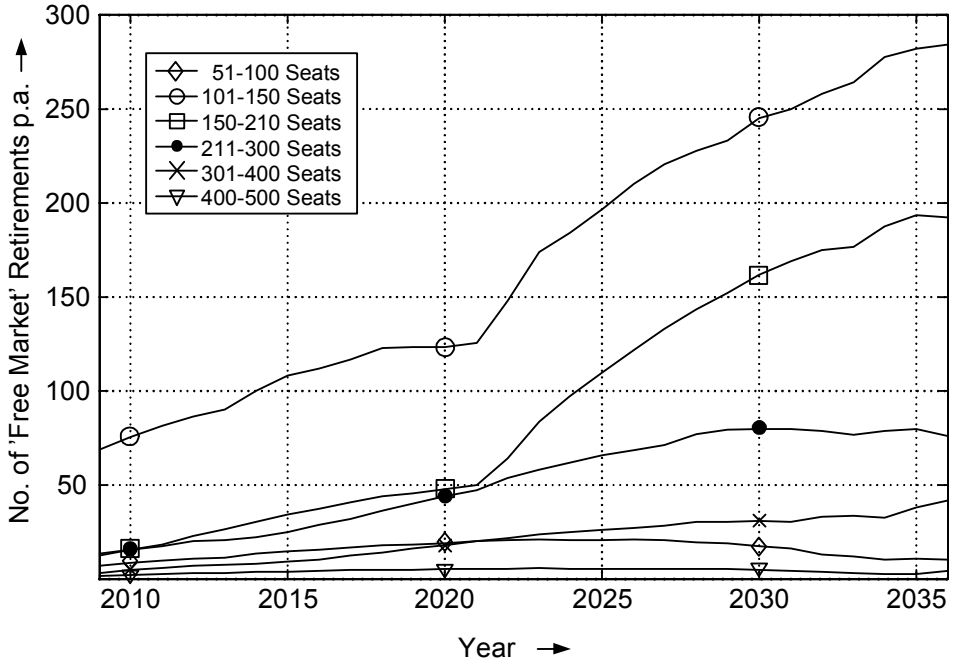

Fig. 5.6 'Free Market' Aircraft Retirements per Year and Seat Category 2009-2036

[1] The seat category of 501 to 600 seats does not feature any free market retirements. Per our definition, the Airbus A380 is the only aircraft to be sold in this category. According to the appropriate retirement curve 'Group 1' in Fig. 5.5, the first A380 could theoretically be retired after 16 years in service (when the curve leaves 100 %). However, as the fleet is small and rather young, the probability that a large number of aircraft is retired in the years 2009 to 2036 is diminutive. Moreover, as long as the A380 is produced (which is assumed to be the case for the entire forecast), a retired aircraft is expected to be replaced by a new A380.

5.4 New Aircraft Introductions and Aircraft Phase-Outs

New aircraft models that are assumed to enter the market in the next decades are presented in this sub-chapter. Further, anticipated phase-outs of predecessors are discussed. Assumptions about new aircraft projects are important to account for their impact on fuel efficiency. As observable from Fig. 5.4, air traffic is forecasted to increase rather than to decrease over the next decades. To avoid global CO_2 from growing as rapidly, its growth needs to be decoupled from the growth in air traffic, i.e. the air traffic system needs to emit less CO_2 per km travelled. There are several means to do this, which include e.g. ATM efficiency gains and the use of bio-fuels. The most obvious (and traditional) approach is however the substitution of existing aircraft with new ones, which are generally technologically advanced and thus more efficient. In the following section future small and regional aircraft are discussed, followed by narrow-body and wide-body aircraft in the sections 5.4.2 and 5.4.3.

5.4.1 Small and Regional Aircraft

A large amount of new aircraft models is assumed to enter the 50 to 150 seat segment over the next years. While entirely new competitors are surging onto the regional market (Sukhoi, Mitsubishi, AVIC, COMAC), Bombardier expands its portfolio by classic medium-range aircraft that are to compete with small variants of the A320 and B737. Boeing and Airbus are expected to introduce successors to the latter ones around the end of the next decade.

It is expected that Sukhoi will deliver its first ***Sukhoi Super Jet*** SSJ100-95 already in 2009. This is in accordance with the actual order book **MRO Prospector 2008b**. The basic variant features a capacity of 95 passengers. A shortened version (SSJ100-75) with only 75 seats capacity is assumed to first enter service after two years in 2011.

It is presumed that work at Mitsubishi is going according to plan with a first delivery of the ***Mitsubishi Regional Jet*** (MRJ) in 2013 (**Mitsubishi 2008**). Mitsubishi intends to build two variants, the 70-seat MRJ-70 and the 90-seat MRJ-90. There was no sign for one of them to be delivered prior to the other. For the study at hand, the introduction of both thus falls into the year 2013.

The industrial consortium *Aviation Industries of China* (AVIC) is about to start series production of the first passenger aircraft to be developed in the People's Republic of China, the ***ARJ21 Xiangfeng***. Similar to the pre-discussed SSJ and MRJ, the ARJ21 features two variants with 70-80 and 90-100 seats. The basic version is the 80-seat ARJ21-700. We presume that it is first delivered according to the order book (**MRO Prospector 2008b**)

already in 2009. The year of first delivery of the stretched ARJ21-900 is taken as 2011, see **AT 2008**.

Bombardier intends to enter the market of larger regional and small medium-range aircraft by the introduction of the ***CRJ1000*** in 2009 and the ***CSeries*** in 2013 (**Kirby 2008**, **Bombardier 2008**). The CRJ1000 is a stretched version of the CRJ900, expanding the capacity of the CRJ family to 100 seats. It is meant as a direct counter to the best-selling large variants of the Embraer E-Jets. The CSeries is a new aircraft model currently under development. It is the first larger-than-regional project of Bombardier. Two variants are currently promoted, the C100, transporting up to 110 passengers and the 130-seat C300. If realized, the CSeries will compete with smaller versions of the Boeing 737 and Airbus A320 aircraft. It is reasonable that Bombardier is able to deliver the first CRJ1000 according to plan in the fourth quarter of 2009, as flight tests are already successfully completed (**Kirby 2008**). A development according to plan is expected for the CSeries and the delivery of the first aircraft to be realizable by 2013.

Airbus and Boeing are both expected to deliver a new short-range aircraft as replacement to their highly successful A320 and 737 families during the next decade. Airbus is presently in the phase of finding an appropriate over-all design for the successor to the A320 family, also known as the ***A30X*** **or** ***NSR***. Even though there has not been a formal program launch yet, Airbus has been extensively exploring novel configurations through both internal and external research, such as the European New Aircraft Concepts Research (NACRE) project (**Wall 2009**).

Boeing has defined its future development milestones in the so-called 'Yellowstone' Project. Subordinate projects are **Boeing *Y1***, a replacement for the present 737 family of aircraft, Y2, a replacement for the present 767 family of aircraft and now been built under the name 787 *Dreamliner*, and Y3, a replacement for the present 777 and 747 aircraft. Today's focus at Boeing is the final development of the production lines for the 787 and 747-8. After that, it is likely that they concentrate on developing a successor to the short-range 737. In June 2007, Boeing announced that a replacement is "... seven or eight years ..." away (**Jane's 2009**).

The expectations regarding increased fuel efficiency are high for the new single aisle aircraft families: "... a 20 % improvement in fuel burn over the best of today's single aisles types ..." is regarded as being essential to justify a launch of the program (**Airline Monitor 2008b,** p. 9). For entry-into-service dates, assumptions of **Airline Monitor 2008b** are adopted. It states that a new Boeing short-range will probably enter the market two years earlier to the Airbus counterpart (Y1 in 2016, A30X in 2018). Reasons for this decision are said to be Boeing's longer experience with carbon fibre technology and a missing incentive for Airbus to replace the best-selling A320 family without the market pressure of a superior competitor product. These dates are in reasonable consistence with **Grimme 2008** who expects both aircraft to enter the world fleet in 2017. Due to the lack of detailed information, both new

aircraft families are assumed to feature variants identical in design specifications to the variants of the 737 and A320 families. They will therefore successively replace all deliveries of the predecessor. All variants are assumed to enter the market in the same year.

The *Commercial Aircraft Corporation of China* (COMAC) released plans to expand the Chinese aircraft manufacture by a 150-seat aircraft. First delivery was planned for 2020, but has now been brought forward to 2016. According to **Francis 2009**, "China wants to ensure it gets its aircraft to market before Airbus and Boeing have a chance to produce new types to replace the Airbus A320 and Boeing 737." For the forecast at hand, the aircraft named ***COMAC 919*** is assumed to be produced according to plan and being brought to the market in 2016.

5.4.2 Medium-Sized Aircraft

There is an urge of several ambitious manufacturers of regional to small aircraft (Embraer, Bombardier, COMAC, AVIC) to also build medium- to large-sized aircraft. It is however assumed that this day is long way off and Airbus and Boeing remain the only manufacturers of medium to large aircraft throughout the entire time span of this forecast. In reality, this assumption may be wrong. However, it is hard to include non-Airbus/non-Boeing large airplane projects in the forecast without having any external input about the details (time, size and likeliness) of these projects. It is further not regarded as being essential for the understanding of the future evolution of CO_2 emissions. Near-future mid-sized aircraft of Airbus and Boeing are the Boeing 787 and Airbus A350.

The **Boeing 787** is a wide-body medium to long-range airliner that is designed to replace the Boeing 767, which first entered airline service in 1982. The basic version, the 787-8, is said to carry 242 passengers in a two class configuration over a design range of 14 484 km. It is now scheduled to enter service in early 2010, which is also assumed for the study at hand. The basic version will be followed by two derivatives. The 787-9 is planned to enter the market in 2012, feature a range of 15 772 km and a capacity of 280 seats. The 787-3, designed for a range of only 5472 km while carrying 317 passengers, is assumed to follow in 2013 (all data by **Airline Monitor 2007**). Boeing thereby satisfies the wish of several airlines for a more efficient medium-range aircraft with a relatively high capacity, a design specification similar to the out-of-production model Airbus A310 and a direct competitor to the A330-300. After Airbus had revealed its plans for the 777-200ER/LR competitor A350-900, Boeing announced a fourth derivative, the 787-10 as a direct counter. It is however unclear if it will ever be built and is therefore not included in the forecast. The 787 is assumed to replace all variants of the Boeing 767, which are considered as being already out of production with beginning of the first year of the forecast.

The **Airbus *A350 XWB*** is a wide-body long-range airliner designed as a direct counter to the long-range versions of the Boeing 787 and Boeing 777. XWB indicates extra wide body, as the cabin cross-section is 0.305 m wider than the body of the A330, yielding more passenger comfort for same number of seats abreast (**Jane's 2009**). Although in some parts comparable, it is assumed that the A350 XWB is not intended to generally succeed the A330.

According to **Rothman 2009**, design for the basic version, the A350-900 was frozen in December 2008, so that Airbus is now mainly concentrating on the industrial phase of development. Projected market-entry is mid-2013. The A350-900 is projected to have a design capacity of 315 passengers in a two-class configuration and a design range of 15 000 km. Two derivative versions are being developed, the smaller A350-800, accommodating 276 passengers and holding a design range of 15 370 km, and the extended A350-1000 with a capacity of 369 passengers and a range of 14 815 km (**Jane's 2009**). The derivatives are said to enter the market one year (-800) and two years (-1000) later than the basic version (**Airline Monitor 2007**). From a comparison of design specifications – i.e. capacity and range – in **Airline Monitor 2007**, the A350-800 is seen as a competitor to the B787-900, the A350-900 as a competitor to the B777-200ER/LR and the A350-1000 as a direct competitor to the B777-300ER. It is further assumed that the A350-800 will replace the long-range version of the A330, the A330-200. This is reasonable as the A350-800 shows similar design specifications and is probably more fuel-efficient. However, for the study at hand, A330-300 deliveries are not affected by the introduction of the A350. The design ranges are regarded as being too different. The market share of the A330-200 linearly decreases from its value in 2013 to zero in 2017. Its delivery thus continues for three years with the A350-800 already being on the market.

5.4.3 Large and Very Large Aircraft

Airbus has recently released the *A380*, a very large aircraft with a nominal seating capacity of 550. For the present, research and development is concentrated on the Airbus A350 XWB and the successor to the A320 family of aircraft. **A new, high-capacity long-range aircraft** (Airbus NLR) to fill the gap between the A350-1000 and the A380 is likely to be the third large project at Airbus. However, Airbus is assumed to be working to capacity for the next ten years with developing and launching the A350 XWB and the A30X. A new long-range aircraft to succeed the A330 and A340 aircraft is therefore not expected to enter the market before 2025. This date is adopted from a study of new aircraft in **Grimme 2008**. Similar to the A30X, no detailed data is yet available for this aircraft. It is thus supposed that the variants of the new model are similar in capacity and range to the A340-2/300, -600 and A330-300.

Neither the actual order book (**MRO Prospector 2008b**) nor market forecasts (**Airline Monitor 2008b**) draw a bright future for the Airbus A340 aircraft. It is thus assumed that no

further A340-200/300 and A340-500 aircraft are produced. Further, the last A340-600 is supposed to be already ordered and to be delivered according to plan in 2011. The A330-300 is however assumed to be sold until replaced by the pre-mentioned new long-range study. The delivery of the new aircraft and the A330-300 are taken to overlap for 3 years, with market shares of the A330 linearly decreasing from the 2024 value to zero in 2028.

Boeing has re-designed large parts of the 747-400 and plans to deliver the first of this supposedly last variant of the 747, the **Boeing *747-8***, in 2010 (**MRO Prospector 2008b**). Similar to Airbus, it is likely that Boeing will then concentrate on developing a new short-range aircraft to succeed the 737 family. After the release of the Y1 in 2016, it is assumed that the aircraft referring to the name **Boeing Y3** (a successor to the 747 and 777 aircraft) will be in their focus of research. The first delivery of Boeing's new large long-range is taken to be in 2027 (**Grimme 2008**). Being a successor to the 747-8, 777-200LR and 777-300ER, its entry-into-service will lead to these aircraft being taken from the market. Again, a linear decrease of the market shares to zero in 2030 is assumed.

The productions of the Boeing aircraft 777-200,-300 and 200ER are believed to be terminated earlier. The order book of the 20th November 2008 does not list any orders for the normal-range variants of the 777-200 and 777-300 aircraft (**MRO Prospector 2008b**). The productions of these models are taken as having ended with the beginning of the forecast. The market forecast of **MRO Prospector 2008a** up to the year 2018 believes the 777-200ER orders to be successively replaced by orders for the newer 777-200LR. Accordingly, the 777-200ER fleet is not growing past 2013. We will thus assume an end-of-production of the 777-200ER in 2014.

5.4.4 Assignment to FESG Seat Categories

For the calculation of market shares and demand, the new aircraft models are assigned to the FESG seat categories following the fleet breakup of similar existing ones, see Table 5.1. The existing models to which the new aircraft are linked in terms of fleet breakup are shown in Table 5.5.

Table 5.5 New Aircraft Models Linked to Similar Existing Ones

New Aircraft	Nominal Seat Capacity	Similar Existing Models
ARJ21, MRJ, SSJ	70	CRJ 700, EMB 170/175
ARJ21-900, MRJ-90, SSJ 100-95	90	CRJ 900, EMB 190
C-Series 110	110	A318, B737-600
CSeries 130	130	A319, B737-700
A30X	107, 124, 150, 185	A320 Family
Y1	110, 126, 162, 180	B737 New Generation
COMAC 919	150	A320

Table 5.5 New Aircraft Models Linked to Similar Existing Ones **(continued)**

New Aircraft	Nominal Seat Capacity	Similar Existing Models
787-3	317	A310
787-8	242	767-300ER
787-9	280	A330-300
A350-800	270	A330-200
A350-900	314	A340-2/300
A350-1000	350	777-300ER
777-200ER Successor	305	777-200ER
777-300ER Successor	365	777-300ER
747-8 Successor	467	747-8
A330/340-300 Successor	295	A340-2/300
A340-600 Successor	380	A340-600

5.4.5 Summary of Assumptions

Fig. 5.7 summarizes entry-into-service and end-of-production years that are adopted for the study at hand and plots them along a time bar.

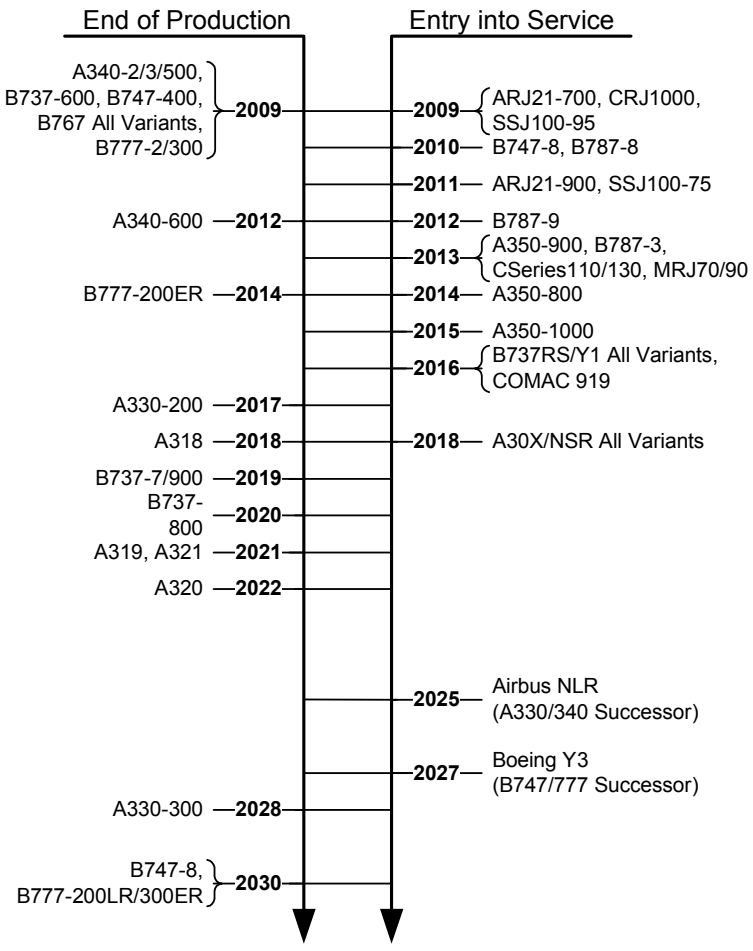

Fig. 5.7 Assumed Entry-into-Service and End-of-Production Dates of Aircraft

5.5 Market Shares

Market share is a measure of how dominant a company or product is in its industry or product category. It is given as the proportion of the total available market that is serviced by the company, e.g. 10 %. On a free market, market share thereby defines the value or attractiveness of a product.

For the fleet forecast at hand, an estimation of future market shares is needed to estimate the penetration of the market by the different aircraft models. Each year, growth rates and aircraft retirements lead to a specific demand for new aircraft in each seat category. This demand, say e.g. 200 aircraft within the 101-150 seat category, is assigned to the available aircraft according to their individual market share, e.g. 50 new A319, 30 new B737-700, etc.

Market shares can be estimated from the number of expected deliveries per aircraft type given in the current aircraft order book (**MRO Prospector 2008b**) and the *Traffic & Fleet Forecast 2008-2030* in **Airline Monitor 2008b**. These 'hypothetical deliveries' per aircraft type are assigned to the FESG seat categories according to Table 5.1 and 5.5. The market share of each aircraft *j* is then calculated from

$$\text{Market Share } S_j = \frac{\text{Individual Aircraft Deliveries per Seat Category}}{\text{Total Deliveries per Seat Category}} = \frac{D_j \cdot f_{C_j}}{\sum_{j=1}^{n} D_j} \quad , \quad (5.4)$$

where f_C is the fraction of the specific aircraft fleet assigned to the seat category C. This approach is schematically shown in Fig. 5.8.

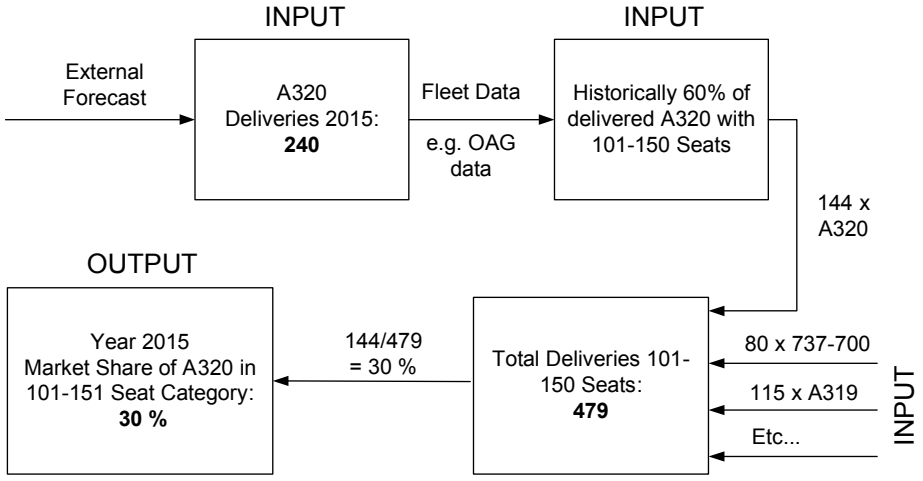

Fig. 5.8 Schematic of Computing Market Shares from Expected No. of Deliveries given in external forecast and seat capacities according to **OAG data 2007**

MRO Prospector 2008b and **Airline Monitor 2008b** do not include information on all considered aircraft. Further assumptions are necessary, especially for the calculation of market shares of the new regional aircraft (AVIC ARJ, Mitsubishi MRJ, Sukhoi SSJ, etc.) and the new large long-range (NLR) aircraft of Airbus and Boeing. It is also necessary to have a closer look at production ramp-ups and phase-outs when new configurations succeed today's models, e.g. A320 → A30X and B737 → Y1. Detailed information about additional assumptions made is found in Appendix B. For simplification, market shares of similar aircraft (if not given by external forecasts) are taken to be identical under normal production conditions (after ramp-up).[1] The transition time from the first delivery of a new model to the last delivery of its predecessor is generally estimated from historical data (**Airline Monitor 2008a**, **MRO Prospector 2008b**) of similar aircraft successions.

According to **Airline Monitor 2008b** and the current order-book (**MRO Prospector 2008b**), with beginning of the forecast, the following aircraft models are assumed as out of production and do not hold any future market shares:

- Airbus: A300, A310, A340-2/3/500
- Boeing: B717, B727, B737-2/3/4/500, B747-1/2/3/400, B757, B767, B777-2/300 (only normal range variants)
- Others: BAe146/AvroJet, DC9, DC10, MD11, MD80, MD90, Fokker 70/100

5.6 Results

The absolute market share for each year of the forecast in terms of total number of aircraft delivered to the world fleet is shown for the different manufacturers in Fig. 5.9. Fig. 5.10 shows market shares per manufacturer alternatively in terms of seats delivered. Note that market share has been originally calculated for each type of aircraft and seat category individually and only afterwards summed up to give market share per manufacturer.

Figs. 5.11 to 5.13 show the size and make-up of the global fleets of regional jet, narrow-body and wide-body aircraft. The number of active aircraft is plotted against the timeframe of the forecast. Note that – similar to the visualization of market shares – the active number of aircraft has been originally calculated for each type of aircraft and seat category individually and only afterwards summed up to give families of aircraft, which are then displayed e.g. as

[1] Exceptions are the new Chinese aircraft ARJ 21 and COMAC 919. It is already public that the ARJ 21 features technology that is rather 'conventional'. The aircraft is largely based on technology originating from the MD90 and only the wing was newly designed (**Spaeth 2008**). As the new regional jets of Bombardier, Mitsubishi and Sukhoi promise to be more efficient, it is assumed that the ARJ is less attractive for western customers. Its world market share is thus roughly the half of the market share of its competitors. Similar assumption is made for the COMAC 919 (50 % market share of the Bombardier CSeries).

Embraer E-Jets or Airbus A320 Family. Type specific results of the fleet forecast – e.g. the market share and active number of E-195 aircraft per seat category and year – can be found in digital form on a compact disc in Appendix D.

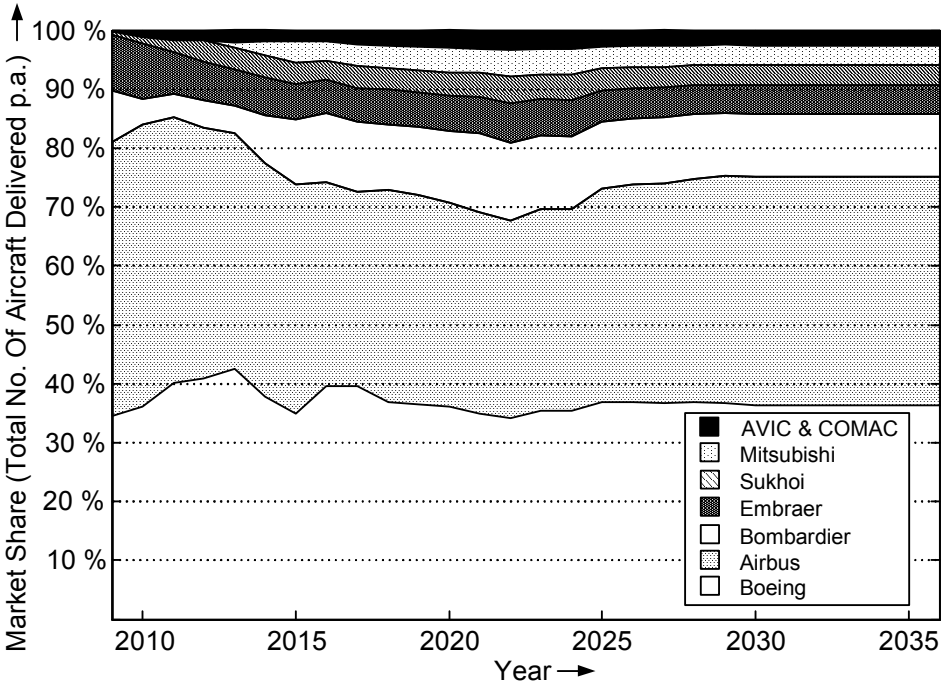

Fig. 5.9 Absolute World Market Share of Total No. of Aircraft Delivered per Manufacturer 2009-2036

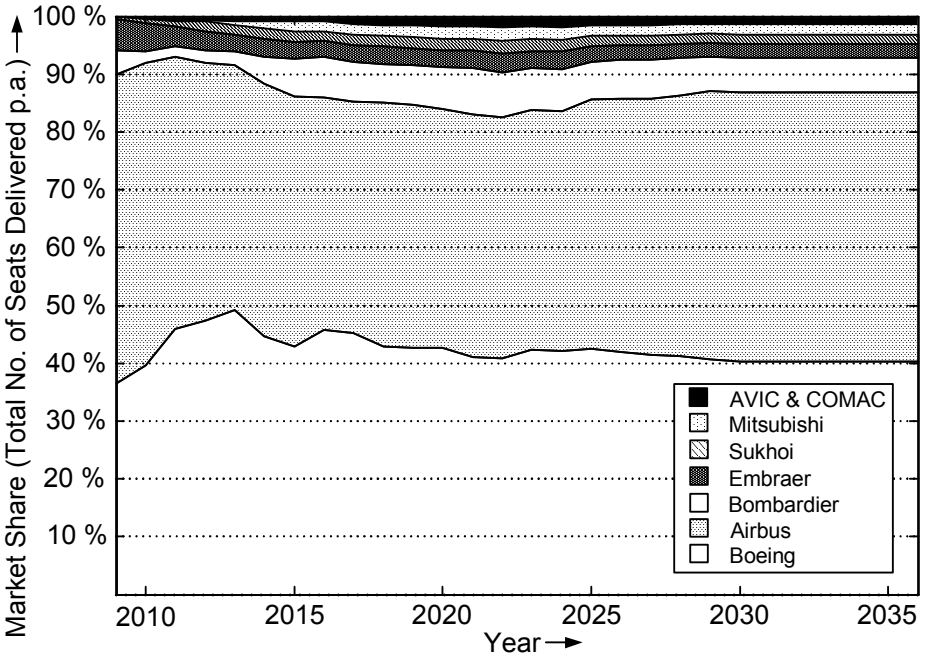

Fig. 5.10 Absolute World Market Share of Total No. of Seats Delivered per Manufacturer 2009-2036

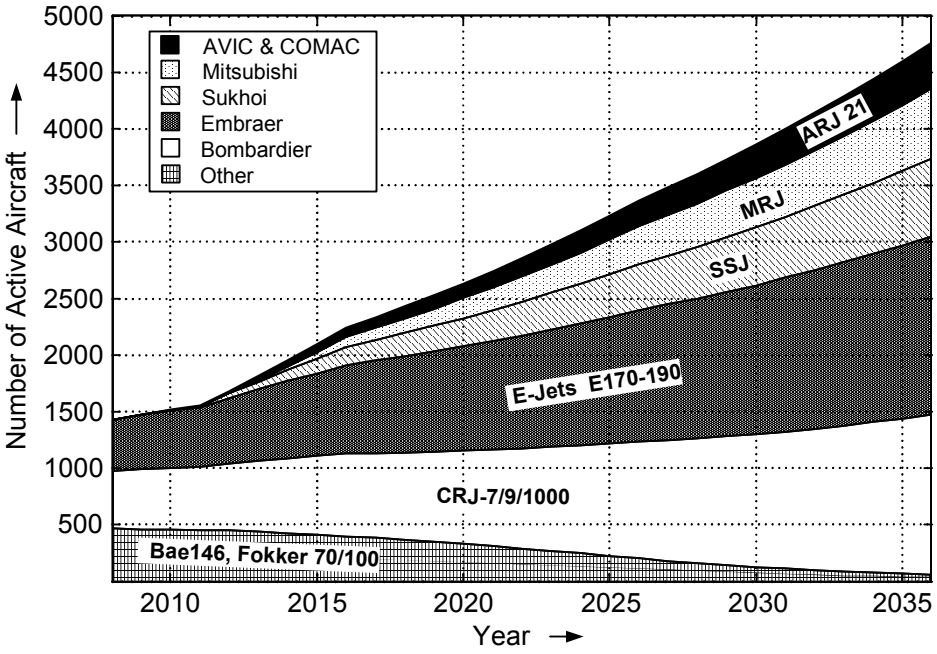

Fig. 5.11 Make-up of the Future World Fleet of Regional Aircraft 2009-2036

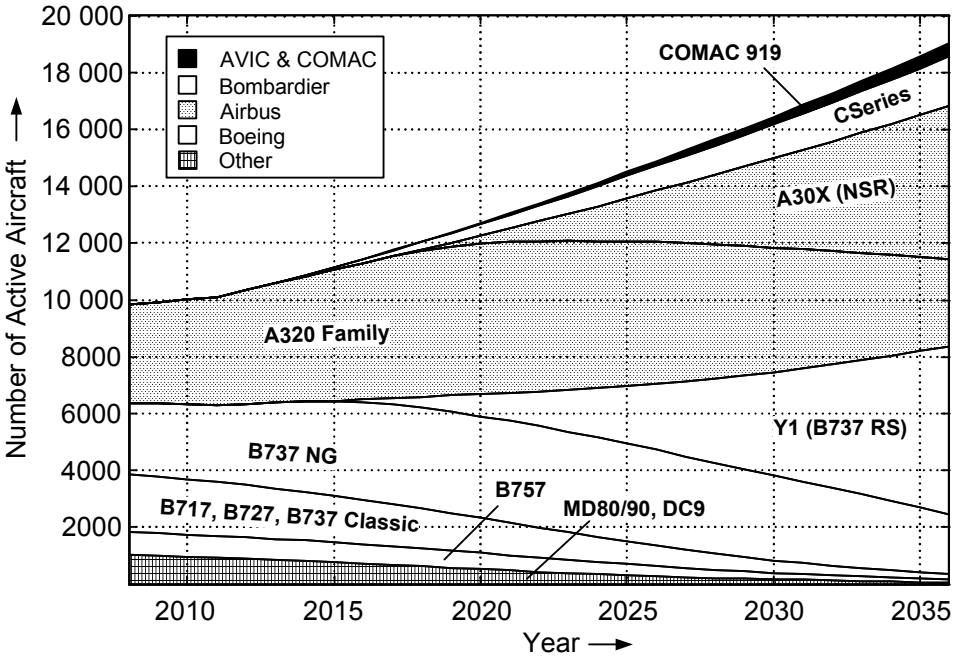

Fig. 5.12 Make-up of the Future World Fleet of Narrow-Body Aircraft 2009-2036

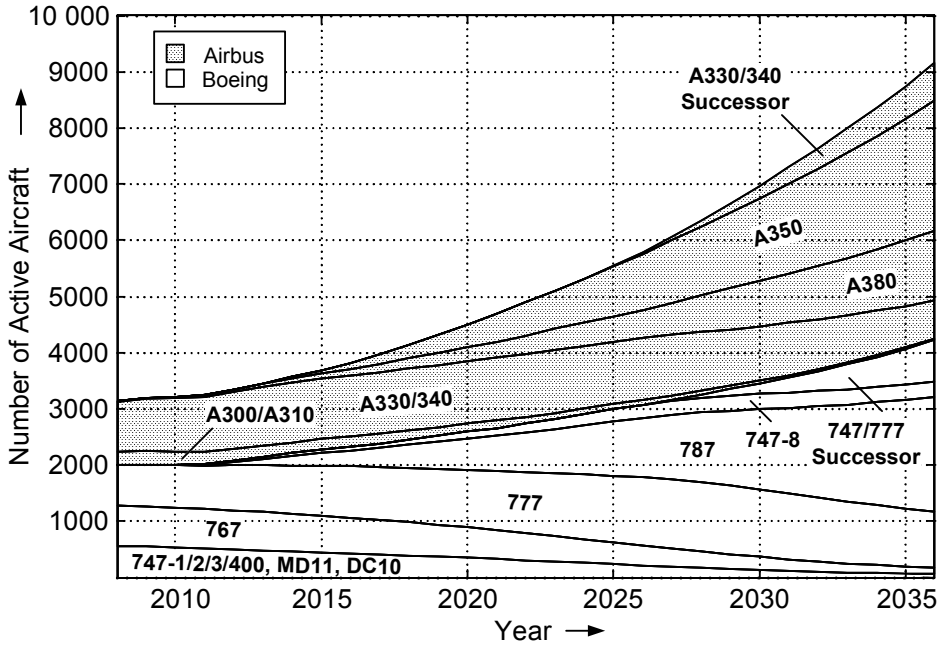

Fig. 5.13 Make-up of the Future World Fleet of Wide-Body Aircraft 2009-2036

5.7 Analysis and Interpretation of Results

5.7.1 Market Shares

The manufacturers of the new regional jets, AVIC, COMAC, Mitsubishi and Sukhoi, feature a combined market share of about 10 % after the production ramp-up. The market shares of today's regional jet market leaders, Embraer and Bombardier, are suffering from this. However, Bombardier is able to recover due to the introduction of the CSeries aircraft in 2013. Both Airbus and Boeing experience a loss in deliveries due to the new Bombardier aircraft competing with the smaller A320 family and 737 aircraft. In the first years of the forecast (2010-2013), Boeing market shares increase due to the new 787 being market leader in the segment of 211-300 seats. With the introduction of the A350 in 2013 however, Airbus is able resume higher shares of the wide-body market. Thus, Boeing is hit by the emergence of two different competitors at the same time, the CSeries on the narrow-body and the A350 on the wide-body market. The decline of market shares of the two major manufacturers is brought to a hold by the launch of the 737 successor in 2016 and the A30X in 2018.

Fig. 5.10 shows market shares alternatively in terms of seats delivered. The influence of the new regional aircraft is noticeably less. Moreover, Boeing's dominance in the wide-body segment (777 and 787 aircraft) and the resulting growth in market shares during the first years of the forecast are easier to observe. As large aircraft are delivered in smaller numbers, but

yield higher market prices, Fig. 5.10 is also more representative in terms of manufacturer's revenue.

5.7.2 Make-up of the Regional Jet Market

The regional jet market (Fig. 5.11) experiences a large growth. The number of active aircraft has more than tripled from 2008 towards the end of the timeframe. Bombardier and Embraer continue to dominate the regional world fleet. However, the new regional jets ARJ21, MRJ and SSJ account for more than one third of the world fleet in 2036. As annual growth rates are low for the years 2009-2011, the advantage of an early introduction of Sukhoi's and AVIC's regional jets over the MRJ is rather small. Nearly all BAe146 and Fokker 70/100 aircraft (408 out of 464) are being retired and replaced by new regional aircraft. However, as there are no successors to the regional aircraft of Embraer and Bombardier, 'new' aircraft account for only 35 % of the entire world fleet in 2036.

5.7.3 Make-up of the Narrow Body Market

There is a large change in the make-up of the narrow body world fleet from 2008, see Fig. 5.12. Almost all out-of-production models (B717, B727, B737 Classic, B757, MD80/90 and DC9) have been replaced by more modern aircraft in 2036. Today's market leaders in the narrow-body segment, the 737 New Generation (NG) and A320 models, are being replaced in 2016 and 2018 respectively. However, the A320 and 737 fleets continue to grow until production ends a few years later. The peak is reached for the 737 NG in 2019 with 3576 aircraft being active, for the A320 in 2021 with 5322 active aircraft. The mean age of the fleets at that time is 14.85 years (A320) and 12.20 years (B737 NG) respectively. The 737 successor Y1 has a small advantage over the A30X in terms of total aircraft deliveries. This is not due to a higher market share (these are more or less identical), but to the earlier market entry in 2016. In 2036, about 70 % of the narrow-body world fleet consists of entirely new aircraft models, including the new Boeing Y1, Airbus A30X, Bombardier C-Series and COMAC 919. The first year in which more 'new' models than 'old' models are in service is 2030. The over-all fleet growth is relatively small when compared to the regional and wide-body market.

5.7.4 Make-up of the Wide Body Market

The development of the world fleet of wide-body aircraft (Fig. 5.13) is marked by the emergence of four new aircraft models: the 787, the A350 and the successor models to the 747/777 and A330/A340 aircraft. In the segment of 211 to 400 seats, the fleet is first dominated by the 777 and A330/A340 aircraft and later by the 787 and A350 aircraft. Throughout the forecast, both Airbus and Boeing aircraft hold nearly an identical share of the cumulative fleet size of these models. In the category of very large aircraft, the number of A380 in the world fleet surpasses the number of 747 in the world fleet in 2025. This is due to the Airbus serving a seat category (501-600 seats), which, according to the forecast of **FESG 2008**, shows high growth rates but is lacking a competitor. Contrary, the new 747-8 has to compete with the A380 in the seat category of 401-500 seats and with the 777 in the 301-400 seat category. Of the three discussed world fleets, the one of wide-body aircraft is the most modern. If we include the A380 in the summation of 'new' aircraft, the number of new aircraft surpasses the number of old ones (767, 777, A330 and A340 included) already in 2027.

5.8 Chapter Summary

In this chapter, a forecast of the size and make-up of the world fleet of turbofan powered passenger aircraft[1] through the year 2036 has been established using annual fleet growth rates that have been determined from a 2008 ICAO/FESG fleet size forecast. Future aircraft retirements have been computed using 'aircraft survival curves' that are based on statistical data. All aircraft have been assigned to seven generic seat categories, which then feature individual annual growth rates and retirements, the sum of which calculates to the annual demand for new aircraft of the respective size. The growth of individual in-production aircraft fleets is then determined by the assigned market share. It is shown that new aircraft work their way only slowly into the world fleet and that a large share of currently active aircraft will probably still be in service many years from now. As the results provide the absolute number of aircraft active per year and type, it is now possible to calculate CO_2 emission and transport performance of the global fleet given that fuel burn and utilization of the individual aircraft is known. The following chapter is thus dedicated to this task.

[1] Note that the analyzed 2008 world fleet does neither regard aircraft types (1) with less than 50 seats, (2) nor of which less than ten aircraft are active (except the Airbus A380) and (3) nor of Russian manufacturers.

6 Global CO_2 Emission Forecast

In the previous chapter, the size and make-up of the future world fleet of turbofan powered passenger aircraft has been projected through the year 2036. In this chapter, the established fleet forecast is employed to assess global CO_2 emissions.

The first section includes information on the approach to calculate global aviation's CO_2 emission from single aircraft fuel consumption and utilization. It includes assumptions made about the fuel efficiency of aircraft active in 2008, the technology implementations on future aircraft and their impact on the aircrafts' fuel efficiency. After the fuel consumption per block hour and the daily utilization for all considered aircraft is set, an elementary or base forecast can be established, which is presented and discussed in subchapter 6.2. The forecast is grounded on the assumption that changes to the fuel/CO_2 efficiency of the global air traffic system come only from technologically advanced future aircraft. In other words, neither technological nor operational measures with the capability to provide benefits to existing aircraft or to existing aircraft programmes are implemented. This forecast is elementary as it allows simulating the potential impact of alternative instruments that have a fleet-wide impact in subchapter 6.3.

6.1 Single Aircraft Contribution

All active aircraft in the world fleet generally contribute to the global emission of CO_2. An aircraft's respective share in global CO_2 emission is dependent on its fuel efficiency and its time in use. If alternative fuels are considered, it will be further a function of the fuel's *specific carbon dioxide emission* (*SCE*), which is the amount of CO_2 emitted per kg fuel burned. The average mass of CO_2 emitted daily from a single active aircraft can be approximated from

$$\text{Daily Aircraft } CO_2 \text{ Emission} = BF \cdot U_d \cdot SCE \quad , \tag{6.1}$$

where BF is the average fuel consumption per block hour and U_d is the average daily utilization (in block hours per day). To compare aircraft of different size and range, it is prudent to calculate fuel burn per seat-km. If block speed, fuel burn per block hour and average capacity are known, this is possible using following equation.

$$SFB = \frac{BF}{v_b n_S f_L} \cdot \frac{1}{10 \rho_F} \quad , \tag{6.2}$$

where f_L is the load-factor, n_S is the number of seats available and ρ_F is the density of the fuel in $kg \cdot m^{-3}$. The result is then in litres per seat and 100 km ($l \cdot 100^{-1} \cdot km^{-1}$). It becomes clear that seat fuel burn *SFB* is not only a function of the fuel consumption per unit time, but also of the block speed – i.e. cruise speed and range – and the ratio of sold to available seats.

For the calculation of global CO_2 emission, block speed v_b and block fuel consumption *BF* of a single aircraft are assumed identical to the average block speed and block fuel consumption of the aircraft's respective fleet. This implies that aircraft of the same model are flown inside a band of flight ranges that allows the linearization of both block time t_b and block fuel weight $W_{F,b}$ over range R. It is a general assumption, which can be found in a great deal of literature dealing with a similar topic.[1] Given that there are no technology changes to the aircraft, block speed and fuel burn are taken as constant during the timeframe of the forecast. This assumes future flight distances (of a single aircraft family) to be relatively consistent with historic data. Even though this corresponds to the assumptions made in a similar fleet forecast by **Grimme 2008**, a more into detail analysis would be needed to justify this approach.

For the study at hand, FESG estimations concerning future utilization growth are adopted for the years 2012 to 2036. In accordance with **FESG 2008,** p. 10, it is assumed that average aircraft utilization per aircraft type experiences a "Total increase of 5 % by 2026", and a "Total increase of 6% by 2036". Growth in between 2007 and 2036 and 2027 and 2036 respectively is assumed exponential. As air traffic is currently affected by a significant economic crisis, see subchapter 5.2, utilization in 2009 is expected 4 % lower than the aircraft utilization in 2008. Utilization is expected to remain low (at 2009 level) also for the following two years. In 2012, air traffic is expected to have recovered and a daily utilization according to FESG estimations is applied. This affects all aircraft considered.

[1] This assumption has been found in several *Aircraft Commerce* articles, see e.g. **Aircraft Commerce 2008b**, in several *Airline Monitor* articles, see e.g. **Airline Monitor 2008c** and in the assumptions made for a similar CO_2 forecast in **Grimme 2008**. It is further an assumption for the calculations of block fuel weight and CO_2 emissions in the *SAS Emissions Calculator* (**SAS 2008**), which has been reviewed by **Forsberg 2002** and has been found to "... provide a reasonable calculation of the environmental impact of specific flights".

6.1.1 Active Fleet of 2008

For the most of currently active aircraft, block speed and fuel burn is adopted from the average of historical fleet data of the last ten years (on a yearly basis). As for some of currently active aircraft models historical data is not readily available, fuel consumption and block speed are adopted from further literature. Consulted literature is listed in Table 6.1. In the following, v_b denotes for the average block speed and *BF* for the average block fuel burn of the respective aircraft fleet.

Table 6.1 Consulted Literature for Fleet Average Fuel Burn per Block Hour and Block Speed

Aircraft	Primary Reference	Validated with
A330-200	**ICAO 2001**	**Aircraft Commerce 2008a**: Ratio of *BF* A330-200/A330-300
A330-300	**ICAO 2001**	**Airline Monitor 2007**
A340-200/300	**Airline Monitor 2007**	**ICAO 2001**
A340-500	**Airline Monitor 2007**	-
A340-600	**Airline Monitor 2007**	**ICAO 2001**
A380-800	**Aircraft Commerce 2007** (5500 nm average flight distance)	**Gmelin 2008**: 12 % less per seat-km than the 747-400
737-600	**Airline Monitor 2007**	**Aircraft Commerce 2008c**
747-300	**Eurocontrol 2004a** Fuel Burn Ratio 747-300/747-200, **Airline Monitor 2008a** Historical Block Fuel 747-200	-
777-200ER	**Aircraft Commerce 2008b**	**Eurocontrol 2004a**: Ratio of In Cruise Fuel Burn 777-200ER/777-300ER
777-200LR	**Aircraft Commerce 2008b**	-
777-300	**Aircraft Commerce 2008b**	-
777-300ER	**Aircraft Commerce 2008b**	**Aircraft Commerce 2001**: 14-17 % lower fuel burn than the A340-600
E-170	**Aircraft Commerce 2008c**	**Airline Monitor 2007**
E-175	**Aircraft Commerce 2008c**	-
E-190	**Aircraft Commerce 2008c**	**Airline Monitor 2007**
E-195	**Aircraft Commerce 2008c**	-
Fokker 70	**Aircraft Commerce 2006**	**Airline Monitor 2008a**: Fokker 100
All Other	Average of Historical Data From 1998 or First Year in Service to 2007 (**Airline Monitor 2008a**)	-

As observable from Table 6.1, data on some aircraft's block fuel burn and block speed is not directly amenable to validation with information given in a second reference. However, the data is reasonable and information on similar aircraft from the same source is readily validated. It is thus assumed that the given data is realistic. Data on the block speed and fuel burn of the different aircraft can be found in Appendix C.

The average seat capacity per aircraft type is calculated from OAG data for the year 2008 (**OAG data 2007**). The approach is similar to identifying the relative share of aircraft flown in different seat categories, see chapter 5.2. The average of available seats per aircraft type for all scheduled flights in 2008 is taken to be the respective fleet average. Detailed results can be found in Appendix C.

Average daily utilization can be determined from single aircraft data given in the MRO Prospector. The MRO document *Aircraft and Engines by Aircraft Model* (**MRO Prospector 2008b**) gives the entry-into-service date and the total number of block hours for each of the regarded aircraft. Dividing the total number of block hours by the number of days in service – i.e. days from entry-into-service to the date the document was updated (20th November 2008) – gives average daily utilization U_d. The major advantage of this approach is that the result is the average utilization over the entire aircraft life. It therefore factors periods of both normal and low utilization, e.g. periods that include major aircraft checks and overhauls. The major disadvantage is that the average utilization over several years is eventually not exactly identical with the average utilization for the base year 2008. It is however assumed that this does not falsify the results of the CO_2 forecast considerably as the relative differences in utilization of the different types of aircraft are expected to be realistic. Computed average U_d of currently active aircraft can be found from the tables in Appendix C.

6.1.2 Future Aircraft Technology Impacts and Fuel Efficiency

It is assumed that eleven entirely new aircraft families enter the market place in the 2030 timeframe. Three of them are regional jet, four are narrow-body and four are wide-body aircraft. Further, two derivatives of already existing aircraft are expected, the CRJ1000 and the 747-8. The entry-into-service dates and market shares for all future aircraft have been already defined for the fleet forecast in chapter 5, see details in Appendix C. Their impact on traffic growth and CO_2 production is now dependent on their respective daily fuel consumption and transport performance.

Future Aircraft with Near- to Medium-term Entry-into-service Date

Eight of the thirteen regarded future aircraft are expected to have a service entry prior to 2015. These projects have already been officially launched by the manufacturers and the general design and major technology features are frozen. Detailed findings of a literature research

concerning the new aircraft is attached through Appendix C. Table 6.2 provides an overview over the most important technology implementations.

Table 6.2 Future Aircraft with Near- to Medium-term Entry-into-Service Date – Assumed Technology Implementations

Aircraft Name	Service Entry	Description	Fuel/CO_2-Relevant Technology Implementations
Bombardier CRJ-1000	2009	Stretched CRJ-900	-
ACAC ARJ21	2009	New regional jet	-
Sukhoi SSJ100	2009	New regional jet	More efficient conventional turbofan
Boeing 747-8	2010	Latest evolutionary 747 variant	New wing design More efficient conventional turbofan
Boeing 787	2010	New medium-sized long-range aircraft, 767 Replacement	Composite primary structures: increased wing span/aspect ratio New wingtip design More efficient conventional turbofan 'No-bleed' engine/ MEA architecture Increased cruising speed
Airbus A350	2013	New medium sized long-range aircraft, 777/787 competitor	Composite/Al-Li primary structures: Reduced empty weight Variable camber wing Improved high lift systems New wingtip design More efficient conventional turbofan Increased cruising speed
Mitsubishi MRJ	2013	New regional jet	Wings and empennage of composite Geared turbofan
Bombardier CSeries	2013	New narrow-body aircraft	Specifically designed for 110-130 seat range Composite/Al-Li primary structures: increased wing span/aspect ratio Geared turbofan

Simply put, fuel efficiency of new aircraft is improved from existing ones by implementing new technologies that are fuel- and/or CO_2-relevant. Even though high fuel efficiency is important to all manufacturers, it must not always be the primary goal. This is also the case for some of the expected future aircraft. For example, the intent behind designing the ARJ21 is rather to gain experience in building commercial aircraft that meet Western certification requirements (**Leithen 2007**). Likewise, Sukhoi emphasized on reducing aircraft purchase, maintenance and operation costs to attract more Western customers. This leads to an aircraft that is "... based on proven advanced technology to minimize technical risks ..." (**Sukhoi 2009**), but does not feature revolutionary fuel-efficient technologies. The bulk in cost reduction for airlines is thus not achieved by lower fuel costs, but through standardized

operation and maintenance procedures. This is the reason for assuming that the ARJ21 and SSJ show no or only a very small improvement from existing aircraft.

Experienced aircraft manufacturers are more likely to implement new technologies and thereby to take the risk of high development cost. This is often due to airlines that demand a certain efficiency improvement from the existing models. For example, both the 787 and A350 will feature some highly innovative technologies such as composite primary structures. Leading aircraft companies can further shift some responsibility in fuel reduction on to the engine manufacturers who are interested in powering aircraft that are likely to be among the best sold in the next decades. This is the reason for technological milestones in engine efficiency to coincide often with new Airbus and Boeing aircraft models, as it is the case for the very high by-pass engines Rolls Royce TrentXWB and General Electric GEnx on the 787 and A350.

An exception to this standard procedure is the geared turbofan (GTF). Here, an entirely new engine architecture that lowers fuel consumption considerably is introduced with new aircraft families of Mitsubishi and Bombardier. The MRJ's fuel burn advantage is assumed to be mainly due to the GTF, as the aircraft does not show other technologies that have a serious potential to reduce fuel consumption. Contrary, the fuel burn advantage of the CSeries is expected to be only partly due to the use of the GTF. A large part is believed to be due to the aircraft being the first to be designed for the seat category of 110 to 130 seats. Its competitors (A318/319, 737-600/700, E-195) suffer in terms of fuel efficiency from being a derivative of generally smaller regional or larger narrow-body aircraft.

A detailed description of all near-to medium-term future aircraft projects regarded in our forecast and their featured technologies is given in Appendix C. Table 6.3 lists fuel reductions over seat fuel burn of comparable reference aircraft that are assumed for the forecast at hand. The reductions in fuel burn are estimations based on manufacturer specifications and a literature research (see Appendix C). The reduction is further in reasonable accordance with the expected improvement of the individual technologies and the parametric study in chapter 3.3.

Table 6.3 Future Aircraft with Near- to Medium-term Entry-into-Service Date – Assumed Reduction in Seat Fuel Burn

Future Aircraft	Reference Aircraft	Reduction in Nominal Seat Fuel Burn
CRJ-1000	CRJ-900	± 0.0 %
ARJ21-700	CRJ-700	± 0.0 %
ARJ21-900	CRJ-900	± 0.0 %
SSJ100-75	E-170	- 2.0 %
SSJ100-95	E-190	- 2.0 %
B747-8	B747-400	- 13.8 %
B787-3	No modern reference available (A300)	(up to - 47.0 %)
B787-8	A330-200 / B767-300ER	ca. - 20.0 %
B787-9	A330-200 / B767-300ER	ca. - 20.0 %
A350-800	B787-9	- 5.5 %
A350-900	B777-200ER	- 23.0 %
A350-1000	B777-300ER	- 20.0 %
MRJ-70	E-170	- 10 %
MRJ-90	E-190	- 10 %
C100	E-195	- 20 %
C300	B737-700	- 20 %

Future Aircraft with Medium- to Long-term Entry-into-Service Date

The remaining aircraft projects are still in a very early stage of development, which does not allow for definite projects of the technology implemented. There is first, Boeing's new short-range, an aircraft project currently titled Y1, which is assumed being delivered from the year 2016 onwards. Similarly, the successor to the Airbus A320 family of aircraft, currently titled A30X, is expected for 2018. New long-range aircraft in the seat range of 300 to 400 from both Airbus and Boeing are anticipated to enter service 2025 and 2027 respectively. Further, a new Chinese aircraft with a capacity for 150 people, the COMAC 919, is due in 2016.

Airbus and Boeing have been engaged in replacement studies for the A320 and 737 for some time now (**Wall 2009**, **Kingsley-Jones 2008b**). It is assumed that they need to deliver an anticipated seat fuel advantage of at least 20 % over the best of today's single-aisle types to give reason for an official program launch (**Airline Monitor 2007**, **Gates 2008**). In **IATA 2008a**, Airbus writes that technical options for the A30X are still being assessed and will be frozen 2009 the earliest. The company further states that "... the A30X will reduce fuel burn and CO_2 emissions in excess of 30 %" (**IATA 2008a,** p. 20). Technologies being assessed for the A30X include laminar flows for drag reduction, advanced composites and alloys for weight reduction, fuel cells as an alternate energy source and geared and open rotor architectures for improved engine efficiency (ibid.). Boeing's current efforts concerning the 737 successor Y1 are similar. The company reduced its airplane-design effort and now focuses on finding appropriate technologies to achieve the anticipated fuel reduction (**Gates 2008**).

While there have been rumours about the intent to build successor aircraft to the 777/747 and A340, there is virtually no information available concerning general design or technology implementations preferred by the manufacturers. An official project launch is probably years away.

Concerning the COMAC 919, there have no details been released besides the plan to co-operate with western engine manufacturers (**Leithen 2007**).

There is an array of new technologies under development that could significantly improve the performance of the aircraft within this longer time scope. However, the further maturing of those technologies is associates with a relatively high degree of uncertainty. Three different technology scenarios are introduced in order to meet these uncertainties. A pessimistic (low) scenario and an optimistic (high) scenario cover the extreme developments and mark the lower and upper boundaries of the 'actual' future technology development; a trend scenario describes a moderate but likely development of aircraft technology levels. Fig. 6.1 gives for the three different scenarios a range of possible technologies that could be integrated into new aircraft. An increasing CO_2 reduction potential (horizontal axis) is in general linked to an increased technology risk (vertical axis).

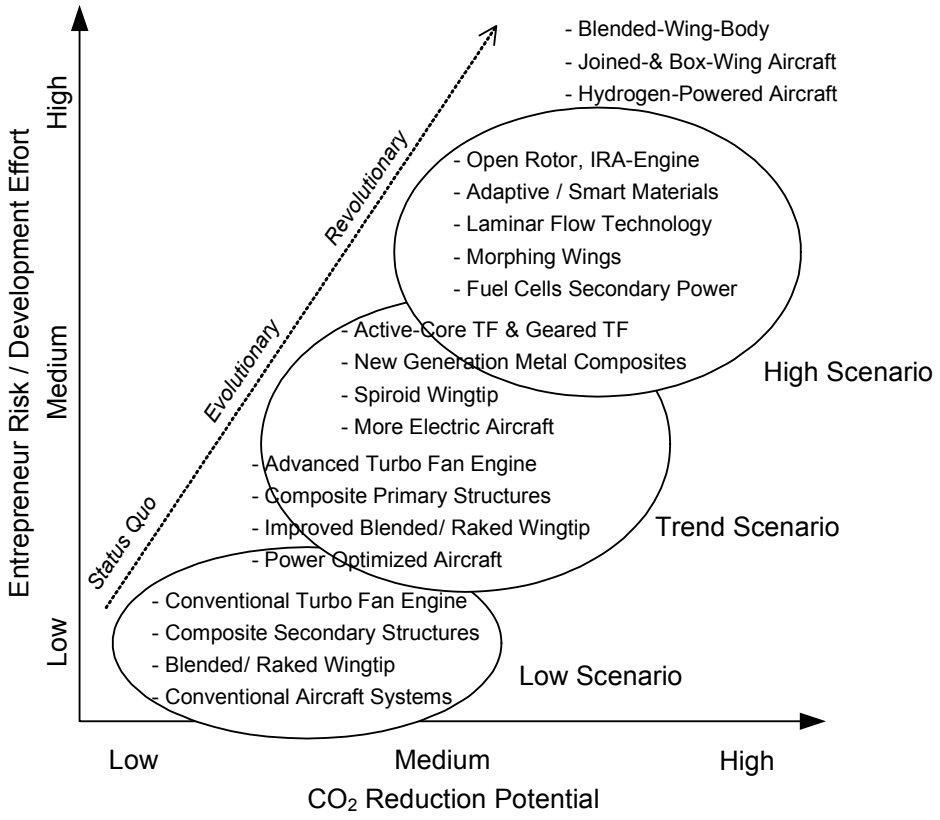

Fig. 6.1 Potential Technologies for Medium- to Long-term Aircraft Projects for Three Different Future Scenarios

The story of the scenarios is summarized in the following:

The **pessimistic scenario** is based on the assumption that the current technology screening brings out that a successor aircraft to the 737 and A320 families providing a 20 % seat fuel reduction is not realizable. This is due to adequate technology being unavailable, immature or too expensive. Both Airbus and Boeing stop development of the Y1 and A30X respectively and continue selling the existing models for the entire time span of the forecast. The decision is fostered by the fact that the current models continue to be ordered and the manufacturers see no need in taking the risk for the development of a new model. Similarly, development of the new Boeing and Airbus long-range aircraft is assumed to be cancelled. While Boeing continues selling the 777 and 747-8, the A350-1000 and A380 remain the only Airbus competitors. Airbus keeps selling the A330-300. The COMAC 919 is released according to plan in 2016 showing similar fuel burn to the A320.

The **optimistic scenario** is based on the assumption that the manufacturers focus on best possible CO_2 reduction. To accomplish this strategy, they are willing to implement also radical and high-risk design changes, such as a forward swept wing for natural laminar flow, open rotor designs and recuperative engines. In accordance with the Airbus statement in **IATA 2008a**, fuel burn of the new narrow-body aircraft shows a reduction in excess of 30 %. Each variant of the A30X and Y1 families features a seat-fuel reduction of 35 % compared to its respective predecessor. The new long-range aircraft are assumed to be the first aircraft to achieve the ACARE Vision 2020 CO_2 reduction goal (see chapter 6.4) through a 40 % fuel reduction over the 777 (A340 and 777 replacements) and over the 747-400 (747 replacement). The COMAC 919 shows fuel consumption similar to the 150-seat A30X variant.

The **trend scenario** is based on the assumption that manufacturers keep up to their business as usual: technical innovations are implemented on a modest scale to not risk high development cost and low customer acceptance. This implies rather evolutionary than revolutionary technologies. Similar to the Boeing 787, Airbus A350 and Bombardier CSeries, the new aircraft feature advanced materials for primary structures and improved, but still conventionally shrouded engines (i.e. advanced or geared turbofans). None of the more radical changes (laminar flow, fuel cell, open rotor, recuperative engine etc.) finds its application. However, the minimum required fuel reduction for the A320 and 737 replacements is achieved. Each variant of the A30X and Y1 families features a seat-fuel reduction of 20 % compared to its respective predecessor. The efficiency of conventional technologies is assumed to have slightly increased from the 787 and A350 when the new long-range aircraft are introduced in the late 2020s. While the 787 and A350 show a seat-fuel advantage of around 20 % over the A330 and 777, this is increased to 25 % for the 777/747 and A340 replacements. Similar to the ARJ21, the intent behind building the COMAC 919 is assumed to be the establishment of a stable Chinese aircraft industry rather than to build

revolutionary fuel-efficient aircraft. It is assumed that due to the company's experience to build the ARJ21, a seat-fuel reduction of 15 % compared to the current A320 is possible.

The assumptions concerning seat fuel reduction for the different scenarios are summarized in Table 6.4.

Table 6.4 Future Aircraft with Medium- to Long-term Entry-into-Service Date – Assumed Reduction in Seat Fuel Burn

Scenario	Future Aircraft	Reference Aircraft	Reduction in Nominal Seat Fuel Burn
Low	A30X	A320 Family	Production Cancelled
(Pessimistic)	Y1	737 NG Family	Production Cancelled
	A340 Successor	777-200ER, 777-300ER	Production Cancelled
	777 Successor	777-200ER, 777-300ER	Production Cancelled
	747 Successor	747-400	Production Cancelled
	COMAC 919	A320	± 0 %
Trend	A30X	A320 Family	- 20 %
(Neutral)	Y1	737 NG Family	- 20 %
	A340 Successor	777-200ER, 777-300ER	- 25 %
	777 Successor	777-200ER, 777-300ER	- 25 %
	747 Successor	747-400	- 25 %
	COMAC 919	A320	- 15 %
High	A30X	A320 Family	- 35 %
(Optimistic)	Y1	737 NG Family	- 35 %
	A340 Successor	777-200ER, 777-300ER	- 40 %
	777 Successor	777-200ER, 777-300ER	- 40 %
	747 Successor	747-400	- 40 %
	COMAC 919	A320	- 35 %

6.1.3 Future Aircraft Operational Performance

The operational performance of future aircraft is adopted or estimated from similar existing aircraft. Block speed v_b and daily utilization U_d are dependent on the cruising speed and the average distance flown. It is thus assumed that existing and future aircraft showing similar cruise Mach numbers and design ranges feature identical block speeds and identical daily block hours. An exception are the 787 and A350 aircraft families. These show considerably increased cruise Mach numbers and design ranges from currently active aircraft. Block speeds for all variants of both 787 and A350 are adopted from **Airline Monitor 2007**. These are in reasonable accordance with the increase in cruise speed and range. For all future aircraft, the relative deviation of average seat capacity from nominal seat capacity is taken to be identical to a comparable reference aircraft. Information on the reference aircraft and the literature used for the estimation of block speed, daily utilization and the deviation from nominal capacity of

future aircraft is listed in Appendix C. The same Appendix further shows the resulting performance data on the prospected future aircraft and contrasts it with obtained performance data on currently active aircraft.

6.2 Base Forecast: Analyzing the Impact of Future Aircraft

A base estimate of future global CO_2 emissions is set up in this subchapter. It assumes that CO_2 benefits to the global fleet are provided only by the emergence of new, i.e. more efficient, aircraft programmes. The base forecast is set up for the three pre-defined scenarios concerning the technology and fuel efficiency of long-term aircraft projects (see Table 6.4). The terms low (pessimistic) scenario, trend (most likely) scenario and high (optimistic) scenario refer to these assumptions. Currently active aircraft and new aircraft delivered of active aircraft programmes do not improve. There are further no CO_2 benefits from improvements of the ATM system and none from the use of alternative fuels considered. Global fuel consumption and CO_2 emission per day is then calculated from

$$\text{World Fleet Fuel Consumption} = \sum_{j=1}^{n_{A/C}} \left(U_d BF\right)_j \quad \text{and} \tag{6.3}$$

$$\text{World Fleet } CO_2 \text{ Emission} = \sum_{j=1}^{n_{A/C}} \left(U_d BF \cdot SCE\right)_j \quad , \tag{6.4}$$

where $n_{A/C}$ is the number of aircraft in the world fleet and SCE is that of kerosene for all aircraft, i.e. 3.15 (kg CO_2 per kg kerosene). Global air traffic per day is calculated in available seat kilometres (ASK) from

$$\text{Air Traffic (in ASK)} = \sum_{j=1}^{n_{A/C}} \left(U_d v_b n_{Seats}\right)_j \quad , \tag{6.5}$$

where n_{Seats} is the single aircraft's seat capacity. The development on the local level, i.e. the development of fuel burn or CO_2 emission per seat-km, can easily be calculated from dividing the outcome of Eq. (6.3) or (6.4) by global daily air traffic, i.e. by the outcome of Eq. (6.5). The reciprocal of seat fuel burn, i.e. ASK per kg fuel, is generally called global fleet fuel efficiency.

6.2.1 Results

Major results of the base forecast are shown below. Fig. 6.2 shows short-term development of world fleet size, traffic (in ASK) and fuel consumption (i.e. CO_2 production) for the years 2008-2015 in comparison to the base year 2008 (indexed as 100). The curves are identical for the pessimistic, optimistic and trend scenario up to the year 2015. They separate with introduction of the 737 replacement Y1 and the COMAC 919 in 2016. Long-term developments with respect to the different scenarios are shown in similar form in Fig. 6.3. Fig. 6.4 shows long-term development of world fleet average seat fuel burn for the different scenarios assuming a 100 % load factor and aircraft flown with average seating capacities. In Fig. 6.5 average seat fuel burn of the global fleets of regional jet, narrow-body and wide-body aircraft are plotted through the year 2036 for the trend scenario. Table 6.5 summarizes forecasted annual average growth rates of world fleet size, traffic (ASK), absolute fuel consumption (i.e. CO_2 production) and average fuel burned (i.e. CO_2 emitted) per seat-km. More detailed results are found in digital format on the compact disc in Appendix D.

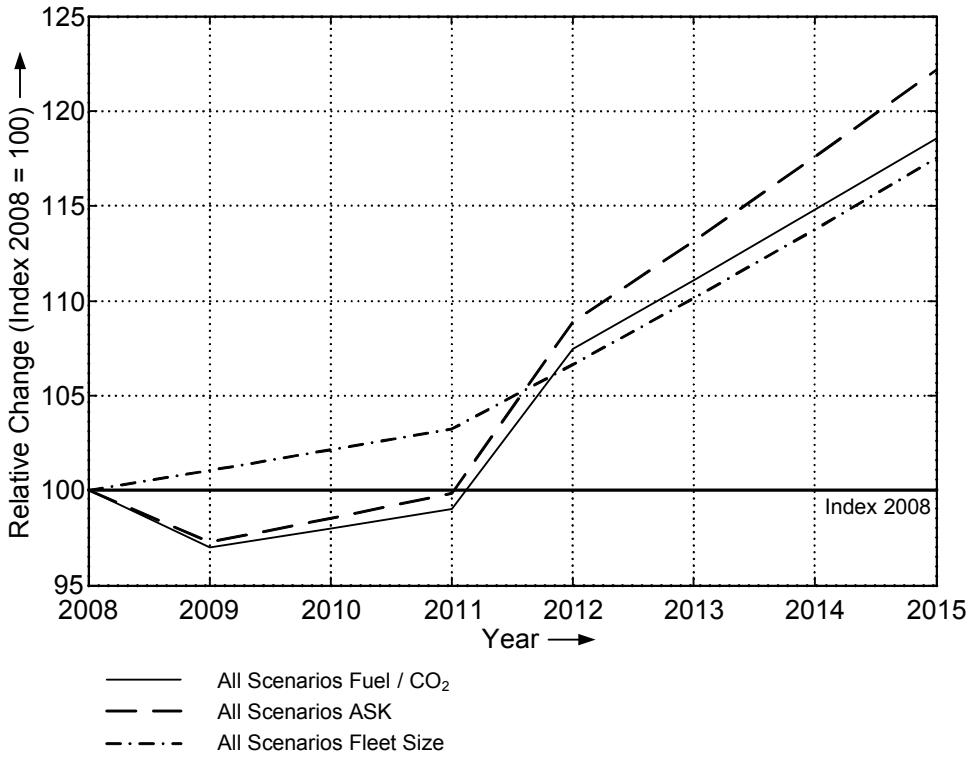

Fig. 6.2 Base Forecast 2009-2015: Relative Growth from Base Year 2008 in World Fleet Size, Daily Available Seat Kilometres (ASK), and Total Daily Fuel Consumption (in kg)

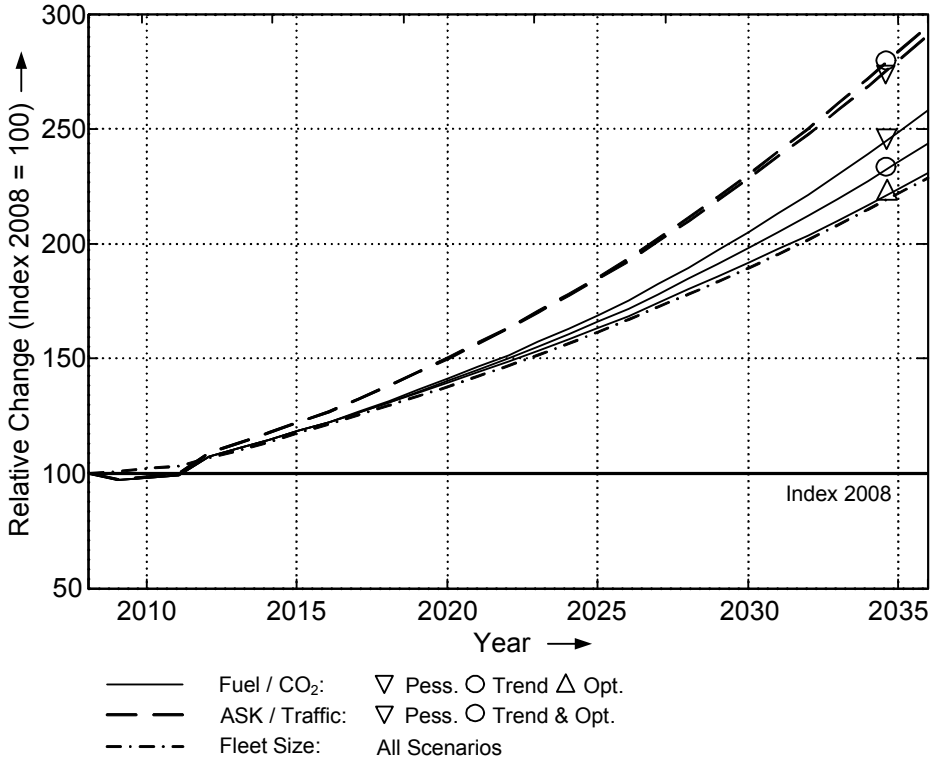

Fig. 6.3 Base Forecast 2009-2036: Relative Growth from Base Year 2008 in World Fleet Size, Daily Available Seat Kilometres (ASK), and Total Daily Fuel Consumption (in kg)

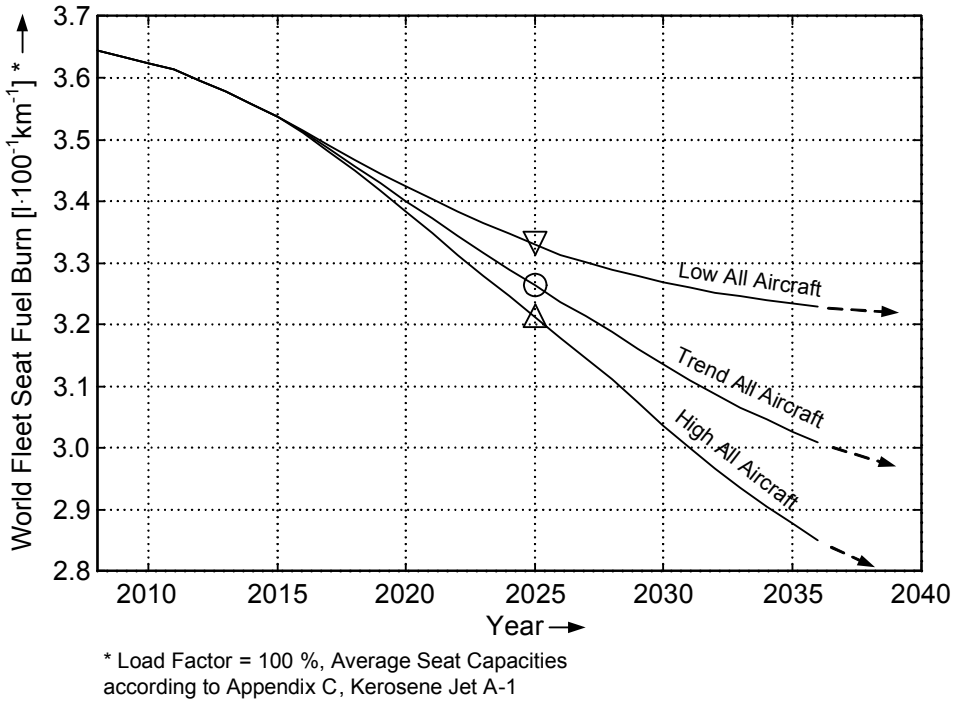

Fig. 6.4 Base Forecast 2009-2036: Development of Global Average Seat Fuel Burn: Pessimistic, Optimistic and Trend Scenarios.

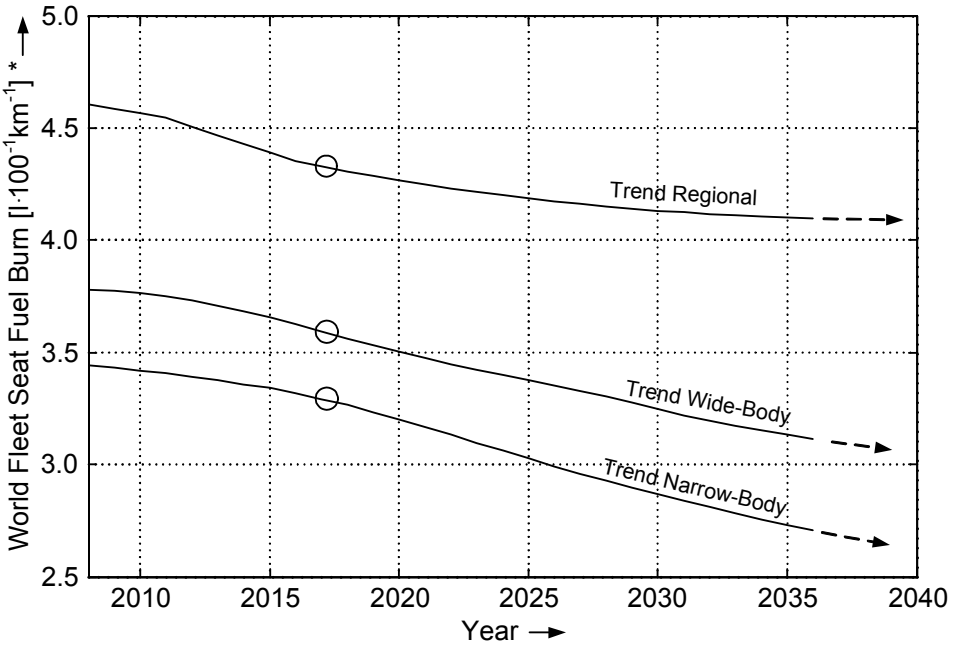

Fig. 6.5 Base Forecast 2009-2036: Development of Global Average Seat Fuel Burn: Regional, Narrow-Body and Wide-Body Fleets (Trend Scenario)

Table 6.5 Base Forecast 2009-2036: Annual average Growth Rates of Fleet Size, ASK, Fuel/CO_2 and Seat Fuel/CO_2

Time Span	Parameter	Annual Average Growth Rates		
		Low (Pessimistic)	Trend (Most likely)	High (Optimistic)
		[%]	[%]	[%]
2009-2016	Fleet Size	2.47	2.47	2.47
	ASK (Traffic)	3.06	3.06	3.06
	Fuel/CO_2	2.60	2.59	2.58
	Seat Fuel/CO_2	- 0.45	- 0.46	- 0.46
2017-2026	Fleet Size	3.23	3.23	3.23
	ASK (Traffic)	4.27	4.30	4.30
	Fuel/CO_2	3.66	3.45	3.27
	Seat Fuel/CO_2	- 0.59	- 0.81	- 0.99
2027-2036	Fleet Size	3.20	3.20	3.20
	ASK (Traffic)	4.21	4.32	4.32
	Fuel/CO_2	3.95	3.56	3.19
	Seat Fuel/CO_2	- 0.26	- 0.73	- 1.08
2009-2036	Fleet Size	3.00	3.00	3.00
	ASK (Traffic)	3.91	3.95	3.95
	Fuel/CO_2	3.46	3.24	3.04
	Seat Fuel/CO_2	- 0.43	- 0.62	- 0.87

6.2.2 Analysis and Interpretation of Results

Absolute Growth in Global Air Traffic and CO_2 Emission

Short-term developments are figured in Fig. 6.2. The implication of the financial/economic downturn is clearly observable for the years 2009 to 2011. While the fleet size is continuously but rather slowly growing, air traffic (represented by ASK), global fuel consumption and global CO_2 emission are lower in 2009 than throughout the base year 2008. This is due to the cutback in daily aircraft utilization. As a result of the growth in fleet size however, both fuel consumption and ASK slightly increase in between 2009 and 2011, even though individual average utilization is constantly lower by 4 % (compared to 2008): global traffic in 2011 is already nearly identical with global traffic in 2008. In 2012, airline economics are expected to have fully recovered and normal FESG utilization rates to be applicable. ASK and global fuel consumption (i.e. CO_2 emission) jump to 108.9 and 107.4 % of their respective 2008 value. Until 2015, total growth exceeds 22.0 and 18.0 % respectively.

The impact of more efficient aircraft on the global production of CO_2 is observable from the decoupling of global ASK and global fuel consumption. Decoupling is possible by an increasing share of new aircraft and a decreasing share of old ones. The decoupling rate is thus a function of demand ('free market' retirements and fleet growth) and the fuel burn advantage over the old aircraft. Accordingly, in Fig. 6.2 decoupling accelerates in between the years 2009 and 2015. This is a combined benefit from new aircraft models being available, increasing retirement rates (see Fig. 5.6) and increased annual fleet growth after airlines slowly recover from the economic crisis.

Long-term developments with respect to the different scenarios are shown in Fig. 6.3. For all scenarios, air traffic (ASK) is expected to have nearly increased threefold by the end of the forecast in 2036.[1] Unsurprisingly, the pessimistic scenario shows the highest increase in fuel consumption and CO_2 emission (258 %) and the optimistic scenario the lowest (231 %). Fuel consumption has increased to 244 % of the 2008 value for the trend scenario. Interestingly, the curve of fuel consumption for the optimistic scenario remains nearly attached to the curve of fleet size. This indicates a constant average daily fuel consumption (and CO_2 production) per aircraft in service with increasing transport performance (ASK).

Annual average growth rates are shown in Table 6.5. In between 2009 and 2016, as a result of the economic crisis, growth rates are rather low. This is bad for the economy, but favourable to the global emission of CO_2, which grows with only 2.6 % p.a. in average. Under normal circumstances (2017-2036), air traffic grows by around 4.3 % p.a., CO_2 by at least 3.23 % p.a. (optimistic scenario).

[1] ASKs are slightly lower for the pessimistic forecast as the A340-600 replacement, which shows a higher capacity and a higher block speed than its competitor 777-300ER, is not introduced.

Global Average Seat Fuel Burn or Fleet Fuel Efficiency

The advance in world fleet fuel efficiency for the different scenarios is easier to observe from Fig. 6.4. It shows the development of average fuel consumption in litres per seat and 100 km of the entire world fleet. Seat fuel consumption in 2015, before the curves of the scenarios separate, is around 3 % lower than in 2008.

Past 2016, the curve of the pessimistic scenario decouples from the other two more explicitly than it does in Fig. 6.3. It is seen that the reduction in seat fuel burn is close to level out by the end of the forecast while the trend and optimistic curves show tendency for further improvement. This is due to the pessimistic assumption that both Airbus and Boeing cancel the development and production of successor aircraft to the A320, A340, 737, 747 and 777. By 2036, only 2.8 % of the world fleet still consists of aircraft that are out of production by the beginning of the forecast (see chapter 5.5). These aircraft are however the only ones being considerably less efficient than the Boeing and Airbus aircraft in production. The remaining chance to replace old aircraft by new ones of the A320, 787 etc. families and thereby to reduce average seat-fuel consumption is thus diminutive. In total, the pessimistic scenario suggests a seat fuel reduction of around 11 % from the active fleet of 2008, the trend scenario a reduction of around 17 % and the optimistic scenario of around 22 %.

The curve for the optimistic scenario reaches an average of 3.0 l per 100 km first in 2031, while the curve for the trend scenario is at 3.01 l in 2036. While it seems that the world fleet of the pessimistic scenario would reach its maximum in efficiency prior to crossing an average of 3.2 l per seat and 100 km, lowest seat fuel burn for the trend and optimistic scenario is expected to come in considerably lower than 3.0 litres. The old A320 and 737 NG families alone still feature fleets of more than 5000 aircraft in 2036 (around 16 % of the world fleet) that are likely to be replaced by the A30X and Y1 in the future.

In Fig. 6.4, the curves of trend and optimistic seat fuel burn show slight kinks whenever new aircraft become available and start improving the overall world fleet efficiency. Similarly, a curve that starts levelling out (e.g. the pessimistic curve) indicates a lack of new, more efficient aircraft. This is observable in Fig. 6.5 as well, where the developments of seat fuel burn of the regional, narrow-body and wide-body fleets in the trend scenario are plotted separately. Efficiencies of the narrow-body and wide-body aircraft fleets improve continuously throughout the forecast. This is due to Airbus and Boeing bringing new aircraft to the market in relatively regular intervals. In comparison, the curve of regional aircraft indicates a strong need for new aircraft past 2015. In the forecast at hand, both Bombardier and Embraer are assumed to continue selling their current regional aircraft (CRJ, E-Jets) for the entire time span with relatively high market shares. If airlines continue to rely on these two manufacturers as prospected, successor aircraft to both aircraft families are necessary in the 2020 timeframe to allow for a similar increase in world fleet efficiency as found for the narrow-body and wide-body aircraft. Alternatively, fuel efficiency increases if Embraer and

Bombardier would lose considerable market shares to the Mitsubishi MRJ, as this is the only regional aircraft that is prospected to show high fuel burn advantage over both CRJ and E-Jets. Additionally, as shown in Fig. 6.5, regional jet aircraft are found to be in general between 20 % to 30 % less efficient than their larger narrow-body and wide-body counterparts. This is in accordance with information given in **Babikian 2006**. In comparison, turboprop-powered regional aircraft achieve similar fuel efficiency to larger turbofans. Average fuel efficiency of the world fleet could thus be increased if the regional jets would be replaced by turboprops. As latter further fly at lower altitudes than regional and larger passenger jets, this would also decrease high-altitude traffic. It should however be noted that there is a trade-off with low passenger acceptance, as regional jets are quieter, travel faster and are publicly regarded as being more modern (**Babikian 2006**).

Comparison to Major External Forecasts

Prior to the year 2000, technological improvements have resulted in an average 1 - 2 % increase in fuel efficiency per year for new production aircraft (**IPCC 1999**). In 1999, the IPCC adopted a forecast of the International Coordinating Council of Aerospace Industries (ICCAIA) saying that, if engine manufacturers continue focusing on improvements in specific fuel consumption (SFC), the annual efficiency improvement for new production aircraft will be 0.95 % between 1997 and 2015, and 0.57 % between 2015 and 2050 (**IPCC 1999**, **GIACC 2009**). Recently, the ICCAIA has set up a new estimate, consisting of two new scenarios. ICCAIA's new scenario 'A' assumes that the intensive current and future research efforts produce an average 0.96 % annual improvement through the year 2050. Its new scenario 'B' requires even higher research commitment and effort than scenario A, and assumes that ambitious EU and US research projects will be funded and successful: an annual improvement of 1.16 % would then be achievable (**GIACC 2009**).

Fig. 6.6 shows the future development of fuel efficiency of new production aircraft for the different ICCAIA scenarios and the three scenarios of the base forecast for the years 2009 through 2030. The average annual improvement is 0.84 % for the trend base scenario, a value in between the assumptions of the 1999 IPCC scenario and that of the new ICCAIA scenario A. For the high base scenario, the annual improvement is 1.26 % and thus reasonably similar to the ICCAIA scenario B. In both trend and high scenarios, the impact of the new short-range and new long-range aircraft is clearly observable. Contrary, the low base scenario shows no improvement beyond 2015 due to the absence of new aircraft. In the years prior to 2015, impacts are mainly due to the introduction of the Boeing 787 in 2010, and the Airbus A350 and Bombardier CSeries in 2013. Disregarding the pessimistic forecast, projections of future aircraft fuel efficiency show high resemblance to the ICCAIA scenarios.

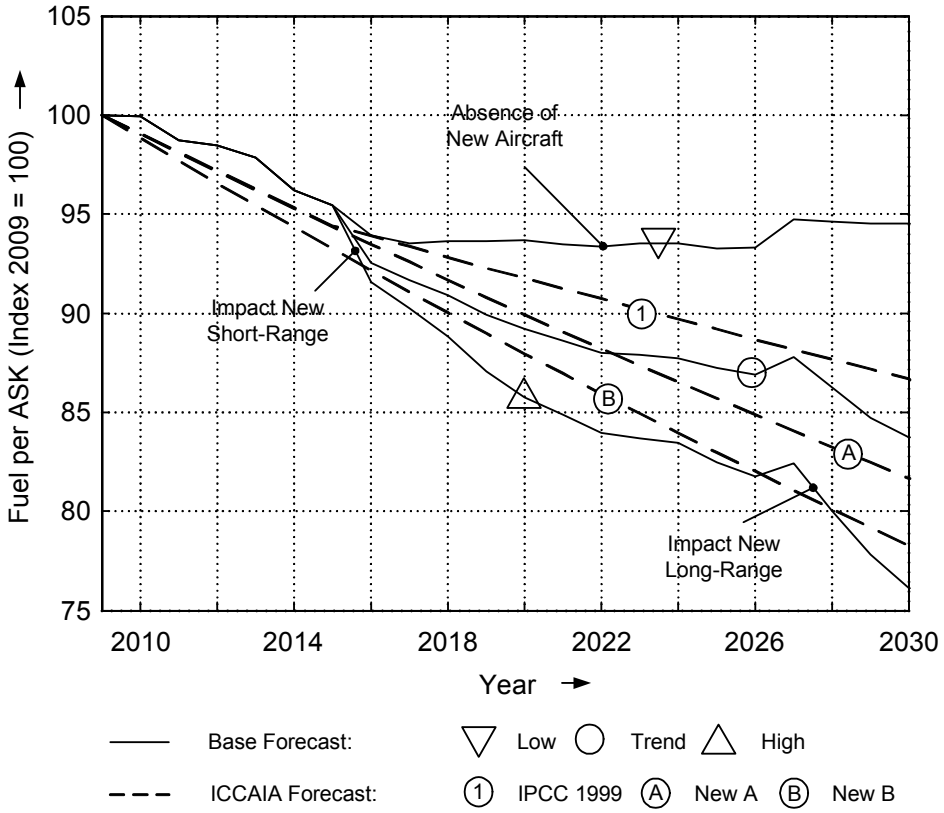

Fig. 6.6 Base Forecast 2009-2030: New Production Aircraft Fuel Efficiency Scenarios

Note that there is a similarity not only in the results but also in the definitions of the base and ICCAIA scenarios. More precisely, both the ICCAIA scenario A and the base trend scenario assume an evolutionary technological advance, while the ICCAIA scenario B and the base high scenario assume revolutionary technologies on-board future aircraft and a broad success for ambitious research projects. This reinforces our assumption of the trend forecast modelling the most realistic case. Both ICCAIA scenarios and FESG fleet growth rates have also been used to model the recent ICAO CO_2 forecast (**ICAO 2009b**). The ICAO forecast can be regarded optimistic, as it adopted the 'high technology scenario' (scenario B) of the ICCAIA and did not re-adjust the basic FESG forecast with respect to the economic crisis.

Consequences for the Future Traffic System

As the **IPCC 1999** writes, "Although fuel efficiency has increased steadily over the past few decades, improvements in fuel efficiency are becoming less dramatic over time". This is due to conventional aircraft technology maturing to efficiencies where improvements are possible only on a small scale. If historical improvements in fleet fuel efficiency should be continued, more radical technological changes – see e.g. the ICCAIA and base forecast 'high technology scenarios' – are necessary. Even though such high annual improvement rates for new aircraft could be achieved, the presented results indicate clearly that the process of increasing over-all

fleet efficiency through the continuous, but rather slow replacement of old aircraft by more efficient ones is not sufficient to stabilize or even lower the over-all carbon footprint of aviation.

Nevertheless, increases in over-all fuel efficiency have traditionally not only come from the introduction of new type of aircraft. In the base forecast, we have disregarded several other measures that have historically provided the fleet with further fuel savings. Most importantly, these are advances in air traffic management (ATM) and operations. Further, existing aircraft and existing production lines have occasionally been updated with new technology. All of these instruments will also help to increase fleet fuel efficiency in future.

The future fuel benefit from advances in ATM technology is however assumed rather small. Today, the world's air traffic environment is already between 92 to 94 % efficient (**CANSO 2008**, **Grimme 2008**). The long-term goals of the Civil Air Navigation Services Organization (CANSO) see system efficiency between 95 to 98 % in 2050, equal to a total increase of 4 % from the level of 2008 (**CANSO 2008**). This calculates to an additional annual improvement in fleet fuel efficiency of 0.1 % between 2009 and 2050. In 2036, the air traffic environment would then be about 2.8 % more efficient then it is today, even though the net benefit in terms of increased capacity will be considerably higher. This has been strongly different in the past: a 4 % ATM efficiency improvement has been achieved only between 1999 and 2005 (**ICAO 2009b**). The low future benefit is due to the system being already highly efficient and further, due to a strong traffic growth. Air traffic control will have to cope with a continuously increasing traffic density and simultaneously lower fuel consumption on individual flights. Even keeping up to current efficiency levels will then be manageable only with large changes to the ATM system (**CANSO 2008**). The European and US airspace might hold a slightly higher potential for improvement, as due to already dense en-route and terminal areas, ATM efficiency today is lower than the average worldwide. Generally, ATM efficiency increases are imaginable that go beyond the maximum efficiency of the current air traffic system. For example, researchers toy with the idea of formation flying in civil aviation, seamless and autonomous global ATC and air-stations on the seas (**Truman 2006**). However, these are extremely challenging concepts that require radical changes in both mission procedures and business models. Hence, they are probably realizable only in the far future (> 2050).

To assess future benefits from operational improvements, the IATA has carried out a survey on possible operations that hold a potential to lower fuel consumption. According to **ICAO 2009b**, their full implementation could lead to an average 5 % fuel saving for the world fleet. If we assume these operations to be fully implemented in 2036, this yields in about 0.17 % additional annual fuel reduction in the time horizon of the fleet forecast.

It is theoretically possible to improve the fuel consumption of individual, already existing aircraft by a technology retrofit. Retrofits incorporate R&D costs and purchasing costs for the operator. The expected cost savings from burning less fuel need to outbalance these costs to

allow for an economically sound implementation. Wingtip technologies (e.g. winglet retrofits) are assumed to provide the highest retrofit potential (**IATA 2008b**). However, wingtip devices need to be individually designed and certified for the respective aircraft. This is generally true for every retrofit that affects the flight performance of the aircraft. A commercially viable implementation is hence imaginable only for aircraft models that feature large world fleets. Due to their small impact, it is assumable that retrofits will play a minor role in increasing the average world fleet fuel efficiency of the future compared to other approaches. Nevertheless, they may increase the profitability of existing aircraft for individual airlines. A comprehensive listing of technologies available for retrofit can be found in **IATA 2008b**.

While retrofits are limited to technologies that result in rather small efficiency increases, existing aircraft programs may be updated with innovations that are more relevant. This includes for example the possibility of an update to an entirely new engine or even material changes to major structural parts (**IATA 2008b**). Some of the most dominate fleets in terms of global fuel consumption in the forecast at hand are the fleets of the A320, 737NG and 777, which are all assumed to be in production with high market shares for at least one decade. Improvements to the existing production lines of these models could thus play a considerable role in reducing world fleet's CO_2 production. As both Airbus and Boeing continue postponing a replacement aircraft to the A320 and 737NG families (**Flight Daily News 2008**, **Gates 2008**, **Kingsley-Jones 2008b**), a re-engineered version could become even more important in terms of increasing fleet fuel efficiency. Similar is true for the regional jet market. The benefit of technology updates to existing production lines are however hard to capture in the forecast at hand, as it cannot be foreseen, which technologies are applicable to certain aircraft without considering a complete redesign. In history, the benefit over an existing model has been rather small. For example, the A320 was launched with the CFM56-5A engine and is now produced with the improved CFM56-B, which offers a 3 % fuel burn advantage over the earlier version (**Safran Group 2008**). According to the **IATA 2008b**, updating the aircraft engines remains the most promising approach in the future.

Not considering retrofits and updates to existing production lines, the forecast at hand suggests a maximum achievable increase in fleet efficiency of 1.3 % annually using traditional technological and operational measures (optimistic scenario). This is however only true for the years 2017 to 2036, after the air traffic industry has completely recovered from the current economic downturn. In the preceding time span 2009-2016, long-term effects of the economic downturn are expected to restrain efficiency growth to annual improvement rates of only 0.73 % (including benefits from advanced ATM and operations).

Finally, there are approaches to improving fleet CO_2 efficiency that go beyond traditional schemes. Some ideas are briefly discussed in the following subchapter.

6.3 Alternative Approaches to CO_2 Reduction

Beyond traditional instruments to increase fleet fuel efficiency, alternative approaches could considerable reduce global CO2 emissions in the future. Currently widely discussed is the use of so-called 'bio'-fuels. Further, independent of technological advances, rethinking the lifetime of both aircraft and their respective programs may also hold high potential.

6.3.1 Using Bio-Fuels

There is the attempt and the desire to use so-called 'bio'-fuels to diminish the over-all carbon footprint of aviation. In this context, bio-fuels term fuels that are derived from plant products. Burning fuel that is made of plants does not generally lower the amount of carbon dioxide emitted on the local, i.e. aircraft level. These fuels are considered CO_2-neutral as the plants absorb carbon dioxide from the atmosphere while growing, which is said to offset the CO_2 emitted by the aircraft engines. In theory, there exist several kind of bio-fuel that are assumed being technologically mature enough in the next decade to be used as a drop-in aviation fuel, see chapter 4.4.1 and Appendix B.4. Today, major unknowns concern the feasibility of growing sufficient feedstock to produce fuel for a wide application. Although 2nd generation bio-fuels promise to need much less farm land than today's fuel crops (**ATAG 2009**), it is still highly uncertain to which maximum quota bio-fuels can replace classic kerosene in aviation and how fast this quota will be reached.

The impact of bio-fuels on aviation CO_2 emission is modelled for two different assumptions concerning the maximum share of bio-fuels in over-all fuel consumption, the first year of major application and the annual rate of increase from an initial share. The first assumption is adopted from the TECH Plus scenario of the International Energy Agency (IEA) in **IEA 2007**. It assumes that bio-fuel holds a share of 25 % of total fuel consumed in the transport sector in 2050. The first year of application and the rate of increase are adopted from **Grimme 2008**. Accordingly, the share is expected to increase linearly between 2010 and 2050. An alternative, highly optimistic scenario is adopted from a document of the Air Transport Action Group (ATAG)[1] (**ATAG 2009**). The scenario assumes a bio-fuel share of 1 % in 2015, 15 % in 2020, 30 % in 2030 and 50 % in 2040. The rate of increase in the years in between is taken as linear. The life-cycle CO_2 emission of the bio-fuel is assumed 10 % that of kerosene, which is according to the current expectations for a 2nd generation bio-fuel that is produced using renewable energy (**IATA 2008b**, **SBAC 2008a**, **Grimme 2008**). For both assumptions, the

[1] The Air Transport Action Group (ATAG) is a coalition of organisations and companies throughout the air transport industry, e.g. Airbus, Boeing, CFM, IATA and Rolls-Royce.

remaining share in fuel burned is assumed kerosene. The impact of both models on the scenarios of the base forecast is modelled in Fig. 6.7.

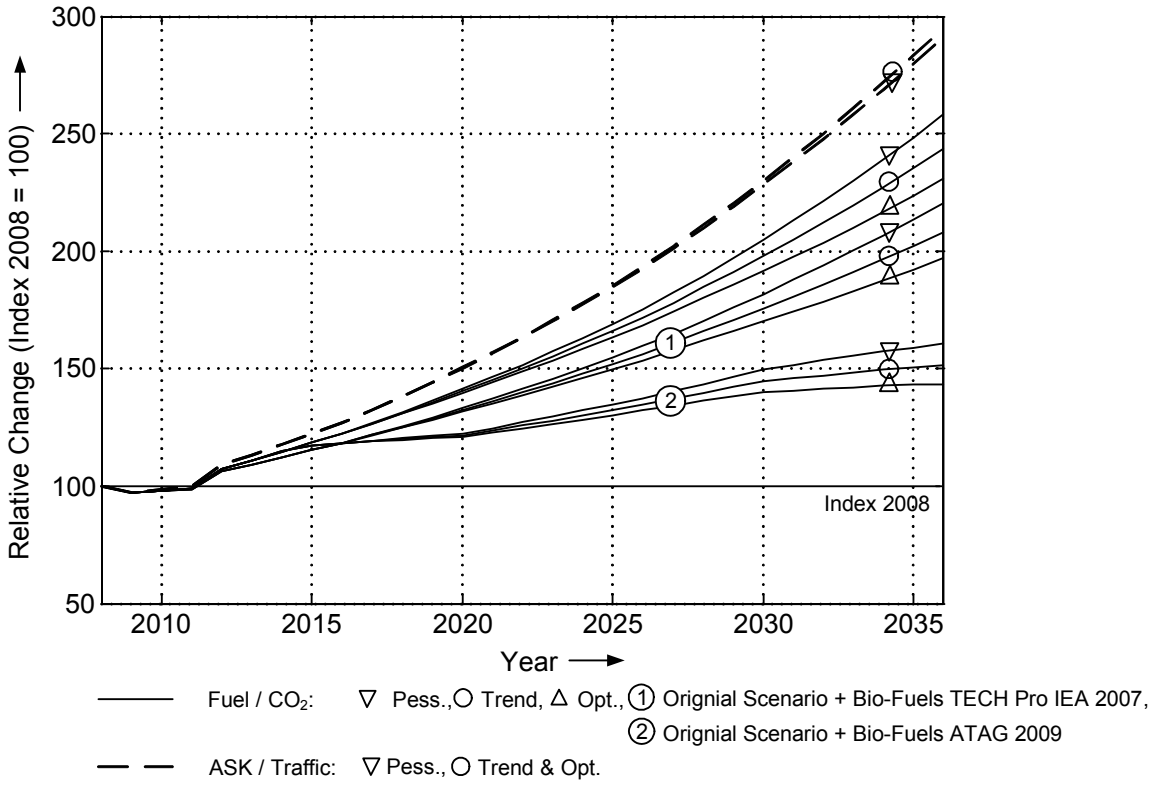

Fig. 6.7 Base Forecast + Bio-Fuel Influence 2009-2036: Relative Growth from Base Year 2008 in World Air Traffic (ASK) and Total Daily CO_2 Emission (Life-Cycle CO_2). **Note:** The Forecast is valid only for a bio-fuel production that is powered by renewable energy, i.e. a life-cycle CO_2 reduction of 90 % over that of kerosene. If the production is powered by fossil fuels, the benefit will be considerably smaller.

As observable from Fig. 6.7, bio-fuels have theoretically a large potential to lower the CO_2 emission of air traffic. The most distinct advantage of bio-fuel over conventional aircraft technology is its 'backward compatibility'. If the blended fuel's characteristics are similar to kerosene, it can be used on both new and old aircraft. As the market penetration with bio-fuel is thus independent of the introduction of new aircraft, benefits show immediately. For the best case, where the optimistic scenario concerning new aircraft and the ATAG scenario of bio-fuels (numbered '2' in Fig. 6.7) fall together, global CO_2 emissions remain below the original 2020 emission level for nearly the entire forecast, even though air traffic shows a strong continuous growth. The returns of using fuel produced from renewable sources are further not only of ecological nature. If carbon trading should become a major cost factor for airlines, bio-fuels help to reduce CO_2 emissions in excess of the reduction in fuel burn. Additionally, when crude oil runs short in the medium-term, cost for regular kerosene could rise above the cost for alternative fuels.

Besides noticing the high potential of bio-fuels, it must be stressed that forecasts concerning their influence on global CO_2 emission hold large uncertainties. This is observable from the discrepancies in assumptions and results of the IEA and ATAG scenario. Further, even though the bio-fuel roadmap of ATAG assumes considerably larger bio-fuel quotas, already a 25 % share in global transport fuel consumption by 2050 (according to the TECH Pro Scenario) is considered a highly optimistic forecast by the IEA (**IEA 2007**). One should also bear in mind that the low growth in CO_2 emission for the ATAG assumptions is due to the fast increase in bio-fuel share between 2015 and 2040. If the annual increase should be kept low past 2040, a similar yearly rate would have to be applied, which stretches the quota beyond the 50 % mark. A high improvement rate is generally only possible if the benefits of more efficient on-aircraft technologies and bio-fuel are combined. In the end, the feasibility of providing large CO_2 benefits for the air traffic system using bio-fuels will depend on the outcome of current research into finding and cultivating appropriate feedstock. The fact that for a considerable reduction in life-cycle CO_2 emission, feedstock for both the fuel itself and its production must be of renewable nature (**SBAC 2008a**), makes this task even more important.

6.3.2 Rethinking Aircraft Production and Life Cycles

It has been found through the set up of the fleet forecast in chapter 5 that the influence of new aircraft on fleet fuel efficiency is not solely dependent on aircraft-specific variables such as the aircraft's fuel advantage over existing models, but also on several organizational parameters and exogenous variables. Two major ones are briefly examined in this subchapter. First, the influence of an early market launch of two major jet airliners on aircraft technology and global fleet fuel efficiency is analyzed. Second, a case study is conducted on the impact of a generally reduced aircraft life and the resulting accelerated fleet turnover. Both studies represent rather uncommon approaches to influence CO_2 emissions. Their aim is to identify organizational handles rather than answering questions of practicability and ultimate impact. These would have to be answered through a more extensive study.

Shortening Aircraft Production Runs

It is shown in Fig. 6.4 that new aircraft are required in regular intervals to guarantee a continuous improvement of fleet fuel efficiency and thus a decoupling of the growth rates of traffic and CO_2. If we assume market shares being unaffected, two main parameters set the impact of a new aircraft on the development of fleet fuel efficiency: The year in which the aircraft becomes available to the market and the magnitude of fuel advantage over the aircraft it replaces. The question that remains is which one of these two influencing factors is of higher importance for the goal of reducing CO2 emissions. In other words, is it beneficial to

global CO2 emissions to delay new aircraft projects for the sake of implementing better technology?

Fig. 6.8 shows the outcome of a small case study on this matter. An alternative scenario to the base trend scenario has therefore been established, assuming Airbus and Boeing to introduce successor aircraft to the A320 and 737 already five years earlier (2013/2011). Due to the earlier design freeze, these aircraft feature less advanced technology and a seat fuel burn that is by only 15.0 % (instead of 20 % in the trend scenario) lower than the one of their respective predecessor.[1] Further assumptions concerning the new aircraft and the rest of the scenario are identical to the trend forecast.[2]

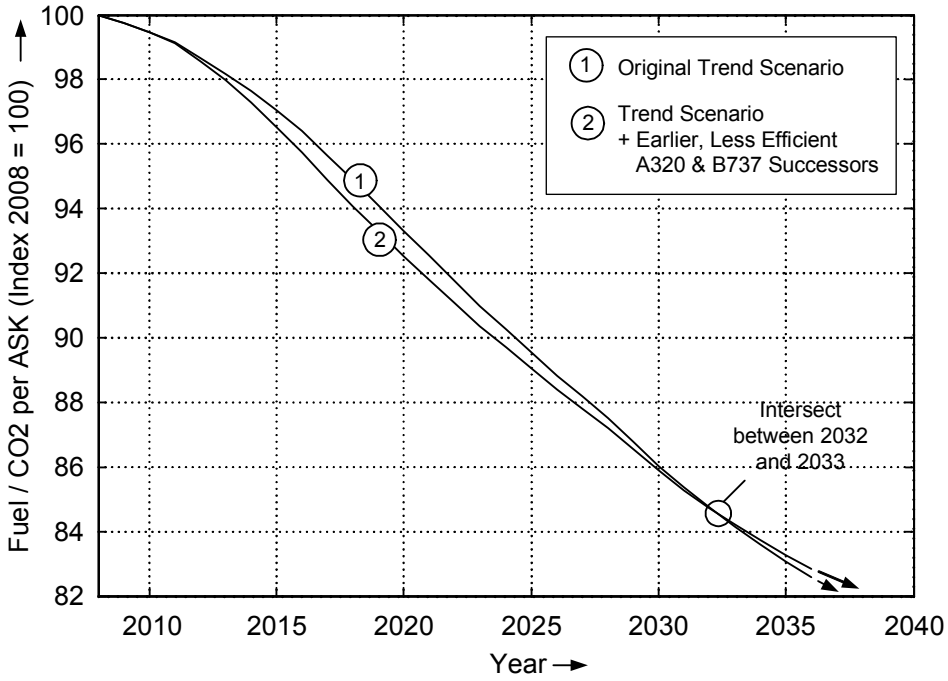

Fig. 6.8 Shortening Aircraft Production Runs: Effect of Earlier A320 and 737 Successors on Global Fleet Fuel Efficiency

As one would expect, the curve for the new scenario (numbered '2') shows a higher annual reduction rate for the years 2011 to 2016. This is reasonable as the new aircraft replace the 737 and A320 earlier and thus start to improve the fleet fuel efficiency prior to the new aircraft in the original forecast. Over the years, the gradient of the curve becomes less steep and is outclassed in annual improvement by the curve representing the original forecast. This is a foreseeable process as the new aircraft in the original forecast show a lower per-seat fuel

[1] Each year of further development is thus assumed to generate a seat fuel advantage of an extra 1.0 %, which is in accordance with historical and future annual improvements in fuel efficiency of new production aircraft: see Fig. 6.6.

[2] Market shares in the early years of production are however slightly higher as the production of the Bombardier CSeries has not yet started (737 replacement) or is started simultaneously (A320 replacement).

burn. Interestingly, fuel burn per seat-km stays however below the trend scenario for many years. It is only after 2032 that fuel efficiency is higher in the original forecast.

According to our calculations, the earlier introduction of the new short-range aircraft saves 47.97 million tonnes of fuel between the years 2011 and 2030. This is about one third of the total fuel burned in 2011 (147.8 million tonnes) and about one sixth of the total fuel burned in 2030 (295.6 million tonnes). Unfortunately, this amount will be lost again shortly after 2036 if seat fuel burn of the two scenarios develops as shown in Fig. 6.8. This can be counteracted by the introduction of a second 737 and A320 replacement in the early 2030s as shown in Fig. 6.9.

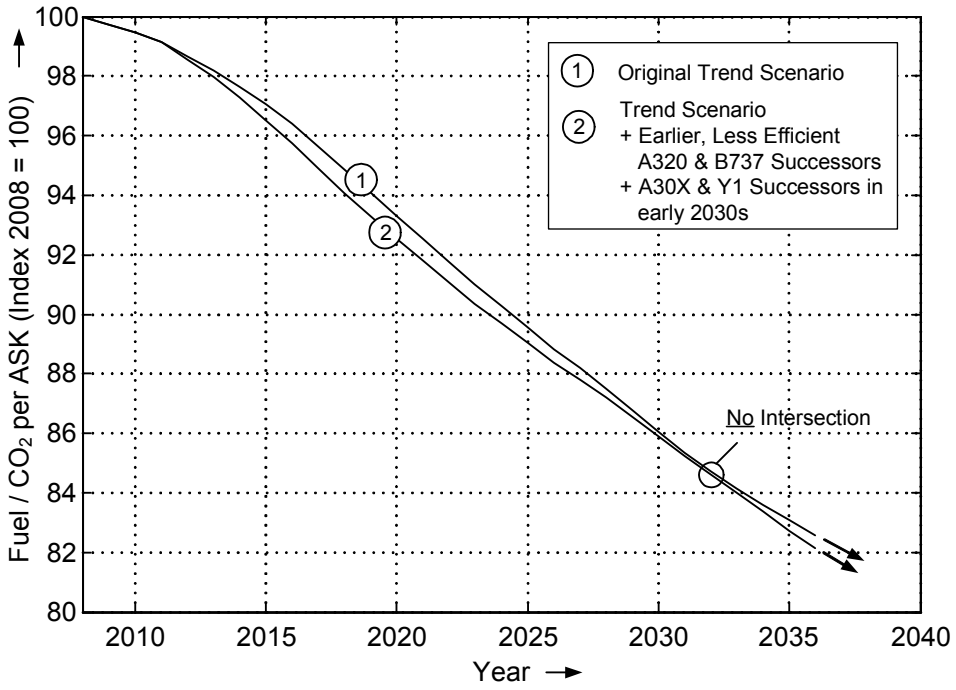

Fig. 6.9 Shortening Aircraft Production Runs: Effect of Additional A30X and Y1 Successors on Global Fleet Fuel Efficiency

For the calculation of the new alternative curve (numbered '2'), a replacement to the Y1 is assumed for 2031 and a replacement to the A30X in 2033. Both aircraft families have accordingly been in production for 20 years. The two new aircraft families show an identical fuel efficiency to the Y1 and A30X in the original trend forecast, i.e. a fuel burn advantage of 20 % over the 737 and A320 respectively. This is only a small improvement from their direct predecessors (around - 6 %) but enough to not being outclassed by the curve of the original forecast. Sometime in the future the curves for the original and the new scenario are expected to merge. This is due to the most efficient aircraft in all seat categories showing a seat fuel consumption that is identical in both scenarios. Again, all other assumptions are adopted from the trend forecast. There is no increase in demand or market shares due to the new aircraft being introduced.

The results of this short case study suggest that albeit the ultimate fuel burn advantage over a predecessor is lower, considerable amounts of fuel and CO_2 could be saved if new aircraft were released earlier. It is further shown that the benefit of an early introduction is preservable only if a follow-up successor model is introduced inside a certain period.[1] Further, the replacement to the first successor is needed to show a seat fuel consumption at least as good as the seat fuel consumption of the originally planned aircraft (here Y1 and A30X of the trend forecast). If over the intervening years an even lower fuel consumption than this is realizable, the benefit will be larger.

The advantage of the early introduction is mainly attributed to two fundamental changes in the forecast. First, delivery of the 737 and A320 ends earlier. This prevents the demand for fleet growth to be met with considerably less-efficient aircraft. Second, the new aircraft and not their respective predecessors replace a large amount of out-of-production aircraft. The earlier aircraft release thereby generates something like an 'efficiency buffer'. The later aircraft release in the original forecast has to first make up for the lost time before its seat fuel advantage can show.

Reducing Aircraft Lifetime

Improvements in the fuel efficiency of new production aircraft translate only slowly to similar improvements in fuel efficiency of the active fleet as older, more inefficient aircraft remain in service for up to 50 years (see Fig. 5.5). Theoretically, the process of fleet modernization could be accelerated by shifting aircraft retirements to earlier ages. For a rough estimate of the potential benefit from earlier retirements, a scenario is established that assumes aircraft to be retired ten years earlier than it is presumed from the survival curves in Fig. 5.5. Therefore, the survival curve 'Group 1' is shifted left by ten years as shown left in Fig. 6.10. The curve is valid for nearly all aircraft regarded in the forecast at hand. Other curves and thus retirements of MD11, 707, 727 and DC10 aircraft remain unaffected. Apart from this change, the scenario is identical in all parts to the original trend forecast. The resulting change in annual aircraft retirements ('free market' retirements) for the years 2009 to 2036 is shown on the right hand side in Fig. 6.10.

[1] For the case study at hand, this period is twenty years, which is in accordance with historical periods of a successful production run (15 to 20 years): see **IPCC 1999**, chapter 7.2.3.

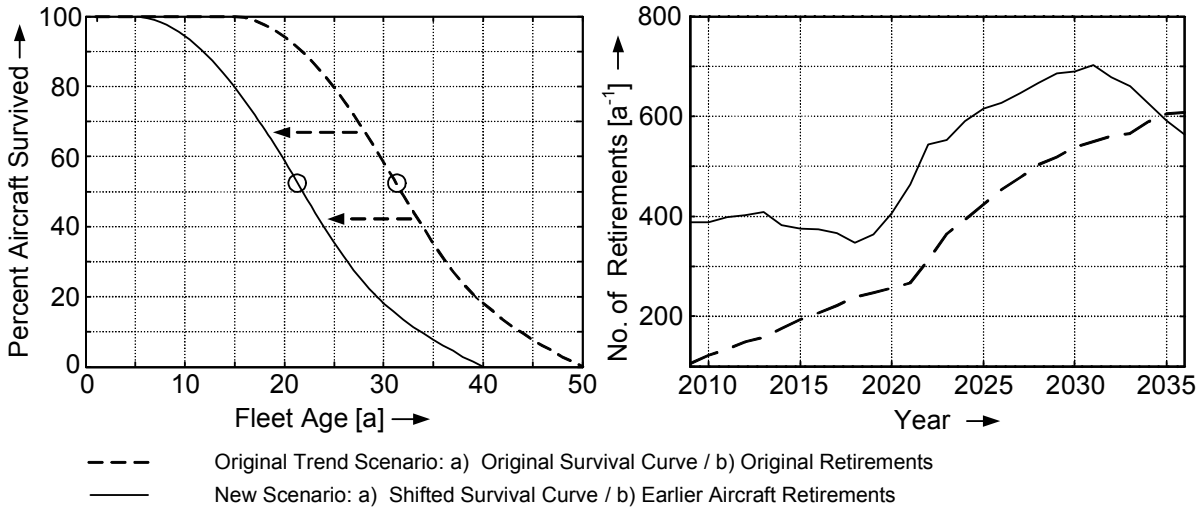

Fig. 6.10 Reducing Aircraft Life: a) Shifted FESG Survival Curve and b) Change in Annual 'Free Market' Retirements

The resulting development of average CO_2 emitted per seat-km for the new scenario is compared to the results of the original forecast in Fig. 6.11. As expected, out-of production aircraft are replaced earlier, which increases the improvement rate and achieves higher fleet efficiencies earlier in time than the regular trend scenario (see curve numbered '2'). However, it is seen that the slope of the curve for earlier retirements is considerably higher only for the early years of the forecast, when rather old aircraft (>20 years) are being retired at higher annual rates (see Fig. 6.11). These retirements mainly concern narrow-body aircraft (737 Classic, MD80/90, etc.) that are replaced to a large extent by aircraft of the A320 and 737 NG families.

From the year 2016 on, when the Boeing Y1 becomes available, both curves '1' and '2' show relatively similar annual improvement rates. This changes in 2025. In the final decade of the forecast, the gradient in the regular forecast is higher even though less aircraft per year are being retired. In fact, the rate of improvement now benefits from large amounts of rather old aircraft still being active. In comparison to the new scenario, where these aircraft are mainly retired in the first decade and replaced by aircraft such as the A320 and 777, they are now being replaced by the considerably more efficient aircraft available in the late 2020s. It seems as if the curves start approaching each other to the end of the time horizon.

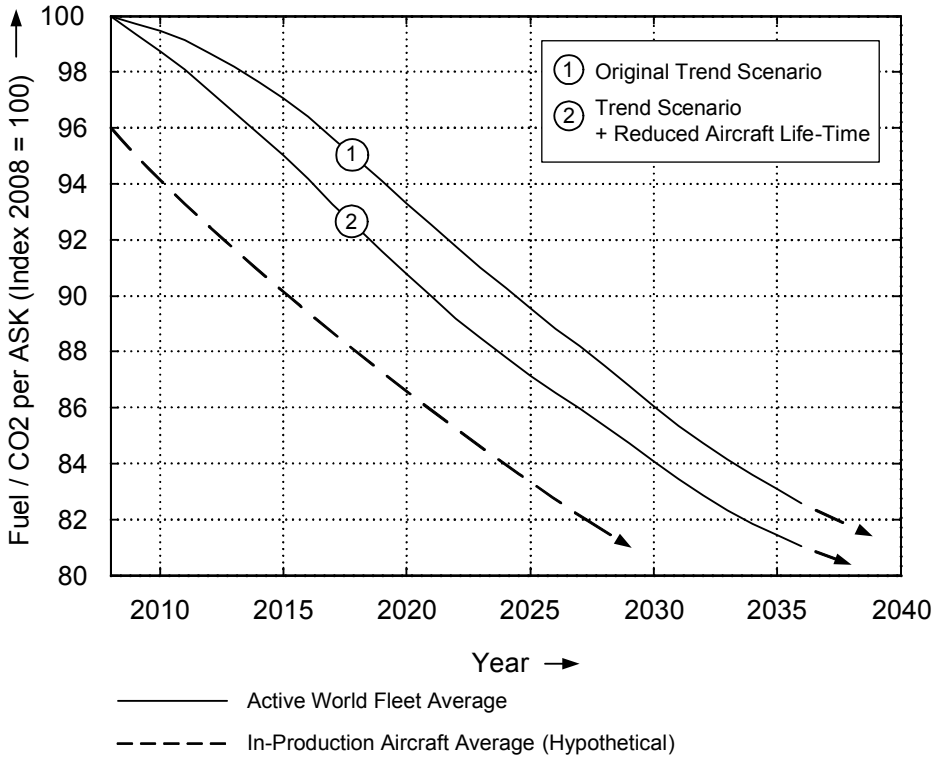

Fig. 6.11 Development of CO_2 emitted per Seat-km 2008-2036 – Aircraft Retirements 10 Years Earlier

The case study at hand suggests that reducing average aircraft life can foster the modernization of the active fleet and thereby assist the reduction of CO_2 emissions per seat-km. This is however only the case if new aircraft are brought to the market in regular intervals. It is important to realize that earlier aircraft retirements can only accelerate the shift to higher fleet efficiencies. Once the whole fleet consists of the most efficient aircraft available, the curves of the original trend and the earlier retirement scenario show the same fuel burn per seat-km. However, the curve with the earlier retirements will reach this level earlier in time. Moreover, a generally reduced aircraft life could provide benefits that go beyond the ones of an accelerated fleet turnover. According to **Greener By Design 2003**, reducing aircraft life could allow for lighter primary structures in new aircraft designs and thus for additional fuel savings for the single aircraft and the global fleet.

Unfortunately, the case study at hand is not sufficient to definitely answer the question whether shifting retirements to earlier ages is beneficial for the global emission of CO_2 or not. This has several reasons. First, the time horizon regarded in the forecast is too short to analyze the long-term development. Second, it might be possible that the advantage shown in Fig. 6.11 is mainly due to the high retirement rates in the first years of the forecast. This is however not a realistic case. If the ages for retirement had been lower in advance, many of these aircraft would have been probably retired prior to 2008. Third, not only the operation but also the production of aircraft generates carbon dioxide. If aircraft life expectancy is lower, more aircraft need to be produced in the same period. This could offset the benefit of

an earlier reduction in fleet fuel burn. In general, a more detailed analysis including calculations of aircraft life-cycle CO_2 is needed to draw definite conclusions.

6.4 Comparison to Environmental Goals

6.4.1 ACARE Vision 2020

The Advisory Council for Aeronautics Research in Europe (ACARE) is a group consisting of members to the European Commission, European research establishments, universities, regulation authorities, manufacturers and other aviation stakeholders. It has been established to provide a strategic research agenda (SRA) and thereby to define the most important goals in European aeronautical research. In 2001, the ACARE set ambitious efficiency, safety and environmental goals to be achieved by the aviation industry by the year 2020. It termed these goals the *Vision 2020*. The Vision 2020 includes environmental goals for the reduction in aircraft noise, NO_x and CO_2. The CO_2 reduction goal is defined as a "... 50% cut in CO_2 emissions per passenger kilometre (which means a 50% cut in fuel consumption in the new aircraft of 2020) ..." (**EC 2001,** p. 14).[1] Even though interpretable as a goal applicable to the average fuel efficiency of all in-production aircraft of the year 2020, there is strong evidence that it applies only to single future aircraft projects, which have their first entry-into-service (EIS) in 2020: see e.g. **ACARE 2002**, pp. 71-82. Comparable in-production aircraft (and engines) of the year 2000 generally act as reference, see e.g. **SBAC 2008b**, **Clarke 2007**.

Due to the ACARE target being valid only for future aircraft projects entering service in 2020, there is no direct comparability to the results of the CO_2 emission forecast at hand. It is however seen from the forecast results of the optimistic scenario that due to missing reduction potential from ATM and operational improvements, future aircraft achieving CO_2 reductions comparable to those envisaged by the Vision 2020 are required to keep up to historical improvement rates in fleet fuel efficiency. Finding and developing potent technologies that provide high fuel reduction benefit is thus of paramount significance for continuously mitigating CO_2 emission of global aviation. The following technologies, which have been identified from the technology survey in chapter 4, could hold potential for achieving the ACARE Vision 2020 goal of a 40 to 45 % CO_2 emission reduction due to on-board aircraft technology in the medium term (2015-2025):

[1] The goal is further subdivided into a 25 % CO_2 reduction due to airframe improvements (aerodynamics and weight), a 15 to 20 % reduction due to engine improvements and a 5 to 10 % reduction due to increased ATM efficiency (**SBAC 2008b**). Thus, only 40 to 45 % need to be achieved by the aircraft 'alone'.

A **25 % fuel reduction due to Airframe technology** might be achievable together from

Aerodynamic improvements:

- Reducing turbulent skin friction drag by disrupting span-wise cyclic flows using Helmholtz resonators or controllable active skin,
- Reducing skin friction drag by maintaining laminar flow using natural laminar flow (NLF) or hybrid laminar flow (HLF) technologies,
- Reducing lift-induced drag by lowering the strength of wing tip vortices using a spiroid wingtip or multiple (active) winglets,
- Reducing lift-induced drag by increasing the wing span using new high-strength lightweight materials,
- Reducing the off-design flying time by tailoring the wing to each flight segment using conventional high-lift systems or morphing wing technology.

Empty weight improvements:

- Reducing structure weight by increasing the specific strength of materials using polymer composites, Al-Li alloys and new generation metal composites (e.g. CentrAl) for primary structures,
- Reducing structure weight by applying new design principles for composite structures (i.e. enabling a departure from current 'black-metal' design),
- Reducing structure weight by designing the aircraft for shorter ranges (multi-stage long-distance travel).

A **15 to 20 % fuel reduction due to Engine technology** might be achievable together from

Thermal efficiency improvements:

- Increasing turbine entry temperatures (TET) using ceramic matrix composites (CMCs) for turbine components, the concept of cooled cooling air and low-NOx combustor technology,
- Increasing over-all pressure ratios (OPR) using titanium metal matrix composites (MMCs) for compressor components, active clearance control (ACC) technology and active surge control (ASC) technology,
- Increasing thermal efficiency using inter-cooled and recuperative engine (IRA) architecture.

Propulsive efficiency improvements:

- Increasing the fan diameter using polymer matrix composites (PMCs) or hollow titanium for the fan and casing,
- Decoupling the fan from the low-pressure (LP) turbine using a geared system,
- Increasing the mass flow through the fan stage using two counter-rotating fan stages and the concept of an open rotor.

In the end, the technological feasibility of achieving the ACARE Goals will not depend on a single technology but on finding an appropriate combination of technologies from the different fields of research. It should also be noted that some of the technologies are beneficial only if implemented on short-range aircraft while others will find application mainly on long-range aircraft. More information on the single technologies is found in chapter 4 and from the tables in Appendix B.

6.4.2 IATA Environmental Targets

The International Air Transport Association (IATA) represents about 230 airlines comprising 93 % of scheduled air traffic. It has set two medium-term, sequential environmental goals for global air transport (**IATA 2009c**), which are

1. 1.5 % average annual improvement in fuel efficiency between 2009 and 2020, and a
2. Carbon-neutral growth from 2020.

If the world fleet develops as assumed for the base forecast in chapter 6.2, the first environmental goal is unlikely to be achieved from technology advances on future aircraft alone. The different scenarios of the base forecast achieve average annual improvement rates of only 0.51 to 0.61 % between 2009 and 2020. An additional 0.27 % from more efficient ATM and operations could then increase the annual improvement rate to about the half of the IATA goal. There are different reasons for this. First, there is the impact of the economic downturn in the early years of the forecast (2009-2015), which is affecting aircraft deliveries and thus delaying the increase in share of new aircraft. Second, currently dominant aircraft families (CRJs, E-Jets, A320, 737NG, A330, 777) remain dominant for many years. It is only after 2015 that the impact of the A30X, Y1, A350 and 787 becomes significant (see Figs. 5.10 to 5.12). Finally, the number of retirements of out-of-production aircraft is small in the first years and thus fleet turnover is a relatively slow process. Nevertheless, there have been multiple instruments identified that could help increasing the annual improvement in fuel efficiency, which are the following:

- **Environmentally proactive operators** can actively influence global fuel efficiency through their buying behaviour. This implies that airlines choose to buy only the most fuel-efficient aircraft in each seat category and thereby increase its market share. In reality, this will however be only partly possible, as the buying decision is dependent on multiple other factors such as the airline's specific route network, customer acceptance, list price and maintenance cost.
- **Aircraft retrofits** can increase future fuel efficiency of already active aircraft. As possible changes are small and cost-intensive, the potential additional annual improvement is assumed rather small (< 0.1 %).

- **Technology updates to active aircraft programmes** could imply larger changes and thus higher additional benefits. Especially updates to the production lines of the A320, 737NG, A330 and 777 aircraft show high potential, as they are expected to be sold with high market shares for at least one decade. If, for example through a new engine, fuel efficiency could be considerably increased, the impact on global seat-fuel burn would be comparable to the release of a new aircraft (see the first case study in chapter 6.3.2).
- **Policy options** could provide incentives for an accelerated fleet turnover. A temporary aircraft scrap-bonus for the duration of the economic downturn could make sooner retirements of old aircraft economically viable. This is also the case for the implementation of an emission cap and trade program as it is planned for the European airspace from 2012. The second case study in chapter 6.3.2 suggests that earlier aircraft retirements could increase the annual fuel efficiency improvement between 2009 and 2020 by more than 0.2 % in average.

It is obvious that annual improvement rates of 1.5 % are realizable only if large efforts are taken by all air traffic stakeholders. Highly fuel-efficient future aircraft are thus only one necessary criterion to reach the target.

Heavily discussed to date is the possibility of a carbon neutral growth, which defines IATA's second environmental goal. That is, traffic growth from 2020 is possible without a further growth in global CO_2 emission. In a visualization identical to Fig. 6.3, the graph representing air traffic (ASK) would then be constantly growing while the graph representing CO_2 emission would level out in 2020 and keep a constant value henceforth. This is possible only if the world fleet is constantly reducing its CO_2 emission per seat-km. If average annual traffic growth is known, the annually required reduction in CO_2 emissions per seat-km can be calculated from

$$\text{CO}_2 \text{ Reduction for Carbon-Neutral Growth} = k_{CO_2} = 1 - \frac{1}{1 + k_{ASK}} \quad . \tag{6.6}$$

where k_{CO2} is the required annual reduction in seat-specific CO_2 and k_{ASK} is the compound annual growth rate (CAGR) in traffic (i.e. ASK). Under normal economic circumstances, traffic is expected to grow annually by around 4.3 % between 2021 and 2036 (see Table 6.5). This calculates to a required average annual reduction in seat-km-specific CO_2 of 4.1 %. The annual reduction realized from using traditional measures is immensely lower for all scenarios in the forecast at hand. For the most optimistic case, average annual reduction is 1.3 % between the years 2021 and 2036. This rate is identical to the historical average (**IPCC 1999**), but still only about one third of the annual CO_2 reduction required to compensate for the increase in traffic.

Regarding the findings of the CO_2 forecast at hand, it is reasonable to state that in the medium-term, annual improvement rates in the order necessary are realizable only through the

combination of revolutionary fuel-efficient future aircraft with a strongly increasing share of bio-fuels in global fuel consumption. The impact of such a highly optimistic scenario is represented by the lowermost curve in Fig. 6.7, where the optimistic base forecast falls together with the bio-fuel scenario given in **ATAG 2009**: CO_2 emissions are on a constant level from 2015 to 2020 and from 2030 to 2036. They also keep below the originally expected 2020 level for almost the entire time horizon of the forecast.

6.5 Chapter Summary

The future development of global air traffic and CO_2 emission has been projected for the world fleet of turbofan-powered passenger aircraft using different future scenarios on technological and operational advances through the year 2036. Both traffic and CO_2 emissions are expected to grow considerably. Air traffic is expected to have increased nearly threefold by the end of the forecast. It has been shown that future aircraft, if implemented according to the fleet forecast in chapter 5, decrease global average seat fuel burn and CO_2 emission continuously, but rather slowly. Only for an optimistic technology scenario, where future aircraft show very high seat-fuel reductions over existing aircraft, historical improvement rates of fleet fuel efficiency can thereby be achieved. Concomitantly, global CO_2 emissions have increased to 231 % of their 2008 level by 2036. Multiple technological and operational measures exist that are capable of providing further benefits across the whole world fleet, of which bio-fuels are expected to hold the highest potential. For an optimistic scenario concerning implementation of the latter, CO_2 emissions are projected to remain below the originally expected 2020 level for nearly the entire time horizon. Concerning important environmental goals, it has been shown that the full potential of multiple technological and operational instruments need to be tapped if the ambitious environmental goals of the IATA are to be accomplished.

7 Summary and Conclusions

Increasing CO_2 emissions and associated fuel consumption of the world's aircraft fleet are a serious threat for both the world climate and the profitability of commercial aviation. CO_2 emission can be analyzed on the local – i.e. single aircraft – and global – i.e. world fleet – level. Methods to reduce CO_2 on the former have been identified and the consequent future evolution of global CO_2 has been estimated.

The mass of CO_2 emitted per kg of fuel burned can be assumed as a pure fuel-specific parameter. For example, kerosene emits 3.15 kg CO_2 per kg of burnt fuel. As fuel consumption and CO_2 emissions are directly linked, technological and operational influences on aircraft CO_2 emission can be quantified utilizing the Breguet range equation, which describes the physics of aircraft in steady level flight. Six technological key variables were isolated. CO_2 emissions are thereby defined by the aircraft's design range R, the engine efficiency η, the aircraft's efficiency in terms of aerodynamic efficiency L/D and empty weight W_E, and the fuel efficiency in terms of heat content H and specific CO_2 emission SCE. The identified variables define major research disciplines into CO_2 reducing aircraft technologies.

A parametric study has been conducted to analyze the influence of the predefined variables on aircraft CO_2 emission. Block CO_2 emissions can be estimated from a modified Breguet equation, which includes semi-empirical formulas for the calculation of fuel burned during taxiing, acceleration to cruise speed, climb to cruise altitude and en-route manoeuvring. The potential influence of the variables has been exemplarily calculated by gradually improving reference parameters of two real-world aircraft, a short-haul narrow-body and a long-haul wide-body aircraft. Calculations have been performed to simulate both retrofits and new aircraft. To quantify the benefit of improving the parameters for a new aircraft design, an iterative computation method has been developed to account for re-sizing effects (snowball effects) on the structure weight and drag polar of the aircraft.

C_{D0} was found to be the dominant part in over-all drag of both reference aircraft. Reducing this parameter thus showed in high fuel and CO_2 savings. Its impact has been outclassed only by improvements in engine efficiency η and fuel heat content H. However, engine efficiency (of conventional turbofans) was found limited by physical laws that might be reached in the medium-term. Re-sizing effects were found to play an important role in tapping the full potential of technological improvements. This applies in particular to component weight reductions, as they feature the best advantage from snowball effects (a factor of around 1.5 to 2.0). Decreasing component weights is thus a powerful technological means for re-sized aircraft only. If induced drag could be reduced significantly, it would have a large impact on CO_2 efficiency. However, improving the two relevant parameters wingspan and Oswald factor resulted in only moderate reductions. Especially benefits from increasing the Oswald factor

were found to be highly limited, as modern aircraft feature factors already close to unity. Design range has not been treated as a variable parameter, but as a fixed design specification. However, literature indicates that there is an optimum range for highest fuel efficiency around 4000 to 6000 km. A coupling between the design range and the reduction potential has been identified. Due to snowball effects, long-range aircraft have a higher benefit from positive technological changes.

A survey on potential technologies for CO_2 reduction comprising improvements in aerodynamics, engine & power, empty weight, alternative fuels and air traffic management (ATM) has been conducted. It is seen that both current aircraft aerodynamics and engines are already at a very high efficiency level for the current design. Large fuel/CO_2 efficiency improvements thus necessitate revolutionary changes such as laminar flow technologies and new engine architecture concepts, rather than further evolutionary development. In comparison, for the reduction of empty weight, the evolutionary development from a metal to a composite aircraft still holds large potential. It has also been shown that there exist several regulatory and operational measures to reduce empty weight considerably. In the field of alternative fuels, some bio-fuels show properties similar to kerosene and could thus find application in short- to medium-term on both new and existing aircraft. Cryogenic fuels (e.g. liquid hydrogen) have also been assessed and shown to be a true alternative only in the long-term. Today's air traffic system has been found to yield already high efficiencies in the order of 93 %. While ATM technology improvements are assumed being necessary to allow for the prospected increase in airspace density, the absolute fuel/CO_2 saving benefit for the air traffic system was found to be relatively low.

In a first step to assess future global CO_2 emission, a method was developed to estimate the future build-up of the world fleet of turbofan-powered passenger aircraft. Today's fleet size and make-up were accessed through an aircraft database giving the number of relevant active aircraft in 2008 as 14 401. Growth rates were adopted from a recent ICAO (FESG) forecast. However, with respect to the current economic downturn, the growth rates of the FESG were adjusted down for the years 2009-2016. Future aircraft retirements were calculated from aircraft survival curves. Eleven entirely new aircraft model families and two derivative models of existing aircraft were identified from a literature survey to have a service entry in the 2030 timeframe. Despite this large number, new aircraft models were found to work their way only slowly into the world fleet. Future aircraft (including the A380) were computed to account for 69 % of the entire world fleet in 2036. The thesis at hand expects world fleet size to have doubled by that time.

In a second step, individual aircraft's fuel efficiency and operational characteristics were introduced. Typical fuel consumption and utilization of currently active aircraft models were accessed from historical recordings of the last ten years. Major technology features of near-term future aircraft (service entry prior to 2015) were found to be frozen and fuel burn characteristics to be obtainable through a literature study. Most of these aircraft will

incorporate technology that is evolutionary advanced from today's aircraft. Increased fuel efficiency is assumed to come mainly from applying composite materials to primary structures and from the use of advanced (still conventional) turbofans. The specific concept bringing the highest CO_2 reduction in this period was found to be the geared turbofan, which is expected to enter service on two aircraft in 2013. The aircraft that are expected to show the highest fuel burn advantage (around 20 %) over currently active models were identified to be the Boeing 787, the Airbus A350 and the Bombardier CSeries. Medium- to long-term aircraft projects with a service entry in the 2015 to 2030 timeframe were found to be still in a very early stage of development, which did not allow for definite projections of the technology implemented. Potential technologies for these aircraft were identified from the technology survey and three scenarios were established to account for different future rates of technology progress and the readiness of manufacturers and airlines to assume risk of high development cost and time for achieving high benefits.

In a final step, the impact of aircraft technologies on future global CO_2 emission has been quantified by combining the results of the fleet forecast with the assumptions of fuel efficiency and operational performance of the individual aircraft. Accordingly, traffic will have increased nearly threefold by 2036. As technologically advanced future aircraft will enter the world fleet to satisfy the increased demand in traffic and to replace aging out-of-production aircraft, over-all fleet fuel and CO2 efficiency will continue to increase. For the base forecast, where benefits were supposed to come only from new technology on future aircraft, per-seat fuel consumption and CO_2 emission in 2036 come in 11 % lower for the pessimistic scenario, 17 % lower for the trend scenario and 22 % lower for the optimistic scenario than in 2008. However, improvements from future aircraft alone are forecasted not being able to keep pace with traffic growth. For the base forecast, global CO_2 emission from aviation was calculated to increase by a factor of 2.58, 2.44 and 2.31 (pessimistic, trend, optimistic) over the entire period. The effects of the economic downturn will lead to low growth rates in traffic and fleet size for the years 2009 through 2016 and thus also to a considerably lower growth in global CO_2 emissions. However, even though beneficial for the global emission of CO_2, on the local level, the economic downturn constrains fleet fuel efficiency to lower improvement rates as the number of new aircraft entering the world fleet will be reduced as well.

Unlike to historic developments, only small additional fuel benefits are expected from advances in the air traffic environment (0.1 % p.a.) and operations (0.17 % p.a.) in the future. As thus, annual improvement rates of considerably more than 1.0 % are achieved only in combination with the optimistic scenario, it is projected that keeping up to historic annual improvement rates in fleet fuel efficiency will be possible only if future aircraft provide radical fuel efficiency leaps.

Beyond traditional instruments to increase fleet fuel efficiency, the benefit of alternative approaches to CO_2 reduction has been assessed. Bio-fuels are shown to have a high potential,

it is however unclear if a large-scale production will be environmentally, ethically and economically feasible. Independent of technological advances are approaches that aim at re-structuring traditional life-cycles of both aircraft and aircraft programs. It has been found that shifting delivery dates to later years for the reason of achieving further technology improvements does not ultimately have to be the best choice for the goal of reducing global CO2 emission. Both the reduction of aircraft lifetime and shortened aircraft production runs – i.e. earlier implementation of successor aircraft – may however positively affect fleet fuel efficiency.

The environmental goal of carbon neutral growth in the medium-term was found being realizable only through the combination of revolutionary fuel-efficient future aircraft with a strongly increasing share of bio-fuels in global fuel consumption.

References

ACARE 2002 ADVISORY COUNCIL FOR AERONAUTICS RESEARCH IN EUROPE (ED.): *Strategic Research Agenda: Volume 2*. Luxembourg: European Communities, 2002

Adams 2008 ADAMS, Charlotte: *Green Engines*, 2008. – URL: http://www.aviationtoday.com/am/categories/commercial/21556.html (2009-06-05)

Airbus 2004 AIRBUS: *Getting to Grips with Fuel Economy*, 2004. – URL: http://www.iata.org/NR/ContentConnector/CS2000/Siteinterface/sites/whatwedo/file/Airbus_Fuel_Economy_Material.pdf (2009-01-16)

Airbus 2007a AIRBUS: *A320 Aircraft Limitations & Features : Aircraft Handling Manual*, 2007. – URL: http://www.scribd.com/doc/6590788/Part-B-A320-A321-English (2009-07-07)

Airbus 2007b AIRBUS: *Global Market Forecast 2007-2026*, 2007. – URL: http://www.airbus.com/store/mm_repository/pdf/att00011423/media_object_file_GMF_2007.pdf (2009-11-04)

Airbus 2009a URL: http://www.airbus.com/en/aircraftfamilies/a350/efficiency/by_nature/cruise.html (2009-07-05)

Airbus 2009b URL: http://www.airbus.com/en/aircraftfamilies/a350/efficiency/a350800_ specifications.html (2009-07-05)

Airbus 2009c AIRBUS: *A320 Israir*, 2009. – URL: http://www.airbus.com/store/photolibrary/AIRCRAFT/CUSTOMER/A320/att00009573/media_object_image_lowres_A320_Israir_mr.jpg (2009-03-31)

Airbus 2009d AIRBUS: *A330: Airplane Characteristics*, 2009. – URL: http://www.airbus.com/fileadmin/documents/Airbus_Technical_Data/AC/AC_A330_01FEB2009.pdf (2009-06-05)

Airbus 2009e AIRBUS: *Taking the Lead : The A350 XWB*, No Date. URL: http://www.eads.com/xml/content/OF00000000400004/7/19/41508197.pdf (2009-07-05)

Aircraft Commerce 2001

AIRCRAFT COMMERCE: *360-seaters in performance test.* In: *Aircraft Commerce*, 15 (2001), pp. 20–25

Aircraft Commerce 2006

AIRCRAFT COMMERCE: *Replacement Options for 80- to 150-Seat Jets.* In: *Aircraft Commerce*, 44 (2006), pp. 36–42

Aircraft Commerce 2007

AIRCRAFT COMMERCE: *Assessing 747-400 Replacement Options.* In: *Aircraft Commerce*, 52 (2007), pp. 40–47

Aircraft Commerce 2008a

AIRCRAFT COMMERCE: *A330 -200 & -300 Fuel Burn Performance.* In: *Aircraft Commerce*, 57 (2008), pp. 16–19

Aircraft Commerce 2008b

AIRCRAFT COMMERCE: *777 Fuel Burn Performance.* In: *Aircraft Commerce*, 60 (2008), pp. 8–9

Aircraft Commerce 2008c

AIRCRAFT COMMERCE: *The economics of downsizing to large RJs.* In: *Aircraft Commerce*, 60 (2008), pp. 31–39

Aircraft Commerce 2009

AIRCRAFT COMMERCE: *Widebody selection : 787/777 versus the A350 family.* In: *Aircraft Commerce*, 62 (2009), pp. 18–22

Airline Monitor 2007 GREENSLET, Edmund S. (ed.): *Profiles of Single and Twin Aisle Aircraft : Prospective Demand, Operating Costs, Prices and Values.* In: *The Airline Monitor*, 20 (2007), No. 6, pp. 11–73

Airline Monitor 2008a

GREENSLET, Edmund S. (ed.): *Block Hour Operating Costs of Passenger Aircraft from 1968 or First Year in Operation.* In: *The Airline Monitor* 21 (2008). – *Microsoft Excel* Spread Sheet

Airline Monitor 2008b

GREENSLET, Edmund S. (ed.): *Commercial Aircraft Monitor: Forecast of the World Jet Transport Market from 2008 to 2030.* In: *The Airline Monitor*, 21 (2008), No. 2

Airline Monitor 2008c

GREENSLET, Edmund S. (ed.): *Commercial Aircraft Monitor : Block Hour Operating Costs by Airplane Type for the Year 2007.* In: *The Airline Monitor*, 21 (2008), No. 3

Airliners Penang 2008

URL: http://airlinerspenang.blogspot.com/2008/07/arj21-advanced-regional-jet-for-21st.html (2009-05-04)

Anders 2007 ANDERS, Hanyo Vera: *User Preferred Trajectories in Commercial Aircraft Operation : Design and Implementation.* Stockholm, KTH, Department of Aeronautical and Vehicle Engineering, Licenciate Thesis, 2007

AT 2008 AEROSPACE TECHNOLOGY: *ARJ21 Regional Jet Aircraft, China*, 2008. – URL: http://www.aerospace-technology.com/projects/arj21/ (2009-04-17)

AT 2009a AEROSPACE TECHNOLOGY: *Airbus A350 XWB Long-Range, Extra-Wide-Bodied Airliner,* 2009. – URL: http://www.aerospace-technology.com/ projects/a350wxb/ (2009-05-07)

AT 2009b AEROSPACE TECHNOLOGY: *Boeing 747-8 Intercontinental Airliner,* 2009. – URL: http://www.aerospace-technology.com/projects/boeing-747-8/ (2009-05-05)

AT 2009c AEROSPACE TECHNOLOGY: *Boeing 787 Dreamliner Long-Range, Mid-Size Airliner*, 2009. – URL: http://www.aerospace-technology.com/ projects/dreamliner/ (2009-05-06)

AT 2009d AEROSPACE TECHNOLOGY: *Bombardier CRJ1000 Regional Jetliner,* 2009. – URL: http://www.aerospace-technology.com/projects/ bombardier_crj1000/ (2009-05-04)

ATA 2009 URL: http://www.airlines.org/operationsandsafety/atc/QandA_RNAV.htm (2009-05-29)

ATAG 2009 AIR TRANSPORT ACTION GROUP: *Beginner's Guide to Aviation Biofuels*, 2009. – URL: http://www.enviro.aero/Content/Upload/File/ BeginnersGuide_Biofuels_WebRes.pdf (2009-06-26)

Babikian 2006 BABIKIAN, Raffi; LUKACHKO, Stephan; WAITZ, Ian: *The Historical Fuel Efficiency Characteristics of Regional Aircraft from Technological, Operational, and Cost Perspectives.* Cambridge: Massachusetts Institute of Technology, 2006. – URL: http://web.mit.edu/aeroastro/people/waitz/publications/Babikian.pdf (2009-06-18)

Bateman 2009 BATEMAN, Louise: *Rolls-Royce engine could cut aircraft carbon emissions by 30 per cent*, 2009. – URL: http://www.greenwisebusiness.co.uk/news/rollsroyce-engine-could-cut-aircraft-carbon-emissions-by-30-per-cent.aspx (2009-07-05)

Bauhaus Luftfahrt 2008 BAUHAUS LUFTFAHRT: *Claire Liner*, 2008. – URL: http://bauhaus-luftfahrt.net/_data/Finale_Claire_Liner_Presentation_English_23-05-2008.pdf (2008-01-14)

Berton 2002 BERTON, Jeffrey: *Advanced Engine Cycles Analyzed for Turbofans With Variable-Area Fan Nozzles Actuated by a Shape Memory Alloy*, 2002. – URL: http://www.grc.nasa.gov/WWW/RT/RT2001/2000/2400berton.html (2009-06-12)

Bock 2007 BOCK, S.; HORN, W.; WILFERT, G.; et al.: *Active Core Engine Technology within the NEWAC Research Program for cleaner and more efficient Aero Engines.* Munich: MTU Aero Engines, 2007. – URL: http://www.newac.eu/uploads/media/No.05_MTU_CEAS_07.pdf (2009-06-10).

Boeing 1996 URL: http://www.boeing.com/commercial/747family/news/1996/news.release.960110-b.html (2009-04-10). – Boeing News Release

Boeing 1998 BOEING: *Airplane Characteristics for Airport Planning : 777-200/300*, 1998. – URL: http://www.boeing.com/commercial/airports/acaps/777_23.pdf (2009-05-07)

Boeing 2005 URL: http://www.boeing.com/news/releases/2005/q4/nr_051114h.html (2009-05-05) – Boeing News Release

Boeing 2007a BOEING: *Airplane Characteristics for Airport Planning : 787 - Preliminary Information*, 2007. – URL: http://www.boeing.com/commercial/airports/acaps/7878.pdf (2009-05-06)

Boeing 2007b BOEING: *B777 Aircraft Handling Manual : Ground Handling Operation Manual,* 2007. – URL: http://www.scribd.com/doc/6590824/Part-B-B777-A330-English (2009-07-07)

Boeing 2008 BOEING: *2008 Environmental Report*, 2008. – URL: http://www.boeing.com/aboutus/environment/environmental_report_08/boeing-2008-environment-report.pdf (2009-05-27)

Boeing 2009a URL: http://www.boeing.com/commercial/787family/specs.html (2009-05-07)

Boeing 2009b BOEING: *Boeing 777 in Flight*, 2009. – URL: http://www.boeing.com/commercial/777family/gallery/17892.html (2009-03-31)

Boeing 2009c BOEING: *Current Market Outlook 2009-2028*, 2009. – URL: http://www.boeing.com/commercial/cmo/index.html (2009-07-07)

Boggia 2004 BOGGIA, S.; RÜD, K: *Intercooled Recuperative Aero Engine.* Munich: MTU Aero Engines, 2004

Bombardier 2007a BOMBARDIER: *CRJ900 NextGen*, 2007. – URL: http://www2.bombardier.com/CRJ/en/NextGen/pdf/CRJ900_EN.pdf (2009-05-05)

Bombardier 2007b BOMBARDIER: *CRJ1000 Next Gen*, 2007. URL: http://www2.bombardier.com/CRJ/en/NextGen/pdf/CRJ1000_EN.pdf (2009-05-05)

Bombardier 2008 URL: http://www.bombardier.com/en/aerospace/media-centre/press-releases/details?docID=0901260d800326db (2009-04-17). – Bombardier Press Release

Bombardier 2009 URL: http://www.nowisthefuture.com/ (2009-05-10)

Bouteiller 2008 BOUTEILLER, X: *Drag Reduction for Nacelle Applications*, 2008. – URL: http://www.kat-net.net/publications/data/64_20081111_bouteiller.pdf (2009-06-10). Proceedings of the KATNET II Drag Reduction Workshop Ascot 2008

Bräunling 2004 BRÄUNLING, Willy J. G.: *Flugzeugtriebwerke : Grundlagen, Aero-Thermodynamik, Kreisprozesse, Thermische Turbomaschinen, Komponenten und Emissionen*. Berlin: Springer, 2004

CAA 2009 CIVIL AVIATION AUTHORITY: *Basic Principles of the Continuous Descent Approach (CDA) for the Non-Aviation Community*, No Date. – URL: http://www.caa.co.uk/docs/68/Basic_Principles_CDA.pdf (2009-03-20)

Cambridge-MIT Institute 2006
URL: http://silentaircraft.org/ (2009-06-12)

CANSO 2008 STOLLERY, Phil: *ATM Global Environment Efficiency Goals for 2050 : Reducing the Impact of Air Traffic Management on Climate Change.* Hoofddorp: Civil Air Navigation Services Organisation, 2008. – URL: http://www.canso.org/cms/showpage.aspx?id=52 (2009-04-06)

Carbone 2008 CARBONE, Achille: *The Green Regional Aircraft ITD*, 2008. – URL: http://www.fp7.org.tr/tubitak_content_files/273/CleanSkyJTI/5_GreenRegionalAircraftITD_AchilleCarbone_AleniaAeronautica.pdf (2009-06-10). Proceedings of the CleanSky Take-Off Conference Brussels 2008

Cavcar 2009 CAVCAR, Mustafa: *The International Standard Atmosphere (ISA)*, No Date. – URL: http://home.anadolu.edu.tr/~mcavcar/common/ISAweb.pdf (2009-06-09)

Clarke 2007 CLARKE, David: *Powering Our Future : Rolls-Royce and the Environment*, 2007. – URL: http://www.apeg.org.uk/programme/pdf/Clarke_presentation.pdf (2009-06-07).

Coppinger 2009 COPPINGER, Rob: *ACARE Prepares for 2010 Overhaul*, 2009. – URL: http://www.flightglobal.com/articles/2009/01/21/321340/acare-prepares-for-2010-overhaul.html (2009-06-20)

Courty 2008 COURTY, J. C: *Drag Reduction Requirements for Civil Applications at Dassault Aviation*, 2008. – URL: http://www.kat-net.net/publications/data/64_20080428_%5B2%5D_joly_courty.pdf (2009-06-09). Proceedings of the KATnet Separation Control Workshop Toulouse 2008

Curry 2008 CURRY, Marty; DUNBAR, Brian: *Beamed Laser Power For UAV*, 2008. – URL: http://www.nasa.gov/centers/dryden/news/FactSheets/FS-087-DFRC.html (2009-04-09)

Daggett 2003a DAGGETT, David L.; EELMAN, Stephan; KRISTIANSSON, Gustav: *Fuel Cell APU for Commercial Aircraft.* Dayton: AIAA, 2003. – AIAA Report AIAA-2003-2660

Daggett 2003b DAGGETT, David L.; KAWAI, Ron; FRIEDMAN, Doug: *Blended Wing Body Systems Studies : Boundary Layer Ingestion Inlets With Active Flow Control.* Hampton: NASA, 2003. – NASA Report NASA/CR-2003-212670

Daggett 2006 DAGGETT, D.; HADALLER, O.; HENDRICKS, R.; et al.: *Alternative Fuels and Their Potential Impact on Aviation.* Hampton: NASA, 2006. – NASA Report NASA/TM-2006-214365

Dodds 2005 DODDS, Will; GE Aviation: *Twin Annular Premixing Swirler (TAPS) Combustor*, 2005. – URL: http://www.techtransfer.berkeley.edu/aviation05downloads/Dodds.pdf (2009-12-06). Proceedings of The Roaring 20th Aviation Noise & Air Quality Symposium Berkeley 2005

Donoghue 2006 DONOGHUE, J. A.: *Cool Burnings.* In: *Air Transport World*, (2006), March 2006, p. 27. – URL: http://www.atwonline.com/magazine/article.html?articleID=1546 (2009-06-12)

Doyle 2009 DOYLE, Andrew: *R-R details Trent XWB development strategy*, 2009. – URL: http://www.flightglobal.com/articles/2009/03/06/323432/r-r-details-trent-xwb-development-strategy.html (2009-05-08)

EC 2001 ARGÜELLES, Pedro; BISCHOFF, Manfred; BUSQUIN, Philippe, et al. (eds.): *European Aeronautics : A Vision for 2020.* Luxembourg: European Communities, 2001

Embraer 2008a EMBRAER: *Embraer 190 Spec Sheet*, 2008. – URL: http://www.embraercommercialjets.com/english/inc/df.asp?Caminho=ejets/doc/SpecSheet_EMBRAER190.pdf (2009-05-09)

Embraer 2008b EMBRAER: *Embraer 175 Spec Sheet*, 2008. – URL: http://www.embraercommercialjets.com/english/inc/df.asp?Caminho=ejets/doc/SpecSheet_EMBRAER175.pdf (2008-05-09)

Embraer 2008c EMBRAER: *Embraer 195 Spec Sheet*, 2008. – URL: http://www.embraercommercialjets.com/english/inc/df.asp?Caminho=ejets/doc/SpecSheet_EMBRAER195.pdf (2009-05-10)

enviro.aero 2008 URL: http://www.enviro.aero/Aviationindustryenvironmentalnews.aspx ?NID=252 (2009-05-26)

Esler 2008 ESLER, David: *The Greening of Business Aviation : Part III*, 2008. – URL: http://www.aviationweek.com/aw/generic/story_channel.jsp?channel=busav&id=news/bca0708p1.xml (2009-01-19)

EU 2004a EU TRANSPORT RESEARCH: *'POA' – research project works to optimise aircraft power use*, 2004. – URL: http://ec.europa.eu/research/transport/news/article_1599_en.html (2009-06-12)

EU 2004b EU TRANSPORT RESEARCH: *ARITMA - Aircraft Reliability Through Intelligent Materials Application*, 2004. – URL: http://ec.europa.eu/research/transport/projects/article_3708_en.html (2009-02-06)

Eurocontrol 2004a EUROCONTROL: *Base of Aircraft Data (BADA) : Aircraft Performance Operational Files Version 3.6.* Brussels: Eurocontrol, 2004

Eurocontrol 2004b EUROCONTROL: *User Manual for the Base of Aircraft Data (BADA) : Revision 3.6.* Brussels: Eurocontrol, 2004

Eurocontrol 2005 EUROCONTROL: *BADA Calculation Tool 3.6: Web Application*, 2005. – URL: http://badaext.eurocontrol.fr/ (2009-03-19). Aircraft Performance Online Calculation Tool

Eurocontrol 2008 EUROCONTROL; Eurocontrol: *Navigation Application & NAVAID Infrastructure Strategy for the ECAC Area up to 2020.* Brussels: Eurocontrol, 2008

Eurocontrol 2009 URL: http://www.atmmasterplan.eu/ (2009-04-06)

Exxon 2008 EXXON: *World Jet Fuel Specifications : 2008 Edition.* Leatherhead: Exxon Mobile Aviation, 2008

FAA 2009 FEDERAL AVIATION ADMINISTRATION: *FAR Part 121 : Operating Requirements: Domestic, Flag, and Supplemental Operations*, 2009. – URL: http://ecfr.gpoaccess.gov (2009-03-03)

Farrar 2007 FARRAR, Charles R.; WORDEN, Keith: *An Introduction to Structural Health Monitoring.* In: *Philosophical Transactions of the Royal Society A*, 365 (2007), pp. 303–315

Faye 2001 FAYE, Robert; LAPRETE, Robert; WINTER, Michael: *Wingtip Devices*, 2009. – URL: http://www.boeing.com/commercial/aeromagazine/aero_17/winglet_story.html#wingtip (2009-01-14)

Feir 2001 FEIR, Jack; Jack B Feir & Associates: *Aircraft Useful Lives, Retirements and Freighter Conversions*, 2001. – URL: http://www.jackfeir.com/JackFeirPresentation.pdf (2009-06-08)

FESG 2007 FORECAST AND ECONOMIC ANALYSIS SUPPORT GROUP: Revised FESG Passenger Aircraft Retirement Methodology / Survivor Curve(s) : CAEP/8 Passenger Aircraft Retirement Curves : Revised as of 1 October 2007. Montréal: ICAO, 2007. – Microsoft Excel Spread Sheet. This Document is enclosed in Digital Format on the Compact Disc in Appendix D

FESG 2008 FORECAST AND ECONOMIC ANALYSIS SUPPORT GROUP; ICAO: FESG Forecast Task Group Progress Report Seattle 11-06-2008. Montréal: ICAO, 2008. – This Document is enclosed in Digital Format on the Compact Disc in Appendix D

Flight Daily News 2008 FLIGHT DAILY NEWS: *Replacement Boeing 737 and Airbus A320 narrowbodies to take longer than planned*, 2008. – URL: http://www.flightglobal.com/articles/2008/05/29/224270/ila-2008-replacement-boeing-737-and-airbus-a320-narrowbodies-to-take-longer-than-planned.html (2009-05-27)

Flight Global 2009 URL: http://www.flightglobal.com/articles/2009/03/30/324411/world-airlines-directory-2009-crisis-management.html (2009-04-12)

Flight International 2006 URL: http://www.flightglobal.com/articles/2006/12/12/ 211030/why-new-wing-is-key-a350-xwb.html (2009-05-07)

Flightglobal 2009 URL: http://www.flightglobal.com/landingpage/mitsubishi%20mrj.html (2009-05-08)

Forrester 2009 FORRESTER, Greg: *WheelTug drives Green Aviation*, 2009. – URL: http://www.wheeltug.gi/press/WheelTug_8June09_Release.pdf (2009-06-13)

Forsberg 2002 FORSBERG, Svante; WERNEMANN, Elisabeth: *Statement of limited review*. Stockholm: Deloitte & Touche, 2002. – URL: http://www.sasems.port.se/Revisorsintyg.pdf (2009-05-15)

Francis 2009 FRANCIS, Leithen: *China fast-tracks 150-seat aircraft programme*, 2009. – URL: http://www.flightglobal.com/articles/2009/03/04/323350/china-fast-tracks-150-seat-aircraft-programme.html (2009-04-17)

GAO 2009 FLEMING, Susan; COLWELL, Cathy; MORRISON, Faye; et al: *Aviation and Climate Change.* Washington, D.C.: United States Government Accountability Office, 2009. – URL: http://gao.gov/new.items/d09554.pdf (2009-06-10)

Gates 2008 GATES, Dominic: *Boeing pushes back design development of 737 replacement jet*, 2008. – URL: http://seattletimes.nwsource.com/html/businesstechnology/2004433395_boeing23.html (2009-05-12)

GE Aviation 2008 URL: http://www.geae.com/genxrightnow/enginedetails.html (2009-05-05)

GE Aviation 2009 URL: http://www.geae.com/engines/commercial/cf34/index.html (2009-04-05)

GIACC 2009 GROUP ON INTERNATIONAL AVIATION AND CLIMATE CHANGE: Working Paper Third Meeting : Review of Aviation Emissions Related Activities within ICAO and Internationally. Montréal: ICAO, 2009. – URL: http://www.icao.int/env/meetings/2009/giacc_3/docs/GIACC3_wp06_en.pdf (2009-07-02)

Global Security 2009 URL: http://www.globalsecurity.org/military/world/europe/a320-schem.htm (2009-05-10)

Gmelin 2008 GMELIN, Tillmann C.; HÜTTIG, Gerhard; LEHMANN, Oliver; Bundesministerium für Umwelt Naturschutz und Reaktorsicherheit: *Zusammenfassende Darstellung der Effizienzpotentiale bei Flugzeugen unter besonderer Berücksichtigung der aktuellen Triebwerkstechnik sowie der absehbaren mittelfristigen Entwicklungen.* Berlin: Bundesministerium für Umwelt Naturschutz und Reaktorsicherheit, 2008. – BMU Report, FKZ UM 07 06 602/01

Gollnick 2008 GOLLNICK, Volker: *Flugzeugentwurf I.* Hamburg, Technical University, Lecture Notes, 2008

Govindasamy 2008 GOVINDASAMY, Sami: *Japan flies solo again*, 2008. – URL: http://www.flightglobal.com/articles/2008/09/23/316320/japan-flies-solo-again.html (2009-08-05)

Grasmeyer 1998 GRASMEYER, Joel M.: *Multidisciplinary Design Optimization of a Strut-Braced Wing Aircraft.* Blacksburg, Virginia Polytechnic, Master Thesis, 1998. – URL: http://scholar.lib.vt.edu/theses/available/etd-4598-173228/unrestricted/Thesis.pdf (2009-01-13)

Gratzer 1992 Patent US 5102068 (1992-07-04). Gratzer, Louis B

Green 2006 GREEN, J. E.: *Küchemann's weight model as applied in the first Greener by Design Technology Sub Group Report: a correction, adaption and commentary.* In: *The Aeronautical Journal*, 1110 (2006), No. 110, pp. 511–516

Greener By Design 2002 STEEDEN, Mike (ed.); Royal Aeronautical Society: *Greener By Design : Improving Operations - The Technology Challenge - Market-Based Options.* London: Royal Aeronautical Society, 2002

Greener By Design 2003 GREEN, John E. (ed.); Royal Aeronautical Society: *Air Travel - Greener By Design : The Technology Challenge.* London: Royal Aeronautical Society, 2003

Greener By Design 2005 GREEN, John E. (ed.); Royal Aeronautical Society: *Air Travel - Greener by Design : Mitigating the Environmental Impact of Aviation: Opportunities and Priorities.* London: Royal Aeronautical Society, 2005

Grimme 2008 GRIMME, Wolfgang: *Measuring the long-term sustainability of air transport – an assessment of the global airline fleet and its CO2-emissions up to the year 2050.* Cologne: DLR, 2008

Gupta 1985 Patent US 4506851 (1985-03-26) Gupta, Alankar; Robert, W.

Hawk 2005 HAWK, Jeff: *The Boeing 787 Dreamliner : More than an Airplane*, 2005. – URL: http://www.aiaa.org/events/aners/Presentations/ANERS-Hawk.pdf (2009-05-06). Proceedings of the AIAA/AAAF Aircraft Noise and Emissions Reduction Symposium Monterey 2005

Heinze 2005 HEINZE, Wolfgang: *Flugzeugentwurf.* Braunschweig, Technical University, Lecture Notes, 2005

Herbert 2007 URL: http://en.wikipedia.org/wiki/File:BWB-Composite.png (2009-04-09)

Hering 2004 HERING, Horst: *VITAL – An Advanced Time-Based Tool for the Future 4D ATM Environment.* No Place: IEEE, 2004. – URL: http://www.eurocontrol.fr/Newsletter/2005/March/Recent_Documents/DASC/3b5.pdf (2009-06-08). IEEE Report 0-7803-8539-X/04

Hone-All 2008 HONE-ALL: *Getting Ready for the Long Haul*, 2008. – URL: http://www.pesmag.co.uk/Issues/September08/PDF/PES_September2008_Subdrilling.pdf (2009-05-05)

Houghton 2003 HOUGHTON, Edward L.; CARPENTER, Peter W.: *Aerodynamics for engineering students.* Amsterdam: Elsevier, 2003

IATA 2008a IATA: Technology Roadmap Report 1st Edition. Geneva: IATA, 2008. – This Document is enclosed in Digital Format on the Compact Disc in Appendix D

IATA 2008b IATA: Technology Roadmap Report 2nd Edition. Geneva: IATA, 2008. – This Document is enclosed in Digital Format on the Compact Disc in Appendix D

IATA 2008c IATA: *IATA 2008 Report on Alternative Fuels*, 2008. – URL: http://www.iata.org/NR/rdonlyres/03FE754C-D30A-4E77-8C92-5A05AF75C614/0/IATA2008ReportonAlternativeFuels.pdf (2009-06-09)

IATA 2009a IATA: *Technology Roadmap Report Technical Annex*, 2009. – URL: http://www.iata.org/NR/rdonlyres/57FC87FB-17AE-419E-A3B9-60F1ED20B712/0/Technology_Roadmap_TechnicalAnnex1.pdf (2009-06-16)

IATA 2009b IATA: *Carbon-Neutral Growth by 2020 : Bold Industry Commitment on Environment*, 2009. – URL: http://www.iata.org/pressroom/pr/2009-06-08-03.htm (2009-06-20). IATA Press Release

ICAO 2001 ICAO: *Working Papers of the Fourth Meeting of the ALLPIRG/Advisory Group : Aircraft Operating Costs (Average per Block Hour)*, 2001. – URL: http://www.icao.int/icao/en/ro/allpirg/allpirg4.htm (2008-09-12)

ICAO 2009a ICAO: *Engine Emissions Databank*, 2009. – URL: http://www.caa.co.uk/default.aspx?catid=702 (2009-03-03)

ICAO 2009b STEELE, Paul: *Industry Goals and Measures to Address CO2 Emissions From Aviation*, 2009. – URL: http://www.icao.int/env/meetings/2009/GIACC_3/Docs/Giacc3_Pres_IndustryGoals.pdf (2009-02-07). ICAO CO_2 Emission Forecast on behalf of ACI, CANSO, IATA and ICCAIA

IEA 2007 GIELEN, Dolf: *Energy Technology Perspectives*, 2007 – URL: http://unfccc.int/files/meetings/dialogue/application/pdf/iea_-_gielen.pdf (2009-06-26). Proceedings of the UNFCCC Dialogue Workshop Bonn 2007

IPCC 1999 PENNER, Joyce E.; LISTER, David H.; GRIGGS, David J.; et al.: *Aviation and the Global Atmosphere.* Cambridge: Cambridge University Press, 1999

IPCC 2007 SOLOMON, S.; QIN, D.; MANNING, M.; et al.: *IPCC : Climate Change 2007 : The Physical Science Basis.* Cambridge: Cambridge University Press, 2007

Jane's 2009 JANE'S: *Jane's all the World's Aircraft 2009.* Couldson: Jane's Information Group, 2009

Japan NIMS 2009 JAPAN NATIONAL INSTITUTE FOR MATERIAL SCIENCE: *Research and Development of Superalloys for Aeroengine Apprications.* No Date. URL: http://sakimori.nims.go.jp/topics/hightemp_e.pdf (2009-06-10)

Jenkinson 2005 JENKINSON, Lloyd R: *Aircraft Data*, 2005. – URL: http://www.soton.ac.uk/~jps7/Aircraft%20Design%20Resources/Lloyd%20Jenkinson%20data/Aircraft%20data/ (2009-03-18)

Jong 2008 JONG, Ed de: *Furanics : Versatile molecules applicable for biofuels and bulk chemicals applications*, 2008. – URL: http://www.rrbconference.org/bestanden/downloads/121.pdf (2009-06-04). Proceedings of the 5th International Conference on Renewable Resources & Biorefineries Ghent 2009

JPDO 2009 URL: http://jpe.jpdo.gov/ee/ (2009-06-04)

Kingsley-Jones 2006 KINGSLEY-JONES, Max: *Airbus's A350 vision takes shape - Flight takes an in-depth look at the new twinjet*, 2006. – URL: http://www.flightglobal.com/articles/2006/12/12/211028/airbuss-a350-vision-takes-shape-flight-takes-an-in-depth-look-at-the-new.html (2009-05-07)

Kingsley-Jones 2007 KINGSLEY-JONES, Max: *Russian Revolution: The Sukhoi Superjet*, 2007. – URL: http://www.flightglobal.com/articles/2007/02/06/211873/russian-revolution-the-sukhoi-superjet.html (2009-05-05)

Kingsley-Jones 2008a KINGSLEY-JONES, Max: *As Airbus A350 takes shape, can it avoid the A380's troubles?*, 2008. – URL: http://www.flightglobal.com/articles/2008/07/08/225120/as-airbus-a350-takes-shape-can-it-avoid-the-a380s.html (2009-05-07)

Kingsley-Jones 2008b KINGSLEY-JONES, Max: *Tomorrow can wait as Airbus and Boeing leave next generation narrowbody development on the back burner*, 2008. – URL: http://www.flightglobal.com/articles/2008/07/09/225122/tomorrow-can-wait-as-airbus-and-boeing-leave-next-generation-narrowbody-development-on-the-back.html (2009-05-11)

Kirby 2007 KIRBY, Mary: *Pictures: Bombardier launches CRJ900 stretch, the CRJ1000, with 38 firm orders and 23 options*, 2007. – URL: http://www.flightglobal.com/articles/2007/02/19/212177/pictures-bombardier-launches-crj900-stretch-the-crj1000-with-38-firm-orders-and-23.html (2009-04-05)

Kirby 2008 KIRBY, Mary: *Bombardier CRJ1000 takes first flight*, 2008. – URL: http://www.flightglobal.com/articles/2008/09/03/315530/bombardier-crj1000-takes-first-flight.html (2009-04-17)

Kroo 2006 KROO, Ilan: *Reinventing the Airplane : New Concepts for Flight in the 21st Century*, 2006. – URL: http://adg.stanford.edu/aa241/AircraftDesign.html (2008-01-13)

Kruse 2008 URL: http://www.tu-braunschweig.de/ism/forschung/ag-flzg/projekte-alt/nefa (2009-06-13)

Küchemann 1993 KÜCHEMANN, D.: *The Aerodynamic Design of Aircraft : A detailed introduction to the current aerodynamic knowledge and practical guide to the solution of aircraft design problems.* Oxford: Pergamon, 1993

Kurzke 2009 KURZKE, Joachim: *Achieving maximum thermal efficiency with the simple gas turbine cycle.* Munich: MTU Aero Engines GmbH, No Date. – URL: http://www.mtu.de/en/technologies/engineering_news/34127Kurzke_AchievingMaximumThermalEfficiencyFinal.pdf (2009-01-25).

Lee 1998 LEE, Jospeh J.: *Historical and Future Trends in Aircraft Performance, Cost, and Emissions.* Cambridge, Massachusetts Institute of Technology, Master Thesis, 1998. – URL: http://www.soton.ac.uk/~jps7/D8%20website/future%20trends%20in%20aircraft%20costs.pdf (2009-06-20)

Leithen 2007 LEITHEN, Francis: *Building a future: The AVIC I ARJ21-700 programme*, 2007. – URL: http://www.flightglobal.com/articles/2007/08/24/216287/building-a-future-the-avic-i-arj21-700-programme.html (2009-04-05)

Lockerby 2008 URL: http://gow.epsrc.ac.uk/ViewGrant.aspx?GrantRef=EP/F004753/1 (2009-05-30)

Maclin 2003 MACLIN, H.; HAUBERT, C.: *Fifty Years Down - Fifty Years to Go.* No Place: AIAA, 2003. – AIAA Release 2003-2788

Mani 2008 MANI, Raghavendran; LAGOUDAS, Dimitris C.; REDINIOTIS, Othon K.: *Active Skin for turbulent Drag Reduction.* In: *Smart Materials and Structures*, 17 (2008), pp. 1–18

Mecham 2006 MECHAM, Michael: *GEnx Development Emphasizes Composites, Combustor Technology*, 2006. – URL: http://www.aviationweek.com/aw/generic/story_generic.jsp?channel=mro&id=news/aw041706p1.xml&headline=GEnx%20Development%20Emphasizes%20Compos (2009-06-12)

Mello 2006 MELLO, Laurent Vieira de: *Aerodynamics of Joined Wing Configurations.* Cranfield, Cranfield University, Master Thesis, 2006. – URL: https://aerade.cranfield.ac.uk/bitstream/1826/1587/1/Thesis%20report.pdf (2009-06-08)

Messier-Dowty 2005 URL: http://www.messier-dowty.com/rubrique.php3?id_rubrique=26 (2009-03-06)

Miller 2008 MILLER, Hugo: *Bombardier May Build 150 CSeries Jets a Year by 2016*, 2008. – URL: http://www.bloomberg.com/apps/news?pid=20601087&sid=aIMzIeMaad.4&refer=home (2009-04-18)

Mitsubishi 2008 MITSUBISHI: *MRJ : Mitsubishi Regional Jet – Flying into the Future*, 2008. – URL: www.mhi.co.jp/en/finance/library/contents/pdf/080331_mrj.pdf (2009-04-17).

Mitsubishi 2009 URL: http://www.mrj-japan.com/main_e.html (2009-05-08)

MRO Prospector 2008a
MRO PROSPECTOR: *Market forecast 2008 / 2013/ 2018*, 2008. – URL: http://mrop.aviationweek.com (2008-10-30). Regularly Updated Web Intelligence Document

MRO Prospector 2008b
MRO PROSPECTOR: *Aircraft and Engines by Aircraft Model*, 2008. URL: http://mrop.aviationweek.com/ (2008-12-09). Regularly Updated Web Intelligence Document

MTU 2007 URL: http://www.mtu.de/GB_2007_en/75.0.html (2009-06-12)

Nangia 2006 NANGIA, R. K.: *Efficiency parameters for modern commercial aircraft.* In: *The Aeronautical Journal*, 110 (2006), No. 1110, pp. 495–510

Nanotechnology 2009 URL: http://www.azonano.com/news.asp?newsid=10144 (2009-04-06)

NEWAC 2009 NEWAC: *Active Core Concept*, 2009. – URL: http://www.newac.eu/uploads/media/Active_Core_Concept.pdf (2009-02-06)

Norris 2008a NORRIS, Guy: *Gearing up for GTF?*, 2008. – URL: http://www.aviationweek.com/aw/blogs/defense/index.jsp?plckController=Blog&plckScript=blogScript&plckElementId=blogDest&plckBlogPage=BlogViewPost&plckPostId=Blog%3A27ec4a53-dcc8-42d0-bd3a-01329aef79a7Post%3A503f32b6-5be4-415c-93c5-421b619ccbf9 (2009-01-27)

Norris 2008b NORRIS, Guy: *Supply Chain Woes and Strike Impact Pushes 747-8 First Flight Into 2010*, 2008. – URL: http://www.aviationweek.com/aw/generic/story_channel.jsp?channel=comm&id=news/747-8EX.xml (2009-05-05)

OAG 2008 URL: http://www.oag.com/oagcorporate/pressreleases/08+oag+reports+a+seven+percent+drop+in+global+airline+capacity.html (2009-04-12). – OAG Press Release

OAG 2009 OAG: *Commercial Aircraft Fleet and Utilization Forecast 2008-2018 : Executive Summary*, 2009. – URL: http://www.oagaviation.com/aviation-reports/reports-camro.htm (2009-04-16)

OAG data 2007 OAG DATA: *MAX : Airline schedules database Dec 07*. Bedfordshire: OAG, 2007

Ostrower 2008 OSTROWER, Jon: *Spiroid Wingtip Technology: The best kept secret in aviation?*, 2008. – URL: http://www.flightglobal.com/blogs/flightblogger/2008/06/spiroid-wingtip-technology-the.html (2009-06-10)

Plohr 2009 PLOHR, Martin: *Comparison of a flight mission calculation and data recorded on-board during the flight*, 2009. – URL: http://www.dlr.de/at/en/DesktopDefault.aspx/tabid-1547/2182_read-3654/gallery-1/gallery_read-Image.20.1837/ (2009-02-06)

PowerJet 2008 URL: http://www.powerjet.aero/?id=200&selt=1 (2009-05-05)

Pratt & Whitney 2008 URL: http://www.pratt-whitney.com/vgn-ext-templating/v/index.jsp?vgnextoid=59ab4d845c37a110VgnVCM100000c45a529fRCRD (2009-05-09)

Raymer 1992 RAYMER, Daniel P.: *Aircraft Design : A conceptual approach*. Washington, D.C.: AIAA, 1992

Riegler 2007 RIEGLER, C.; BICHLMAIER, C.: *The Geared Turbofan Technology : Opportunities, Challenges and Readiness Status.* Munich: MTU Aero Engines, 2007

Rolls Royce 2008 URL: http://www.rolls-royce.com/trent_1000/1000.htm (2009-05-06)

Rosato 2004 ROSATO, Donald Vincent; ROSATO, Dominick V.: *Reinforced plastics handbook.* Oxford: Elsevier, 2004

Roskam 1997 ROSKAM, Jan; LAN, Chuan-Tau E.: *Airplane aerodynamics and performance.* Lawrence: DARcorporation, 1997

Roskam 2002 ROSKAM, Jan: *Airplane design.* Lawrence: DARcorporation, 2002

Rothman 2009 ROTHMAN, Andrea: *Airbus Says A350 on Course for First Delivery in 2013 (Update2)*, 2009. – URL: http://www.bloomberg.com/apps/news?pid=20601085&sid=aXEUgElSbQA0&refer=europe (2009-04-15)

Ruijgrok 2005 RUIJGROK, G. J. J.; VAN PAASSEN, D. M.: *Elements of Aircraft Pollution.* Delft: Delft University Press, 2005

Safran Group 2008 URL: http://www.safran-group.com/article.php3?id_article=2304 (2009-05-26)

SAS 2008 SAS: *Emission Calculator*, 2008. – URL: http://www.sasems.port.se/EmissionCalc.cfm?lang=1&utbryt=0&sid=geninfo&left=geninfo (2009-05-15)

SBAC 2008a LAMBERT, Carrie: *SBAC Aviation and Environment Briefing Papers 4: Alternative Aviation Fuels*. London: Society of British Aerospace Companies, 2008. – URL: http://www.sbac.co.uk/pages/92567080.asp (2008-10-24)

SBAC 2008b WATSON, Mark; LAMBERT, Carrie: Society of British Aerospace Companies: *SBAC Aviation and Environment Briefing Papers No.7 : ACARE Explained.* London: Society of British Aerospace Companies, 2008. – URL: http://www.sbac.co.uk/pages/92567080.asp (2009-06-12)

Scheiderer 2008 SCHEIDERER, Joachim: *Angewandte Flugleistung : Eine Einführung in die operationelle Flugleistung vom Start bis zur Landung.* Berlin: Springer, 2008

Schlichting 2001 SCHLICHTING, Hermann; TRUCKENBRODT, Erich: *Grundlagen aus der Strömungsmechanik : Aerodynamik des Tragflügels (Teil I)*. Berlin: Springer, 2001

Scholz 1999 SCHOLZ, Dieter: *Flugzeugentwurf.* Hamburg, Hochschule für Angewandte Wissenschaften, Lecture Notes, 1999

Scholz 2009 SCHOLZ, Dieter: *Aircraft Systems Overview : Secondary Power Systems - Today and Tomorrow,* 2009. – URL: http://www.mp.haw-hamburg.de/pers/Scholz/Aero/Aero_PRE_SWAFEA_09-04-24.pdf (2009-06-12)

Seibel 2003 SEIBEL, Michael; FLÜH, Hans-Jürgen: *Flugzeug-Strukturkonstruktion.* Hamburg, Hochschule für Angewandte Wissenschaften, Lecture Notes, 2003

Shell 2008 URL: http://www.shell.com/home/content/media/news_and_library/press_releases/2008/visit_merkel_choren_17042008.html (2009-03-06)

Shell 2009 MIDGLEY, Robert: Shell Presentation on Alternative Fuels, Long Term Perspective. Lecture at AERONET Workshop, Manchester, 2009-07-01

Shelton 2006 SHELTON, Andrew; TOMAR, Agvinesh; PRASAD, J. V.R.; et al.: *Active Multiple Winglets for Improved Unmanned-Aerial-Vehicle Performance.* In: *Journal of Aircraft*, 43 (2006), No. 1, pp. 110–116

Sims 2009 SIMS, Ralph; TAYLOR, Michael; SADDLER, Jack; et al.: *IEA's Report on 1st- to 2nd-Generation Biofuel Technologies*, 2009. – URL: http://www.renewableenergyworld.com/rea/news/article/2009/03/ieas-report-on-1st-to-2nd-generation-biofuel-technologies (2009-06-27)

Sinnett 2007 SINNETT, Mike: *787 No-Bleed Systems : Saving Fuel and Enhancing Operational Efficiencies*, 2007. – URL: www.boeing.com/commercial/aeromagazine (2009-01-29)

Smarsly 2006 SMARSLY, Wilfried: *Aero Engine Materials*, 2006. – URL: http://www.mtu.de/en/technologies/engineering_news/others/061221_smarsly_materials.pdf (2009-06-10)

Spaeth 2008 SPAETH, Andreas: *Die Wende am Himmel : Neue Hersteller von effizienten und umweltfreundlicheren Regionaljets drängen auf den Markt. Sie kommen aus Russland, China und Japan*, 2008. – URL: http://www.sueddeutsche.de/automobil/778/310706/text/ (2009-04-21)

Steinke 2006a STEINKE, Sebastian: *Airbus unveils A350 XWB*, 2006. In: *Flug Revue*, (2006), No. 9, p. 26. – URL: http://www.flug-revue.rotor.com/FRheft/FRHeft06/FRH0609/FR0609b.htm (2009-05-07)

Steinke 2006b STEINKE, Sebastian: *Boeing Launches 747-8*, 2006. In: *Flug Revue*, (2006), No. 1. – URL: http://www.flug-revue.rotor.com/FRHeft/FRHeft06/FRH0601/FR0601f.htm (2009-05-05)

Streit 2008 STREIT, Thomas; LIERSCH, Carsten: *Design of a Transonic Wing with Natural Laminar Flow for the EC Project NACRE*, 2008. – URL: http://www.kat-net.net/publications/data/64_20081111_streit.pdf (2009-01-20). Proceedings of the KATnet II Drag Reduction Workshop Ascot 2008

Sukhoi 2009 URL: http://www.sukhoi.org/eng/planes/projects/ssj100/characteristic/ (2009-05-05)

Sweetman 2000 SWEETMAN, Bill: *Flights of fancy take shape*, 2000. – URL: http://www.janes.com/defence/air_forces/news/idr/idr000704_1_n.shtml (2009-01-14)

Takemoto 2007 TAKEMOTO, Paul: *Automatic Dependent Surveillance-Broadcast (ADS-B) : Fact Sheet*, 2007. – URL: http://www.faa.gov/news/fact_sheets/news_story.cfm?newsId=7131 (2009-05-29)

Techno Science 2009 TECHNO SCIENCE: *CRJ1000*, 2009. – URL: http://techno-science.net/illustration/Aero/CRJ1000/CRJ1000.jpg (2009-04-05)

Torenbeek 1997 TORENBEEK, Egbert: *Cruise Performance And Range Prediction Reconsidered.* In: *Progress in Aerospace Sciences*, 33 (1997), 5/6, pp. 285–321

Truman 2006 TRUMAN, T.; GRAAF, A. de (eds.): *Out of the Box : Ideas about the Future of Air Transport.* Den Haag: ASTERA-ACARE, 2006

UAC Russia 2008 UAC RUSSIA: *Superjet 100*, 2008. – URL: http://www.uacrussia.ru/common/img/uploaded/superjet_100/SSJ_chertyozh_3_vida.png (2009-05-05)

University of Greenwich 2008 URL: http://fseg.gre.ac.uk/NACRE/details.html#programme (2009-06-10)

Viscotchi 2006 VISCOTCHI, Florentina: *Aviation Operational Measures for Fuel and Emissions Reduction Workshop : Weight Management*, 2006. – URL: http://www.icao.int/env/WorkshopFuelEmissions/Presentations/Viscotchi.pdf (2009-01-16). Proceedings of the ICAO Fuel and Emission Reduction Workshop Montréal 2006

Volvo Aero 2007 URL: http://www.volvo.com/volvoaero/global/en-gb/products/Engine+components/commercial_engines/commercial_engines.htm?TAB=15 (2009-05-07)

Waitz 2006 WAITZ, Ian; LUKACHKO, Stephan; WILLCOX, Caren; et al.: *Architecture Study for the Aviation Environmental Portfolio Management Tool.* Cambridge: Massachusetts Institute of Technology, 2006

Wall 2009 WALL, Robert: *Airbus Refines A30X Design*, 2009. – URL: http://www.aviationweek.com/aw/generic/story_generic.jsp?channel=awst&id=news/aw020909p3.xml (2009-02-15)

Wallace 1998 WALLACE, Lane E.: *Airborne Trailblazer*, 1998. – URL: http://oea.larc.nasa.gov/trailblazer/SP-4216/toc.html (2009-01-19)

Walz 2009 WALZ, Martha: *The Dream of Composites*, No Date. URL: http://www.rdmag.com/ShowPR~PUBCODE~014~ACCT~1400000100~ISSUE~0611~RELTYPE~PR~ORIGRELTYPE~FE~PRODCODE~00000000~PRODLETT~BM.html (2009-05-06)

WheelTug 2009 URL: http://www.wheeltug.gi/ (2009-06-13)

Willems 1998 WILLEMS, Frank; Eindhoven University of Technology, Faculty of Mechanical Engineering, Section Systems and Control: Valve Selection for Compressor Surge Control. Eindhoven: Eindhoven University of Technology, 1998 (Report WFW 98.042)

Appendix A

Appendix to the Parametric Study

This appendix provides further information on the approach to calculating the impact of parametric variations in chapter 3. Appendix A.1 documents the process of finding appropriate assumptions/formulas to calculate 'lost fuel' weights for the phases of take-off, climb, manoeuvre, descent and ground operation that find application in the parametric study. Appendix A.2 gives information on the approach to calculate efficiencies of the two reference aircraft from the *Base of Aircraft Data* (BADA) aircraft performance files (**Eurocontrol 2004a**). Detailed results of the parametric variations for all four cases are included as *Microsoft Excel* spreadsheets on a compact disc in Appendix D. Besides the data on fuel burn, the results contain information on the impact of snowballs on aircraft weight, wing area and drag.

A.1 Assumptions concerning 'Lost Fuel'

In chapter 3.1.1, an equation is introduced that allows to calculate the fuel weight required for a hypothetical cruising flight over **the entire mission range**, i.e. from take-off to touch-down. As the fuel burned is actually transporting payload over a range, this fuel can be regarded as 'useful' fuel (as efficiency of a vehicle can be defined as the product of payload and range divided by the energy consumed). According to the definition in **Torenbeek 1997**, all additionally consumed fuel is then 'lost fuel', as it is burned without increasing the aircraft's transport performance.

This is different to the definition of fuel weights found in other literature concerning preliminary aircraft design, e.g. in **Roskam 2002** and **Raymer 1992**. Here, cruise fuel weight is calculated with a similar equation to the one used in the parametric study, it however accounts for **only a part of the mission range**. Fuel weight for the phases take-off, climb and descent is then calculated from so-called mission mass/weight fractions, which are defined by the ratio of final to initial aircraft weight. For example, if the mission weight fraction is 0.90, ten percent of the initial aircraft weight is assumed fuel that is consumed during this phase of flight. The mission mass/weight fraction thus includes not only 'lost fuel', but also 'useful fuel', that is, the portion of the fuel fraction that accounts for the useful distance over ground. Table A.1 shows mission mass/weight fractions for different mission phases suggested by **Roskam 2002** and **Raymer 1992**.

Table A.1 Historical Mission Segment Weight Fractions from **Roskam 2002** and **Raymer 1992**

Phase	W_f/W_i	Source
Engine Start and Warm-up	0.990	**Roskam 2002,** p. 12, Table 2.1: Transport Jets
Taxi	0.990	Ibid.
Take-off	0.995	Ibid.
Climb	0.980	Ibid.
Descent	0.990	Ibid.
Landing Taxi, Shutdown	0.992	Ibid.
Warm-up and Take-off	0.970	**Raymer 1992,** p. 16, Table 3.2
Climb	0.985	Ibid.
Landing	0.995	Ibid.

In the following sections, assumptions in **Roskam 2002**, **Torenbeek 1997** and further literature concerning fuel weights for the different block segments (exclusive of the cruise segment) are compared. It is then tried to identify the method that best represents realistic fuel weights. This method is then adopted for the calculation of fuel weights in the parametric study.

A.1.1 Lost Fuel for Ground Operation

Ground operation includes engine start and warm-up, pre-flight taxi and landing taxi. Mission range is assumed being unaffected from ground operations. Thus, ground fuel is regarded as 100 % lost fuel. Ground fuel fractions are further not included in the computation of aircraft take-off weight. This has two reasons. First, fuel for pre-flight operation is consumed prior to take-off and can be neglected. Second, fuel for post-flight ground operation is typically taken from the reserves and is not accounted for separately (**Torenbeek 1997**).

Engine Start and Warm-Up, Pre-Flight Taxiing

Pre-take-off fuel weight, if calculated with the weight fractions give by **Roskam 2002**, would account for around 2.03 % of aircraft take-off weight. For an Airbus A320 with a typical take-off weight around 60 000 kg this calculates to around 1 218 kg of fuel. For a Boeing B777 ($W_{TO} \approx 200\,000$ kg), the same weight percentage gives 4060 kg of burned fuel. As these fuel amounts seem to be rather large (the design fuel weight for an A320 on a 5600 km range mission is only about 22 000 kg (**Jenkinson 2005**)), further investigation on typical taxi fuel loads was conducted. The results are:

- The ground handling operation manuals for the two aforementioned aircraft give much lower values. According to **Airbus 2007a**, standard taxi fuel, which is "a standard quantity of fuel to cover engine starts and ground manoeuvres until start of take-off", is 200 kg for the A320. This is only around 0.33 % of take-off weight. Similarly, standard taxi fuel for the B777 **Boeing 2007b** is 400 kg. This gives a weight fraction of only 0.2 % W_{TO}.
- The landing and take-off (LTO) cycle defined by the International Civil Aviation Organisation (ICAO) gives historical/statistical values for the time aircraft are taxiing. Fuel consumed for pre-flight ground operations can then be estimated using the ICAO engine emissions databank (**ICAO 2009a**). It gives a fuel flow of 0.296 $kg \cdot s^{-1}$ for the GE90-94B engine in idle, which is used on the B777-200ER. The all-up time for taxi/ground idle according to the LTO cycle is 26 min. Assuming that about half of this time is due to pre-flight operation, a B777-200ER with two running engines would then consume 230.88 kg of fuel. Using the same assumptions, an A320 equipped with two CFM56-5B2/2 turbofans would need 102.18 kg of fuel (0.131 $kg \cdot s^{-1}$). This results in a take-off weight fraction of 0.12 % for the B777 and a take-off weight fraction of 0.17 % for the A320.

From the information given above, it seems reasonable to assume a lower pre-take-off fuel weight fraction for a typical operation than suggested by **Roskam 2002**. The data given by **Boeing 2007b** and **Airbus 2007a** is somewhere in between the relatively small fuel amounts calculated from the ICAO LTO cycle and the large fuel amounts calculated from **Roskam 2002**. The shift from the lower values is in accordance with an extra allowance for engine start and warm-up. The weight fraction calculated for the A320 (0.33 %) is hence considered as being representative for short-haul narrow-body aircraft, the weight fraction calculated for the B777 (0.2 %) is considered as being representative for long-haul wide-body aircraft.

Post-Flight Ground Operations

After touch-down, the engines still consume fuel for taxiing the aircraft to the arrival gate. **Roskam 2002** assumes this fuel to account for 0.8 % of landing weight. For an Airbus A320-200, operational empty weight is 41,310 kg, design payload is 14 250 kg and design fuel weight is 17 940 kg (**Jenkinson 2005**). If we assume that around 5 % of design fuel weight is reserve fuel – i.e. not burned on the design mission –, the landing weight of the aircraft is around 56 457 kg. According to **Roskam 2002**, fuel for landing-taxi then calculates to 452 kg. Using the same assumptions, (design-) landing weight of a Boeing 777-200ER is 173 536 kg – with an operating empty weight of 138 120 kg, a design payload of 29 450 kg and a design fuel weight of 119 327 kg. Accordingly, landing taxi fuel weight is 1388 kg.

Similar to the calculations of pre-take-off fuel further above, the fuel weights calculated from **Roskam 2002** turn out to be rather large. Thus, in agreement with the considerations for pre-take-off fuel weight further above, a fuel weight of 0.33 % W_{TO} for narrow-bodies and of 0.2 % W_{TO} for wide-bodies will be applied for landing-taxi. This is admissible as taxi fuel flow (idle) for a given engine is independent of aircraft weight according to **ICAO 2009a**. Hence, assuming a similar taxi time, landing- and pre-flight-taxi fuel will be nearly identical.

A.1.2 Lost Fuel for Flight Operation

In flight, fuel flow in the segments of take-off, climb to cruise altitude, manoeuvre and descent is different to the fuel flow in cruise. These segments need to be either separated from the cruise flight (e.g. **Roskam 2002**, **Raymer 1992**) or further allowances need to be added to a fuel weight calculated from a cruise flight over the entire mission range (e.g. **Torenbeek 1997**). The following sections discuss fuel weights resulting from both methods. In general, the latter approach seems to suit our case of application better than the former. This is mainly due to Torenbeek's calculations of lost fuel being semi-empirical. They take account of major changes in the mission profile and aircraft efficiency and therefore agree with the basic idea of a parametric study. In comparison, the mission mass/weight fractions suggested by **Roskam 2002** and **Raymer 1992** are fully empirical. They are based on historical/statistical values and do not allow for future improvements.

Take-Off and Climb to Cruise Altitude

According to the weight fractions found in **Roskam 2002**, take-off and climb fuel accounts for around 2.49 % of aircraft take-off weight. This implies a constant factor, unchanging with aircraft efficiency.

To find out if a constant weight fraction as proposed by **Roskam 2002** provides a realistic fuel weight fraction, consumed fuel, time and covered distance of different aircraft during climb was calculated using the *BADA Calculation Tool* (**Eurocontrol 2005**). Results were produced for 23 aircraft climbing to 35 000 ft (10 668 m). The results are shown in Table A.2 and Table A.3.

Table A.2 Climb Fuel, Time and Distance covered of 10 Narrow-Body Aircraft (**Eurocontrol 2005)**

Aircraft	Ma_{cr}	W_{TO}	h_{cr}	**Climb Time**	**Distance Covered**	ΔW_F	$\Delta W_F/W_{TO}$
	[-]	[kg]	[ft]	[min]	[km]	[kg]	[%]
A319	0.78	60000	35 000	18.12	211.50	1389.30	2.32
A320	0.78	64000	35 000	21.82	264.65	1729.80	2.70
A321	0.78	72000	35 000	21.33	255.58	1931.90	2.68
B712	0.72	46000	35 000	17.03	183.72	1130.40	2.46
B733	0.76	52500	35 000	16.55	193.35	1353.00	2.58
B734	0.74	58000	35 000	17.42	197.79	1506.30	2.60
B735	0.74	52000	35 000	17.98	202.98	1367.40	2.63
B736	0.78	55000	35 000	13.88	153.72	1237.10	2.25
B737	0.78	60000	35 000	15.62	174.09	1406.60	2.34
B738	0.78	65300	35 000	17.98	205.02	1599.60	2.45
Mean				**17.77**	**204.24**		**2.50**

Table A.3 Climb Fuel, Time and Distance of 13 Wide-Body Aircraft (**Eurocontrol 2005)**

Aircraft	Ma_{cr}	W_{TO}	h_{cr}	**Climb Time**	**Distance Covered**	ΔW_F	$\Delta W_F/W_{TO}$
	[-]	[kg]	[ft]	[min]	[km]	[kg]	[%]
A306	0.79	140000	35 000	19.43	229.46	3251.10	2.32
A310	0.80	120000	35 000	13.48	160.38	2416.30	2.01
A332	0.82	190000	35 000	18.62	232.06	4024.50	2.12
A333	0.82	174000	35 000	18.42	228.54	3915.30	2.25
A343	0.80	210000	35 000	23.73	277.61	5231.40	2.49
B742	0.82	255800	35 000	16.03	201.31	6320.10	2.47
B743	0.84	310000	35 000	22.68	291.69	8100.40	2.61
B744	0.84	285700	35 000	14.37	185.01	5127.80	1.79
B762	0.78	140000	35 000	19.82	226.13	3074.10	2.20
B763	0.78	150000	35 000	17.23	197.42	3106.50	2.07
B764	0.78	158800	35 000	16.83	194.83	3113.80	1.96
B772	0.84	208700	35 000	17.95	215.57	4211.10	2.02
B773	0.84	237600	35 000	22.23	273.73	5691.10	2.40
Mean				**18.90**	**229.45**		**2.21**

The average weight fraction for climb fuel is 2.5 % of take-off weight for narrow-body aircraft (Table A.2). This is coherent with the weight fraction given by **Roskam 2002**, 2.49 %. The standard deviation from 2.5 % is 0.16 %. Hence, fuel burn for climb can be approximated using a constant factor of 2.5 % for 68.3 % of the aircraft with an error of ± 0.16 % and for 95.4 % of the aircraft with an error of ± 0.32 %. Bearing in mind that the fuel consumption for climb is only a small fraction of the over-all block fuel, considering the average fuel fraction to be 2.5 % of take-off weight seems to be a reasonable approach for current narrow-body aircraft.

For long-haul wide body aircraft (Table A.3), cruise fuel weight is even more dominant, and most likely, small errors in calculations of climb fuel will not dramatically falsify the calculations of the over-all fuel weight. However, the average fuel weight fraction for climb is

less than suggested by **Roskam 2002** and should hence be used. For the aircraft listed above, the standard deviation from 2.21 % is 0.24 %.

Nevertheless, it is important to realize that **constant weight fractions can only produce realistic climb fuel weights as long as aircraft efficiency parameters do not differ largely from the reference aircraft**. When considering profound technology changes – as for example a change to liquid hydrogen (LH_2) as aviation fuel – a calculation should be used that allows for these changes. From **Torenbeek 1997** we can derive an alternative method that takes into account at least some of the influencing factors. For this approach, lost fuel for lifting the aircraft to cruise altitude and accelerating it to cruise speed is calculated from an energy balance,

$$\Delta W_F \eta_{Climb} \frac{H}{g} = W_{TO} \left(h_{Cr} + \frac{v_{Cr}^2}{2g} \right) \quad , \tag{A.1}$$

where ΔW_F is the fuel consumed, η_{Climb} the average engine efficiency for climb, h_{Cr} the initial cruise altitude and v_{Cr} the initial cruise speed. Using above formula, **Greener By Design 2003** obtained a take-off weight fraction of 1.52 % for a kerosene-powered aircraft (H typically 43 $MJ \cdot kg^{-1}$) lifted to 35 000 ft (10 668 m) and accelerated to Mach 0.85. Unfortunately, as engine efficiency is a function of flight speed and altitude, η_{Climb} is not easily calculated and Eq.(A.1) is unpractical to use. Hence, for the parametric study at hand, a mixture of the two aforementioned approaches – a constant weight fraction and the calculation from an energy balance – will be used. For this purpose, the average climb efficiency that results from the weight fraction calculated by **Greener By Design 2003** is considered as being representative of current aircraft ($\eta_{Climb} = 21$ %). It is assumed further, that engine efficiency for climb is directly related to engine efficiency in cruise: if cruise efficiency is changed, climb efficiency will be changed proportionally. Eq.(A.1) can then be rewritten to give climb fuel as

$$\Delta W_F = W_{TO} \frac{\left(h_{Cr} + \frac{v_{Cr}^2}{2g} \right)}{0.21 \left(\frac{\eta_{Cr,New}}{\eta_{Cr,Ref}} \right) (H/g)} \quad , \tag{A.2}$$

where the index *New* denotes for the new aircraft and the index *Ref* for the reference aircraft.

At first sight, the weight fractions calculated by **Greener By Design 2003** seem small in comparison to the weight fractions resulting from **Roskam 2002** and **Eurocontrol 2005**. It is important however to note the difference. **Roskam 2002** and **Eurocontrol 2005** imply that a certain range is covered during the climb. When calculating cruise fuel, this range has to be taken off the mission range. Contrary, Torenbeek's lost fuel is accounting only for the extra energy needed from lifting and accelerating the aircraft: no range is covered. Thus, when

calculating cruise fuel, the over-all mission range is used. To generate more comparable weight fractions, cruise fuel over the climb distance needs to be added to the fuel calculated from the simple energy balance. For exemplarily reason, this has been done for the same set of aircraft listed above. Cruise performance parameters for the aircraft were taken from **Eurocontrol 2004a**. Results are shown below in Table A.4 and Table A.5.

Table A.4 Climb Fuel Weight Fractions calculated from Eq.(A.2) for 10 Narrow-Body Aircraft

Aircraft	Ma_{cr}	h_{cr}	$\Delta W_F/W_{TO}$ **Lost Fuel Eq.(A.2)**	**Distance Covered**	$\Delta W_F/W_{TO}$ **Distance Eq.(3.1)**	$\Delta W_F/W_{TO}$ **Total**	$\Delta W_F/W_{TO}$ **Eurocontrol 2005**
	[-]	[ft]	[%]	[km]	[%]	[%]	[%]
A319	0.78	35 000	1.45	211.50	0.95	2.40	2.32
A320	0.78	35 000	1.45	264.65	1.16	2.61	2.70
A321	0.78	35 000	1.45	255.58	1.20	2.65	2.68
B712	0.72	35 000	1.41	183.72	0.94	2.36	2.46
B733	0.76	35 000	1.44	193.35	1.05	2.49	2.58
B734	0.74	35 000	1.43	197.79	1.05	2.48	2.60
B735	0.74	35 000	1.43	202.98	1.22	2.65	2.63
B736	0.78	35 000	1.45	153.72	0.78	2.23	2.25
B737	0.78	35 000	1.45	174.09	0.82	2.27	2.34
B738	0.78	35 000	1.45	205.02	0.95	2.41	2.45
Mean				**204.24**		**2.46**	**2.50**

Table A.5 Climb Fuel Weight Fractions calculated from Eq.(A.2) for 13 Wide-Body Aircraft

Aircraft	Ma_{cr}	h_{cr}	$\Delta W_F/W_{TO}$ **Lost Fuel Eq.(A.2)**	**Distance Covered**	$\Delta W_F/W_{TO}$ **Distance Eq.(3.1)**	$\Delta W_F/W_{TO}$ **Total**	$\Delta W_F/W_{TO}$ **Eurocontrol 2005**
	[-]	[ft]	[%]	[km]	[%]	[%]	[%]
A306	0.79	35 000	1.46	229.46	0.92	2.38	2.32
A310	0.80	35 000	1.47	160.38	0.66	2.13	2.01
A332	0.82	35 000	1.49	232.06	0.77	2.25	2.12
A333	0.82	35 000	1.49	228.54	0.80	2.28	2.25
A343	0.80	35 000	1.47	277.61	0.96	2.43	2.49
B742	0.82	35 000	1.49	201.31	0.92	2.41	2.47
B743	0.84	35 000	1.50	291.69	1.16	2.66	2.61
B744	0.84	35 000	1.50	185.01	0.75	2.25	1.79
B762	0.78	35 000	1.45	226.13	0.94	2.39	2.20
B763	0.78	35 000	1.45	197.42	0.75	2.20	2.07
B764	0.78	35 000	1.45	194.83	0.75	2.20	1.96
B772	0.84	35 000	1.50	215.57	0.74	2.24	2.02
B773	0.84	35 000	1.50	273.73	0.94	2.44	2.40
Mean				**229.45**		**2.33**	**2.21**

As can be seen above, the take-off weight fractions calculated from Eq.(A.2) seem to match the much more detailed computations from the BADA Calculation Tool (**Eurocontrol 2005**) with only small deviations. It can be observed that the standard deviation for the narrow-bodied aircraft is noticeably less (0.08 %) than for the wide-bodied aircraft (0.19 %). For both type of aircraft however, the standard deviation is less than calculating with a simple constant factor. Further, as Eq.(A.2) is semi-empirical, it adopts the lost fuel weight fraction to changes

in engine efficiency and fuel heat content. Torenbeek's approach is thus more suitable for a parametric study and is adopted for the thesis at hand.

En-Route Manoeuvring

Roskam 2002 and **Raymer 1992** do not include allowances for the extra energy needed when performing typical mission manoeuvres. To account for the additional fuel burn, a semi-empirical formula from **Torenbeek 1997** will be adopted:

$$\Delta W_F = W_{TO} \frac{0.0025}{\eta_{Cr}} \quad , \tag{A.3}$$

where η_{Cr} is the over-all engine efficiency for cruise. For modern turbofans with cruise efficiencies around 35 to 40 %, the additional fuel for manoeuvring is then around 0.71 to 0.63 % W_{TO}. Again, the formula allows for a re-calculation of the fuel weight fraction with changing engine efficiency.

Descent

Similar to take-off and climb, **Roskam 2002** gives fuel weight for descent as a ratio of initial to final weight. From Table A.1 we get for transport aircraft

$$\frac{W_{Landing}}{W_{Cr,f}} = 0.990 \quad , \tag{A.4}$$

where $W_{cr,f}$ is the aircraft weight at the end of a cruise flight. Again, Roskam's weight ratio assumes a range that is covered during the segment. In comparison, **Torenbeek 1997** and **Greener By Design 2003** assume that the fuel consumed during descent, approach and landing is equal to the fuel used during a cruising flight over the same distance. If we presume that the distance covered during descent is approximately equal to the distance covered during climb (see Table A.5), this approach results in weight fractions that are consistent with the weight fraction given by **Roskam 2002** above: see Table A.6.

With respect to economic and ecological aspects, a late descent with the engines running in idle would be most favourable. According to the *Flight Crew Operating Manual* (given in **Scheiderer 2008**) an A320 (weight at top of descent = 45 000 kg) descending from 35 000 ft (10 668 m) to 1500 ft (457 m) would then consume only 134 kg of fuel. This is a weight

fraction W_f/W_i of only 0.997. For final landing, thrust is increased, so that the over-all fuel fraction from the *top of descent* until touchdown will be slightly higher.

Table A.6 Descent Fuel Weight Fractions calculated from **Roskam 2002** and **Torenbeek 1997**

Aircraft	Ma_{cr}	h_{cr}	**Distance Covered**	W_f/W_i **Assumed Cruise Flight over Descent Distance (Torenbeek 1997)**	$\Delta W_F/W_{TO}$ **Fixed Fuel Fraction (Roskam 2002)**
	[-]	[ft]	[km]	[%]	[%]
A319	0.78	35 000	211.50	0.9904	0.990
A320	0.78	35 000	264.65	0.9882	0.990
A321	0.78	35 000	255.58	0.9878	0.990
B717-200	0.72	35 000	183.72	0.9905	0.990
B733	0.76	35 000	193.35	0.9893	0.990
B734	0.74	35 000	197.79	0.9894	0.990
B735	0.74	35 000	202.98	0.9876	0.990
B736	0.78	35 000	153.72	0.9921	0.990
B737	0.78	35 000	174.09	0.9917	0.990
B738	0.78	35 000	205.02	0.9904	0.990
Mean			**204.24**		**2.50**

In the real world however, due to high dense air traffic and ATC regulations, this procedure is rare. Often, pilots get the order to start descending long before the optimum point (top of descent) is reached (**Scheiderer 2008**). In consequence, the engines need to produce thrust while descending and the fuel consumption is higher. Busy airports may also have *Standard Terminal Arrivals* (STARs), where the aircraft are guided verbally to a specified holding stack. This holding stack is normally at an altitude of 6000 to 7000 ft (1882 to 2134 m). Depending on the traffic density, additional fuel is consumed while loitering. The final approach is then realized by "stair stepping down" in altitude (**Anders 2007**). Normally, the aircraft gets clearance to descend to an altitude of typically 3000 ft (914.4 m) (**CAA 2009**). The aircraft would then fly level for several miles before starting the final approach (see Fig. A.1). These level flights, especially when flaps and landing gear are deployed, may increase safety (by vertical separation) but burn considerably more fuel than a continuous descent in idle. A "real world aircraft" will therefore show a fuel weight for descent, approach and landing that is somewhere in between the values calculated from **Torenbeek 1997** or **Roskam 2002** and the idle descent given in aircraft operating manuals.

As no additional allowances are made for final loitering and approaching phases, assuming a cruising flight over the same distance (as proposed by **Torenbeek 1997** and exemplarily calculated for Table A.6 seems tolerable for current aircraft and ATC regulations and will be adopted for the parametric calculations. Nevertheless, one should bear in mind that regulation authorities, research institutions and industry are permanently working on improving the air traffic system and on-board equipment. Some airports have already implemented continuous descent approaches (**Anders 2007**). According to the long-term strategy of **Eurocontrol 2008**, continuous descent approaches should be implemented for most European terminal

areas in the year 2020. This may then allow shifting the weight fraction for descent closer to optimum (descent with engines in idle).

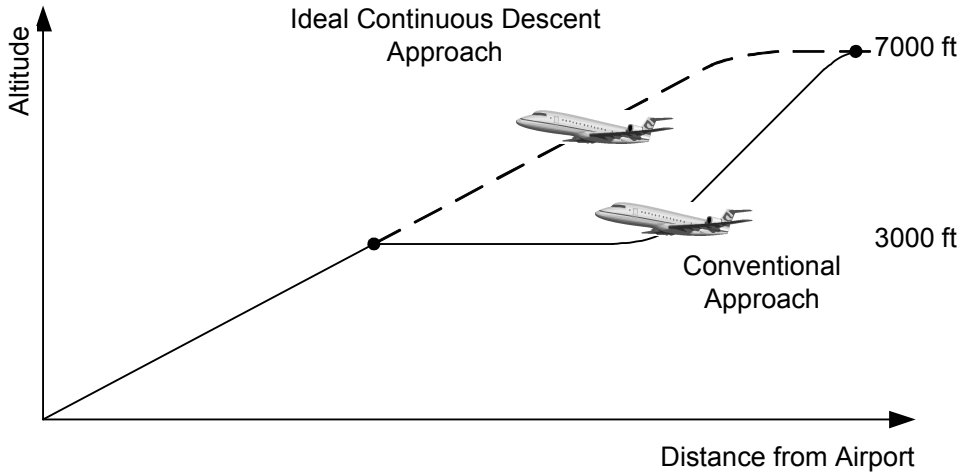

Fig. A.1 Ideal Continuous Descent Approach/Conventional Approach Schematic

A.2 BADA Aircraft Files

It was decided to use real existing aircraft as reference aircraft for the parametric study to increase the informative value. Information on the performance of many existing aircraft can be conducted from the *Eurocontrol Base of Aircraft Data* (BADA) aircraft performance database. The data are given in the form of ASCII files that contain coefficients from which the pre-discussed efficiency parameters can be calculated. For each aircraft, BADA includes three ASCII files:

- *.apf-files: These files contain airline procedure parameters such as standard climb speeds and cruise Mach numbers.
- *.opf-files: These files contain operations performance parameters such as the design weights, parameters on the drag polar and the thrust specific fuel consumption.
- *.ptf-files: These files contain data on the fuel flow calculated from the *.apf- and *.opf-files. However, the fuel flow is only a "snapshot" (given in $kg \cdot s^{-1}$) for three constant standard weights at different altitudes.

For the purpose of the parametric analysis, nearly all necessary data are given in the *Operational Performance Files* (*.opf). The cruise Mach number is the only parameter not found herein and will be taken from the *Airline Procedure File* (*.apf). For demonstration, the *.opf-file for the Airbus A320-212 (Option 2) aircraft is shown in Fig. A.2.

```
CCCCCCCCCCCCCCCCCCCCCCCCCCCCCCCCCCCCCCCCCCCCCCC A320__.OPF CCCCCCCCCCCCCC/
CC                                                                          /
CC                AIRCRAFT PERFORMANCE OPERATIONAL FILE                     /
CC                                                                          /
CC                                                                          /
CC      File_name: A320__.OPF                                               /
CC                                                                          /
CC      Creation_date: Apr 30 2002                                          /
CC                                                                          /
CC      Modification_date: May 14 2004                                      /
CC                                                                          /
CD                                                                          /
CC====== Actype ============================================================/
CD   A320__          2 engines    Jet                          M            /
CC   Airbus A320-212 with CFM56_5_A3 engines                 wake           /
CC                                                                          /
CC====== Mass (t) ==========================================================/
CC    reference      minimum      maximum     max payload  mass grad  /
CD     .64000E+02   .39000E+02   .77000E+02   .21500E+02   .28000E+00 /
CC====== Flight envelope ===================================================/
CC     VMO(KCAS)       MMO         Max.Alt       Hmax        temp grad  /
CD     .35000E+03   .82000E+00   .39000E+05   .34354E+05  -.13000E+03 /
CC====== Aerodynamics ======================================================/
CC Wing Area and Buffet coefficients (SIM)                                  /
CCndrst Surf(m2)     Clbo(M=0)       k           CM16                       /
CD 5   .12260E+03   .10400E+01   .22700E+00   .00000E+00                   /
CC   Configuration characteristics                                          /
CC n Phase  Name    Vstall(KCAS)    CD0          CD2         unused     /
CD 1 CR   Clean     .14500E+03   .24000E-01   .37500E-01   .00000E+00 /
CD 2 IC   1         .12000E+03   .24200E-01   .46900E-01   .00000E+00 /
CD 3 TO   1+F       .11400E+03   .39300E-01   .39600E-01   .00000E+00 /
CD 4 AP   2         .10700E+03   .45600E-01   .38100E-01   .00000E+00 /
CD 5 LD   FULL      .10100E+03   .83800E-01   .37100E-01   .00000E+00 /
CC   Spoiler                                                               /
CD 1      RET                                                              /
CD 2      EXT                               .00000E+00   .00000E+00 /
CC   Gear                                                                  /
CD 1      UP                                                               /
CD 2      DOWN                  .31200E-01   .00000E+00   .00000E+00 /
CC   Brakes                                                                /
CD 1      OFF                                                              /
CD 2      ON                                .00000E+00   .00000E+00 /
CC====== Engine Thrust =====================================================/
CC         Max climb thrust coefficients (SIM)                              /
CD     .13605E+06   .52238E+05   .26637E-10   .10290E+02   .58453E-02 /
CC      Desc(low)    Desc(high)   Desc level   Desc(app)    Desc(ld)  /
CD     .94370E-02   .31014E-01   .15000E+05   .13000E+00   .34000E+00 /
CC      Desc CAS     Desc Mach    unused       unused       unused    /
CD     .31000E+03   .78000E+00   .00000E+00   .00000E+00   .00000E+00 /
CC====== Fuel Consumption ==================================================/
CC   Thrust Specific Fuel Consumption Coefficients                          /
CD     .94000E+00   .10000E+06                                             /
CC   Descent Fuel Flow Coefficients                                        /
CD     .88900E+01   .81926E+05                                             /
CC   Cruise Corr.    unused       unused       unused       unused    /
CD     .10600E+01   .00000E+00   .00000E+00   .00000E+00   .00000E+00 /
CC====== Ground ============================================================/
CC        TOL          LDL         span         length       unused    /
CD     .21900E+04   .14400E+04   .34100E+02   .37570E+02   .00000E+00 /
CC=========================================================================/
FI                                                                          /
```

Fig. A.2 Operational Performance File (*.opf) for the A320 (**Eurocontrol 2004a**)

For the calculation of the efficiency parameters of the reference aircraft, the following parameters are imported from the *.opf-files (underlined values of Fig. A.2):

- Maximum mass, i.e. maximum take-off weight W_{MTO}, here 77 t (77000 kg)
- Wing surface area S, here 122.6 m^2
- Zero-lift drag coefficient C_{D0} for the clean (cruise) configuration, here 0.024

- C_{D2} for the clean (cruise) configuration, which is generally known as the *k*-factor and accounts for the increase in drag due to lift, i.e.

$$C_{D2} = k = \frac{S}{\pi \cdot b^2 e} \quad \text{, here 0.0375.} \tag{A.4}$$

- The thrust specific fuel consumption for zero flight speed C_{f1}, here 0.94 kg·min^{-1}·kN^{-1}
- A fuel flow factor to account for the *TSFC* being dependent on flight speed C_{f2}, here 100 000 knots (51444 m/s) and
- A cruise fuel flow factor $C_{f,Cr}$, which is a correction factor for the thrust specific fuel consumption in cruise, here 1.06.

For a given cruise altitude, atmospheric parameters can be conducted from the ICAO standard atmosphere (e.g. **Cavcar 2009**). The aerodynamic efficiency of the reference aircraft at the beginning of the cruise flight is then calculated from

$$C_{L,i} = \frac{2W_{Cr,i}}{\rho_{Cr} Ma_{Cr} a_{Cr} S} \quad , \tag{A.5}$$

$$C_{D,i} = C_{D0} + C_{D2} C_{L,i}^2 \quad , \tag{A.6}$$

$$\left(L/D\right)_i = \frac{C_{L,i}}{C_{D,i}} \quad , \tag{A.7}$$

where ρ_{Cr} is the density of the air at the cruising altitude. $W_{Cr,i}$ is calculated by subtracting the lost fuel for lifting and accelerating the aircraft from the take-off weight. The Oswald factor can be calculated from Eq.(A.5). The thrust specific fuel consumption in cruise is calculated in accordance with BADA's user manual **Eurocontrol 2004b** from

$$TSFC_{Cr} = \frac{C_{f1} \cdot \left(1 + \frac{Ma_{Cr} a_{Cr}}{C_{f2}}\right) C_{f,Cr}}{60\,000} \quad , \tag{A.8}$$

where the unit of *TSFC* is converted from kg·min^{-1}·kN^{-1} to kg·s^{-1}·N^{-1} concomitantly. Over-all engine efficiency is then given by

$$\eta_{Cr} = \frac{Ma_{Cr} a_{Cr}}{TSFC_{Cr} H} \quad , \tag{A.9}$$

where *H* is the calorific value of the fuel, taken as 43 MJ·kg^{-1} for kerosene.

Appendix B

Appendix to the Technology Survey

This appendix provides summarized information on CO_2 reducing technologies that were introduced in chapter 4. The technologies are grouped in tables according to their respective research discipline and field of interest, e.g. *Aerodynamics – Reducing Skin Friction Drag*, in the appendices B 1 to B.4.

In addition to the information given in chapter 4, the following tables give information about major limitations, trade-offs and challenges associated with the technologies, the expected timeframe they could be available for commercial series production and their potential of reducing CO_2 emissions. The definitions of table entries for the categories 'Availability' and 'Potential CO_2 Red.' are shown in Table B.1. Entries for both reflect trends found from estimates in literature. Nevertheless, **given ranges are not claimed definite**.

Many of the listed technologies were found through a technology survey for IATA's *Technology Roadmap* Project. The survey was conducted by participation of the German Aerospace Centre (DLR) Hamburg from summer 2008 to spring 2009. Participants from industry and academia collected the information in close cooperation. The results of the survey were published in May 2009 and can be found in the *Technical Annex* to the *Technology Roadmap Report* (3rd ed.), see **IATA 2009a**.

Table B.1 Definition of Table Entries concerning Availability and CO2 Reduction Potential of Technologies

Category	Entry	Description
Availability[1]	Current	Available today
	Short	Could become available between 2010-2015
	Medium	Could become available between 2016-2025
	Long	Could become available past 2025
	Continuous	Continuous improvement process from small scale to large scale application
	Unknown	Unknown
Potential CO2 Red.[2]	Negative	Negative Impact
	Low	< 5 %
	Medium	5 to 10 %
	High	> 10 %
	All ranges	All ranges (low to high) possible
	Unknown	Unknown

[1] Applies to the earliest date a series production is **technologically feasible**, if development is fostered by airlines and authorities. Does **not include** an assessment about the **economic feasibility**. Concerning **bio-fuels**: does **not include** an assessment about the **feasibility of finding appropriate feedstock**.

[2] Applies to expected potential reduction in CO_2 emissions per seat-km compared to current state of the art in-production aircraft.

B 1. Aerodynamics: Technologies

Table B.2 Aerodynamics – Reducing Skin Friction Drag

Technology	Description	Limitations/Trade-Offs/Challenges	Availability	Potential CO_2 Red.	Reference
... by smoothing outer surfaces				**Low**	
New Manufacturing Methods and Composite Materials for current designs	Rivet free joining methods decrease no. of roughness elements	Depending on specific manufacturing method or material	Current, Continuous	Low to Medium	-
Drag Reduction Coatings	Nanotech, lotus, films, liquid coatings etc.; Different possible approaches: 1. Smoothing the surface 2. Keeping the airframe clean	Eventually expensive + time-consuming with low benefit	Current	Low	**Wallace 1998**
… by disrupting span-wise cyclic Flows				**Medium to High**	
Riblets (Passive)	Force cyclic flows to follow stream-wise "ridges and valleys"	Surface contamination	Medium	Medium	**Houghton 2003 IATA 2008a Lockerby 2008**
Dimples (Passive)	Randomized surface roughness elements	Need to be further investigated	Medium	Medium	**Lockerby 2008**
Helmholtz Resonators(Passive)	Resonators create span-wise oscillating micro-jets	Need to be further investigated (eventually contamination)	Medium	Medium to High	**Lockerby 2008**
Controllable Active Skin	Create travelling surface waves that induce span-wise vorticity	Controlling is complex, system weight and power input	Medium to Long	Medium	**Lockerby 2008 Mani 2008**
… by maintaining laminar Flow				**High**	
Natural Laminar Flow (NLF)	Shaping the airfoil: airflow is only gently accelerating over the front part of the wing surfaces; drag reduction on wing, tail, nacelles	Long chord (high Reynolds numbers), high speed + high sweep; not applicable to current larger than regional aircraft, surface contamination	Medium	High	**Greener By Design 2003, 2005 Houghton 2003 IATA 2008a**
Hybrid Laminar Flow (HLF)	Active suction or blowing to re-energize boundary layer; drag reduction on wing, tail, nacelles	Long chord (high Reynolds numbers); unresolved problems on system side: increase in weight, power required, maintenance time; surface contamination	Medium to Long	High	**Greener By Design 2003, 2005 Houghton 2003 IATA 2008a**
Forward-Swept Wing	Allows for greater applicability of laminar flow as wing sweep is reduced	Stability	Medium	High	**Streit 2008**
Gapless/Seamless High-Lift Devices	Allow for greater applicability of laminar flow as early transition is avoided	Need to be further investigated	Medium	High	**Courty 2008 Carbone 2008**

Table B.2 Aerodynamics – Reducing Skin Friction Drag (cont'd)

Technology	Description	Limitations/Trade-Offs/Challenges	Availability	Potential CO_2 Red.	Reference
… by reducing the relative wetted Area				**High**	
Reducing Fin and Horizontal Tail Areas	Improved aerodynamics allow for smaller surfaces; current research on laminar flow or double-hinged control concepts (NACRE Project); Active Stability (see Table A.3); V-Tail aircraft (NEFA Project)	Depending on specific technology	Medium	Medium	**Courty 2008 Kruse 2008 University of Greenwich 2008**
Blended Wing-Body (BWB)	merge the wings with the fuselage and thereby eliminate non-lifting fuselage and tail surfaces	Problems concerning passenger transports (e.g. a pressurized cabin, emergency evacuation, etc.)	Long	High	**Greener By Design 2003**, 2005 **IATA 2008a**

Table B.3 Aerodynamics – Reducing Form Drag

Technology	Description	Limitations/Trade-Offs/Challenges	Availability	Potential CO_2 Red.	Reference
… by Streamlining				**Low**	
Avoiding Fuselage Tail Base Areas	Avoiding early flow separation	APU Integration, landing ground clearance	Current	Low	**Roskam 1997**
Blended Wing Body (BWB)	Improved aerodynamic shape without limiting passenger comfort	Problems concerning passenger transports (e.g. a pressurized cabin, emergency evacuation, etc.)	Long	Low to Medium	**Greener By Design 2003**, 2005 **IATA 2008a**
… by avoiding Flow Separation on small Disturbances				**Low**	
Detail Design	Reducing Protuberances such as antennas, access panels, windshield wipers, NACA inlets, gaps etc.	Depending on specific Technology (e.g. Gapless High-lift Devices)	Current, Continuous	Low	**Roskam 1997**
… by active or passive Separation Control				**Low**	
Passive Systems	Constant generation of stream wise vortices through fixed devices; e.g. wing fence, vortex generators, leading-edge strake	Use on commercial aircraft mostly unnecessary; increase drag when not in use	Current	Negative	**Houghton 2003**
Active Systems	Active suction or blowing to remove 'tired parts' of boundary layer	increase in system weight, power required, maintenance time; surface contamination; regarded having minor importance to HLF	Unknown	Low	**Houghton 2003**
Boundary Layer Ingesting Engine Inlet (BLI)	engines use their inlets to ingest the boundary layer; mainly for BWB aircraft	Probably unattractive for current aircraft design; risk of engine efficiency decrease due to low-energy air inflow	Long	Medium	**Daggett 2003b IATA 2008a**

Table B.4 Aerodynamics – Reducing Induced Drag

Technology	Description	Limitations/Trade-Offs/Challenges	Availability	Potential CO_2 Red.	Reference
… by Using Wing-Tip Devices				**Low to Medium**	
Traditional Devices (Winglet, Wingtip Fence, Raked Wingtip)	Reduce strength of wingtip vortices	Wing-root bending moment	Current	Low	**Houghton 2003 Faye 2001**
Spiroid Wingtip	Spiraling and reattaching (to wing surface) wingtip device. Further decreasing wing induced drag	Wing root bending moment	Medium	Medium	**Gratzer 1992 Ostrower 2008**
Multiple (active) Winglets	Split the single tip vortex into multiple lower strength vortices, Rigid system known as 'wing-grid', active system is 'mission-adaptive'	Wing root bending moment; complex system; need to show benefit on large aircraft	Long	Medium	**Shelton 2006**
... by Reducing Trim-Drag				**Low**	
Rearward centre of gravity (Passive)	Reduces trim force needed from the horizontal stabilizer; moving heavy equipment to back of aircraft, manage passenger seating configuration, etc.	Stability	Current	Low	**Viscotchi 2006 Roskam 1997**
Active Stability	Reduces trim force needed from the horizontal stabilizer by pumping fuel into special trim tanks in the aft of the aircraft	Complex system needed, considerable benefit only on long-haul flights	Current	Low	**Airbus 2004 Greener By Design 2003**
… by Increasing the Wing Span (the Aspect Ratio)				**High**	
New high-strength, light-weight materials	Could allow for an increase in wing span without weight penalties	Depending on specific material	Current, Continuous	All ranges	**Greener By Design 2005**
Use of turbulent boundary layer control	Could allow for thicker wing profiles and lower wing bending moments	Depending on system	Depending on system	Unknown	**Greener By Design 2005**
Reduction of the cruise Mach number	Could allow for thicker wing profiles (lower wave drag) and lower wing bending moments	Risk of reduced aircraft utilization, customer acceptance	Current	Unknown	**Greener By Design 2005**
Folding wing tips	Could allow for optimum wing design on very large aircraft (wing span >80 m)	Risk of increase in wing weight due to system weight; only attractive for large aircraft	Current	Low	**Greener By Design 2005 IATA 2008a**
Strut- or Truss-Braced Wing (TBW) Designs	Support the wing with a truss or a strut and thereby reduce the wing root bending moment	Risk of exceeding 80 m wing span airport restriction	Long	High	**Grasmeyer 1998 IATA 2008a**
Joined- or Box-Wing Designs	A second, forward swept wing joins the main wing either in the middle (joined-wing) or at the tips (box-wing), thereby reducing the wing root bending moment	Large unknowns concerning aerodynamics, manufacturing methods and direct operating costs (DOCs)	Long	High	**Mello 2006 Kroo 2006 Bauhaus Luftfahrt 2008**

Table B.5 Aerodynamics – Reducing Interference Drag

Technology	Description	Limitations/Trade-Offs/Challenges	Availability	Potential CO_2 Red.	Reference
Finding an appropriate geometric layout of all airplane components	Reduce early flow separation and the departure from optimum wing design	Unknown	Current, Continuous	All Ranges	**Roskam 1997**
Well designed fairings and fillets	Reduce early flow separation	Unknown	Current, Continuous	Low to Medium	**Roskam 1997**
Buried engines	Bury the engines in the airframe, thereby reduce nacelle drag and interference drag; mainly for BWB aircraft, supports BLI technology	Probably unattractive for current aircraft design; risk of engine efficiency decrease; disadvantages for maintenance, exchangeability and protection against engine burst	Long	Unknown	**Greener By Design 2005 IATA 2008a**
Distributed multi-fan propulsion	Many small propulsion systems (e.g. multiple fans) instead of a few large ones: reduce interference with wing and fuselage, can potentially be buried and used with BLI technology	To date no specific implementation known; Several integration issues (e.g. transmission weight and possible additional drag)	Long	Medium	**IATA 2008a GAO 2009**

Table B.6 Aerodynamic s – Reducing Wave Drag

Technology	Description	Limitations/Trade-Offs/Challenges	Availability	Potential CO_2 Red.	Reference
Supercritical wing designs	Specifically tailored airfoils to keep shock waves at minimum strength	Trade-offs with other drag forms, e.g. laminar flow designs (require different airfoils)	Current, Continuous	Low	**Houghton 2003**
Increased wing sweep	Reduce the effective Mach number of the airflow advancing the wing	Trade-offs with other drag forms, e.g. laminar flow designs (require a low wing sweep); engine integration problematic	Current	Low	**Houghton 2003**
Active or passive boundary layer control	Spread the shock into multiple shocks of lower strength, e.g. by active or passive bumps, suction or blowing	Risk of weight penalty; system power input and control need to be further investigated	Unknown	Low	**Greener By Design 2005 Houghton 2003**

Table B.7 Aerodynamics – Reducing Off-Design Flying Time

Technology	Description	Limitations/Trade-Offs/Challenges	Availability	Potential CO_2 Red.	Reference
Mission-Adaptive Wing (MAW)	Allows the wing to change its section airfoil shapes during flight and thus to be continuously tailored to each flight segment;	Multiple steps needed from current designs to a fully morphing wing; large unknowns concerning smart materials and control;	Short (A350, B787), Continuous	All ranges	**Greener By Design 2005 IATA 2008a**

B 2. Aircraft Engines and Secondary Power: Technologies

Table B.8 Aircraft Engines and Secondary Power – Increasing Thermal Efficiency

Technology	Description	Limitations/Trade-Offs/Challenges	Availability	Potential CO_2 Red.	Reference
… by Increasing Turbine Entry Temperature (TET)				**Medium**	
Advanced Ni-based super-alloys	Alternative materials to conventional Ni-alloys for turbine elements with moderate increase in heat resistance	Unknown	Short	Low	**Japan NIMS 2009.**
Ceramic Matrix Composites (CMCs)	Alternative materials to conventional Ni-alloys for turbine elements with large increase in heat resistance	Unknown	Short	Medium	**Gmelin 2008 IATA 2008a Smarsly 2006**
New Coating Materials for Thermal Barrier Coating (TBC)	Provides life-extension and protection to heat-resistant engine elements beyond their melting temperature range; new materials include CMC and Niobium-Silicon	Current technology not being considered fully monitorable and reliable, thus not fully exploitable	Conventional TBC: Current; New Materials: Continuous	Low to Medium	**IATA 2008a Smarsly 2006**
Cooled Cooling Air for Turbine Blades	Lower the temperature of the cooling air by guiding it along the secondary (fan) flow; increase in heat resistance of turbine material	Increased Levels of thermal stress expected in HP turbine blades and the heat exchanger; risk of pressure losses in the secondary flow	Medium	Medium	**Gmelin 2008 Bock 2007**
Low NO_x Combustor Technology, Lean-Burn Combustors	Allow for constant or reduced NO_x emission with increasing TET; include the TAPS, TALON X and RQL Technology	Trade-off in further increasing TET and strongly reducing NO_x; Combustor efficiencies are already very high and difficult to improve	1st Gen: Current 2nd and 3rd Gen.: Medium	Medium to High	**Dodds 2005 Donoghue 2006 IATA 2008a**
... by Increasing Over-all Pressure Ratios (OPR)				**Medium**	
Titanium Metal Matrix Composites (MMCs)	Alternative materials to titanium for compressor elements with higher heat capability	High production costs; unknowns in structural mechanics and quality testing methods	Short	Medium	**IATA 2008a Smarsly 2006**
Active Clearance Control (ACC)	Actively control clearance between the compressor rotor blades and the casing	Accurate sensors for measuring tip clearance need to be developed; final controlling yet to be solved	Medium	Medium	**Bock 2007 NEWAC 2009**
Active Surge Control (ASC)	Suppressing flow instabilities, thereby increasing core efficiency at low mass flow rates	Control and application of the system and the calculation of aerodynamic stability is complex	Medium	Medium	**Bock 2007 NEWAC 2009**
Cooled Cooling Air on HPC Rear Cone	Reduces material temperatures, thereby allowing for a change in material or thickness (the rear cone of the HPC is un-cooled on current engines)	Benefits are unclear; risk of pressure losses in the secondary flow	Medium	Unknown	**Bock 2007**

Table B.8 Aircraft Engines and Secondary Power – Increasing Thermal Efficiency (cont'd)

Technology	Description	Limitations/Trade-Offs/Challenges	Availability	Potential CO_2 Red.	Reference
… by Minimizing Pressure Losses				**Medium**	
Increased heat resistance of the turbine material	Allows for reduction of bleed air from the compressor if TET held constant	Trade-off with possibility to increase TET with higher heat resistance	Depending on enabling technology	Low to Medium	-
Active Cooled Cooling Air	Control amount of cooling (bleed) air from the HP compressor, thereby reduce unnecessary pressure losses	Unknowns concerning the reliability of the system	Medium	Medium	**Bock 2007**
More Electric Airplane (MEA) Architecture / No-Bleed Engine	No bleed air taken from the engines for hydraulic / pneumatic aircraft systems, eliminate pressure losses behind the LP compressor	Trade-off with an increase in electric power requirement	Short	Low to Medium	**Daggett 2003a Gmelin 2008 Sinnett 2007**
... by Inter-Cooling and Recuperation				**High**	
Inter-cooled aero engine	Inter-cooling the air exiting the LP compressor, thereby reducing energy needed from the HP compressor	Risk of pressure losses in the secondary flow; complex; high benefits only in combination with heat recuperation from the exhaust gases (see below)	Long	Low (without recuperator)	**Boggia 2004 Gmelin 2008**
Recuperative aero engine	Rise in turbine inlet temperature is partly achieved by recycling heat from the exhaust gases	Highly complex system; Risk of weight increase and pressure losses	Long	Medium	**Boggia 2004 Gmelin 2008**
Inter-cooled Recuperative Aero Engine (IRA)	Combines the benefit of inter-cooling and recuperation	See 'Intercooled' and 'Recuperative'	Long	High	**Boggia 2004 Gmelin 2008**

Table B.9 Aircraft Engines and Secondary Power – Increasing Propulsive Efficiency

Technology	Description	Limitations/Trade-Offs/Challenges	Availability	Potential CO_2 Red.	Reference
… by improving Current Designs				**Medium**	
Polymer Matrix Composite (PMC) for fan blades	Lightweight composite material; allows for an increase in fan diameter (BPR) without weight penalties	Foreign Object Damage (FOD, Impact) design, erosion resistant coatings; quality testing methods	Current and Short	Medium	**IATA 2008a Smarsly 2006**
Advanced hollow titanium fan blades	Lightweight titanium material; allows for an increase in fan diameter (BPR) without weight penalties	More complex manufacturing process	Current	Medium	**IATA 2008a**
Laminar Flow Nacelle (Natural and Hybrid)	1. Reduces nacelle drag; 2. Could possibly allow for larger fan/nacelle diameters and increased BPR	See Aerodynamics 'NLF' and 'HLF'	NLF: Short (B787) HLF: Unknown	Low	**Greener By Design 2003**
... by new Engine Concepts				**High**	
Variable fan exhaust nozzle	Varies fan pressure ratios (FPR) in flight; allows optimum FPRs for large fans	System weight and control; considerably benefits only very large fans; used only for flight testing so far	Unknown	Unknown (rather low)	**Berton 2002 Gmelin 2008**
Geared Turbofan (GTF)	Decoupling the fan from the LP turbine by using a gear; allows both components to run at their respective optimum speeds	Current design is working only at low and medium thrust ranges (up to A320 size): risk of too high temperatures in the gear;	Short	Medium to High	**Gmelin 2008 IATA 2008a MTU 2007**
Two-Stage Counter-Rotating Turbofan (CRTF)	Allows for an increase of the mass flow (lower specific thrust, higher BPR) without increasing the fan diameter; reduces internal drag as fixed stator vanes after the fan stage are removed	Mechanical installation complicated and requires more maintenance	Medium to Long	High	**Gmelin 2008 IATA 2008a**
Open Rotor, Un-Ducted Fan (UDF), Propfan Concepts	Fan is rotating outside the nacelle; allows for ultra-high BPR (>>20)	Risk of increased noise, vibration and weight; cabin safety issues (impact of fan blades); challenging engine-airframe integration	Medium	High	**Gmelin 2008 IATA 2008a**
Counter-Rotating Integrated Shrouded Propfan (CRISP)	Combining the benefit of the counter-rotating fan and the geared turbofan in a shrouded design	See CRTF and GTF	Long	High	**Gmelin 2008 MTU 2007**
Distributed Propulsion Systems	Many small propulsion systems instead of a few large ones, thus increasing BPR semi-independent of the engine external diameter; Realized e.g. by multiple flow paths and fans driven by a single gas turbine; Improved engine-airframe integration	Has not been researched in depth so far: no prototype been constructed, gearing of the multiple fans may be difficult; eventually only interesting for BWB aircraft	Long	Unknown	**Cambridge-MIT Institute 2006 IATA 2008a**

Table B.10 Aircraft Engines and Secondary Power – Lowering Fuel Consumption of the Aircraft Systems

Technology	Description	Limitations/Trade-Offs/Challenges	Availability	Potential CO_2 Red.	Reference
Improved efficiency of system sub-parts (aircraft engines remain primary power source)	Increased efficiency of the consumers, improved efficiency in power generation; i.e. fibre-optic links for flight control, LEDs for cabin lighting, etc.	Depending on the respective technology	Continuous	Low to Medium	**IATA 2008b Scholz 2009**
Smooth out the peaks in power demand	Systems for power generation designed for smaller peak demands; e.g. deploying flaps sequentially	Unknown	Current, Continuous	Low to Medium	**EU 2004a**
More Electric Engine Architecture (MEA)	More energy-efficient and reliable, power supply better matches power demands, no bleed air from the engine; enabler for fuel cell as secondary power source	Risk of increased weight and engine shaft power off-take, unknowns concerning benefits	Continuous, first major application 2010 (B787)	Low to Medium	**EU 2004a Sinnett 2007**
Fuel cell for current APU services	Zero-emission technology; provides energy for on-ground services and redundancy	Depending on the type of fuel cell used; In general: hydrogen supply (carried in extra tanks or produced on-board), system weight, heat production & thermal insulation, primarily electric systems required, costs	Medium	Low	**IATA 2008a**
Fuel cell as primary source for secondary power	Zero-emission power supply for all aircraft systems	See above	Long	Medium	**IATA 2008a**
Solar Power	Use of photovoltaic cells applied to the aircraft outer surfaces; regenerative, zero-emission technology	Current technology has very low power density; unlikely to improve to being useful for commercial aviation; trade-offs with aerodynamics (e.g. laminar flow)	Long	Low	**IATA 2008a**
Landing-gear drive	Ground movements per electric motor on nose or main wheel; engines shut down for taxi	Unknown; (Eventually weight, control and reliability)	Short	Low	**WheelTug 2009**

B 3. Aircraft Empty Weight: Technologies

Table B.11 Aircraft Empty Weight – Reducing Structure Weight

Technology	Description	Limitations/Trade-Offs/Challenges	Availability	Potential CO_2 Red.	Reference
... by using new materials for aircraft structures				**High**	
Composite (CFRP) primary structures	Higher strength-to-weight ratio; corrosion resistance	Impact resistance, manufacturing methods, conductivity, high development and certification costs	Current; first large application 2010 (B787)	High	**IATA 2008a**
Al-Li alloys	Higher bending strength and lower density; attractive fatigue properties; improved fracture toughness	Currently more expensive and difficult to process	Current	Medium	**IATA 2008a**
Al-Mg-Sc alloys	Newest Al-alloy under development; excellent corrosion resistance	High cost of scandium	Medium	Unknown	**IATA 2008a**
Advanced Ti-alloys	High strength-to-weight ratio; could be alternative to steel applications	High cost	Current	Medium	**IATA 2008a**
First generation metal-composites	High fatigue resistance, offers possibility for load monitoring and damage detection; e.g. GLARE, ARALL	Technical problems when fabricating thick forms	Current	Medium	**IATA 2008a**
New generation metal-composites	Higher strength-to-weight ratio than many carbon-fibre-reinforced plastics (CFRP); high fatigue and impact resistance; e.g. CentrAl	Unknown; (Might be more expensive to produce)	Short to Medium	High	**IATA 2008a**
(Nano-) tailored materials	Next generation materials; structures being specifically tailored to fit their respective loading (e.g. being flexible in one direction, while being stiff in another); seen as important enabler for morphing structures (see below)	Still under principle investigation; might find first large-scale application rather in military aviation; probably high development, manufacturing and maintenance cost	Long (Large-Scale)	High	**IATA 2008a**
Adaptive / smart materials	Next generation materials; can be internally actuated to adopt their properties to different loadings during flight and to change the structural shape; e.g. Flexible Matrix Composites (FMCs), shape memory alloys (SMAs), pneumatic artificial muscles (PMAs) and piezo-ceramic actuators; seen as important enabler for morphing structures (see below)	See '(Nano-) tailored materials'	Long (Large-Scale)	High	**IATA 2008a**

Table B.11 Aircraft Empty Weight – Reducing Structure Weight (cont'd)

Technology	Description	Limitations/Trade-Offs/Challenges	Availability	Potential CO_2 Red.	Reference
... by using new manufacturing technologies				**Medium**	
Metal structures – new welding technologies	Rivet-free joining techniques; reduce empty weight and decrease friction drag; potential enabler for laminar flow; e.g. electron-beam welding, friction stir welding, laser beam welding	Most welding technologies are designed for a specific metal alloy; manufacturing might be more expensive	Current	Low to Medium	**IATA 2008a**
Composite structures – manufacturing technologies	Rivet-free joining techniques; reduce empty weight and decrease friction drag; potential enabler for laminar flow; e.g. braiding, stitching, gluing	Quality testing methods, reparability	Current	Low to Medium	-
... by reducing additional loads / load multipliers				**All ranges**	
Advanced active load alleviation	Actively uses control surfaces to reduce or distribute the loads on the wing; might allow for reduction in wing and empennage gust load factors and wing root bending moments	More advanced systems are complex and use morphing/shaping materials: eventually high development risk and cost; reliability; load sensoring	Simple systems: current, fully morphing wing: long	All ranges	**IATA 2008a**
Active wing vibration damping	Actively damping wing vibration and thus allowing for lighter structures;	See "Advanced active load alleviation" above	Medium	Unknown	**EU 2004b**
Certification - Lower structural reserve factors	Enabled by structural health monitoring systems and more reliable materials / maintenance procedures	Quality testing methods; acceptance from passengers and certification authorities;	Long	All ranges	**Greener By Design 2005**
... by new design concepts/configurations				**High**	
New design principles for composite structures	Composite structures are currently designed as-if being metal structures (black-metal-design): this does not fully exploit material potential	High development/certification risk and cost	Current, Continuous	High	-
Design for reduced aircraft life	Reduced weight and accelerated fleet turnover	Airline and passenger acceptance; Increased fleet turnover/production rates could increase life-cycle CO_2: recycling issues; costs	Undefined	Unknown	**Greener By Design 2005**
Morphing structures / aircraft	Seamless variations in wing/empennage area, section airfoil shapes and camber; structures change their shape and material properties to adopt to different mission segments and loadings; flexible wings that do without conventional control surfaces etc.; most important enablers are adaptive/smart materials and tailored materials (see above)	Still under principle investigation; might find first large-scale application rather in military aviation; probably high development, manufacturing and maintenance cost	Medium, Continuous	High	**IATA 2008a**

Table B.11 Aircraft Empty Weight – Reducing Structure Weight (cont'd)

Technology	Description	Limitations/Trade-Offs/Challenges	Availability	Potential CO_2 Red.	Reference
... by new design concepts/configurations (cont'd)				**High**	
Hybrid- or Blended-Wing-Body (BWB) concepts	Improved lift/load distribution, improved aerodynamics (reduced relative wetted area)	Problems concerning passenger transports (e.g. a pressurized cabin, emergency evacuation, etc.)	Long	High	**Greener By Design 2003**, 2005 **IATA 2008a**
Strut- or Truss-Braced-Wing (TBW) concepts	Support the wing with a truss or a strut and thereby reduce the wing root bending moment	Risk of exceeding 80 m wing span airport restriction; unknowns concerning aerodynamics	Long	High	**Grasmeyer 1998** **IATA 2008a**
Joined or Box-Wing concepts	A second, forward swept wing joins the main wing either in the middle (joined-wing) or at the tips (box-wing), thereby reducing the wing root bending moment	Large unknowns concerning aerodynamics, manufacturing methods and direct operating costs (DOCs)	Long	High	**Mello 2006** **Kroo 2006** **Bauhaus Luftfahrt 2008**
... by reducing transported fuel weight				**High**	
Certification - Reduced fuel reserve requirements	Enabled by more reliable systems/aircraft/ATM etc.	Quality testing methods; acceptance from passengers and certification authorities;	Undefined	Low	**Greener By Design 2005**
Multi-stage long-distance travel	Breaking down ultra-long distance journeys (e.g. 15 000 km) into several medium-range journeys (e.g. 3 flights à 5000 km)	Passenger and airline acceptance (increased over-all time to travel)	Current	High	**Greener By Design 2003**, 2006
Air-to-air refuelling for civil aviation	Carrying fuel for mission sections rather than the whole mission; advanced multi-stage travel	Safety and ATM issues; high navigational performance needed on-board and for ATC; trade-off with fuel consumption of the tanker aircraft	Long	High	**Truman 2006**

Table B.12 Aircraft Empty Weight – Reducing System and Fixed Equipment Weight

Technology	Description	Limitations/Trade-Offs/Challenges	Availability	Potential CO_2 Red.	Reference
... by reducing engine weight				**Low**[1]	
Polymer matrix composite (PMC) for the fan	Lighter specific material weight	See Table B.9	Current and short	Low	**IATA 2008a** **Smarsly 2006**
Metal matrix composite (MMC) for the compressor	Lighter specific material weight	See Table B.8	Short	Low	**IATA 2008a** **Smarsly 2006**
Ceramic matrix composite (CMC) for the turbine	Lighter specific material weight	See Table B.8	Short	Low	**Gmelin 2008** **IATA 2008a** **Smarsly 2006**
Reduce the number of compressor and turbine stages	Shorter and lighter core architecture	Depending on the specific technology	Current, Continuous	Low	**Greener By Design 2003**

[1] It is assumed that savings in engine component weight are rather used for increasing engine efficiency (higher BPR and OPR) than for reducing engine weight

Table B.12 Aircraft Empty Weight – Reducing System and Fixed Equipment Weight (cont'd)

Technology	Description	Limitations/Trade-Offs/Challenges	Availability	Potential CO_2 Red.	Reference
... by reducing engine weight (cont'd)				**Low**[1]	
Blisk and Bling technology for the compressor	Blade Integrated Disk and Integral Bladed Metal Matrix Ring; Lighter specific compressor weight	Adjustment of the manufacturing and maintenance processes	Short to Medium	Low	**Greener By Design 2005 IATA 2008a**
No-bleed engine architecture	Remove the systems (ducts, gearbox parts, etc) belonging to the bleed air system	See 'More Electric Engine Architecture (MEA)', Table B.10	Short (B787)	Low	**Sinnett 2007**
... by reducing flight system weight				**Low to Medium**	
Fly-By-Light	Fiber-optic links between flight computer and control sufaces; lighter wiring	High cost of software verification and validation	Medium	Low	**IATA 2008a**
Wireless flight control	Wireless links between flight computer and control surfaces; no wiring	High cost, reliability, radio-frequency interference	Long	Low	**IATA 2008a**
Variable camber and morphing wing concepts	Weight savings due to smaller actuators, less parts, etc.	See Table B.7	Short (A350), Continuous	Medium	**IATA 2008a**
... by reducing landing gear weight				**Medium to High**	
Titanium metal matrix composites(Ti-MMC)	Lighter specific material weight	High cost	Medium	Low to Medium	**Messier-Dowty 2005**
Terrestrial and automated landing	Aircraft designed with lightweight emergency or no landing gear	Large changes to airport and aircraft design; passenger acceptance	Long	Medium to High	**Truman 2006**
... by reducing fixed equipment weight				**Medium**	
Different lightweight materials for interiors	Lighter specific material weight; carbon-fibre reinforced plastics, honeycomb material etc.	Depending on the specific material	Current, Continuous	Medium	-
High-strength Glass Microspheres	Lighter specific material weight of resin in interior plastics	Unknown	Current	Medium	**IATA 2008b**
LEDs for cabin lighting	Lightweight, energy efficient cabin lighting	Costs	Current	Low	**IATA 2008b**
... by reducing moisture (insulation) weight				**Low**	
'Zonal dryers' and drain apparatus for liquid condensate	Lower the increase in system weight due; zonal dryer: pumping dry air through the insulations	No considerable challenges; (small weight increase)	Current	Low	**Gupta 1985 enviro.aero 2008**

[1] It is assumed that savings in engine component weight are rather used for increasing engine efficiency (higher BPR and OPR) than for reducing engine weight

B 4. Alternative Fuels

Table B.13 Alternative Fuels – Reducing life-cycle CO_2

Technology	Description	Limitations/Trade-Offs/Challenges	Availability	Potential CO_2 Red.	Reference
... Drop-In Fuels				**High**[1]	
Biomass-to-Liquid (BTL)	Bio-Fuel; Also known as synthetic kerosene; can be produced from both cellulose and fat-based biomass; properties similar to kerosene, thus good drop-in choice	Finding appropriate feed-stock; Production process inefficient; high production and high fuel cost	Current	High	**SBAC 2008a**
Hydrogenated Oils	Bio-Fuel; Can be produced only from fat-/oil-based plant-matter; similar properties to kerosene expected; cheaper in production and end-price than BTL;	Finding appropriate feed-stock; production process still under development	Short	High	**SBAC 2008a**
'Furanics'	Bio-Fuel; Also known as furans or HMF fuel; can be produced from biomass that allows the production of glucose; similar properties to kerosene expected	Finding appropriate feed-stock; Production process still under development; costs and final CO_2 benefit unclear	Short to Medium	High (unclear)	**Jong 2008 IATA 2008a**
Fatty acid methyl esters (FAMEs)	Bio-Fuel; Also known as bio-diesel or transesterification fuel; can be produced only from fat-/oil- based plant matter; similar production to hydrogenated oils; cheap production	Finding appropriate feed-stock; Dissimilar properties to kerosene: can be used only in FAME/kerosene-blends; FAMEs and feedstock is better used for land transportation	Current	Low to Medium	**SBAC 2008a**
Alcohols (Ethanol, Methanol)	Bio-Fuel; Can be produced from both cellulose and fat-based biomass; cheap production	Finding appropriate feed-stock; Very low energy density; practically unusable in aviation	Current	Negative	**SBAC 2008a**
Coal-to-Liquid (CTL)	Produced from coal; similar production to BTL; ready and certified drop-in fuel	No bio-fuel, non-regenerative; Considerably worse life-cycle CO_2 than kerosene	Current	Negative	**SBAC 2008a**
Gas-to-Liquid (GTL)	Produced from natural gas; similar production to BTL; ready and certified drop-in fuel	No bio-fuel, non-regenerative; Similar or worse life-cycle CO_2 compared to kerosene	Current	Negative to very low	**SBAC 2008a**

[1] The assessment of life-cycle CO_2 for bio-fuels and liquid hydrogen is based on the assumptions that the production is powered with biomass or nuclear energy; if the production is powered with conventional fuels, life-cycle CO_2 may be similar or even worse to kerosene (**SBAC 2008a**).

Table B.13 Alternative Fuels – Reducing life-cycle CO_2 (cont'd)

Technology	Description	Limitations/Trade-Offs/Challenges	Availability	Potential CO_2 Red.	Reference
... Cryogenic Fuels				**High**[1]	
Liquid Hydrogen	Very high weight specific energy content; zero-CO_2 emission	Very low volume specific energy content; pressurization needs large and heavy fuel tanks; considerable changes to the aircraft and infrastructure	Long	High	**Daggett 2006** **SBAC 2008a**
Liquid Methane	Bio-fuel if produced from biomass; High weight specific energy content; can eventually produced from captured CO_2; more similar to kerosene than liquid hydrogen	Low volume specific energy content; pressurization needs large and heavy fuel tanks; considerable changes to the aircraft and infrastructure	Long	High	**SBAC 2008a** **Nanotechnology 2009** **IPCC 1999**

[1] The assessment of life-cycle CO_2 for bio-fuels and liquid hydrogen is based on the assumptions that the production is powered with biomass or nuclear energy; if the production is powered with conventional fuels, life-cycle CO_2 may be similar or even worse to kerosene (**SBAC 2008a**).

Appendix C

Appendix to the Global Fleet and CO_2 Emission Forecasts

This appendix provides data that is used to establish the fleet and CO_2 forecast in chapter 5. Appendix C.1 gives information and data on the calculation of future market shares. Appendix C.2 lists data on the fuel consumption and transport performance of aircraft active in 2008. Appendix C.3 presents findings of a literature study on future aircraft available in the short- to medium term (< 2015) and lists data on the fuel consumption and transport performance of the future aircraft regarded in the forecast. Detailed results for all calculations of future fleet size and composition, fuel consumption and CO_2 emission are found on a compact disc (Appendix D) in the form of *Microsoft Excel* spreadsheets.

C.1 Market Shares

Market shares are approximated from expected deliveries in the current order book given in the *MRO Prospector* (**MRO Prospector 2008b**), the *Traffic & Fleet Forecast 2008-2030* in **Airline Monitor 2008b** and further literature. These 'hypothetical deliveries' D per aircraft type j are assigned to the FESG seat categories according to 2008 OAG data (**OAG data 2007**). The market share of the aircraft in the seat category C is then calculated from

$$\text{Market Share } S_j = \frac{\text{Individual Aircraft Deliveries per Seat Category}}{\text{Total Deliveries per Seat Category}} = \frac{D_j \cdot f_{C_j}}{\sum_{j=1}^{n} D_j} \quad , \text{(C.1)}$$

where f_C is the fraction of the specific aircraft fleet assigned to the respective seat category. This approach is schematically shown in the main body of the thesis in Fig. 5.8.

As, the current order book and **Airline Monitor 2008b** do not include information on all considered aircraft, further assumptions are necessary, especially for the calculation of market shares of the new regional aircraft (AVIC ARJ, Mitsubishi MRJ, Sukhoi SSJ, etc.) and the new large long-range aircraft of Airbus and Boeing in the late 2020s. It is also necessary to have a closer look at production ramp-ups and phase-outs when new configurations succeed today's models, e.g. A320 → A30X and B737 → Y1. The assumptions for all different aircraft are listed below.

C.1.1 'Hypothetical Deliveries' for Calculating Market Shares

The assumptions given below concern the 'hypothetical deliveries' *D* from which the market shares are calculated according to Eq.(C.1). 'Order Book' is a synonym for the order book according to **MRO Prospector 2008b**. 'Forecast Airline Monitor' stands for the fleet forecast found in **Airline Monitor 2008b**. The resulting market shares per aircraft type, seat category and year can be found in sub-appendix C.1.2. The information on hypothetical deliveries is given as:

Aircraft Name: Year(s) of interest: Deliveries adopted from Source or similar Aircraft (*Further Information on Source*). *Further Information on the Aircraft in General*

below. Tables C.1a through C.1c provide the resulting values for *D*.

Regional Aircraft

ACAC ARJ21-700: 2009-2011: Order Book, 2012-2036: 50 % of average CRJ-700/E-170

ACAC ARJ21-900: 2011-2013: identical to first years ARJ21-700 (2009-2011), 2012-2036: 50 % of average CRJ-900/E-190

Bombardier CRJ-700: 2009: Order Book, 2010-2030: Forecast Airline Monitor, 2031-2036: identical to 2030

Bombardier CRJ-900: 2009: Order Book minus 2 (*deliveries of the CRJ-1000*), 2010-2030: 50 % Forecast Airline Monitor CRJ-900, 2031-2036: identical to 2030

Bombardier CRJ-1000: 2009: 2 aircraft (*first delivery in fourth quarter*), 2010-2030: 50 % Forecast Airline Monitor CRJ-900, 2031-2036: identical to 2030

Embraer E-170: 2009: Order Book, 2010-2030: 60 % Forecast Airline Monitor E-170/175 (*pro rata order book 2009*), 2031-2036: identical to 2030

Embraer E-175: 2009: Order Book, 2010-2030: 40 % Forecast Airline Monitor E-170/E175 (*pro rata order book 2009*), 2031-2036: identical to 2030

Embraer E-190: 2009: Order Book, 2010-2030: 84.5 % Forecast Airline Monitor E-190/195 (*pro rata order book 2009*), 2031-2036: identical to 2030

Embraer E-195: 2009: Order Book, 2010-2030: 15.5 % Forecast Airline Monitor E-190/195 (*pro rata order book 2009*), 2031-2036: identical to 2030

Mitsubishi MRJ-70: 2013: identical to first year SSJ100-75, 2014-2036: linear increase to average of CRJ-700/E-170 in 2015

Mitsubishi MRJ-90: 2013: identical to first year SSJ100-95, 2014-2035: linear increase to average of CRJ-900/E-190

Sukhoi SSJ100-75: 2011-2013: identical to first years SSJ100-95 (2009-2011), 2014-2036: average of CRJ-700/E-190

Sukhoi SSJ100-95: 2009-2011: Order Book, 2014-2036: average of CRJ-900/E-190

Table C.1a 'Hypothetical Deliveries' for Calculating Market Shares – Regional Aircraft

Year	ARJ21		CRJ			E-Jets				MRJ		SSJ	
	-700	-900	-700	-900	-1000	-170	-175	-190	-195	-70	-90	-75	-95
2009	4	-	57	43	2	15	10	71	13	-	-	-	6
2010	13	-	20	15	15	18	12	66	12	-	-	-	14
2011	18	4	20	15	15	18	12	51	9	-	-	6	18
2012	10	13	20	20	20	18	12	46	9	-	-	14	33
2013	10	18	20	15	15	18	12	42	8	6	6	18	29
2014	10	18	20	20	20	18	12	51	9	13	21	19	36
2015	10	18	20	20	20	18	12	51	9	19	36	19	36
2016	10	20	20	20	20	18	12	59	11	19	40	19	40
2017	12	23	30	25	25	18	12	68	12	24	47	24	47
2018	13	26	30	27	27	21	14	76	14	26	52	26	52
2019	14	27	35	30	30	21	14	76	14	28	53	28	53
2020	16	28	40	37	37	24	16	76	14	32	57	32	57
2021	12	21	30	25	25	18	12	59	11	24	42	24	42
2022	16	25	40	30	30	24	16	68	12	32	49	32	49
2023	20	26	50	35	35	30	20	68	12	40	52	40	52
2024	20	33	50	45	45	30	20	85	15	40	65	40	65
2025	20	33	50	45	45	30	20	85	15	40	65	40	65
2026	20	34	50	47	47	30	20	89	16	40	68	40	68
2027	20	36	50	50	50	30	20	93	17	40	72	40	72
2028	20	36	50	50	50	30	20	93	17	40	72	40	72
2029	20	39	50	55	55	30	20	101	19	40	78	40	78
2030	20	43	50	60	60	30	20	110	20	40	85	40	85
2031	20	43	50	60	60	30	20	110	20	40	85	40	85
2032	20	43	50	60	60	30	20	110	20	40	85	40	85
2033	20	43	50	60	60	30	20	110	20	40	85	40	85
2034	20	43	50	60	60	30	20	110	20	40	85	40	85
2035	20	43	50	60	60	30	20	110	20	40	85	40	85
2036	20	43	50	60	60	30	20	110	20	40	85	40	85

Narrow-Body Aircraft

Airbus A318: 2009: Order Book, 2010-2017: Forecast Airline Monitor, 2018: end of production. *A318 and A30X-18 productions do not overlap due to small annual production*.

Airbus A319: 2009: Order Book, 2010-2017: Forecast Airline Monitor, 2018: Forecast Airline Monitor minus production A30X-19, 2019-2021: linear decrease from 2018 to zero in 2021. *A319 and A30X-19 productions overlap for three years (according to history 737-300 and 737-700)*.

Airbus A320: 2009: Order Book, 2010-2017: Forecast Airline Monitor, 2018: Forecast Airline Monitor minus production A30X-20, 2019-2022: linear decrease from 2018 to zero in 2022. *A320 and A30X-20 productions overlap for four years (according to history 737-400 and 737-800)*

Airbus A321: 2009: Order Book, 2010-2017: Forecast Airline Monitor, 2018: Forecast Airline Monitor minus production A30X-21, 2019-2021: linear decrease from 2018 to zero in 2021. *A321 and A30X-21 productions overlap for three years (according to history 737-300 and 737-700).*

Airbus A30X-18: 2018-2036: Forecast Airline Monitor, 2031-2036: identical to 2030

Airbus A30X-19: 2018: 47 aircraft (*according to historical second year deliveries of A319*), 2019-2020: Forecast Airline Monitor minus production A319, 2021-2030: Forecast Airline Monitor, 2031-2036: identical to 2030

Airbus A30X-20: 2018: 58 aircraft (*according to historical second year deliveries of A320*), 2019-2020: Forecast Airline Monitor minus production A320, 2021-2030: Forecast Airline Monitor, 2031-2036: identical to 2030

Airbus A30X-21: 2018: 22 aircraft (*according to historical second year deliveries of A321*), 2019-2020: Forecast Airline Monitor minus production A321, 2021-2030: Forecast Airline Monitor, 2031-2036: identical to 2030

Boeing 737-600: no further deliveries according to Order Book and Forecast Airline Monitor

Boeing 737-700: 2009: Order Book, 2010-2015: Forecast Airline Monitor, 2016: Forecast Airline Monitor minus production Y1-700, 2017-2019: linear decrease from 2016 to zero in 2019. *737-700 and Y1-700 productions overlap for three years (according to history 737-300 and 737-700).*

Boeing 737-800: 2009: Order Book, 2010-2015: Forecast Airline Monitor, 2016: Forecast Airline Monitor minus production Y1-800, 2017-2020: linear decrease from 2016 to zero in 2020. *737-800 and Y1-800 productions overlap for four years (according to history 737-400 and 737-800).*

Boeing 737-900: 2009: Order Book, 2010-2015: Forecast Airline Monitor, 2016: Forecast Airline Monitor minus production Y1-900, 2017-2019: linear decrease from 2016 to zero in 2019. *737-900 and Y1-900 productions overlap for four years (according to history 737-300 and 737-700).*

Boeing Y1-600: 2016-2030: Forecast Airline Monitor, 2031-2036: identical to 2030

Boeing Y1-700: 2016: 65 aircraft (*according to historical first year deliveries of 737-800*), 2017-2018: Forecast Airline Monitor minus production 737-700, 2019-2030: Forecast Airline Monitor, 2031-2036: identical to 2030

Boeing Y1-800: 2016: 65 aircraft (*according to historical first year deliveries of 737-800*), 2017-2019: Forecast Airline Monitor minus production 737-800, 2020-2030: Forecast Airline Monitor, 2031-2036: identical to 2030

Boeing Y1-900: 2016: 65 aircraft (*according to historical first year deliveries of 737-800*), 2017-2018: Forecast Airline Monitor minus production 737-900, 2019-2030: Forecast Airline Monitor, 2031-2036: identical to 2030

Bombardier C100: 2013: identical to first year production SSJ100-95, 2014-2016: linear increase to 75 aircraft p.a. in 2016 (*according to **Miller 2008**: "Bombardier may build 150 CSeries Jets a Year by 2016"*), 2017-2036: identical to 2016 (*no further production increase according to competitors A318/A30X-18 and 737-600/Y1-600*)

Bombardier C300: 2013: identical to first year production SSJ100-95, 2014-2016: linear increase to 75 aircraft p.a. in 2016 (*according to **Miller 2008**: "Bombardier may build 150 CSeries Jets a Year by 2016"*), 2017-2036: relative changes in production identical to Y1-700 production, base value: 75 p.a.

COMAC 919: 2016-2018: identical to first years ARJ21-700 (2009-2011), 2019-2036: 50 % Bombardier C300

Table C.1a 'Hypothetical Deliveries' for Calculating Market Shares – Narrow-Body Aircraft

Year	A320 Family				A30X				B737			Y1				CSeries		Com
	318	319	320	321	18	19	20	21	700	800	900	600	700	800	900	100	300	919
2009	10	102	253	66	-	-	-	-	57	285	31	-	-	-	-	-	-	-
2010	5	100	250	56	-	-	-	-	90	215	25	-	-	-	-	-	-	-
2011	5	110	267	50	-	-	-	-	90	215	25	-	-	-	-	-	-	-
2012	5	120	275	45	-	-	-	-	105	200	30	-	-	-	-	-	-	-
2013	5	120	240	45	-	-	-	-	105	200	30	-	-	-	-	6	6	-
2014	5	120	240	45	-	-	-	-	100	180	30	-	-	-	-	29	29	-
2015	5	120	240	45	-	-	-	-	80	165	30	-	-	-	-	52	52	-
2016	5	120	235	45	-	-	-	-	65	155	25	5	65	65	65	75	75	4
2017	5	110	220	50	-	-	-	-	43	116	17	5	97	129	93	75	75	13
2018	-	93	192	88	5	47	58	22	22	78	8	5	118	167	102	75	75	18
2019	-	62	144	59	5	78	101	51	-	33	-	5	140	207	110	75	75	38
2020	-	31	96	30	5	109	144	90	-	-	-	5	140	240	120	75	75	38
2021	-	-	48	-	5	100	112	90	-	-	-	5	100	160	90	75	58	29
2022	-	-	-	-	5	110	170	100	-	-	-	5	110	170	100	75	63	32
2023	-	-	-	-	5	130	220	110	-	-	-	5	130	220	110	75	75	38
2024	-	-	-	-	5	155	230	150	-	-	-	5	155	230	150	75	89	45
2025	-	-	-	-	5	190	290	195	-	-	-	5	190	290	195	75	110	55
2026	-	-	-	-	5	215	310	220	-	-	-	5	215	310	220	75	124	62
2027	-	-	-	-	5	230	330	230	-	-	-	5	230	330	230	75	133	66
2028	-	-	-	-	5	235	350	250	-	-	-	5	235	350	250	75	136	68
2029	-	-	-	-	5	235	355	255	-	-	-	5	235	355	255	75	136	68
2030	-	-	-	-	5	245	375	265	-	-	-	5	245	375	265	75	141	71
2031	-	-	-	-	5	245	375	265	-	-	-	5	245	375	265	75	141	71
2032	-	-	-	-	5	245	375	265	-	-	-	5	245	375	265	75	141	71
2033	-	-	-	-	5	245	375	265	-	-	-	5	245	375	265	75	141	71
2034	-	-	-	-	5	245	375	265	-	-	-	5	245	375	265	75	141	71
2035	-	-	-	-	5	245	375	265	-	-	-	5	245	375	265	75	141	71
2036	-	-	-	-	5	245	375	265	-	-	-	5	245	375	265	75	141	71

Wide-Body Aircraft

Airbus A330-200: 2009: Order Book, 2010-2013: Forecast Airline Monitor, 2014-2017: linear decrease from 2013 production to zero in 2017 (*succeeded by A350-800 in 2014*)

Airbus A330-300: 2009: Order Book, 2010-2025: Forecast Airline Monitor, 2026-2028: linear decrease from 2025 production to zero in 2028 (*succeeded by Airbus A330/340-Replacement in 2025*)

Airbus A340-600: 2009: Order Book, 2010-2011: Forecast Airline Monitor, 2012: end of production

Airbus A350-800: 2014: Order Book, 2015-2017: linear increase to Forecast Airline Monitor A350-800 plus A330-200, 2018-2030: Forecast Airline Monitor A350-800 plus A330-200, 2031-2036: identical to 2030

Airbus A350-900: 2013: Order Book, 2014-2030: Forecast Airline Monitor, 2031-2036: identical to 2030

Airbus A350-1000: 2015: Order Book, 2016-2030: Forecast Airline Monitor, 2031-2036: identical to 2030

Airbus A380-800: 2009: Order Book, 2010-2030: Forecast Airline Monitor, 2031-2036: identical to 2030

Airbus NLR 1 (A330-300 and A340-200/300 Replacement): 2025: 22 (*according to historical first year production A340-2/300*), 2026-2030: linear increase to identical production rate as Boeing 777-200 Replacement in 2030, 2031-2036: identical to 2030

Airbus NLR 2 (A340-600 Replacement): 2025: 6 (*according to historical first year production A340-600*), linear increase to identical production rate as Boeing 777-300 Replacement in 2030, 2031-2036: identical to 2030

Boeing 747-8: 2010: Order Book, 2011-2026: Forecast Airline Monitor, 2027-2030: linear decrease from 2026 production to zero in 2030 (*succeeded by Boeing 747 Replacement in 2027*)

Boeing 777-200ER: 2009: Order Book, 2010-2013: 26.3 % Forecast Airline Monitor 777-200ER/LR (*pro rata Order Book 2009*), 2014: end of production (*succeeded by 777-200LR and 787-9, according to* ***MRO Prospector 2008a***)

Boeing 777-200LR: 2009: Order Book, 2010-2013: 73.6 % Forecast Airline Monitor 777-200ER/LR, 2014-2026: 100 % Forecast Airline Monitor 777-200ER/LR, 2027-2030: linear decrease from 2026 production to zero in 2030 (*succeeded by Boeing 777-200 Replacement in 2027*)

Boeing 777-300ER: 2009: Order Book, 2010-2026: Forecast Airline Monitor, 2027-2030: linear decrease from 2026 production to zero in 2030 (*succeeded by Boeing 777-300 Replacement in 2027*)

Boeing 787-3: 2013: Order Book, 2014-2030: Forecast Airline Monitor, 2031-2036: identical to 2030

Boeing 787-8: 2010: Order Book, 2011-2030: Forecast Airline Monitor, 2031-2036: identical to 2030

Boeing 787-9: 2012: Order Book, 2013-2030: Forecast Airline Monitor, 2031-2036: identical to 2030

Boeing Y3 (777-200 Replacement): 2027: 13 (*according to historical first year production 777*), 2028-2029: Forecast Airline Monitor 777-200ER/LR minus production 777-200LR, 2030: 100 % Forecast Airline Monitor 777-200ER/LR, 2031-2036: identical to 2030

Boeing Y3 (777-300 Replacement): 2027: 13 (*according to historical first year production 777*), 2028-2029: Forecast Airline Monitor 777-300 minus production 777-300ER, 2030: 100 % Forecast Airline Monitor 777-300, 2031-2036: identical to 2030

Boeing Y3 (747 Replacement): 2027: identical to first year production 747-8, 2028-2029: Forecast Airline Monitor 747-8 minus production 747-8, 2030: 100 % Forecast Airline Monitor 747-8, 2031-2036: identical to 2030

Table C.1c 'Hypothetical Deliveries' for Calculating Market Shares – Wide-Body Aircraft: Airbus

Year	A330		A340	A350			A380	New Large Long-Range	
	-200	-300	-600	-800	-900	-1000	-800	-1	-2
2009	48	37	3	-	-	-	21	-	-
2010	70	30	3	-	-	-	30	-	-
2011	70	25	3	-	-	-	35	-	-
2012	50	25	-	-	-	-	35	-	-
2013	50	25	-	-	5	-	35	-	-
2014	38	25	-	16	40	-	35	-	-
2015	25	25	-	42	40	1	35	-	-
2016	13	25	-	67	40	30	35	-	-
2017	-	25	-	95	50	45	35	-	-
2018	-	25	-	95	50	45	35	-	-
2019	-	25	-	95	50	45	35	-	-
2020	-	25	-	90	50	50	35	-	-
2021	-	25	-	60	40	40	30	-	-
2022	-	25	-	70	45	45	35	-	-
2023	-	30	-	90	50	55	40	-	-
2024	-	30	-	100	60	65	40	-	-
2025	-	30	-	105	70	80	40	22	6
2026	-	20	-	105	70	80	40	30	25
2027	-	10	-	105	70	80	40	37	44
2028	-	-	-	105	75	80	40	45	62
2029	-	-	-	135	90	100	50	52	81
2030	-	-	-	135	90	100	50	60	100
2031	-	-	-	135	90	100	50	60	100
2032	-	-	-	135	90	100	50	60	100
2033	-	-	-	135	90	100	50	60	100
2034	-	-	-	135	90	100	50	60	100
2035	-	-	-	135	90	100	50	60	100
2036	-	-	-	135	90	100	50	60	100

Table C.1d 'Hypothetical Deliveries' for Calculating Market Shares – Wide-Body Aircraft: Boeing

Year	747	777			787			New Large Long-Range		
	-8	-200ER	-200LR	-300ER	-3	-8	-9	-1	-2	-3
2009	-	5	14	9	-	-	-	-	-	-
2010	3	9	26	45	-	4	-	-	-	-
2011	30	8	22	40	-	75	-	-	-	-
2012	30	7	18	35	-	90	16	-	-	-
2013	25	7	18	30	5	90	45	-	-	-
2014	25	-	25	30	10	90	50	-	-	-
2015	25	-	30	35	10	90	55	-	-	-
2016	25	-	35	40	15	75	70	-	-	-
2017	25	-	35	45	15	75	70	-	-	-
2018	25	-	35	50	15	75	75	-	-	-
2019	25	-	35	50	15	75	75	-	-	-
2020	25	-	40	55	15	75	75	-	-	-
2021	15	-	30	35	15	55	55	-	-	-
2022	20	-	30	45	15	55	65	-	-	-
2023	25	-	40	60	20	70	80	-	-	-
2024	25	-	50	65	20	75	90	-	-	-
2025	25	-	50	75	25	80	110	-	-	-
2026	25	-	50	75	25	80	110	-	-	-
2027	22	-	37	62	25	80	110	13	13	3
2028	15	-	25	41	25	85	110	25	34	10
2029	7	-	12	21	25	100	125	48	79	18
2030	-	-	-	-	25	100	125	60	100	30
2031	-	-	-	-	25	100	125	60	100	30
2032	-	-	-	-	25	100	125	60	100	30
2033	-	-	-	-	25	100	125	60	100	30
2034	-	-	-	-	25	100	125	60	100	30
2035	-	-	-	-	25	100	125	60	100	30
2036	-	-	-	-	25	100	125	60	100	30

C.1.2 Market Shares per Year and Seat Category

Below, calculated market shares for the years 2009 to 2036 are listed per seat category and aircraft. These are calculated from Eq.(C.1) using the 'hypothetical deliveries' given above. The deliveries are assigned to the seat categories according to the relative share of aircraft flown in the respective seat class. This fraction is initially adopted from 2008 OAG data (**OAG data 2007**). However, for in-production aircraft the value is not constant. It may change due to different market conditions (growth rate and fierceness of competition) in the seat categories. An example is the 787-3. It is initially assumed that 76 % of the aircraft's fleet is sold in the 211 to 300 seat category and only 24 % in the seat category of 301 to 400 seats (the nominal seating capacity of the 787-3 is 317 passengers). As the average annual growth rate is however higher for aircraft with more than 300 seats, more 787-3 are sold in the latter category. Thus, by 2020, already around 42 % of the aircraft's fleet is flown in the seat category of 301 to 400 seats. This is an automatic effect that results from growth rates being applied directly to the different fleet fractions. Detailed results are contained in digital format (Excel spreadsheets) on the enclosed compact disc (Appendix D).

Table C.2a Market Shares in the 51-100 Seat Category 2009-2036

Year	A318	A30X	ARJ21	B737-800	Y1	CRJ	Cseries	EMB E-Jets	MRJ	SSJ
-	[%]	[%]	[%]	[%]	[%]	[%]	[%]	[%]	[%]	[%]
2009	1.01	-	1.84	0.09	-	46.96	-	47.32	-	2.76
2010	0.60	-	7.21	0.08	-	27.72	-	56.62	-	7.76
2011	0.60	-	11.06	0.09	-	27.66	-	47.32	-	13.27
2012	0.53	-	7.65	0.07	-	29.35	-	39.40	-	22.99
2013	0.53	-	9.27	0.07	-	24.25	0.58	36.92	5.82	22.55
2014	0.42	-	7.54	0.05	-	22.92	2.80	32.74	12.70	20.82
2015	0.38	-	6.87	0.04	-	20.66	4.97	29.53	18.77	18.77
2016	0.35	-	6.72	0.04	0.01	18.98	6.90	29.99	18.50	18.50
2017	0.30	-	6.94	0.02	0.03	21.24	6.29	27.73	18.72	18.72
2018	-	0.27	6.86	0.01	0.03	20.62	5.34	29.06	18.90	18.90
2019	-	0.18	6.87	0.01	0.03	22.31	4.79	27.77	19.02	19.02
2020	-	0.14	6.83	-	0.03	24.46	4.15	26.42	18.99	18.99
2021	-	0.16	6.73	-	0.02	22.92	5.27	27.08	18.91	18.91
2022	-	0.12	6.87	-	0.02	23.64	4.11	26.94	19.15	19.15
2023	-	0.09	6.98	-	0.02	25.16	3.43	25.96	19.18	19.18
2024	-	0.07	6.67	-	0.01	25.71	2.86	26.10	19.28	19.28
2025	-	0.07	6.59	-	0.02	25.78	2.74	26.14	19.33	19.33
2026	-	0.06	6.49	-	0.02	25.83	2.60	26.25	19.37	19.37
2027	-	0.06	6.39	-	0.02	26.08	2.47	26.21	19.39	19.39
2028	-	0.06	6.34	-	0.02	26.12	2.41	26.23	19.41	19.41
2029	-	0.05	6.19	-	0.02	26.36	2.23	26.26	19.44	19.44
2030	-	0.05	6.04	-	0.01	26.52	2.07	26.32	19.50	19.50
2031	-	0.05	5.99	-	0.01	26.55	2.02	26.33	19.52	19.52
2032	-	0.05	5.94	-	0.01	26.58	1.98	26.34	19.55	19.55
2033	-	0.05	5.88	-	0.01	26.62	1.95	26.35	19.57	19.57
2034	-	0.04	5.84	-	0.01	26.65	1.91	26.36	19.59	19.59
2035	-	0.04	5.79	-	0.01	26.68	1.87	26.38	19.62	19.62
2036	-	0.04	5.74	-	0.01	26.71	1.84	26.39	19.64	19.64

Table C.2b Market Shares in the 101-150 Seat Category 2009-2036

Year	A320 Fam.	A30X	B737	Y1	ARJ21	COMAC 919	Cseries	EMB E-Jets
-	[%]	[%]	[%]	[%]	[%]	[%]	[%]	[%]
2009	68.20	-	30.15	-	-	-	-	1.65
2010	64.24	-	34.26	-	-	-	-	1.50
2011	65.85	-	32.59	-	0.48	-	-	1.08
2012	64.47	-	32.99	-	1.54	-	-	1.00
2013	60.99	-	33.72	-	1.92	-	2.48	0.89
2014	57.03	-	29.56	-	1.61	-	10.87	0.92
2015	55.18	-	23.79	-	1.52	-	18.62	0.89
2016	44.69	-	16.58	14.17	1.37	0.41	21.89	0.89
2017	41.69	-	11.49	21.37	1.57	1.24	21.69	0.96
2018	32.41	13.15	5.97	24.05	1.65	1.62	20.11	1.04
2019	22.60	22.08	1.04	28.29	1.72	3.39	19.84	1.03
2020	13.43	31.11	-	29.24	1.88	3.43	19.85	1.04
2021	5.94	36.07	-	28.02	1.94	3.59	23.32	1.12
2022	-	42.26	-	28.06	2.15	3.64	22.75	1.14
2023	-	43.89	-	28.40	1.97	3.62	21.15	0.98
2024	-	43.18	-	28.85	2.26	3.81	20.80	1.10
2025	-	44.34	-	29.32	1.93	3.86	19.62	0.93
2026	-	44.25	-	29.66	1.87	3.97	19.35	0.91
2027	-	44.37	-	29.77	1.87	4.00	19.07	0.91
2028	-	44.80	-	29.72	1.85	3.97	18.77	0.89
2029	-	44.80	-	29.59	2.03	3.94	18.63	1.00
2030	-	44.96	-	29.58	2.15	3.94	18.36	1.02
2031	-	44.94	-	29.56	2.18	3.94	18.36	1.03
2032	-	44.91	-	29.54	2.21	3.94	18.36	1.04
2033	-	44.88	-	29.52	2.24	3.93	18.37	1.05
2034	-	44.86	-	29.50	2.27	3.93	18.37	1.06
2035	-	44.83	-	29.48	2.30	3.93	18.38	1.07
2036	-	44.80	-	29.46	2.33	3.93	18.39	1.08

Table C.2c Market Shares in the 151-210 Seat Category 2009-2036

Year	A320 Fam.	A30X	B737	Y1	COMAC 919	B787-8
-	[%]	[%]	[%]	[%]	[%]	[%]
2009	40.33	-	59.67	-	-	-
2010	45.40	-	54.49	-	-	0.11
2011	45.12	-	53.76	-	-	1.12
2012	45.97	-	52.86	-	-	1.17
2013	43.67	-	55.09	-	-	1.24
2014	45.83	-	52.72	-	-	1.45
2015	47.57	-	50.73	-	-	1.71
2016	36.47	-	36.42	25.44	0.42	1.25
2017	32.13	-	23.99	41.36	1.33	1.18
2018	32.17	9.12	13.30	42.87	1.51	1.03
2019	22.86	17.48	5.18	50.41	3.04	1.03
2020	13.14	27.09	-	55.87	2.90	1.00
2021	5.27	35.20	-	55.34	3.14	1.04
2022	-	40.34	-	55.48	3.21	0.97
2023	-	39.41	-	56.41	3.15	1.02
2024	-	40.95	-	54.93	3.18	0.93
2025	-	41.21	-	54.96	3.05	0.78
2026	-	41.49	-	54.66	3.13	0.71
2027	-	41.39	-	54.76	3.17	0.67
2028	-	41.57	-	54.74	3.02	0.67
2029	-	41.57	-	54.70	2.96	0.76
2030	-	41.47	-	54.85	2.95	0.73
2031	-	41.45	-	54.87	2.94	0.73
2032	-	41.44	-	54.89	2.94	0.73
2033	-	41.43	-	54.90	2.93	0.74
2034	-	41.42	-	54.91	2.93	0.74
2035	-	41.41	-	54.92	2.93	0.74
2036	-	41.41	-	54.92	2.93	0.74

Table C.2d Market Shares in the 211-300 Seat Category 2009-2036

Year	A320 Fam.	A30X	A330	A340	A 350	Airbus New Large Long-Range	B737	Y1	B777	B787	Boeing New Large Long Range
-	[%]	[%]	[%]	[%]	[%]	[%]	[%]	[%]	[%]	[%]	[%]
2009	2.45	-	80.89	0.37	-	-	9.91	-	6.38	-	-
2010	1.67	-	75.97	0.29	-	-	6.59	-	12.37	3.12	-
2011	0.98	-	47.39	0.19	-	-	4.40	-	7.29	39.74	-
2012	0.84	-	34.67	-	-	-	5.00	-	5.91	53.59	-
2013	0.70	-	29.18	-	1.69	-	4.20	-	4.60	59.64	-
2014	0.61	-	21.14	-	16.66	-	3.61	-	2.86	55.12	-
2015	0.57	-	15.46	-	24.20	-	3.30	-	3.09	53.38	-
2016	0.49	-	10.01	-	29.97	-	2.34	6.06	3.07	48.05	-
2017	0.50	-	5.70	-	38.48	-	1.46	6.01	3.05	44.80	-
2018	0.87	0.22	5.61	-	37.76	-	0.68	6.15	3.18	45.53	-
2019	0.59	0.53	5.61	-	37.76	-	-	6.74	3.17	45.61	-
2020	0.30	0.98	5.62	-	36.42	-	-	7.47	3.53	45.68	-
2021	-	1.38	7.54	-	34.30	-	-	7.66	3.24	45.87	-
2022	-	1.41	6.80	-	35.70	-	-	7.74	3.38	44.97	-
2023	-	1.26	6.61	-	35.85	-	-	6.89	3.66	45.73	-
2024	-	1.50	5.88	-	36.17	-	-	8.27	3.75	44.43	-
2025	-	1.61	4.94	-	33.04	4.66	-	8.97	3.44	43.33	-
2026	-	1.78	3.23	-	32.46	6.68	-	9.93	3.39	42.54	-
2027	-	1.83	1.57	-	31.64	8.41	-	10.16	2.63	41.43	2.33
2028	-	1.93	-	-	30.73	9.98	-	10.66	1.67	40.43	4.61
2029	-	1.69	-	-	32.42	9.82	-	9.23	0.70	38.66	7.49
2030	-	1.70	-	-	31.53	11.11	-	9.32	-	37.64	8.69
2031	-	1.70	-	-	31.62	11.09	-	9.34	-	37.79	8.45
2032	-	1.70	-	-	31.68	11.08	-	9.36	-	37.91	8.26
2033	-	1.70	-	-	31.74	11.06	-	9.36	-	38.03	8.10
2034	-	1.70	-	-	31.79	11.04	-	9.37	-	38.15	7.95
2035	-	1.70	-	-	31.82	11.03	-	9.37	-	38.24	7.83
2036	-	1.70	-	-	31.86	11.02	-	9.38	-	38.34	7.70

Table C.2d Market Shares in the 301-400 Seat Category 2009-2036

Year	A330	A340	A350	Airbus New Large Long-Range	B747-8	B777	B787-3	Boeing New Large Long-Range
-	[%]	[%]	[%]	[%]	[%]	[%]	[%]	[%]
2009	32.22	7.25	-	-	-	60.53	-	-
2010	14.22	3.27	-	-	1.84	80.66	-	-
2011	12.45	3.24	-	-	14.96	69.35	-	-
2012	12.41	-	-	-	20.10	67.49	-	-
2013	12.91	-	1.69	-	20.07	63.64	1.69	-
2014	9.68	-	14.92	-	16.98	54.69	3.73	-
2015	7.70	-	16.83	-	14.88	56.79	3.80	-
2016	5.05	-	32.09	-	10.68	47.75	4.42	-
2017	3.83	-	39.26	-	8.95	44.07	3.88	-
2018	3.74	-	38.45	-	8.38	45.61	3.82	-
2019	3.75	-	38.65	-	8.05	45.71	3.85	-
2020	3.47	-	38.48	-	7.14	47.32	3.59	-
2021	4.68	-	41.41	-	5.50	43.59	4.82	-
2022	4.12	-	41.07	-	6.23	44.33	4.25	-
2023	3.93	-	38.66	-	5.96	46.96	4.49	-
2024	3.44	-	40.23	-	5.02	47.39	3.92	-
2025	2.96	-	41.80	2.67	4.12	44.26	4.20	-
2026	1.86	-	39.51	9.10	3.70	41.86	3.96	-
2027	0.92	-	38.82	15.31	3.05	32.61	3.88	2.88
2028	-	-	39.66	21.41	2.03	21.76	3.88	5.61
2029	-	-	42.91	24.43	0.82	9.53	3.40	8.85
2030	-	-	42.90	30.13	-	-	3.41	11.58
2031	-	-	42.86	30.18	-	-	3.41	11.69
2032	-	-	42.85	30.22	-	-	3.42	11.77
2033	-	-	42.82	30.23	-	-	3.43	11.86
2034	-	-	42.80	30.24	-	-	3.44	11.94
2035	-	-	42.79	30.25	-	-	3.44	12.00
2036	-	-	42.79	30.25	-	-	3.46	12.06

Table C.2e Market Shares in the 401-500 and 501-600 Seat Category 2009-2036

	401- 500 Seat Category			501-600 Seat Category
Year	A380-800	B747-8	Boeing New Large Long-Range	A380-800
-	[%]	[%]	[%]	[%]
2009	100.00	-	-	100.00
2010	92.08	7.92	-	100.00
2011	55.09	44.91	-	100.00
2012	58.36	41.64	-	100.00
2013	65.81	34.19	-	100.00
2014	67.43	32.57	-	100.00
2015	67.77	32.23	-	100.00
2016	67.71	32.29	-	100.00
2017	67.07	32.93	-	100.00
2018	64.35	35.65	-	100.00
2019	62.18	37.82	-	100.00
2020	60.43	39.57	-	100.00
2021	67.20	32.80	-	100.00
2022	63.36	36.64	-	100.00
2023	60.48	39.52	-	100.00
2024	59.72	40.28	-	100.00
2025	59.00	41.00	-	100.00
2026	58.32	41.68	-	100.00
2027	55.42	35.73	8.85	100.00
2028	43.70	21.22	35.08	100.00
2029	32.75	6.44	60.81	100.00
2030	24.87	-	75.13	100.00
2031	23.27	-	76.73	100.00
2032	21.94	-	78.06	100.00
2033	20.84	-	79.16	100.00
2034	19.89	-	80.11	100.00
2035	19.06	-	80.94	100.00
2036	18.32	-	81.68	100.00

C.2 Performance Data on Active Aircraft 2008

Tables C.3a through C.3.c list data on currently active aircraft that finds it application in the final CO_2 forecast (in alphabetical order). In large part, the data represents a historical average (exceptions to this are listed in the main body in Table 6.1). Fuel burn per block hour *BF* and average block speed v_b is based on fleet recordings from 1998 to 2007 (**Airline Monitor 2008a**). Daily utilization U_d is the average utilization over the entire life of the regarded aircraft (**MRO Prospector 2008b**). The average capacity is the average number of scheduled available seats for 2008 in **OAG data 2007**. Nominal seat fuel burn and transport performance in ASK is calculated for an aircraft flying with nominal capacity and a load factor of 100 %. Average seat fuel burn and transport performance in ASK is calculated for an aircraft flying with average capacity and a load factor of 100 %. An average density of kerosene Jet A-1 of 800 $kg \cdot m^{-3}$ is assumed. Many wide-body aircraft are flown in average with a considerably lower capacity than their nominal one. This leads to an increase in per-seat fuel consumption. For many narrow-body aircraft, especially for the new generation 737 family, this is vice versa. The CO_2 forecast is based on the average capacity (seat fuel burn and ASK).

Table C.3a Fuel Consumption and Operational Performance – Active Regional Aircraft 2008

Aircraft Name	***BF***	v_b	U_d	**Nom. Capacity**	**Av. Capacity**	**Nom. Seat Fuel Burn**	**Av. Seat Fuel Burn**	**Av. ASK p. Day**
[-]	[$kg \cdot h^{-1}$]	[$km \cdot h^{-1}$]	[$h \cdot day^{-1}$]	[Seats]	[Seats]	[$l \cdot km^{-1} \cdot 100^{-1}$]	[$l \cdot km^{-1} \cdot 100^{-1}$]	[1000·km]
BAe146	1801	411	5.27	91	96	6.02	5.70	208
CRJ-700	1363	534	6.91	70	69	4.55	4.62	255
CRJ-900	1575	520	6.38	86	82	4.40	4.62	272
E-170	1272	523	6.53	75	72	4.05	4.22	246
E-175	1339	523	6.36	70	79	3.85	4.05	263
E-190	1554	539	6.80	98	96	3.68	3.75	352
E-195	1635	539	6.22	108	106	3.51	3.58	355
Fokker 70	1870	487	6.00	79	79	6.08	6.08	231
Fokker 100	2021	487	5.62	107	103	4.85	5.04	282

Table C.3b Fuel Consumption and Operational Performance – Active Narrow-Body Aircraft 2008

Aircraft Name	*BF*	v_b	U_d	Nom. Capacity	Av. Capacity	Nom. Seat Fuel Burn	Av. Seat Fuel Burn	Av. ASK p. Day
[-]	[kg·h^{-1}]	[km·h^{-1}]	[h·day^{-1}]	[Seats]	[Seats]	[l·km^{-1}·100^{-1}]	[l·km^{-1}·100^{-1}]	[1000·km]
A318	1997	600	7.71	107	112	3.89	3.72	518
A319	2346	610	7.85	124	129	3.88	3.73	617
A320	2433	626	8.21	150	155	3.24	3.14	797
A321	2820	642	7.67	185	180	2.97	3.05	886
B717	1862	485	7.10	106	112	4.52	4.28	386
B727	4190	588	4.21	169	145	5.27	6.14	360
B737-200	2515	484	5.63	120	115	5.41	5.64	314
B737-300	2340	543	7.19	128	135	4.21	3.99	527
B737-400	2394	543	7.01	150	146	3.67	3.77	556
B737-500	2219	532	6.60	118	114	4.42	4.57	400
B737-600	1908	595	6.29	110	111	3.64	3.61	416
B737-700	2165	613	6.76	126	137	3.50	3.22	567
B737-800	2392	605	6.95	162	168	3.05	2.94	706
B737-900	2574	634	6.73	180	188	2.82	2.70	802
B757-200	3233	647	8.63	200	195	3.12	3.20	1090
B757-300	3627	661	8.88	243	237	2.82	2.89	1392
DC-9	2513	459	5.25	125	111	5.47	6.16	268
MD-80	2848	568	7.05	150	141	4.18	4.45	564
MD-90	2502	575	5.45	153	143	3.56	3.81	448

Table C.3c Fuel Consumption and Operational Performance – Active Wide-Body Aircraft 2008

Aircraft Name	*BF*	v_b	U_d	Nom. Capacity	Av. Capacity	Nom. Seat Fuel Burn	Av. Seat Fuel Burn	Av. ASK p. Day
[-]	[kg·h^{-1}]	[km·h^{-1}]	[h·day^{-1}]	[Seats]	[Seats]	[l·km^{-1}·100^{-1}]	[l·km^{-1}·100^{-1}]	[1000·km]
A300-Classic	5155	654	5.07	266	244	3.70	4.04	810
A300-600	5155	654	6.79	266	259	3.70	3.80	1151
A310	4464	710	8.50	230	204	3.41	3.85	1232
A330-200	5336	764	11.22	253	248	3.45	3.52	2128
A330-300	5666	764	9.90	295	282	3.14	3.29	2135
A340-200/300	6662	805	12.39	295	266	3.51	3.89	2651
A340-500	8479	805	13.37	313	252	4.21	5.23	2711
A340-600	7874	805	12.75	380	325	3.22	3.76	3334
A380	12201	813	9.26	555	500	3.38	3.75	3763
B747-100	10775	764	4.90	366	387	4.82	4.56	1447
B747-200	10775	764	8.12	366	358	4.82	4.93	2220
B747-300	11477	813	9.24	412	390	4.28	4.53	2930
B747-400	10194	813	11.58	410	367	3.82	4.27	3455
B767-200	4353	706	5.65	224	182	3.44	4.24	726
B767-200ER	4353	706	10.38	224	182	3.44	4.24	1333
B767-300	4688	728	6.65	230	226	3.50	3.56	1094
B767-300ER	4688	728	10.53	230	214	3.50	3.76	1640
B767-400ER	5071	707	11.20	304	263	2.95	3.41	2082
B777-200	6484	782	7.49	305	295	3.40	3.52	1727
B777-200ER	6420	789	10.70	305	295	3.34	3.45	2489
B777-200LR	7064	789	10.77	305	292	3.67	3.83	2480
B777-300	7001	789	8.35	365	357	3.04	3.11	2351
B777-300ER	6932	789	9.51	365	341	3.01	3.22	2558
DC-10	7971	759	8.52	250	274	5.25	4.79	1772
MD-11	7377	779	10.69	323	289	3.67	4.10	2405

C.3 Data on Future Aircraft

Future aircraft regarded in the forecast can be roughly divided into aircraft available in short- to medium-term and aircraft available in the more long-term. Former represent aircraft projects, where the design process is finished or already well advanced. As the basic design and technology is frozen already, expected fuel burn and transport performance can be accessed from a literature study, see below. Due to the uncertainty of technology implementations, this is not possible for more distant aircraft projects. The forecast of the main-body is thus based on three scenarios, which consider different technology improvements and fuel consumptions for these aircraft. Data on the expected fuel burn and transport performance of all regarded future aircraft can be found from appendix C.3.2.

C.3.1 Literature Study: Aircraft with Short- to Medium-term Entry-into-Service Date

Bombardier CRJ-1000

The Bombardier CRJ-1000 is a stretched version of the CRJ-900 with a nominal seating capacity of 100 passengers. It is powered by two rear-mounted CF34-8 engines, conventional turbofans with a BPR of 5:1. The same engines power the CRJ-700/900 and Embraer E-170/175 aircraft. The wing is in large part identical to the CRJ900 wing. However, the wing tip and wing leading-edge were redesigned. The fuselage is a simple stretch from the CRJ900. A schematic of the aircraft is shown in Fig. C.1.

In short, the CRJ-1000 is a simple stretch from the CRJ-900, but with slightly refined technology (wing). For the forecast at hand, it seems reasonable to assume that the CRJ-1000 will burn the same amount of fuel per seat-km as the CRJ-900. This may seem a rather conservative approach, as Bombardier expects the CRJ-1000 to achieve 30 % reduced carbon dioxide emissions compared to older generation aircraft with similar passenger capacity currently in operation (**Kirby 2007**). However, with 4.40 litres per 100·km nominal seat fuel burn, the CRJ-1000 consumes 27 % less than the BAe146 (6.02 litres per 100 seat-km) and 10 % less than the Fokker 100 (4.85 litres per 100 seat-km). Seat fuel consumption of the CRJ-1000 is still higher than of its direct counterpart Embraer E190 (3.68 litres per 100 seat-km). Nevertheless, this is in accordance with engine data given by **GE Aviation 2009**: the Embraer E190 is equipped with wing-mounted CF34-10 engines that feature a lower *TSFC*. As the long-range cruising speeds of the CRJ-1000 and CRJ900 are identical (0.78 Ma) and design ranges are close (2761 km, 2414 km), block speed (523 $km \cdot h^{-1}$) and daily utilization (6.38 h) are adopted from the CRJ-900 (All data by **GE Aviation 2009**, **AT 2009d**, **Bombardier 2007a** and **Bombardier 2007b**)

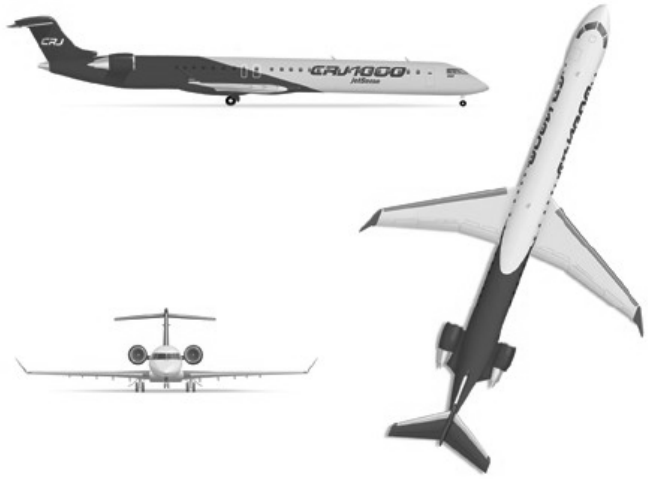

Fig. C.1 Bombardier CRJ1000 Schematic (**Techno Science 2009**)

ACAC ARJ21

The ACAC ARJ21-700 represents an entirely new regional jet family. However, the technology is rather conventional. The design of the fuselage originates largely from the MD90 aircraft, which production was licensed to Chinese aerospace companies by McDonnell Douglas (today Boeing) (**Spaeth 2008**). Even though the ARJ21-700 is a considerably smaller aircraft, the similarity in design to the MD90 and its predecessors MD80 and DC9 is apparent in Fig. C.2. The aircraft is powered by rear-mounted CF34-10 turbofans (BPR 5:1) that are also in use on the Embraer E190 and E195 aircraft (**GE Aviation 2009**). Only the wing was newly designed by Antonov (**Spaeth 2008**). The ARJ21-700 is expected to be followed by a stretched and refined version, the ARJ21-900 in 2011. According to **Leithen 2007** and **AT 2008**, ACAC and Bombardier are planning to intensify cooperation for the larger aircraft. The ARJ21-900 could thus benefit from newer technology. For example, in comparison to the -700, ACAC wants the horizontal and vertical stabilizer of the -900 to be composite as well as parts of the fuselage (**Leithen 2007**).

It is important to mention that the intent behind building the ARJ21 is not to build a revolutionary fuel-efficient aircraft. For ACAC, the aim is rather to gain experience in building commercial aircraft that meet Western certification requirements (**Leithen 2007**). As the technology featured is thus rather conventional, both aircraft are expected to show seat fuel consumption similar to the Bombardier CRJs. Seat fuel consumption for the ARJ21-700 is adopted from the CRJ-700 (4.55 litres per 100 seat-km), while seat fuel consumption for the ARJ21-900 is adopted from the CRJ-900 (4.40 litres per 100 seat-km). Due to the intensified cooperation with Bombardier, the ARJ21-900 (100 seats) could eventually feature newer technology and be slightly more fuel-efficient. However, this is unclear and is not

regarded in the forecast at hand. Utilization and block speed of both aircraft is adopted from the CRJ900 (6.38 h, 523 km·h^{-1}). This is reasonable as cruising speeds are identical (0.78 Ma) and design ranges are comparable (ARJ21-700: 2225 km, CRJ900: 2414 km).

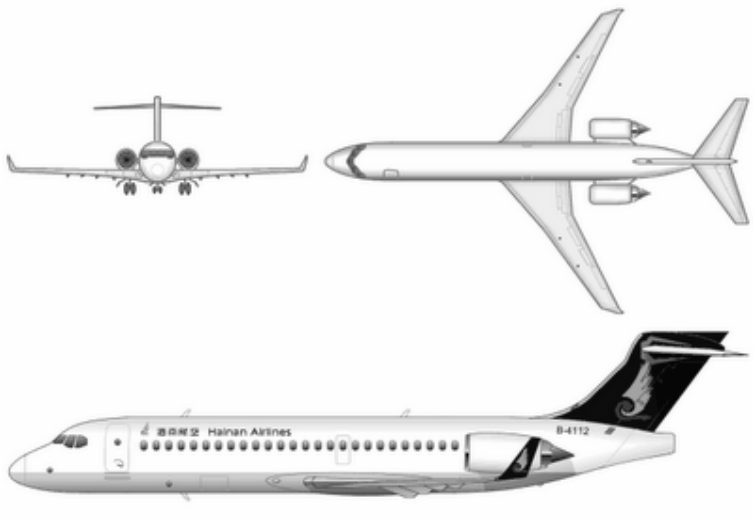

Fig. C.2 ACAC ARJ21-700 Schematic (**Airliners Penang 2008**)

Sukhoi SSJ

The Sukhoi SSJ100 is the first Russian airliner designed specifically to meet Western certification standards. As observable from Fig. C.3, the design resembles rather narrow-body aircraft like the Boeing 737 and Airbus A320 than traditional regional jets (see e.g. Fig. C.1 and Fig. C.2). This is mainly due to the wider fuselage and wing-mounted engines. Sukhoi decided in an early design stage for a cabin layout seating five passengers abreast. According to **Kingsley-Jones 2007**, Sukhoi Aviation Holding director general Michail Pogosyan believes that a four-abreast layout is not optimal for aircraft beyond 70 seats. Similar to the Embraer E-Jets, the SSJ family is further designed for longer ranges (2900 - 4550 km) than traditional regional jets (All data by **Kingsley-Jones 2007** and **Sukhoi 2009**).

In comparison to the ARJ-21 and CRJ1000, the SSJ100 was entirely new-designed. However, the focus was not only on fuel efficiency. To make the aircraft more attractive to Western customers, Sukhoi emphasized mainly on reducing aircraft purchase, maintenance and operation costs. This leads to an aircraft that is "...based on proven advanced technology to minimise technical risks ..." (**Sukhoi 2009**), but does not feature revolutionary, fuel-efficient technologies. The bulk in cost reduction for airlines is thus not achieved by lower fuel costs, but through standardized operation and maintenance. Nevertheless, with the Sukhoi SuperJet, a whole new regional-jet-engine enters the world fleet, the PowerJet SaM146. Snecma (France) and NPO Saturn (Russia) developed the engine in a joint venture. Although being a

conventional turbofan with a BPR of only 4.43, TSFC (0.0178 $kg \cdot h^{-1} \cdot kN^{-1}$) is reduced in comparison to the CF34-10 (Embraer E-190, 0.0184 $kg \cdot h^{-1} \cdot kN^{-1}$) by 3.2 % (All data by **Sukhoi 2009**, **PowerJet 2008** and **GE Aviation 2009**).

As cruising speeds (0.78 Ma) and design ranges are similar, utilization and block speed of the E-190 (6.8 h, 539 $km \cdot h^{-1}$) are adopted for the SSJ100-95 and of the E-170 (6.53 h, 523 $km \cdot h^{-1}$) for the SSJ100-75. Due to the new engine, the SSJ100-95 features a fuel consumption 2 % lower than its competitor E-190 **Spaeth 2008**. The fuel reduction is assumed to be applicable to the fuel burn per seat-km. An identical seat fuel reduction in comparison to the E-170 is expected for the SSJ100-75. Fuel burn per 100 seat-km of the -95 then calculates to 3.60 and of the -75 to 3.97 litres.

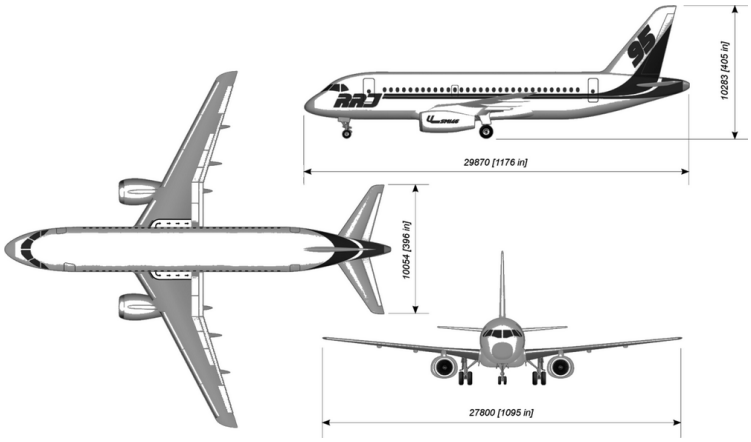

Fig. C.3 Sukhoi SSJ100-95 Schematic (former RRJ-95) (**UAC Russia 2008**)

Boeing 747-8 Intercontinental

The Boeing 747-8 Intercontinental is the latest evolutionary variant of the 747 family of aircraft. The original design was lengthened by 5.6 m to allow for a higher capacity (410 → 467 seats nominal) and thereby to fill the gap between the large variants of the 777 and the Airbus A380. The 747-8 is the first 747 to be stretched (**Boeing 2005**). Apart from this, the basic design of the fuselage is identical to the predecessor. According to **Hone-All 2008**, "... some carbon fibre reinforced plastics will be utilized in the airframe. However, structural changes will mostly be evolutionary rather than revolutionary." This is in accordance with **AT 2009b**, who believe that the 747-8 "...will be of aluminium rather than composite construction."

Main technological changes concern the wing. While sweep and basic design of the wing are kept to reduce development cost, the wing is thickened to transport more fuel.[1] It is thereby reached that the range is increased from the standard 747-400 without auxiliary tanks in the tail. Further, slightly bent-up raked wingtips replace the winglets of the 747-400 to lessen the influence of wingtip vortices and thus to save fuel (**Steinke 2006b**). Main flight controls are still mechanical (**Steinke 2006b**), however the 747-8 features fly-by-wire spoilers and outboard ailerons (**Norris 2008b**). To allow for the increased number of passengers and range (increased take-off weight) without changing the wing's overall area, the wing root is strengthened (**Norris 2008b**).

The 747-8 features four conventionally shrouded high-bypass turbofans. The GEnx-2B67 engine is the only powerplant available for the 747-8. It is a derivative of the GEnx engine developed for the 787 and features a considerably higher BPR (8.0) than the engines available for the 747-400 (4.8 – 5.3). A fan case and fan blades made out of lightweight composite material make this possible. Further, the over-all pressure ratio (OPR) is noticeably increased (**GE Aviation 2008**). As the aircraft systems on the 747-8 are kept conventional, the engine variant for the 747 will be adapted to provide bleed air for the systems (**Steinke 2006b**). The GEnx-2B67 has been flight tested in February 2009 (**Norris 2008b**). Results are not yet available. Accurate information about the over-all increase in engine efficiency is thus difficult to give. However, **GE Aviation 2008** says that the GEnx family of engines provides up to 15 % better specific fuel consumption than the engines it replaces. It should be noted that all GEnx engines feature a so-called *Twin Annular Premixing Swirler* (TAPS) combustor that considerably lowers NO_x emissions. The TAPS combustor mixes fuel and air prior to ignition and achieves a lower flame temperature – i.e. lower NO_x emission.

It is important to consider the intent behind designing the 747-8. Boeing mainly focused on two aspects. First, the new 747 should have the ability to serve more distant city pairs, i.e. the range had to be extended. Second, the new 747 should have the ability to operate on smaller and more airports than the A380, i.e. the aircraft's wings should not become too large. Both characteristics are important to allow the 747-8 to fit into the long-term 'point-to-point' fleet strategy of Boeing. Further, the commonality of the 747-8 with former 747 variants allows pilots to fly the 747-8 without complex re-training. This will attract customers for whom the A380 is too large and too 'new', i.e. too expensive.

For the study at hand, information of the *Boeing 2008 Environment Report* (**Boeing 2008**) concerning performance of the 747-8 is adopted. It states that the 747-8 shows a 16 % fuel burn advantage over the 747-400. This calculates to a 13.8 % reduction in nominal seat fuel burn. The 747-8 is thus assumed to burn 3.30 litres per 100 seat-km in a nominal capacity layout. This is about 2.5 % less than the nominal seat fuel burn of the A380-800. Block speed

[1] Further, "The wing is deeper, particularly at the root, and has a steeper twist angle to create additional lift inboard. In place of the complex double- and triple-slotted flaps of the current 747, the trailing edge of the -8 is configured with simpler 777-style double and single-slotted flaps." (**Norris 2008b**)

is expected to be identical to the 747-400, as cruising speeds (0.85 Ma) are identical and design ranges are similar (13 149 and 14 816 km).

Boeing 787

The Boeing 787 is an entirely new family of aircraft succeeding the Boeing 767. Three versions are expected to enter service in the years 2010-2013. The basic version, 787-8, replaces the 767-300(ER) and -200(ER), the stretched 787-9 replaces the 767-400ER. Both aircraft are long-range variants with design ranges of 14 484 km (-8) and 15 772 km (-9). Unlike, the third aircraft variant 787-3 is optimized for short ranges up to 5472 km (**Airline Monitor 2007**). The 787-3 is not comparable to any variant of the 767 family. The concept of a wide-body short-range aircraft is more comparable to the out-of-production models Airbus A300, A310-200 and McDonnell Douglas DC10-10. Even though the 787 is a classic cantilever aircraft, in terms of technical improvements, it can be regarded being revolutionary. The technical improvements described in the following are valid for all 787 variants.

The largest change concerns the material selection for major aircraft parts, see Fig. C.4. According to **Hawk 2005**, 50 % of the 787 material is composite and only 20 % aluminium. In comparison, only 12 % of the Boeing 777 and 25 % of the A380 structure is made of composites (**Walz 2009**). The relative share of composite material on the 767 is even considerably less (**Rosato 2004**). According to **Walz 2009**, the 787-8 will therefore be lighter by 30 000 to 40 000 lb (13 608 to 18 144 kg) than its direct competitor Airbus A330-200. However, if we compare the Airbus A330-200 and Boeing 787-8 from the actual *Airplane Characteristics for Airport Planning* Manuals (**Airbus 2009d**, **Boeing 2007a**), the ratio of empty weight to maximum take-off weight (W_E/W_{MTO}) is nearly identical (≈ 0.52) and so is the specific empty weight per passenger (≈ 473 kg).[1] Besides the potential weight reduction, the 787 composite fuselage features further advantages. As composites do not corrode and fatigue like metals, the cabin altitude could be lowered to 1.8 km (instead of the typical 2.4 km) and the cabin humidity be increased. This results in a higher passenger comfort (**Walz 2009**). Further, as will be seen below, the use of composites probably allowed for an increase in wing span.

The wings of the 787 are conventionally backswept and virtually fully turbulent. However, in comparison to the 767-300ER, the wing span of the -8 and -9 versions is increased by more than 10 metres (47.6 m → 58.8 m). From aerodynamic theory and the parametric study, we expect the aerodynamic efficiency to have largely increased. The increase in span has

[1] According to **Airbus 2009d**, W_{MTO} of the A330-200 is 230 000 kg and the typical W_E is 119 600 kg. The A330-200 transports 253 passengers over a range of 14 353 km (**Airline Monitor 2007**). According to **Boeing 2007a**, W_{MTO} of the 787-8 is around 219 539 kg and the typical W_E is 114 532 kg. The 787-8 transports 242 passengers over a range of 14 484 km (**Airline Monitor 2007**).

probably been made possible by the use of composite material for nearly the entire wing. Similar to the 747-8, the 787-8 and -9 feature slightly bent-up raked wing-tips to lessen the induced drag component. Due to the highly shortened range of the 787-3, its wing span is shortened by roughly 7.6 metres with respect to the 787-8 wing. To prevent induced drag to rise dramatically, the raked wing-tips were thus replaced by blended winglets (All data by **AT 2009c**).

The engines available for all variants of the 787 are the General Electric GEnx and the Rolls Royce Trent 1000. Both engines are conventionally shrouded high by-pass turbofans. However, both engines feature very high bypass-ratios, the GEnx a BPR of 9.1 - 9.6 and the Trent 1000 a BPR of 10.0 - 11.0. In comparison to the engines available for the 767, the BPR has nearly doubled (BPR of the GE CF6-80C2, P&W 4000-94 and RR RB211 around 5.0). The increase in fan diameter is possible by using new lightweight material for the fan blades and case. These components are made of titanium on the Trent 1000 and of composite material on the GEnx. Engine theory suggests the propulsive efficiency of the 787 engines to have largely increased from the ones on the 767. Due to higher over-all pressure ratios (OPR), thermal efficiencies of both engines are likely to have increased as well. The Trent features an OPR around 50, while the GEnx features an OPR around 45. For comparison, the engines used on the 767 feature an OPR around 30. Further, both engines are 'bleed-free', i.e. no bleed-air is taken from the engines to power the aircraft systems. Instead, pneumatic aircraft systems are replaced by electrical ones on the 787. Even though the generators on the engines need to produce higher electrical power, this is said to reduce over-all energy taken from the engines by 35 % (**Sinnett 2007**). If secondary system losses are lower, the thermal efficiency of the engine increases (**Gmelin 2008**). Additionally, the over-all efficiency benefits from a higher cruising speed of the 787 – 0.85 Ma instead of 0.8 (767) and 0.82 Ma (A330).

According to **Adams 2008**, fuel consumption efficiency of the Trent 1000 is around 13 to 14 % higher than for the Trent 700 which is on use on the A330. **GE Aviation 2008** states that the GEnx features a specific fuel consumption that is up to 15 % better than the one of the engines it replaces. These values indicate a reduction of thrust specific fuel consumption in the order of 10 to 13 % from the 767 and A330.

Another technological innovation found on the 787 is the laminar flow nacelle. The nacelle features very smooth composite surfaces that allow attaining natural laminar flow over the entire nacelle if it is maintained and cleaned regularly. According to the findings of **IATA 2008a**, the 787 thereby saves 30 000 gallons (90 845 kg kerosene) of fuel per year and aircraft.

Airline Monitor 2007 expects the 787 variants to burn 4542 $kg \cdot h^{-1}$ (-8), 5148 $kg \cdot h^{-1}$ (-9) and 3331 $kg \cdot h^{-1}$ (-3) of fuel per block hour and to obtain block speeds of 813 $km \cdot h^{-1}$ (-8, -9) and 676 $km \cdot h^{-1}$ (-3). If flown with full capacities of 242 and 280 passengers, the fuel burn per seat and 100 km is then typically 2.89 l (-8) and 2.83 l (-9). This is around 20 % less than the seat

fuel consumption of the A330-200 and 767-300ER (3.62 l, 3.45 l), which are comparable in size and range. The assumption of **Airline Monitor 2007** is thereby in accordance with the information given by **Boeing 2009a**, that the 787 uses "... 20 percent less fuel than any other airplane of its size." If the 787-3 is flown with full capacity (317 passengers), it burns only 1.94 l per seat and 100 km. The strong reduction of around 30 % from the seat fuel consumption other 787 variants is due to the shorter range and the associated reduction in take-off weight.[1]

It is believed that the assumption of a 20 % seat fuel reduction in comparison to the A330-200 and 767-300ER is in reasonable accordance with the technological improvements of the 787 mentioned above. It is further assumed that the efficiency increase is primarily due to an improvement in aerodynamics and engine efficiency. The wide application of composite material is seen rather as an enabler for the increase in wing span and a higher passenger comfort than for a reduction in payload specific empty weight. The results of the parametric variation of engine efficiency in chapter 3.3 of the main body show a reduction in block fuel weight of around 15 to 20 % for a 13 to 15 % efficiency increase as prospected by **GE Aviation 2008** and **Rolls Royce 2008**. Adding the benefit from increasing the wing span by 10 m, an over-all reduction of 20 % seems realistic. The application of bleed-free engines and a laminar flow nacelle is an important step to foster the use of new technology on aircraft. Even if the benefit for the 787 may be rather small, it allows the practical wide-range testing of the technology. Thereby more radical changes and benefits for future aircraft could be made possible.

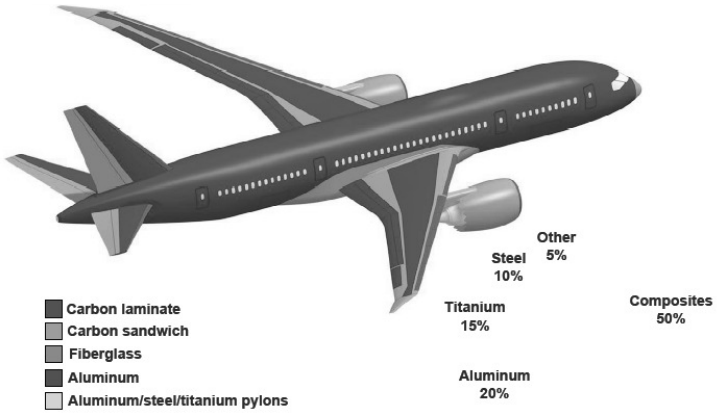

Fig. C.4 Material Distribution on Major Structural Parts of the Boeing 787 (**Hawk 2005**)

[1] The maximum take-off weight of the 787-3 is expected to be only 165 000 kg, 54 000 kg less than the W_{MTO} of the 787-8 and even 80 000 kg less than the W_{MTO} of the 787-9 (**Boeing 2009a**).

Airbus A350 XWB

The Airbus A350 XWB is a new family of wide-body long-range aircraft to compete with the Boeing 777 and the 787-9. It is expected to succeed the productions of the Airbus A340 and A330-200. Even though the A350 competes with only one variant of the 787, technological improvements are highly influenced by the 787 design. All A350 variants feature a very long range, similar to the extended range and long-range versions of the 777 and the 787. The A350 is a classic cantilever aircraft with two wing-mounted engines.

The relative share by weight of composite material used on the A350 is similar to the one of the 787. Information given in literature concerning the actual share varies from 45 % (**AT 2009a**) to 53 % (**IATA 2008a**). Another advanced material in use on major aircraft parts is Aluminium-Lithium (Al-Li). Together, the relative share of advanced materials on the A350 is around 62 % (**Steinke 2006a**). Contrary to the 787, the A350 fuselage is not constructed of single-piece composite barrels. Instead, Airbus applies what they call a 'four shell skin panel concept': carbon fibre skin panels, doublers, joints and stringers are attached to aluminium frames (see Fig. C.5). According to **Airbus 2009e.**, this allows for an easier reparability, as panels can be removed and substituted. Aluminium frames were chosen for an improved energy absorption and electrical conduction (ibid.). As on the 787, the use of composite material for large parts of the fuselage allows for an increase in cabin humidity and a decrease in cabin altitude for higher passenger comfort.

Airbus states that due to the wide application of new material the manufacturer's empty weight per seat of the A350 is around 12 % lower than the one of the 777 (**Airbus 2009e**). Recent Airbus calculations give manufacturer's empty weight ($W_{E,M}$) of the A350-900 as 115 700 kg (**Kingsley-Jones 2008a**). This is 11 % less $W_{E,M}$ per seat than calculated for the 777-300ER and 9 % less than calculated for the 777-200ER.[1]

The wing of the A350 is a conventional backswept and virtually fully turbulent cantilever. Similar to the 787, it is primarily made of composite and features a wingspan (64.7 m) and area (442 m^2) similar to the 777-200LR and 777-300ER (**Kingsley-Jones 2008a**, **Flight International 2006**). To allow for an increase in Mach number from 0.82 (A330) to 0.85, the wing's leading edge is swept by 35° instead of 32°. The general design of the wing is seen in Fig. C.6. It resembles the wing design of the 787, especially as both aircraft families use a similar wingtip device to lessen induced drag. However, while Boeing uses three wings of different size and area, each one designed for the specific needs of the different aircraft variants, Airbus applies the same wing to the A350-800, -900 and -1000 (**Airbus 2009b**).

[1] According to **Aircraft Commerce 2001**, the 777-300ER manufacturer's empty weight is 151 031 kg and typical operating empty weight is 169 644 kg. Manufacturer's empty weight of the 777-200ER was not retrievable. It is calculated assuming an identical relative difference between the operating empty weight and the manufacturer's empty weight as for the 777-300ER. Typical operating empty weight of the 777-200ER is 138 100 kg (**Boeing 1998**), calculated manufacturer's empty weight is thus 122 950 kg. Typical seating capacities of 314 (A350-900), 365 (777-300ER) and 305 (777-200ER) are assumed (**Airline Monitor 2007**).

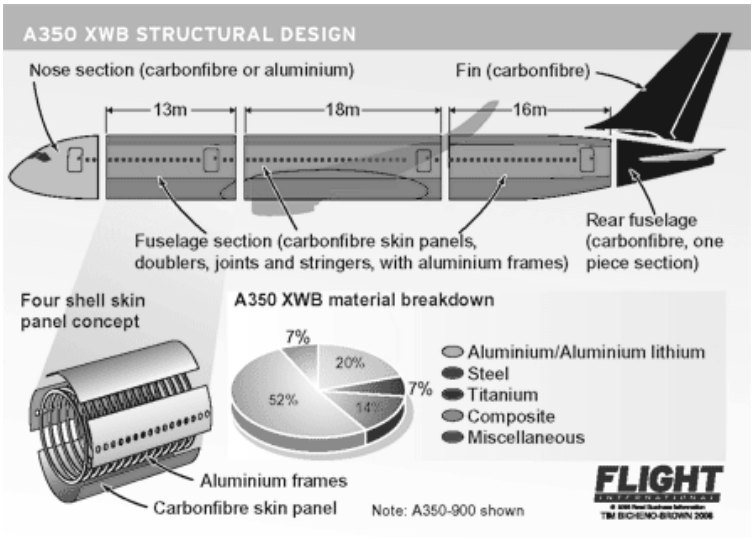

Fig. C.5 Airbus A350 XWB Structural Design (**Kingsley-Jones 2006**)

The wing of the A350 features some rather unapparent, but still innovative technology. First, the outboard flaps are deployed stream-wise rather than normal to the rear spar as usual. This is a very simple technique, but reduces drag created by the flap fairing. Second, the spoilers are used to control the gap between the trailing edge of the wing and the leading edge of the flap by deflecting down. Thereby the high lift performance is optimized (**Kingsley-Jones 2008a**). Third, as **Aircraft Commerce 2009** explains, "The flight computer will perform in-flight trimming of the inboard and outboard flaps, to create a variable camber wing that adapts to different flight conditions."

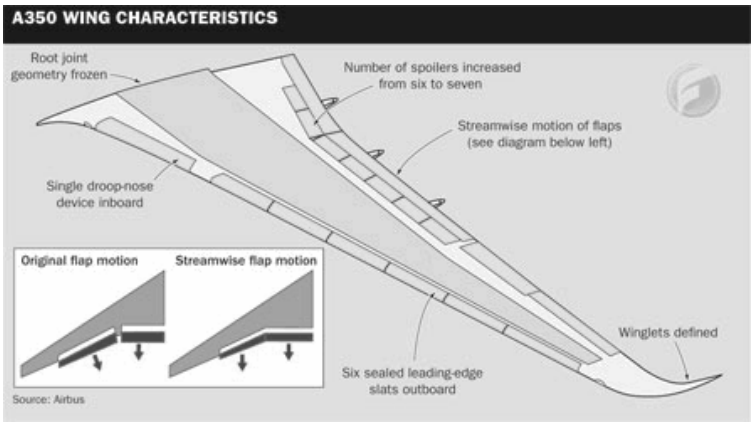

Fig. C.6 Airbus A350 XWB Wing Characteristics (**Kingsley-Jones 2008a**)

As for the moment, only one type of engine is available for the Airbus A350, the Rolls Royce Trent XWB. It is a high-bypass three-shaft shrouded turbofan and the most modern of the Trent family, which also powers the A380 and 787. The general design of the Trent XWB is derived from the 787's Trent 1000. It is thus expected that it incorporates similar technology.

However, according to **Doyle 2009**, the manufacturer "…has made some significant advances even compared with the Trent 1000". Even though the final design is not yet available to public, it is published that the Trent XWB is the first Trent to feature a two-stage intermediate-pressure turbine, Blisk technology for the compressor (weight savings) and a mechanism to control the bleed air for the turbine blades (smaller losses). Similar to the Trent 1000, a large fan has been made possible by titanium fan blades and housing (All data by **Doyle 2009**). In comparison to the Trent 1000, the Trent XWB still supplies the aircraft systems with bleed air. "...according to Airbus's calculations, purely electrical systems add to the maintenance costs with virtually no cost or weight advantages", says **Steinke 2006a**.

The first Trent XWB is designed for the use on the A350-900 and features a BPR of 9.3 (**Doyle 2009**). The over-all pressure ratio will probably be near the OPR of the Trent 1000 (OPR 50.0). The A350-900 competes with the 777-200ER, which is available with the General Electric GE90-94B (BPR 8.3, OPR 40.5), Rolls Royce Trent 892/895 (BPR 5.7-6.2, OPR 41.5) and Pratt & Whitney PW4090 (BPR 5.8-6.4, OPR 39.2) (**MRO Prospector 2008b**, **ICAO 2009a**). The difference in engine OPRs and BPRs between the 777-200ER and the A350-900 are not as large as between the 767 and 787. This suggests that also the difference in engine efficiencies is not as big. According to **Doyle 2009**, the manufacturer expects the Trent XWB to show a relative 15 % improvement from the Trent 700 in terms of fuel burn. Thrust specific fuel consumption (TSFC) of the Trent 700 on the A330-200 can be calculated from data given in **Eurocontrol 2004a**. The typical TSFC of the 777-200ER in cruise (**Eurocontrol 2004a**) is 10 % smaller. A 15 % improvement from the Trent 700 thus indicates a relative reduction in TSFC in the order of 3 to 4 % from the engines of the 777-200ER.

A relatively detailed list on Airbus' expectations concerning the performance of the A350 can be found in **Airbus 2009e**. Herein, Airbus sets the A350-900 as datum and states that the 777-200ER burns 30 % more block fuel per seat. Similarly, the 777-300ER is expected to consume 25 % more fuel per seat than the A350-1000 and the 787-9 to consume 6 % more fuel per seat than the A350-800 (ibid.). From this, we can assume the block fuel per seat of the A350-900 to be 23 % less than the one of the 777-200ER, the block fuel per seat of the A350-1000 to be 20 % less than the one of the 777-300ER and the block fuel per seat of the A350-800 to be 5.5 % less than the one of the 787-9. This is in reasonable accordance with information on the current Airbus website (**Airbus 2009a**): "... the aircraft will be highly efficient ... while reducing fuel consumption and CO2 emissions by up to 25 % compared to other aircraft in this category." Other sources expect more radical seat fuel savings with reductions of 30 % or even above (**Steinke 2006a**, **Airline Monitor 2007**, **Aircraft Commerce 2009**). However, for the sake of conservatism, we are adopting the Airbus expectations for the forecast at hand. As cruise Mach and design range of the A350 variants equal cruise Mach and design range of the 787-9, it is assumed that block speeds of these aircraft are identical (813 $km \cdot h^{-1}$).

The relative improvement from 777 efficiency parameters is highest for the empty weight per seat. It is thus assumed that this is the key enabler for the rather radical seat fuel reduction. This is unlike the 787, where the increase in efficiency is mainly attributed to the increase in wing span and engine efficiency. Nevertheless, Airbus and Rolls Royce put large effort in optimizing wing design and engine efficiency, which of course have their contributions to the fuel reductions. The introduction of unconventional technologies on the wing of the A350 is believed to be an important indicator for the willingness of manufacturer's to apply novel technology. This is similar to the more electric aircraft architecture and laminar flow nacelle on the 787. It is further believed that this is strongly driven by the attractiveness of eco-efficient technologies as end-customers (passengers) have become more ecologically sensitive over the last decade.

Mitsubishi MRJ

With the Mitsubishi Regional Jet (MRJ), yet another new manufacturer of medium to large regional jets is surging onto the market. The 70 and 90 seat aircraft compete with the Bombardier CRJs, smaller variants of the Embraer E-Jets and the new regional aircraft of Sukhoi and ACAC. The MRJ is a conventional regional aircraft with cantilever wings, a four seat-abreast cabin and wing-mounted engines. It is one of the first aircraft to be powered by a geared turbofan (GTF). Besides the engine, only little technical details have been released about the aircraft (**Flightglobal 2009**).

The general design and materials breakdown of the MRJ is seen in Fig. C.7. The design resembles the one of the Embraer E-Jets. This is also true for the four seats abreast cabin layout. Contrary to the 787 and A350, the MRJ is still a largely metal aircraft (58 % aluminium, 28 % carbon fibre). Nevertheless, the wings and empennage are primarily made of composites, which is new for regional jets of this size. This could indicate weight savings. However, this is not underpinned by a comparison of maximum take-off weights with the E-Jets. The long-range version of the MRJ-70 features a W_{MTO} (40 200 kg) nearly identical with the long-range version of the E-175 (40 370 kg). The MRJ-70LR thereby transports 80 passengers over a range of 3300 km and the E-175 78 passengers over a range of 3706 km. The take-off weight per seat-km is thus even slightly lower for the Embraer aircraft. The same is true for a comparison of the MRJ-90LR with the E-190 (**Mitsubishi 2009**, **Embraer 2008b**, **Embraer 2008a**). The MRJ uses winglets similar to the ones in use on the CRJs and E-Jets to lessen the influence of wingtip vortices and thus to reduce induced drag.

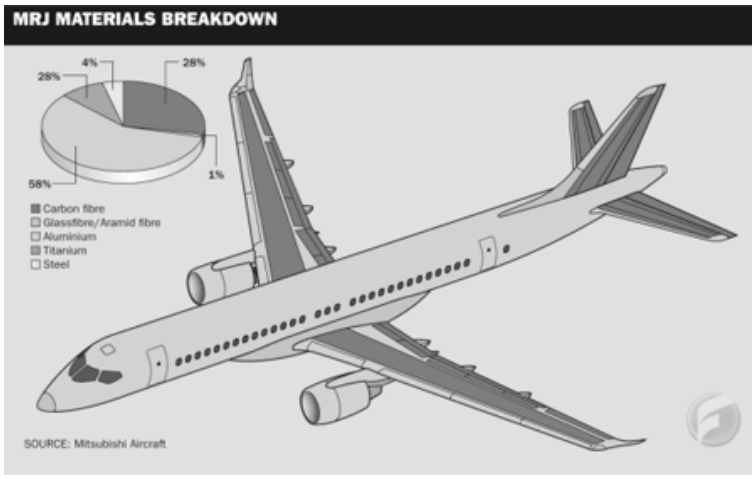

Fig. C.7 Mitsubishi MRJ Materials Breakdown (**Govindasamy 2008**)

The MRJ is powered by the Pratt & Whitney PW1000G, which is the first engine to use a geared fan. This allows both the low pressure turbine and the fan to rotate at their respective optimal speeds (see Appendix B and main body chapter 4.2.). The slow turning fan allows for an increase in fan diameter as blade tip speeds are reduced. The PW1000G thus features a by-pass ratio of 8.0, which is noticeably more than the BPR of other regional jet engines. For comparison, the GE CF34 that is in use on the CRJs, ARJs and E-Jets features a BPR of only 5.0. A geared fan further allows fan blades to be built lighter and the number of blades to be reduced to about the half of conventional turbofans. This benefits the weight of the engine. Weight is also saved on the low-pressure compressor and turbine as the number of stages can be reduced with the LP turbine rotating at higher speeds. Even though the gearing mechanism adds extra weight to the engine, the GTF is therefore still lighter than conventional turbofans. The combined benefits of the weight savings and increased component efficiencies are expected to lower specific fuel consumption by 12 % compared to similar state-of-the-art engines. (All data by **IATA 2008a**, **Aircraft Commerce 2008c**, **Pratt & Whitney 2008**, **GE Aviation 2009**)

Mitsubishi prospects fuel savings of over 20 % over similar sized regional aircraft (**Mitsubishi 2009**). From the information on technical details given to date, the geared turbofan PW1000G seems to be the only revolutionary technology found on the MRJ that truly enables considerable fuel reductions. The results of the parametric study in chapter 3.3 of the main body suggest that block fuel weight of narrow-body aircraft drops by approximately 12 to 13 % if TSFC is reduced by 12 %. The impact on block fuel is influenced by the design range of the aircraft. As the design range of the MRJ is smaller than the design range of the narrow-body aircraft regarded in chapter 3.3, a reduction of only 10 % in block fuel is anticipated for the regional aircraft. It is thus assumed that the MRJ-70 burns nominally 10 % less fuel per seat-km than the similar E-170 and the MRJ-90 10 % less fuel per seat-km than the similar E-190. This is in agreement with Mitsubishi's prospected fuel savings: the seat fuel burn of the two MRJ variants is then 21 and 27 % lower than the seat

fuel burn of the CRJ-700 and -900 respectively. Block speed for the MRJ is adopted from the Bombardier CRJ family of aircraft, as Cruise speeds (0.78 Ma) and design ranges (1480 - 3330 km) are similar.

Bombardier CSeries

The Bombardier CSeries is a new family of aircraft designed specifically for the 100- to 130-seat market. Its main competitors are the best-selling Embraer E-190/195 and smaller variants of the Airbus A320 and Boeing 737 family of aircraft. The CS100 and CS300 are classic cantilever aircraft with wing-mounted engines and feature ranges of 4704 km (basic variant) and 5463 km (extended range variant). The CSeries is one of the two aircraft families to launch series production of a new type of engine, the geared turbofan.

The CS100 and CS300 highly benefit from the fact that they are not downsized from larger aircraft (like the A318 and B737-600) or upsized from smaller aircraft (like the E-195), but specifically designed for their respective seat range. The result is a more efficient wing and fuselage design, even without implementing technological innovations. This is observable from Fig. C.8: the shortened A318 features a wing and cabin width too large for its capacity, for the E-195 this is vice versa. A more coherent design has positive effects on the aerodynamics and weights of an aircraft.

Fig. C.8 Top views of Airbus A318, Embraer E-195 and Bombardier CS100 (**Global Security 2009**, **Embraer 2008c**, **Bombardier 2009**)

Similar to the Boeing 787 and Airbus A350, the CSeries is constructed to a large part of advanced materials (see Fig. C.9). Wings, empennage, rear fuselage and engine pods are

made of composite material, which accounts for a total of 46 % of manufacturer's empty weight. The main fuselage is made of aluminium-lithium (24 % $W_{E,M}$). Manufacturer's or operating weight empty is not yet available. Take-off weight of the CS100 basic variant (54 749 kg) is however close to the advanced-range (AR) variant of the E-195 (52 290 kg). Both aircraft feature a range of 4074 km, while the CS100 transports 110 passengers and the E-195 108 passengers. The cruising speed of the CS100 is with 0.78 Ma however considerably higher than the cruising speed of the E-195 (0.75 Ma) (**Bombardier 2009**, **Embraer 2008c**).

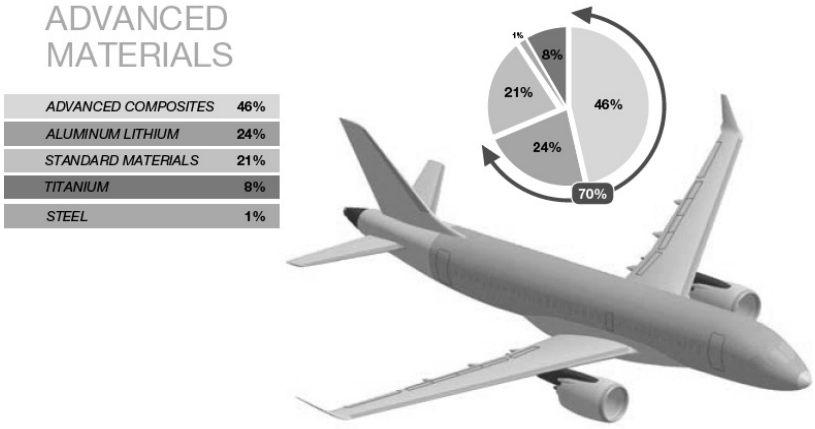

Fig. C.9 Bombardier CSeries Materials Breakdown (**Bombardier 2009**)

In comparison to the wings of the A318 and E-195, the wing of the CSeries features a high aspect ratio, similar to the wing of the 787 (see Fig. C.8). This has probably been made possible by the extensive use of composite material for the wing. A wing of a higher aspect ratio (larger span, smaller area) improves aerodynamic efficiency and is thus expected to reduce fuel burn.

The CSeries is the second family of aircraft that is solely powered by the geared turbofan PW1000G. With a bypass ratio of 12.0 (**IATA 2008a**), the CSeries engine has the highest BPR of any turbofan that has been produced up to the year 2013. The PW1000G for the CSeries have a higher thrust range than the geared turbofans for the MRJ, the benefits are however identical. Similar to the MRJ engine, Pratt & Whitney expect TSFC to come in 12 % lower than the TSFC of today's state-of-the-art engines (ibid.).

Bombardier 2009 states that the CSeries has a fuel burn advantage of at least 20 % over any in-production aircraft in its class. Regarding the benefits of a general design that is closer to optimum, an increased wing aspect ratio and a TSFC reduction of 12 %, this seems reasonable. According to **Airline Monitor 2007**, today's most efficient aircraft in the class of

the CS100 is the E-195 with a nominal seat fuel burn of 3.51 litres per 100 seat-km[1]. Accordingly, the CS100 is expected to burn 20 % less, i.e. 2.81 litres per 100 km[2]. This results partly from a lower fuel burn per block hour and partly from a higher block speed (598 km·h^{-1} instead of 539 km·h^{-1}). The higher block speed results from a higher cruising speed and longer design ranges and is taken as the average of the block speeds of the A318 and 737-600. In comparison to the Airbus and Boeing narrow-bodies, the seat fuel consumption of the CS100 is around 20 to 23 % lower. Today's most efficient aircraft in the class of the CS300 is the 737-700 with a seat fuel burn of 3.50 litres per 100 km[3]. We will thus assume the CS300 to burn only 2.80 litres per 100 km[4], i.e. 20 % less. The block speed of the CS300 is taken as the average of the block speeds of the 737-700 and A319 (611 km·h^{-1}).

C.3.2 Performance Data on Future Aircraft

Operational performance of future aircraft is adopted from similar existing ones. This concerns block speed, daily utilization and the average deviation from the nominal seat capacity. Table C.4 lists reference aircraft to the different future models.

Tables C.5a, C.5b and C.5c list resulting performance data on the future aircraft. For comparability, the tables also include data on similar in-production aircraft. Nominal seat fuel burn and transport performance in ASK is calculated for an aircraft flying with nominal capacity and a load factor of 100 %. Average seat fuel burn and transport performance in ASK is calculated for an aircraft flying with average capacity and a load factor of 100 %. An average density of kerosene Jet A-1 of 800 kg·m^{-3} is assumed.

[1] With a nom. capacity of 108 passengers and a load factor of 100 %
[2] With a nom. capacity of 110 passengers and a load factor of 100 %
[3] With a nom. capacity of 126 passengers and a load factor of 100 %
[4] With a nom. capacity of 130 passengers and a load factor of 100 %

Table C.4 Reference Aircraft and Literature for the Estimation of Future Aircraft Operational Performance

Future Aircraft	Reference Aircraft / Literature for Estimation of		
	Block Speed	**Daily Utilization**	**Deviation from nom. Seat Capacity**
CRJ-1000	CRJ-900	CRJ-900	CRJ-900
ARJ21-700/900	CRJ-900	CRJ-900	CRJ-900
SSJ100-75/95	E-170/190	E-170/190	E-170/190
747-8	747-400	747-400	747-400
787-3	**Airline Monitor 2007**	767-300	767-300
787-8	**Airline Monitor 2007**	A330-200	A330-200
787-9	**Airline Monitor 2007**	777-200ER	777-200ER
A350-800	**Airline Monitor 2007**	787-9	787-9
A350-900	**Airline Monitor 2007**	777-200ER	777-200ER
A350-1000	**Airline Monitor 2007**	777-300ER	777-300ER
C100	A318, 737-600	A318, 737-600	E-195
C300	A319, 737-700	A319, 737-700	737-700
A30X	A320 Family	A320 Family	A320 Family
Y1	737 NG Family	737 NG Family	737 NG Family
A340 Replacement	A340 Family	A340 Family	A340 Family
777 Replacement	777 Family	777 Family	777 Family
747 Replacement	747-400	747-400	747-400

Table C.5a Fuel Consumption and Operational Performance – Future and In-Production Regional Aircraft

Aircraft Name	***BF***	v_b	U_d	**Nom. Capacity**	**Av. Capacity**	**Nom. Seat Fuel Burn**	**Av. Seat Fuel Burn**	**ASK**
[-]	[kg·h^{-1}]	[km·h^{-1}]	[h·day^{-1}]	[Seats]	[Seats]	[l·km^{-1}·100^{-1}]	[l·km^{-1}·100^{-1}]	[1000·km]
70-Seaters								
CRJ-700	1363	534	6.91	70	69	4.55	4.62	255
E-170	1272	523	6.53	75	72	4.05	4.22	246
ARJ21-700	1515	520	6.38	80	76	4.55	4.78	253
SSJ100-75	1296	523	6.53	78	75	3.97	4.14	256
MRJ-70	1170	534	6.91	75	72	3.65	3.80	266
90-Seaters								
CRJ-900	1575	520	6.38	86	82	4.40	4.62	272
E-190	1554	539	6.80	98	96	3.68	3.75	352
CRJ-1000	1831	520	6.38	100	95	4.40	4.62	316
ARJ21-900	1831	520	6.38	100	95	4.40	4.62	316
SSJ100-95	1522	539	6.80	98	96	3.60	3.68	352
MRJ-90	1238	520	6.38	90	88	3.31	3.38	292

Table C.5b Fuel Consumption and Operational Performance – Future and In-Production Narrow-Body Aircraft

Aircraft Name	***BF***	v_b	U_d	**Nom. Capacity**	**Av. Capacity**	**Nom. Seat Fuel Burn**	**Av. Seat Fuel Burn**	**ASK**
[-]	[kg·h^{-1}]	[km·h^{-1}]	[h·day^{-1}]	[Seats]	[Seats]	[l·km^{-1}·100^{-1}]	[l·km^{-1}·100^{-1}]	[1000·km]
110-Seaters								
A318	1997	600	7.71	107	112	3.89	3.72	518
B737-600	1908	595	6.29	110	111	3.64	3.61	416
E-195	1635	539	6.22	108	106	3.51	3.58	355
C100	1477	598	7.00	110	108	2.81	2.86	452
A30X-18								
- central	1598	600	7.71	107	112	3.11	2.97	518
- high	1298	600	7.71	107	112	2.53	2.41	518
Y1-600								
- central	1526	595	6.29	110	111	2.91	2.89	416
- high	1240	595	6.29	110	111	2.37	2.35	416
130-Seaters								
A319	2346	610	7.85	124	129	3.88	3.73	617
B737-700	2165	613	6.76	126	137	3.50	3.22	567
C300	1782	611	7.30	130	141	2.80	2.58	631
A30X-19								
- central	1877	610	7.85	124	129	3.10	2.98	617
- high	1525	610	7.85	124	129	2.52	2.42	617
Y1-700								
- central	1732	613	6.76	126	137	2.80	2.58	567
- high	1407	613	6.76	126	137	2.28	2.10	567
150-Seaters								
A320	2433	626	8.21	150	155	3.24	3.14	797
B737-800	2392	605	6.95	162	168	3.05	2.94	706
A30X-20								
- central	1946	626	8.21	150	155	2.59	2.51	797
- high	1581	626	8.21	150	155	2.11	2.04	797
Y1-800								
- central	1914	605	6.95	162	168	2.44	2.35	706
- high	1555	605	6.95	162	168	1.98	1.91	706
COMAC 919								
-low	2433	626	8.21	150	155	3.24	3.14	797
-central	2068	626	8.21	150	155	2.75	2.67	797
-high	1581	626	8.21	150	155	2.11	2.04	797
180-Seaters								
A321	2820	642	7.67	185	180	2.97	3.05	886
B737-900	2574	634	6.73	180	188	2.82	2.70	802
A30X-21								
- central	2256	642	7.67	185	180	2.38	2.44	886
- high	1833	642	7.67	185	180	1.93	1.98	886
Y1-900								
- central	2059	634	6.73	180	188	2.26	2.16	802
- high	1673	634	6.73	180	188	1.83	1.75	802

Table C.5c Fuel Consumption and Operational Performance – Future and In-Production Wide-Body Aircraft

Aircraft Name	***BF***	v_b	U_d	**Nom. Capacity**	**Av. Capacity**	**Nom. Seat Fuel Burn**	**Av.Seat Fuel Burn**	**Av. ASK**
[-]	[kg·h^{-1}]	[km·h^{-1}]	[h·day^{-1}]	[Seats]	[Seats]	[l·km^{-1}·100^{-1}]	[l·km^{-1}·100^{-1}]	[1000·km]
Medium-Sized Wide-Body								
A330-200	5336	764	11.22	253	248	3.45	3.52	2128
A330-300	5666	764	9.90	295	282	3.14	3.29	2135
B767-200	4353	706	5.65	224	182	3.44	4.24	726
B767-300	4688	728	6.65	230	226	3.50	3.56	1094
B767-200ER	4353	706	10.38	224	182	3.44	4.24	1333
B767-300ER	4688	728	10.53	230	214	3.50	3.76	1640
B767-400ER	5071	707	11.20	304	263	2.95	3.41	2082
A350-800	4691	813	10.70	270	261	2.67	2.76	2271
B787-3	3331	676	6.65	317	295	1.94	2.09	1327
B787-8	4542	813	11.22	242	237	2.89	2.95	2164
B787-9	5148	813	10.70	280	271	2.83	2.92	2355
Large Wide-Body								
A340-200/300	6662	805	12.39	295	266	3.51	3.89	2651
A340-500	8479	805	13.37	313	252	4.21	5.23	2711
A340-600	7874	805	12.75	380	325	3.22	3.76	3334
B777-200ER	6420	789	10.70	305	295	3.34	3.45	2489
B777-200LR	7064	789	10.77	305	292	3.67	3.83	2480
B777-300ER	6932	789	9.51	365	341	3.01	3.22	2558
A350-900	5245	813	10.70	314	304	2.57	2.66	2641
A350-1000	5481	813	9.51	350	327	2.41	2.58	2528
A340-2/300 Replacement								
-Central	4752	805	12.39	295	266	2.50	2.78	2651
-High	3802	805	12.39	295	266	2.00	2.22	2480
A340-600 Replacement								
-Central	5523	805	12.75	380	325	2.26	2.64	3334
-High	4419	805	12.75	380	325	1.81	2.11	3334
B777-200LR Replacement								
-Central	4815	789	10.77	305	292	2.50	2.61	2480
-High	3852	789	10.77	305	292	2.00	2.09	2480
B777-300ER Replacement								
-Central	5199	789	9.51	365	341	2.26	2.42	2558
-High	4159	789	9.51	365	341	1.81	1.93	2558
Very-Large Wide-Body								
A380-800	12201	813	9.26	555	500	3.38	3.75	3763
B747-400	10194	813	11.58	410	367	3.82	4.27	3455
B747-8	10010	813	11.58	467	418	3.30	3.68	3936
B747 Replacement								
-Central	8708	813	11.58	467	418	2.87	3.20	3936
-High	6967	813	11.58	467	418	2.29	2.56	3936